The Biomechanical Characteristics of

Human Skin

A thesis presented for the Degree of

Doctor of Philosophy of the

University of Strathclyde

by

Colin Henry Daly, BSc

47 Auchinloch Road
Lenzie.   August 1966.

ACKNOWLEDGEMENTS

CONTENTS

ABSTRACT

"The Biomechanical Properties of Human Skin"

The aims of the research project described in
the thesis were to investigate the mechanical properties
of skin, to develop relevant analytical concepts and to
explore clinical applications.

Chapter I gives a review of the published
literature, consisting of a brief description of the
anatomy of skin, a more detailed survey of the nature and
mechanical properties of the components of skin and a
critical review of all known work on the mechanical
properties of skin.

The pilot experiments which were carried out to
define the nature and extent of the problems involved in
testing skin are described in Chapter II.

Various theoretical approaches to describe the
behaviour of skin are considered in Chapter III, including
a semi-empirical network concept and the general theory of
continuum mechanics applied to biological tissue.

Chapter IV contains a detailed description of
the development of testing methods up to and including the
highly refined uniaxial, constant strain rate technique
which was eventually used. Stress relaxation and creep
tests are also described. The results obtained are
analysed in Chapter V.

Various attempts to develop *in vivo* testing
techniques are described in Chapter VI and possible clinical
applications of the work covered in this thesis are discussed
in Chapter VII.

There is an extensive bibliography and various appendices, presenting the details of experimental and analytical techniques which were not fully discussed in the main text.

No separate list of the mathematical notation employed is given as each symbol is explained as it arises.

I.1   <u>Anatomy of Human Skin</u>

The skin is the largest organ of the human body and is responsible for several very important functions.-

(i)   containment of body fluids and tissues
(ii)   protection from physical and biological environment
(iii)   control of body temperature
(iv)   control of blood pressure
(v)   sensation of touch, pain and temperature.

Skin is a stratified tissue consisting of two distinct layers, the epidermis and the dermis, as shown in Fig I.1.

The epidermis is the body's shield against its environment and also restricts the loss of body fluids by evaporation. The epidermis itself consists of several layers as shown in Fig I.2. As a result of cell division occurring mainly in the basal layer, epidermal cells are constantly moving away from the dermis towards the skin surface. The layered appearance results from changes in the shape and character of the cells during this process. The stratum malpighii consists of living epithelial cells of cuboidal form. This layer merges gradually into the stratum granulosum in which the cells become squamous in form and granules of the horny protein keratin appear within them. The stratum corneum consists of dead, horny, fully keratinised cells which resemble scales. This layer is much thicker over the palms and soles where the skin is subjected to considerable pressure. Also in these regions a thin fourth layer, the stratum lucidum, consisting of hyalin, is found between the stratum granulosum and the stratum corneum.

Fig I.3   The Dermis Showing the Papillary and
           Reticular Layers (Stain: Haemotoxylin
           and Eosin).
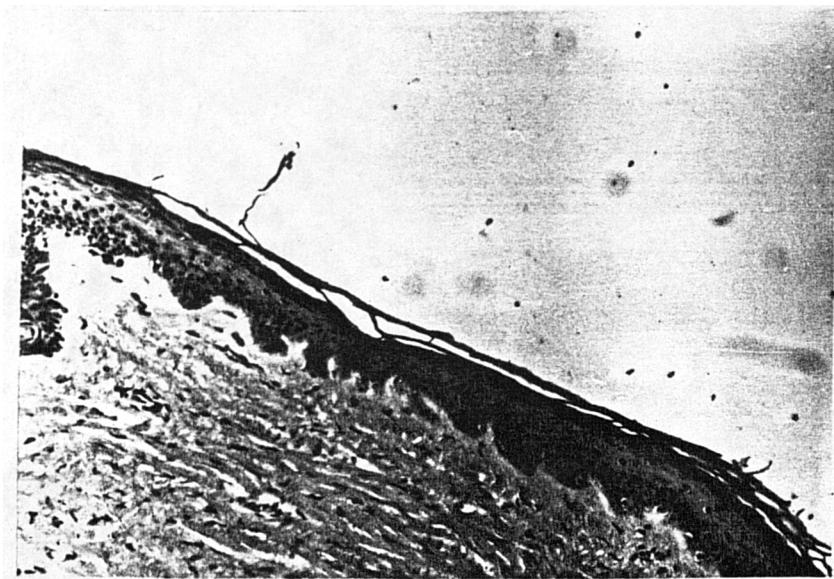
Fig I.4   The Dermis-Epidermis Junction (Stain:
           Haemotoxylin and Eosin).

Chapter I

Review of Literature
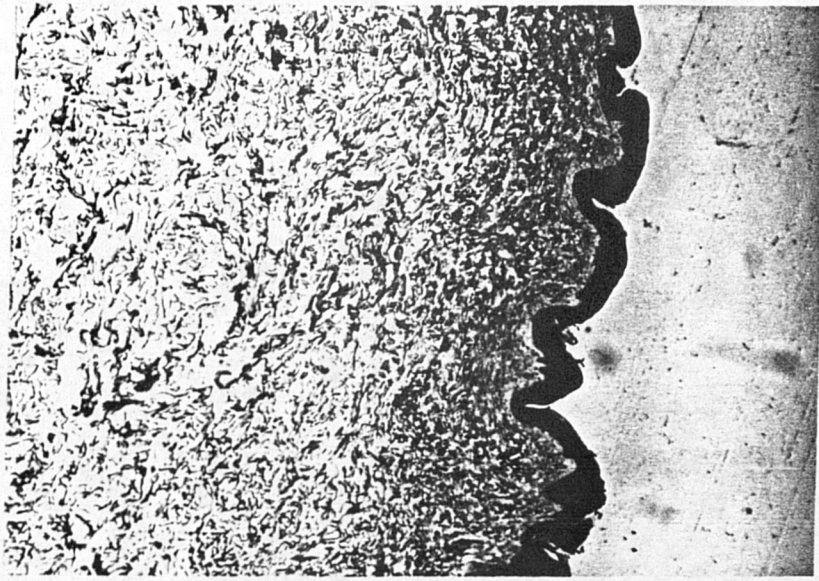
Fig I.1   Transverse Section of Skin Showing the
           Dermis and Epidermis (Stain: Haemotoxylin
           and Eosin).
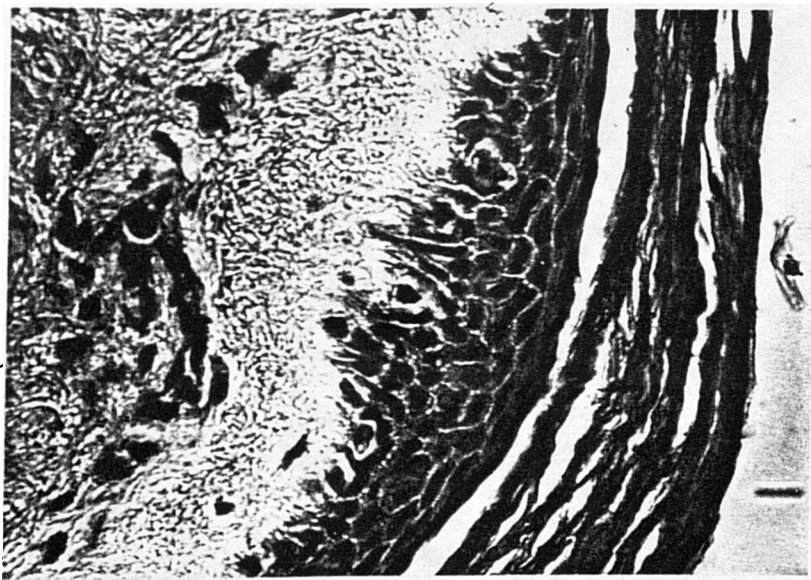
granulosum

Fig I.2   The Epidermis, Showing its Layered Structure
           (Stain: Haemotoxylin and Eosin).

The dermis consists of a microscopic meshwork of the fibrous proteins collagen and elastin, permeated by an amorphous ground substance (Fig I.3).

The papillary layer of the dermis consists of interwoven meshes of delicate collagen, elastin and reticulin fibres and a dense capillary bed. This layer nourishes and supports the epidermis.

The reticular layer consists of coarse collagen fibre bundles arranged in an apparently randomly oriented network.

The junction between the basal layer of the epidermis and the papillary layer of the dermis is corrugated, as shown in cross-section in Fig I.4, so that there is a mechanical keying effect. The cells of the basal layer also send very delicate processes into the dermis.

Beneath the skin proper there is a layer consisting of globules of fat supported by a fine connective tissue framework. This framework is continuous with the dermis and with the connective tissue sheaths of the superficial skeletal muscles.

The blood circulation system of the skin is very complex and allows both the total blood volume and the blood flow rate in the skin to be varied within wide limits. The skin is thus able to play a major rôle in the control of blood pressure and body temperature.

Various discrete structures found in the skin are shown in Fig I.5.

The most important of these are the sweat glands which play a major part in the control of body temperature.
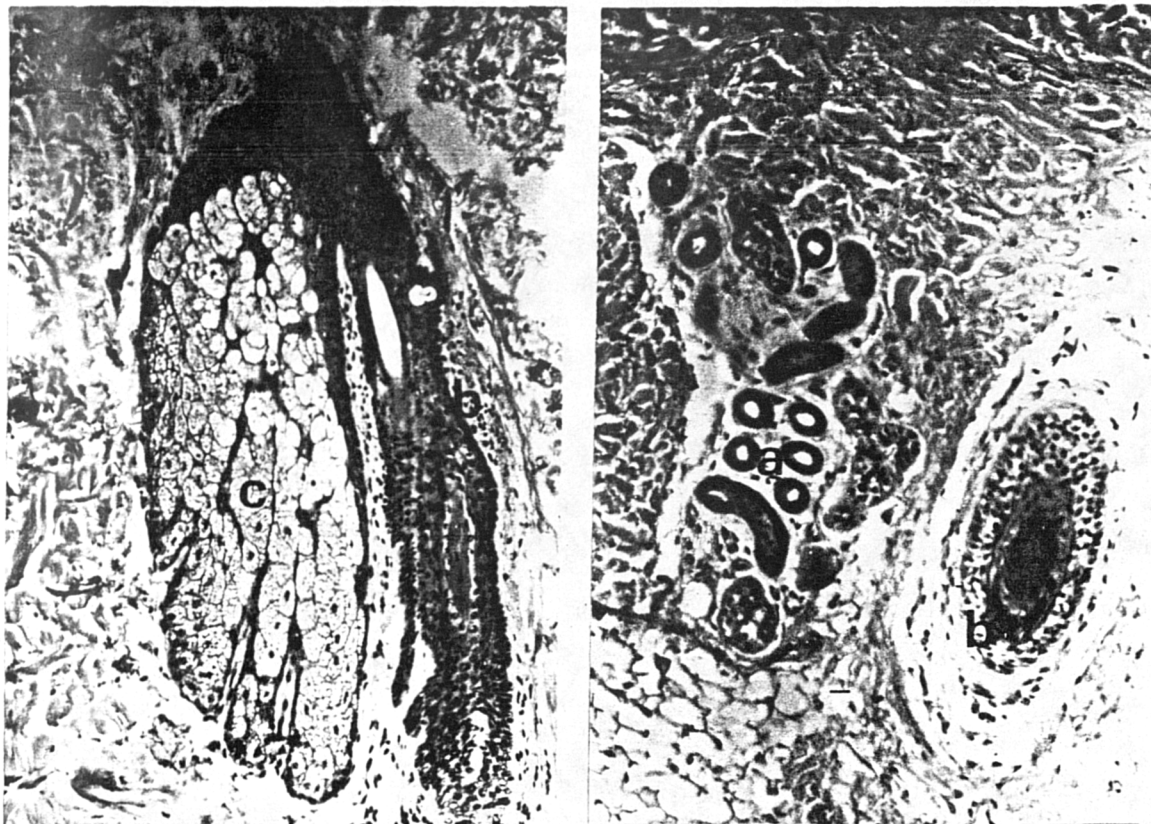
Fig I.5   Cutaneous Appendages (Stain: Haemotoxylin
           and Eosin).
           (a)   eccrine sweat gland
           (b)   hair follicle
           (c)   sebaceous gland.

Sebaceous glands produce a waxy secretion which spreads over the skin surface and helps to preserve the skin "condition".

Typical Composition by Weight of Skin

Water	62-70%
Elastin	0.7-1.4%
Reticulin	0-12%
Collagen	29-37%

I.2 **Mechanical Characteristics of the Fibrous Proteins and Ground Substance of the Dermis**

In considering the mechanical properties of the dermis it is pertinent to consider first the nature and mechanical properties of its constituent parts. These are:-

(i)   The collagen network
(ii) The elastin network
(iii) The reticulin network
(iv) The ground substance

I.2.1 **Collagen structure**

This fibrous protein is the major constituent of skin, representing about 72% by weight of dry, fat-free human skin (Rothman 1954).

Proteins are a group of organic substances of very high molecular weight constructed from a small number (about 20) of relatively simple amino acid "building blocks".

FIG I.6 - GENERAL MOLECULAR STRUCTION OF AMINO ACID. THE GROUP R DETERMINES THE SPECIFIC ACID.

AMINO ACID.

AMINO ACID.

DIPEPTIDE.   WATER.

FIG. I.7. CONDENSATION OF TWO AMINO ACIDS PRODUCES DIPEPTIDE. THIS PROCESS CAN BE REPEATED MANY TIMES TO FORM POLYPEPTIDE.

Amino acids have the general molecular form shown in Fig.I.6
and are able to condense together as shown in Fig I.7 to form
long chain molecules called polypeptides.   These large
molecules can then combine in even more complex configurations
to form proteins, the particular protein formed depending on
the amino acid composition of the polypeptide chains.

     Various analyses of the amino acid composition of
collagen (Lowther 1963; Ramachandran 1963; Wood 1964) show that
it contains approximately 30% by weight of glycine, the
simplest of the amino acids.   The presence of large quantities
of this small molecule allows the polypeptide chains to
approximate closely to one another, thus forming a structure of
high mechanical strength.   Collagen also contains about 14%
by weight of hydroxyproline.   This amino acid is not found in
significant amounts in other proteins and can thus be used in
the assay of collagen (Neuman and Logan 1950: Stegemann 1958).

     The currently accepted model of the collagen
molecule (Rich and Crick 1961; Ramachandran 1963) consists of
three polypeptide chains connected together by hydrogen bonds
between carbonyl and imino groups.   The molecule is of the
complex "coiled coil"   form shown in Fig I.8 and is a rigid
rod-like particle about 2800 $\overset{\circ}{A}$ in length and 10-15 $\overset{\circ}{A}$ in
diameter (1 $\overset{\circ}{A}$ = 10^{-8} cm.).

     In naturally occurring collagen fibrils these
molecules are joined together as shown in Fig I.9.   In human
skin collagen the fibrils have a mean diameter of 1000 $\overset{\circ}{A}$
(Gross and Schmitt 1948).

     Further aggregation of fibrils results in the
collagen fibres which are visible under the light microscope.
In the human dermis these fibres vary in width from 2 to 40
microns.

(a) SINGLE CHAIN POLYPEPTIDE LEFT HAND HELIX.

200A

(b) SINGLE CHAIN L.H. HELIX IS ITSELF COILED
INTO A RIGHT HAND HELIX.

(c) THREE CHAIN "COILED COIL" STRUCTURE OF
COLLAGEN MOLECULE.

FIG.I.8.-FORMATION OF COLLAGEN MOLECULE FROM
THREE POLYPEPTIDE CHAINS.

2800A°   700A
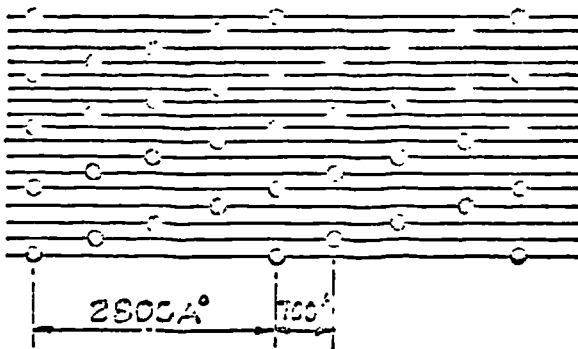
COLLAGEN FIBRIL
MAGNIFICATION:120,000
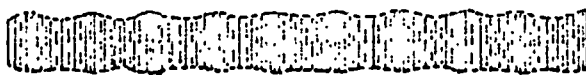
FIG.I.9.-COLLAGEN MOLECULES JOIN UP IN PARALLEL
ARRAYS STAGGERED BY ONE QUARTER OF THEIR LENGTH.
THIS RESULTS IN THE CHARACTERISTIC 700A° STRIATIONS
FOUND WHEN COLLAGEN FIBRILS ARE VIEWED
UNDER THE ELECTRON MICROSCOPE.

Much work remains to be done on collagen to
describe the methods by which collagen molecules join to form
fibrils and by which fibrils join to form fibres.

I.2.2   The mechanical properties of collagen
        Investigations of the mechanical properties of
collagen have been conducted on collagen fibres by Hall
(1951 a), (1951 b), (1952), Mitton and Morgan (1960), Morgan
and Mitton (1960) and Morgan (1960 b).   Various forms of
connective tissue which consist predominantly of collagen
fibres arranged in parallel bundles have also been studied.
These were rat tail tendon (Partington and Wood 1963),
human fascia lata (Gratz 1931), canine tendon (Laban 1962)
and human plantaris tendon (Walker, Harris and Benedict
1964).

(Note: In this and subsequent sections of this chapter, it
will be seen that those papers referring to simpler forms of
the tissue concerned are reviewed first.   For example the
work on collagen fibres and the very fine rat tail tendons
is discussed before the work on the more complex fascia
lata and canine and human tendons.   When papers refer to
similar work they are reviewed in chronological order).

        Hall (1951 a) investigated the creep behaviour
(i.e. the time variation of strain at constant stress) of
collagen fibres obtained from ox hide.   The fibres were
cemented to fine glass loops with 1 cm. of fibre between the
loops.   The testing apparatus consisted of a balance beam
with a chain loading system.   The fibre extension was
measured by an optical lever system.   This measurement included
any extension of the glass loops but no attempt was made to

Extension

4

3 β 𝑓𝑓𝑓

2

1

Test No.

Test conditions:-
20°C 7.0pH in water
Fibre load 25 g. for 200 mins.
Unloaded rest time between tests 21 hrs.

50	100	150	200

Time - minutes
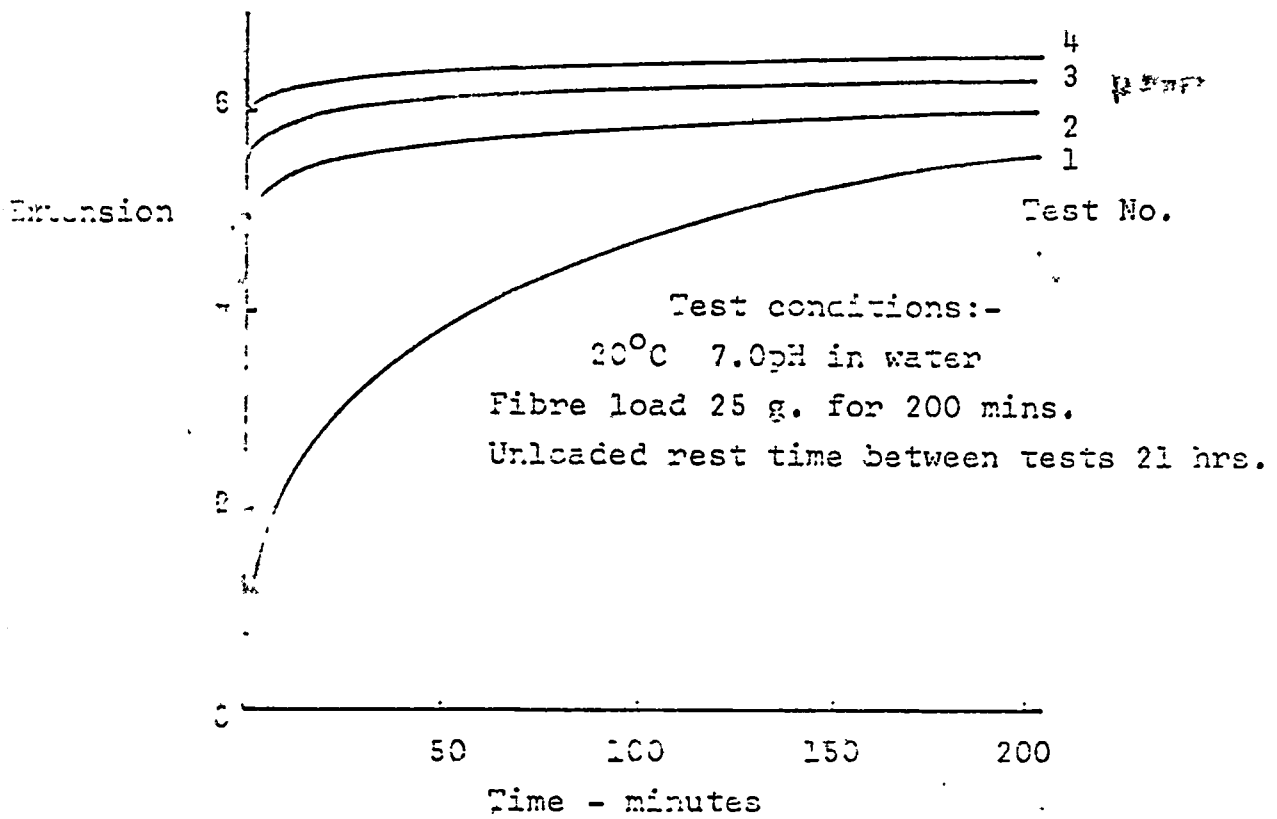
Fig I.10   Repeated creep tests on single
            collagen fibre (Hall 1951 a)

C

B

Extension

recoverable
extension

Permanent
set

Total
extension

A

Time
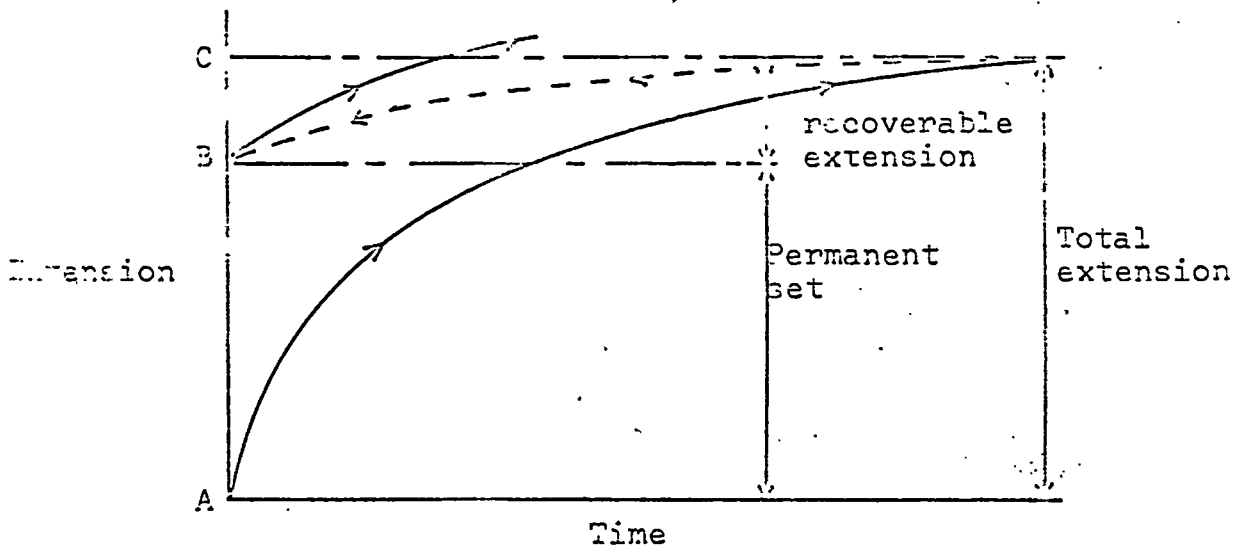
Fig I.11   Permanent and recoverable parts of
            collagen fibre extension (Hall 1951 a)

ascertain the magnitude of this error. The fibres were tested in water at pH7.0 and 20°C ±0.1°C.

Fig I.10 shows the result of a series of consecutive tests on a single fibre.

Fig I.11 shows how Hall split the fibre extensions into two parts:-

(i) A plastic extension resulting in permanent set (AB in fig)

(ii) A recoverable, viscoelastic extension (BC in fig).

Hall suggested that the plastic extension signified the breakdown and reforming at different sites of hydrogen bonds and that the viscoelastic effects were attributable to the fibre ground substance.

Using the same apparatus, Hall (1951 b) investigated the variation with pH of the load-extension properties of collagen. The chain loading system was motor driven to give a loading rate of approximately 4 gm./min.

It was found that fibres were not significantly affected by variations of pH between 4.5 and 10.0.

A typical load-extension curve of a fibre tested at pH7.0 is shown in Fig I.12. Hall noticed that this curve approached an asymptote (AB in fig). By measuring the slope of this asymptote he obtained values of Young's Modulus between 71 and 210 kg./mm². Although the number of fibres considered was small, there appeared to be a relation between the fibre cross-sectional area and this "modulus", small cross-sectional areas giving high values of modulus. No explanation of this phenomenon was offered.
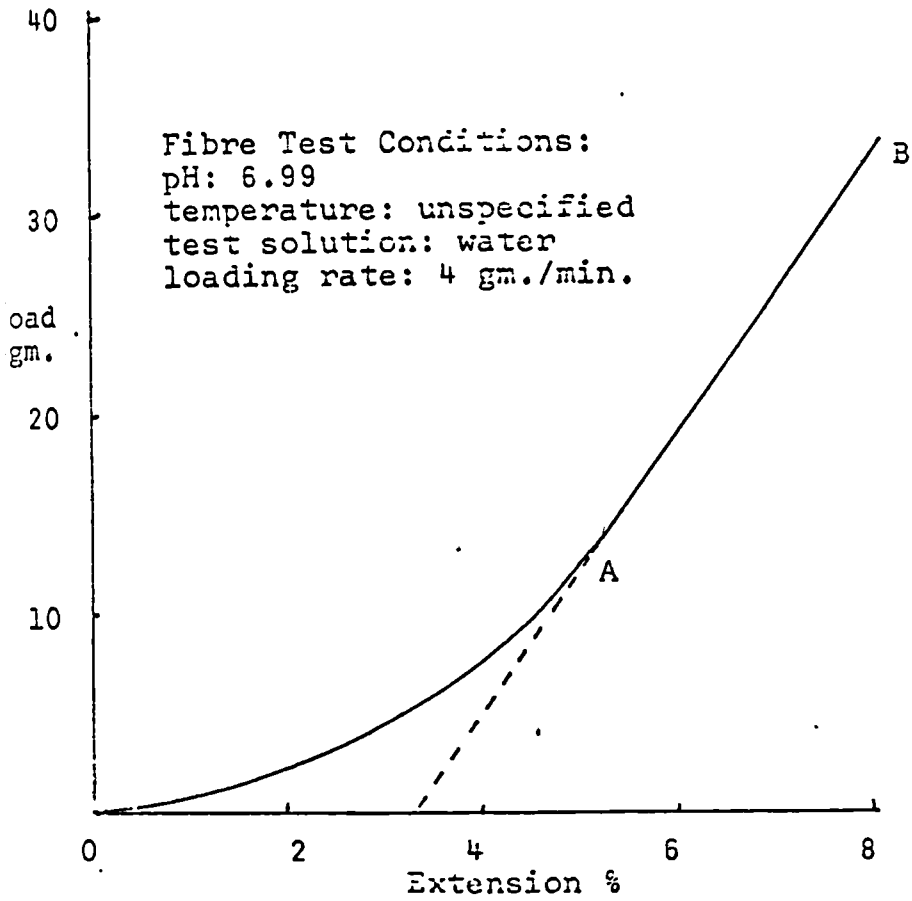
Fig I.12. Load-Extension Curve for Single Collagen Fibre
(Hall 1951 b)

1.5

$\Delta E = \int_0^{\ell} (\frac{\partial E}{\partial \ell}) d\ell$: Internal energy change

$\Delta \Phi = \int_0^{\ell} (\frac{\partial Q}{\partial \ell}) d\ell$: Entropy change

1.0

0.5

0.5

0

2   4   6   8   10
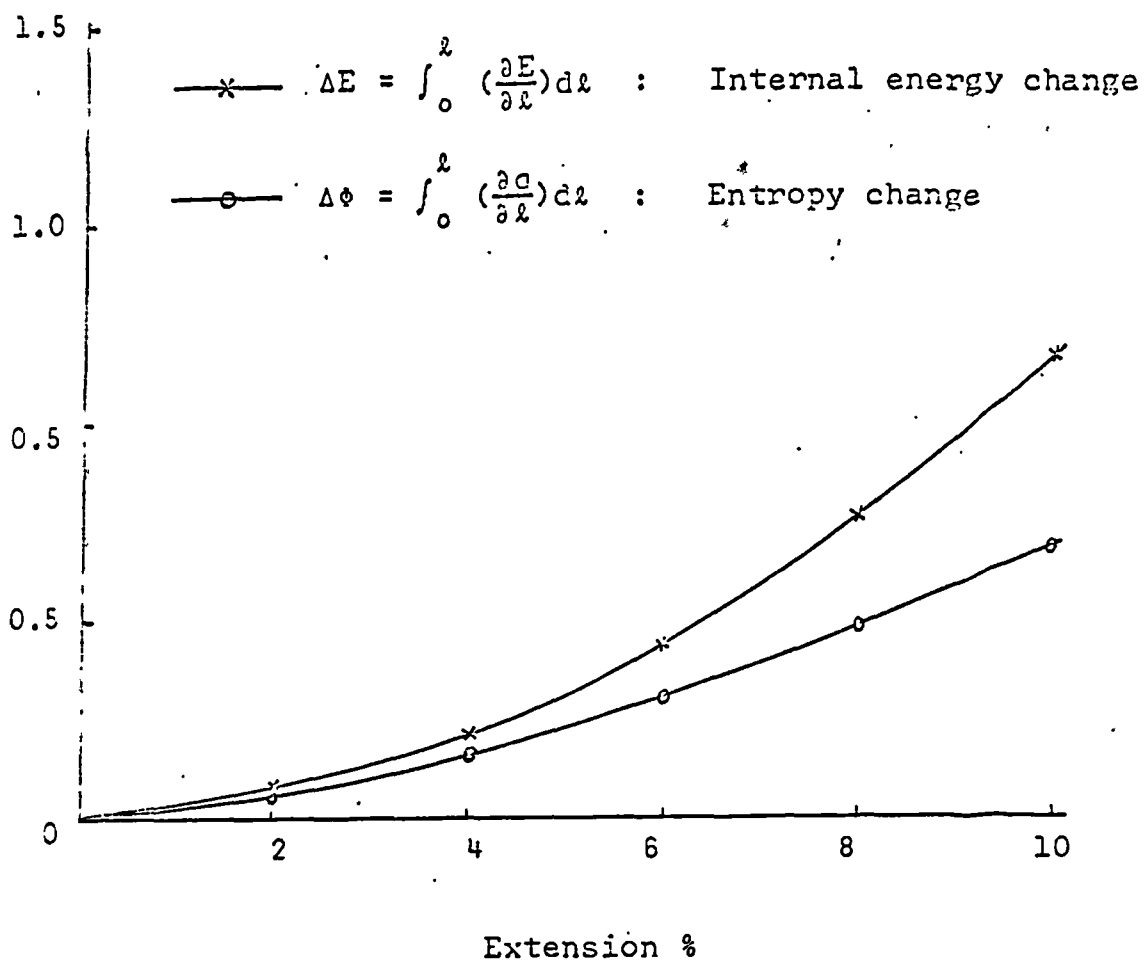
Extension %

Fig I.13   Change in internal energy and entropy of
a single collagen fibre v. extension

at 7.0pH, both internal energy and entropy increase with
extension.   This behaviour is not consistent with elastomer
theory.   Hall suggested that collagen had a structure
similar to that of extended rubber but he did not suggest
any theoretical explanation of the behaviour of this type
of structure.

Morgan (1960 b); Mitton and Morgan (1960) and
Morgan and Mitton (1960) described an intensive study of the
stress-strain curves of several hundred collagen fibres
obtained from ox hide.

Morgan (1960 a) described the apparatus used
for these tests.   This was basically similar to that used
by Hall but was able to test eight fibres simultaneously.
The fibres were tested in air of known temperature and
relative humidity.

Because of the irregular cross-sections of the
fibres, their tensile strengths were expressed in terms of a
parameter, called the breaking length, given by

$$\frac{\text{breaking load on fibre}}{\text{weight per unit length of fibre}} \text{ kilometres}$$

Multiplying this quantity by the density of the
fibre gives the tensile strength of an equivalent uniform
fibre.   The values of tensile strength quoted below were
obtained using a value of 1.39 gm./c.c. for the density of
raw hide (Kanagy and Wallace 1943).

The tensile strength of the fibres varied from
37 kg./mm.^{2} for thin fibres to 14 kg./mm.^{2} for thick fibres.
It was also found that short fibres were generally stronger
than long fibres.   The authors attributed both of these
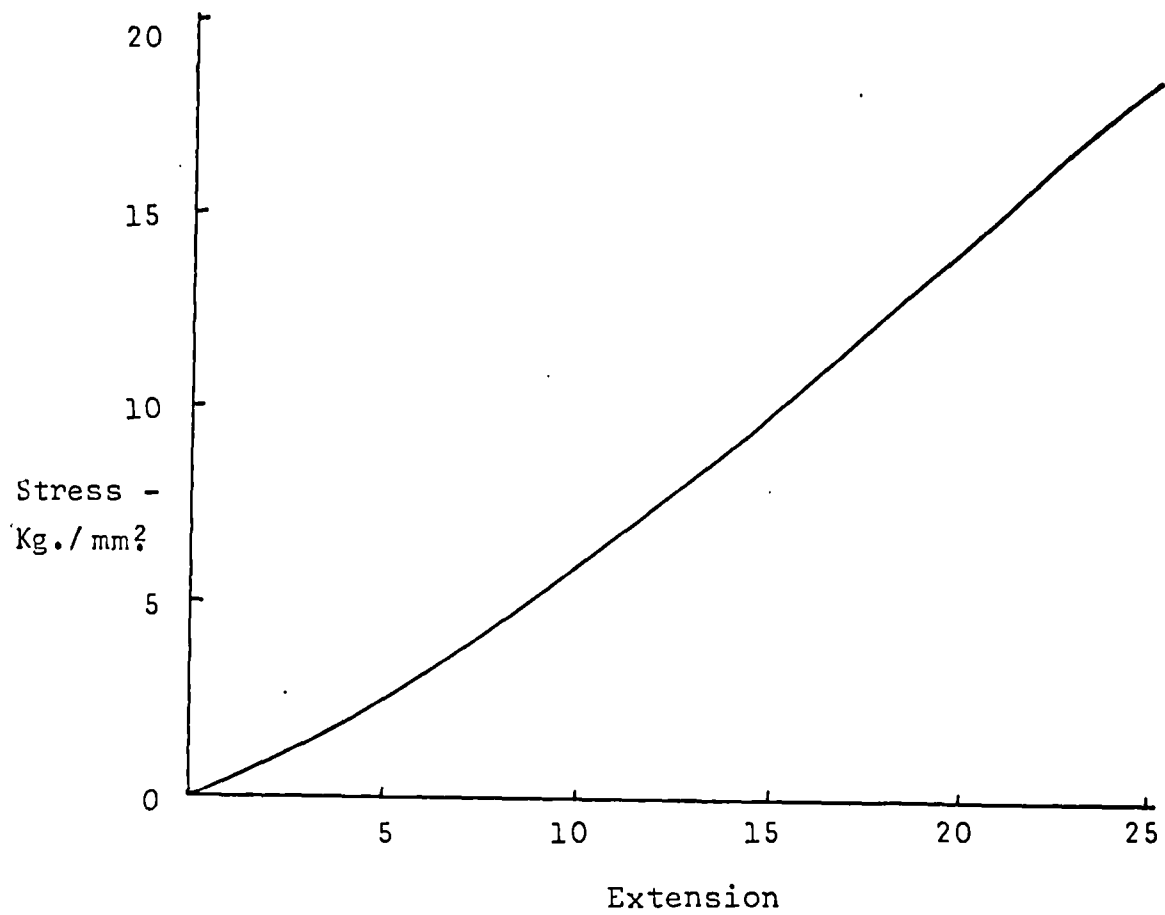
Fig I.14   Stress-extension curve for single collagen
fibres - average result from 395 fibres
(Morgan 1960 b)

effects to the variation in fibre cross-section along its length. This implies that thick fibres have a greater relative variation in cross section than thin fibres.

Various mechanical preconditioning techniques had no significant effect on the ultimate strength of the fibres. Changes in relative humidity had an appreciable effect, the maximum fibre strength occurring at 35% R.H. Taking this maximum as 100, the strength at saturation (100% R.H.) was 78 and at dryness (0% R.H.) it was 92.

The rate of loading had a pronounced effect on the tensile strength, maximum values being recorded at a loading rate of 12 g./min. when the fibres were tested at 0, 33 and 66% R.H. At 100% R.H. no maximum was found below 24 g./min. the highest loading rate used.

The stress-strain curves found during this test programme were analysed by Morgan (1960 b). The average curve found from 395 fibres is shown in Fig I.14. This could be adequately expressed by a power law expression of the form

$$\sigma = 0.386 \ E^{1 \cdot 23}$$

where E' = strain and σ = fibre stress - Kg./sq.mm.

The weight per unit length has a marked effect on the load-extension curve, thin fibres (i.e. fibres with low weights per unit length) being more extensible under the same load than thick fibres. Morgan failed to show that if, by taking account of the effective fibre cross-sectional area, the results are plotted on a stress-strain basis, then thin fibres are less extensible at the same stress than thick fibres. This again suggests that thick fibres have a greater relative variation in cross-section than thin fibres.

0.3

0.2

Stress -
Kg./sq.
mm.   0.1

Fibre cross-section
area = 0.085 sq. mm.

0

0.005   0.01   0.015   0.02
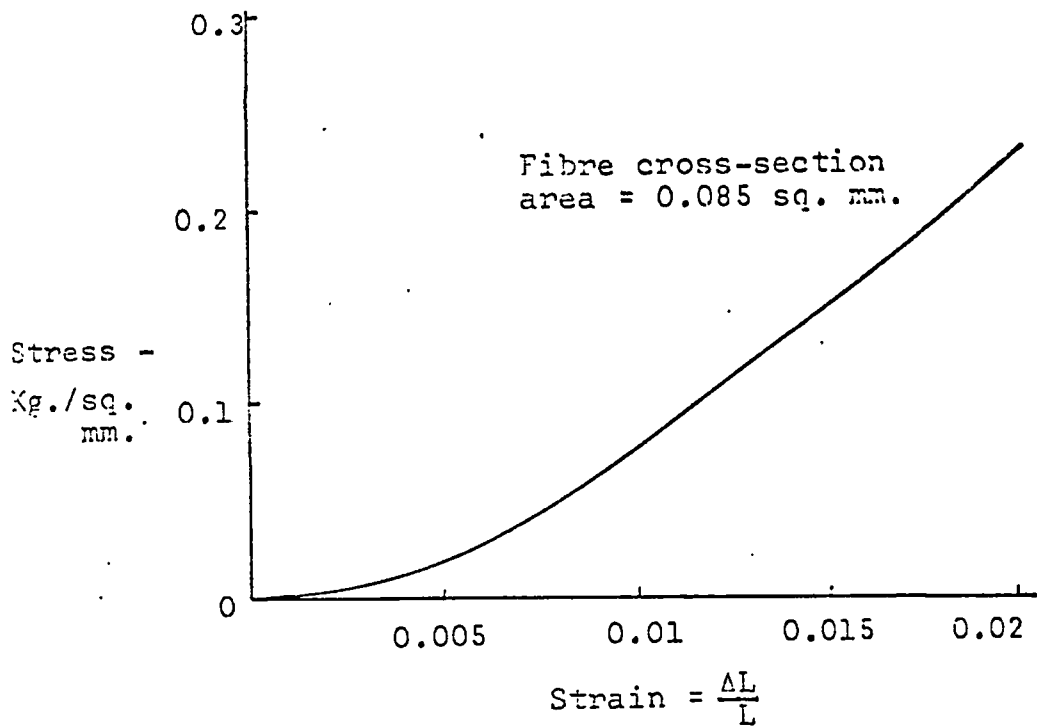
Strain = $\frac{\Delta L}{L}$

Fig I.15   Stress-strain curve for rat tail tendon
            (Partington and Wood 1963)

30

20

Load -
(Units not
given)   10

1
2
3
4
Test No.

0

0.005   0.01   0.015   0.02

Strain = $\frac{}{L}$
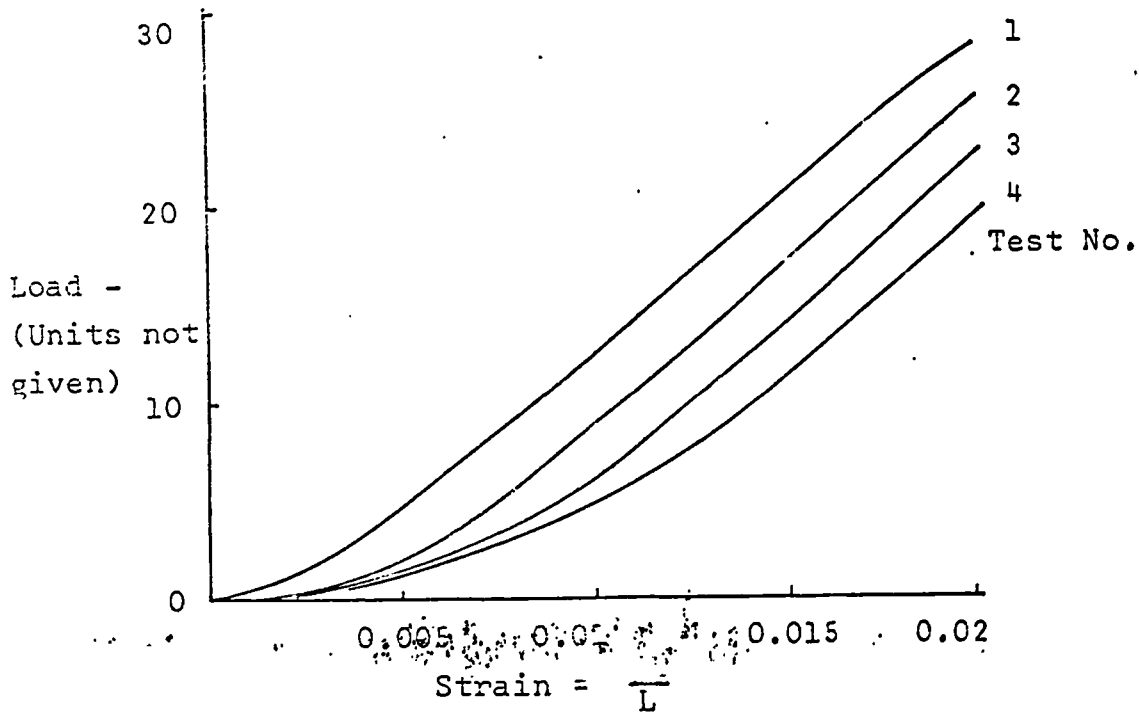
Fig I.16   Repeated load-extension tests on rat tail
            tendon (Partington and Wood 1963)

The effect of increasing humidity was to increase fibre extensibility. The rate of loading had little effect on the shape of the load-extension curve.

Although Morgan was able to obtain a satisfactory fit to his results with a power law expression, he pointed out that this was a purely empirical approach giving no information as to the physical interpretation of collagen deformation. He therefore compared his results with various other theoretical approaches but was unable to obtain any agreement.

Partington and Wood (1963) investigated the effect of various enzyme treatments on the mechanical properties of rat tail tendon. These tendons are about 5 cm. long and about 0.3 mm. in diameter. They consist of parallel bundles of collagen fibres oriented along the axis of the specimen.

Load extension curves were obtained using a simple apparatus which extended the specimens at a constant strain rate of 1%/min. During test, the tendons were immersed in a constant temperature bath of physiological fluid at $25^{\circ}C$.

A typical stress-strain curve obtained from an untreated tendon is shown in Fig I.15. The extension was restricted to 2% as it was found that permanent deformation occurred at extensions greater than about 3%.

Repeated load-extension tests gave the result shown in Fig I.16. Although there was a pronounced increase in extensibility between successive tests, the slope of the final straight line part of each curve was found to be the same. The authors were therefore able to test specimens before and after a particular enzyme treatment and then to assume that any variation in this final slope was due to the treatment. A set of untreated control specimens was tested
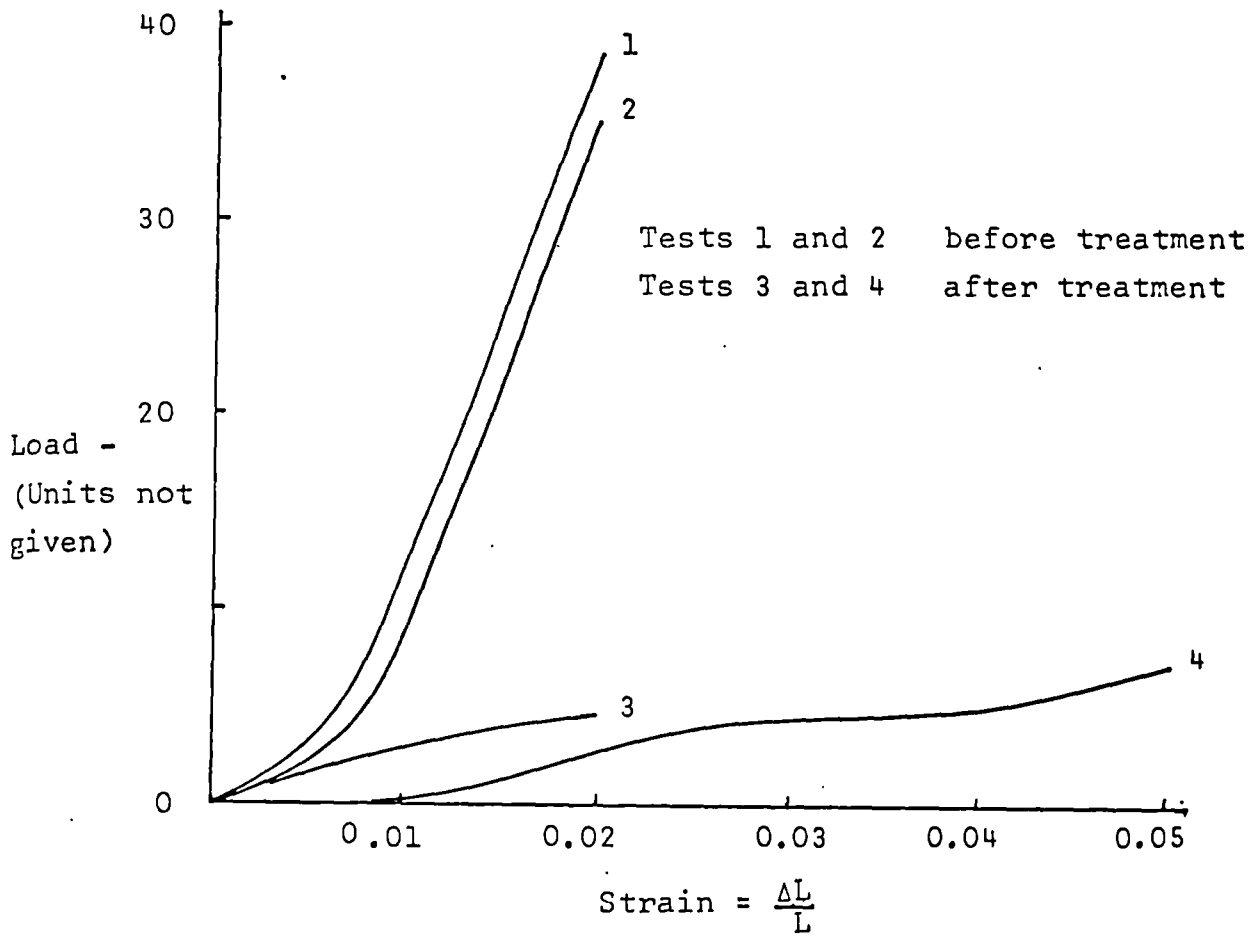
Fig I.17   Effect on load-extension curve of treating
           tendons with hyaluronidase (Partington and
           Wood 1963)

as a check.

A group of tendons which were treated with the enzyme hyaluronidase A gave the result shown in Fig I.17. As the effect of this enzyme is to break up the long chain molecules of the ground substance in which the collagen fibres in the tendon are embedded, the importance of this substance in providing the bond between collagen fibres is clearly shown.

Gratz (1931) investigated the mechanical properties of human fascia lata. This is the tough, fibrous sheath around muscles. It consists of a sheet of thick parallel collagen bundles oriented along the direction in which the fascia is normally subject to tension. The material is thus very strong in this direction but is very weak in the transverse direction.

A strip of fascia was tested in an unspecified standard engineering tensile test machine. The test was presumably carried out in air, no precautions being taken to control temperature or humidity. Also, no allowance was made for the viscoelastic nature of the material. In view of these omissions, the results obtained are of doubtful value except that the shape of the stress-strain curve is of interest in connection with the network theory of skin elasticity which is developed in Chapter III. A typical stress-strain curve obtained by Gratz is shown in Fig I.18.

The investigations carried out by Laban (1962) into the mechanical properties of canine tendon were reported in a rather superficial manner and are of doubtful value because of the primitive test techniques employed. The specimens were tested in oxygenated Ringer's solution at 37°C and 7pH. The specimen was held between grips in a horizontal position and, as no attempt seemed to be made to support the weight of the grips, there must have been a
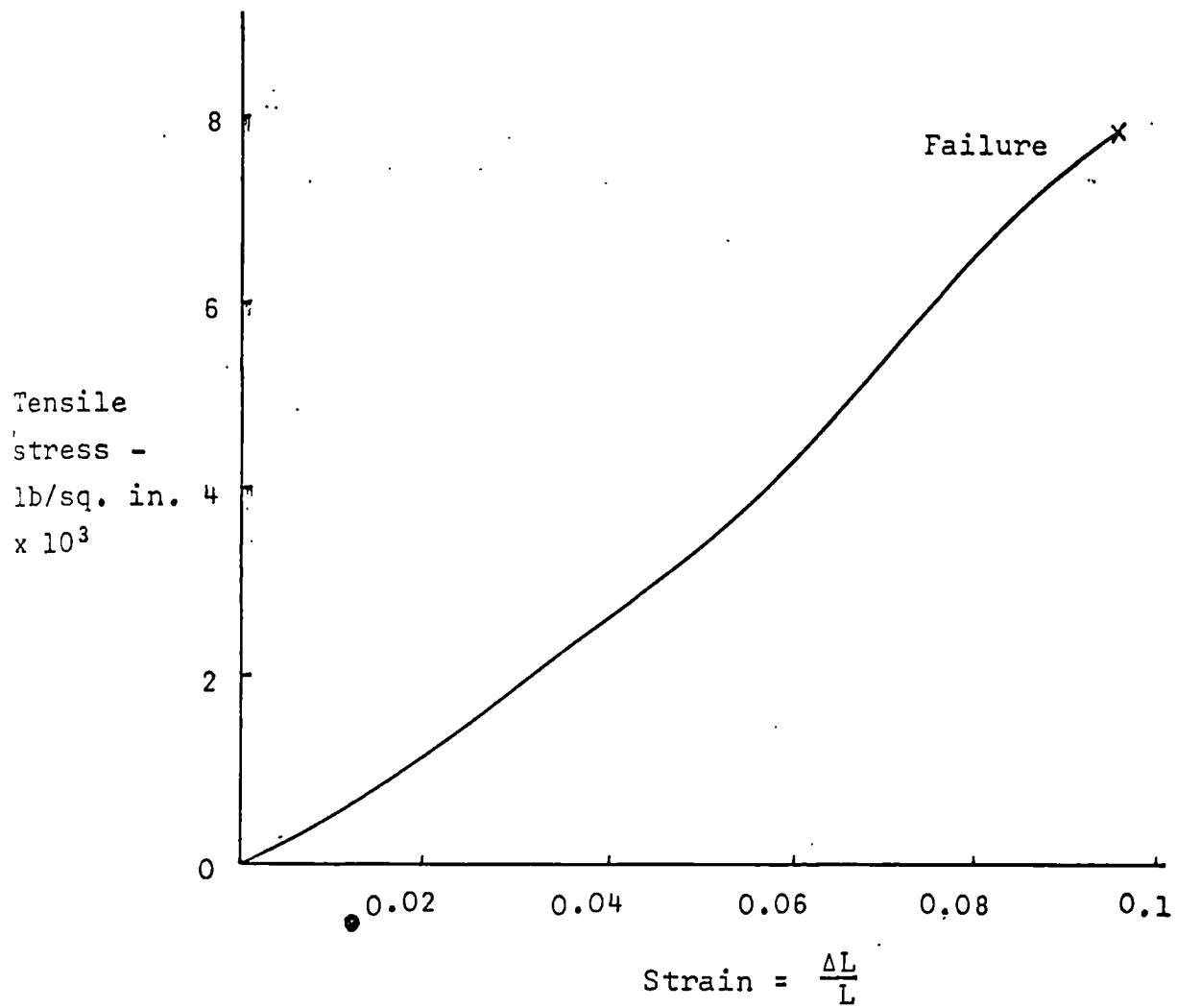
Fig I.18   Stress-strain curve for human fascia lata
(Gratz 1931)

considerable zero error in the measurement of extension.

The grips employed were of the self-tightening, wedge action type so that a certain amount of grip movement must have taken place during load application. This gave rise to further error in the extension measurement. No details were given of the time between the application of successive load increments. This was surprising as the author also carried out creep tests on the tendons and must have appreciated the importance of allowing for the visco-elastic nature of the material. For these reasons, the stress-strain results obtained by Laban are of little value.

Walker, Harris and Benedict (1964) have investigated the mechanical properties of specimens of human plantaris tendon obtained at autopsy.

The testing technique used was very crude and showed a distinct lack of appreciation of the complex mechanical properties of biological materials.

The specimens were tested in air with no control of temperature or humidity. The load was applied in discrete increments with strain being measured on a gauge length at each increment. No account was taken of the creep effects which must have occurred during this process. The initial measurement of gauge length was made with the specimen in the testing rig adjusted so that "impending tension prevailed". This suggests the possibility of a large zero error in strain measurement.

Not surprisingly, a very large scatter was found in the results. The only information of any significance that can be deduced from this work is that the tensile strength of human plantaris tendon varied from 10,600 lb/sq. in. to 21,300 lb/sq. in. These values agree well with the figures quoted by Cronkite (1936).

I.2.3   Elastin structure

Elastin, or yellow connective tissue, is the other major connective tissue component of the dermis, accounting for 2-4 per cent. of the fat-free dry weight of human skin (Montagna 1956, Rothman 1954).   The elastic fibres in the dermis form a complex mesh interwoven with the collagen network (Dick 1947).   They are more numerous in the papillary layer and may play some part in anchoring the epidermis to the dermis (Montagna 1956).   The fibres are thinner than those of collagen and are observed to run into one another, thus forming a continuous structure, whereas collagen fibres are separate entities.

The most striking difference between collagen and elastin is that elastin exhibits long-range elasticity with little viscoelastic side-effects, i.e. when the load is removed from a stretched elastin fibre it will snap back almost instantly to its original length.

Electron microscope and X-ray diffraction studies of unstretched elastin show that this protein has a highly disordered structure.   Elastin has a content similar to collagen of the amino acids, glycine and proline but the content of other amino acids is markedly different.   In particular, it has a negligible content of hydroxyproline and hydroxylysine which are thought to impart rigidity to the collagen molecule.   Collagen fibres, thermally shrunk or swollen in acid solution,exhibit an X-ray diffraction pattern similar to that of elastin (Ramachandran 1963). The same author has also observed traces of a collagen-like X-ray diffraction pattern from stretched elastin fibres. He points out, however, that this may be due to some traces of collagen remaining in the purified elastin used for the

experiment. Ramachandran and Santhanam (1957) have suggested
that the elastin molecule has a similar triple helical
structure to that of collagen, but that it is in the
thermally shrunk state at normal temperature. In this
condition, the long molecules are not rigid. Because of
thermal agitation they contort themselves into more probable
configurations than the fully extended state of the collagen
molecules. There must also be a small number of strong,
covalent cross-links between the molecules as elastin is
a very stable protein being insoluble except in very strong
reagents. It is thus thought that elastin behaves in a
similar manner to elastomers such as lightly vulcanised
rubber (Ayer 1964).

I.2.4   The mechanical properties of elastin

The mechanical properties of elastic tissue have
been investigated for samples of this tissue in the form of
single fibres (Carton, Dainauskas and Clark 1962), ligament
(Wood 1954) and blood vessels (Banga and Balo 1961; Bergel
1961). An explanation of these properties in terms of
elastomer theory has been put forward by King and Lawton
(1950; 1951; 1960).

Carton et al. (1962) tested elastin fibres
dissected from ligamentum nuchae taken from freshly
slaughtered beef cattle. A small fragment of ligament
was mounted between very small clamps and was then dissected
until only a single fibre was left connecting the two
bundles of fibres in the clamps. This system was mounted
vertically with the bottom clamp replaced by a hook weighing
1.5 mg. The weight of this hook was neglected in the load-
extension measurements which were carried out in Ringer-Locke
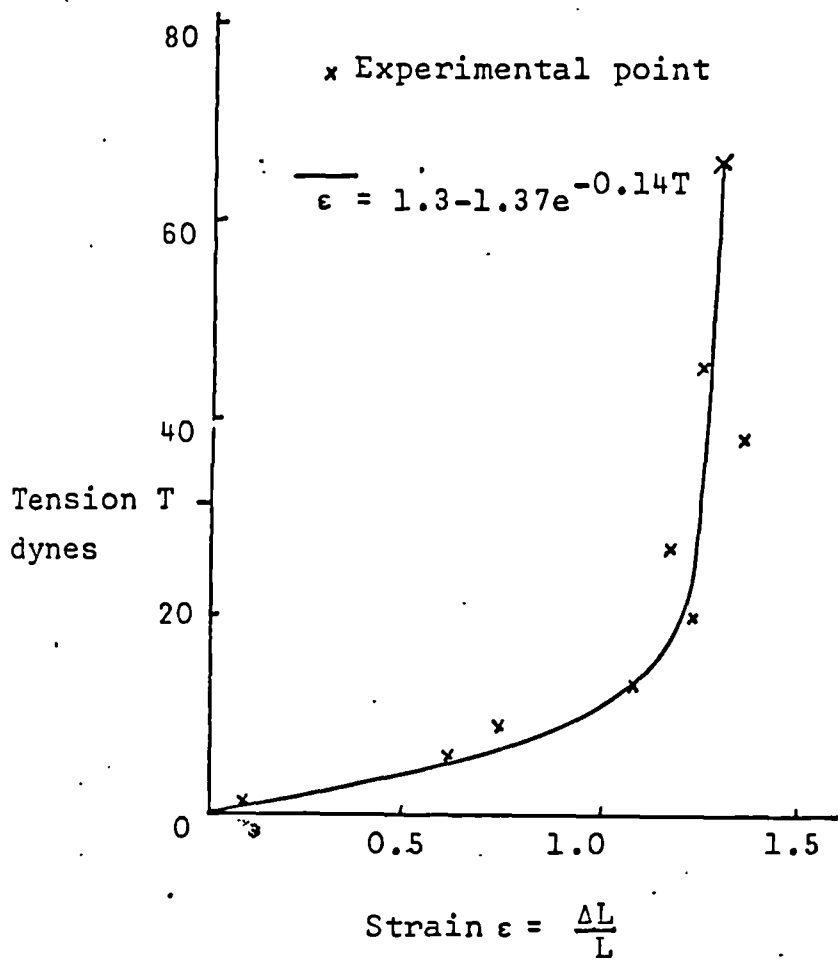
Fig I.19   Tension-strain curve for single elastin
fibre (Carton et al. 1962)

solution at a temperature of 37 ±0.5°C. A convenient gauge length between suitable landmarks on the fibre was measured with a micrometer microscope, the mean length taken being 350 microns. The fibre diameter was about 9 microns. Load extension curves were obtained by loading the hook with suitable weights and measuring the gauge length. No creep effects were noted over a period of 2 minutes.

Using an empirical expression of the form

$$e = 1.3 - A \exp^{-bT}$$

where   e = strain

           T = applied tension in dynes

    A, b = constants

the authors obtained a good fit to the experimental data. Fig I.19 shows a typical result. This shows that, although the weight of the hook (1.5 mg.) was neglected, it must in fact have made a considerable contribution to the initial extension of the fibre.

Tests were also carried out on small strips of ligament for comparison purposes. It was found that these strips were much more extensible than the fibres taken from the same ligament. The authors suggested that this was due to the branching network arrangement of the fibres in the ligament.

Wood (1954) also experimented with strips of ligamentum nuchae both in the native state and after various treatments. A typical result of a test on native ligament is shown in Fig I.20. The testing technique used was described by Wood and Chamberlain (1954). The specimens were tested at a constant,but unspecified, rate of extension. Testing was carried out in a constant temperature
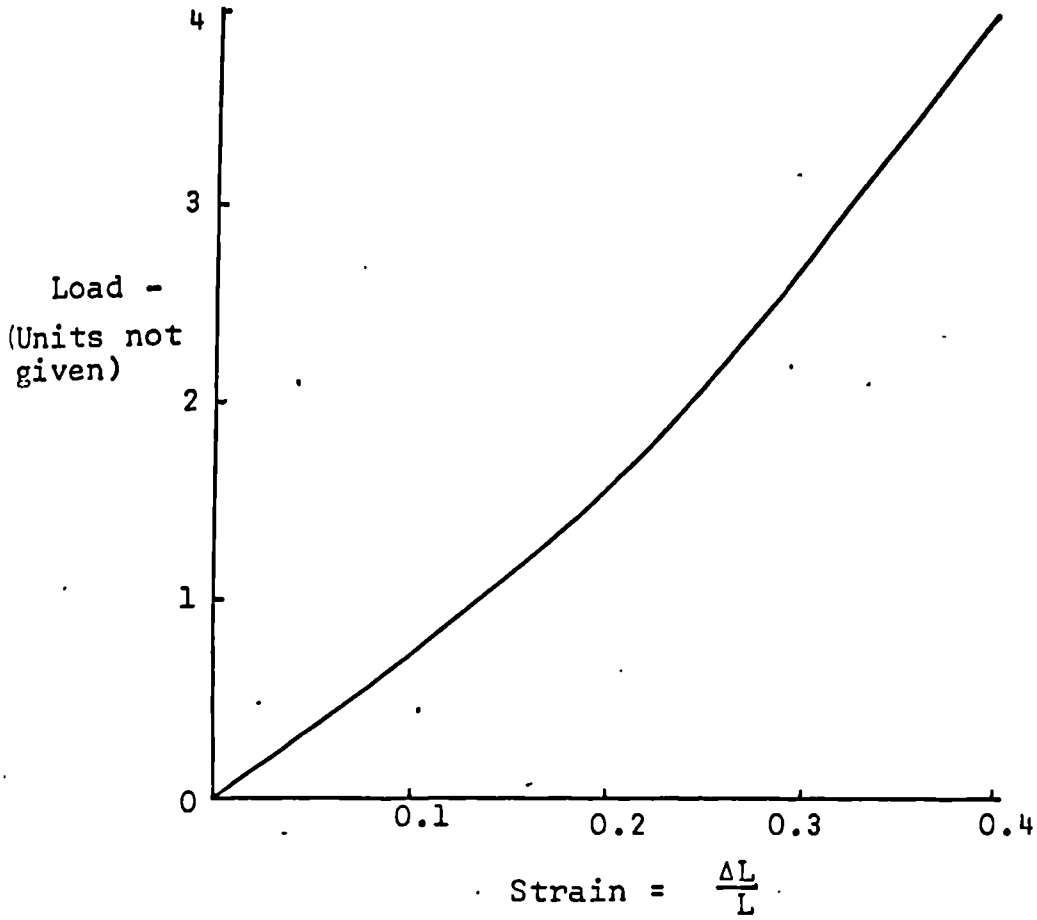
Fig I. 20   Load v. strain for a strip of bovine
ligamentum nuchae (Wood 1954)
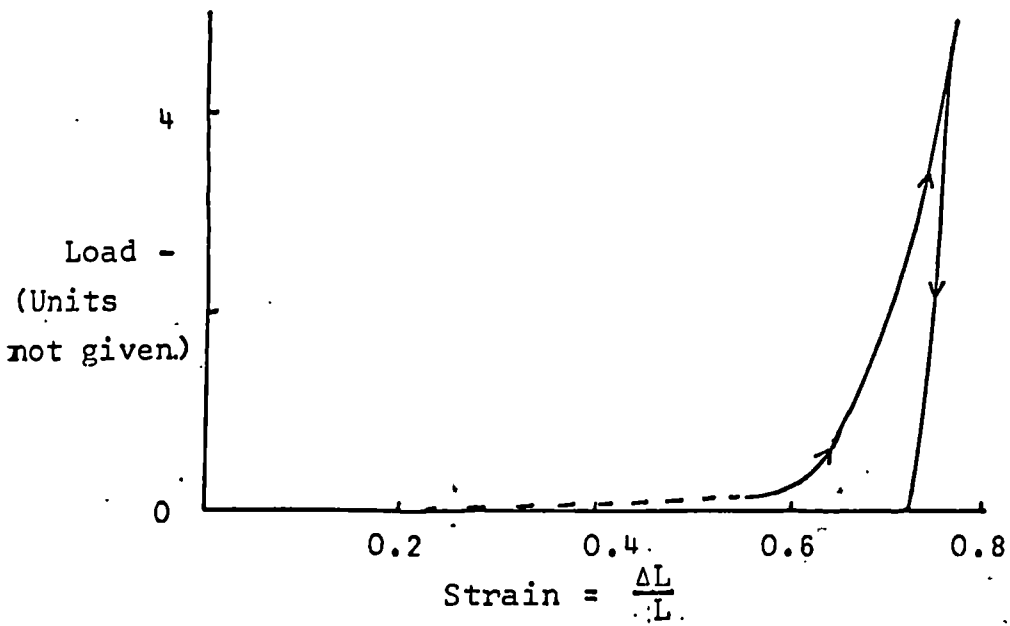
Fig I.21   Load v. strain curve after treatment
of ligament to destroy elastin
(Wood 1954)

water bath at 25.5°C.

As the load-extension curves for native tissue were found to be reasonably linear up to extensions of 20%, and as some of the treated specimens ruptured at about 30% extension, Wood restricted his observations to the range 0-20% extension.

Wood investigated the effect on the tensile test behaviour of ligament after treating the specimens so as to:-

(i)   Remove elastin
(ii)   Remove collagen
(iii)   Degrade the ground substance

After removal of elastin, the ligament showed plastic extension under very small load up to about 70% extension (Fig I.21).   This extension was not recoverable. Beyond this extension the material became much more rigid and behaved in a manner typical of collagen fibres.   Wood suggested that these phenomena are most likely due to the extension and orientation of a loose collagen meshwork.

Various treatments to remove collagen from the ligament resulted in widely differing results.   These effects were much greater than the collagen content of 17% dry weight and the negligible strength contribution of the collagen meshwork at 20% extension would have led one to expect.   Wood therefore concluded that these effects must be due to changes in the ground substance and/or elastin.

Treatment with the enzyme, hyaluronidase, to destroy the ground substance produced a marked weakening effect. It was therefore likely that those collagen-removing treatments which weakened the ligament did so by destroying the
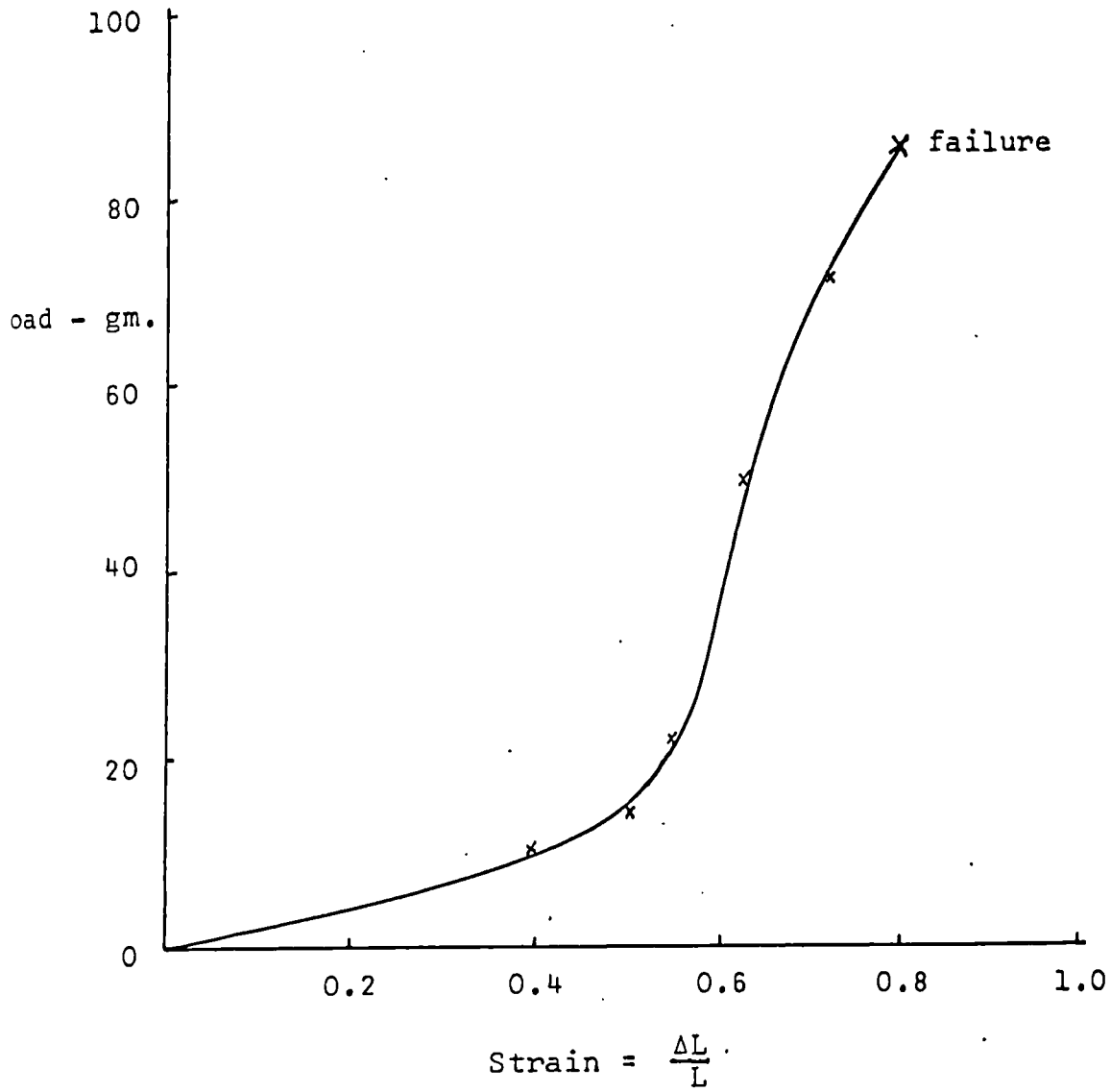
Fig I.22 Load v. strain for human carotid artery
(Banga and Balo 1961)

ground substance.   Wood suggested that those treatments
which strengthened the ligament did so by increasing the
number of cross-linkages between the elastin molecules in
the manner outlined by King and Lawton (1950).

The walls of arteries contain a large proportion
of elastin.   Banga and Baló (1961) investigated the
mechanical behaviour of strips of human carotid artery
taken at autopsy.   The age range covered was from 14 to 89
years.

Thin rings of artery were excised and cut to form
strips 1.2 to 1.7 centimetres in length.   The wet weight of
these specimens was from 5 to 43.5 mg.   The specimens were
tested in Ringer's solution at 22°C.   The equipment used
was a modified chemical balance.

Although the load-extension curves obtained (Fig
I.22) were markedly non-linear, the authors expressed their
results in terms of an elastin "modulus" given by

$$\frac{\text{load at 50\% extension}}{\text{area of cross-section of unstressed specimen}}$$

The cross-section area was computed from the wet weight,
assuming a specific gravity of 1.12.

It was found that this elastic modulus varied
with the wet weight.   No explanation for this variation
was offered but, to enable further comparisons to be made,
only those results obtained from specimens weighing between
22 and 30 mg. were considered.

The "elastic modulus" was found to increase with
age and with the degree of atherosclerosis (hardening of the
arteries) present.

Bergel (1961) investigated the pressure-radius
relations for lengths of excised arteries held at their
original *in situ* lengths.   The vessels used were the major

arteries of dogs. All tests were carried out at room temperature (18-22°C) in Ringer's solution. A 6 cm. length of artery was held vertically at its *in vivo* length between supports of a suitable diameter. Pressure was applied internally, in steps of 20 mm. Hg up to a maximum of 240 mm. Hg with a pause of 2 minutes at each step. The diameter of the specimen was measured at a point midway between the supports.

Bergel was aware that artery was a non-linear material, i.e. that the elastic modulus varies with stress. He therefore plotted his results in terms of an elastic modulus calculated for each loading increment.

It was found that this incremental modulus increased with internal pressure. The author suggested that this was due to the transfer of stress from the elastin and smooth muscle components of the artery wall which carry the initial stress to the collagen component which must be supporting the major part of the stress at the higher pressures. The values of incremental modulus obtained at high pressure were of the same order as elastic moduli found for collagen.

King and Lawton (1950; 1951; 1960) have in investigated the behaviour of elastic-rich tissues in terms of the elastomer theory developed by Wall (1942 a; 1942 b; 1943), James and Guth (1941; 1943; 1944; 1947) and Treloar (1943). The derivation of this theory is discussed in Chapter III and Appendix A.II. In particular, King and Lawton derived pressure-radius relations for a thin spherical elastomer shell and for a thin elastomer cylinder with various boundary conditions.

The thin shell theory was compared with pressure-volume relationships of cat bladder obtained by Simeone

and Lampson (1937). Good agreement was found up to an increase in diameter of over 200%.

The thin cylinder expression was compared with pressure-volume relations obtained by Hallock and Benson (1937) from isolated specimens of human aorta. Again, good agreement was obtained. A definite relation was found between age and one of the parameters in the equation. The interpretation of this in terms of the elastomer theory suggested that a greater number of cross-linkages between the long chain elastomer molecules in the artery wall appeared with advancing age.

This work suggests that the mechanical properties of elastin and of tissues rich in elastin can be adequately described by elastomer theory. However, when other tissue components, such as collagen, muscle and ground substance, are present in appreciable amounts, this theory is no longer applicable.

I.2.5   Reticulin

Reticulin is the least understood of the fibrous components of skin. Physically and chemically it is similar to collagen. The fibrils are thinner than those of collagen but show the same regular 700 Å striations under the electron microscope. In human skin, reticulin fibres are found chiefly in the papillary layer of the dermis and around hair follicles, sweat glands and blood vessels. The dermis of the human embryo contains only reticulin fibres and, during wound-healing, the fibres which are formed initially appear to be of reticulin. In both cases the reticulin is either transformed into or replaced by true collagen. For this reason, reticulin is believed to be a primitive form of collagen.

Nothing is known of the mechanical properties of
reticulin because of the difficulty of obtaining samples.
It is probably similar to collagen in this respect and, as
it makes up only 0.38% of the dry weight of skin (Montagna
1956) its contribution to the mechanical properties of skin
can reasonably be neglected.

I.2.6   Ground substance

In the dermis, the term 'ground substance' is used
to describe the amorphous, semi-fluid substance contained in
the spaces between the fibres and fibrils. It contains no
free fluid although it has a large water content. The major
constituents of the ground substance are a group of substances
known as mucopolysaccharides. These are long chain carbo-
hydrates. The most important mucopolysaccharides in the
dermis are hyaluronic acid and chondroitin sulphate B.
There is also a small content of substances called glyco-
proteins, these being proteins containing a small amount of
carbohydrate.

The large water content of the ground substance is
mainly in the form of water molecules bound to hyaluronic
acid. Montagna (1956) suggested that a very thin film of
water around the fibres and fibrils in connective tissue
could also account for a considerable volume of water in
view of the very large total surface area of the fibres.

In contrast to the comparatively inert collagen
and elastin, the ground substance plays a considerable part
in the metabolic activity of the skin (Muir 1964). It is
found to increase in quantity at sites of wound repair
(Delaunay and Bazin 1964). This suggests that the ground
substance is involved in the manufacture of collagen fibrils
and fibres from the collagen molecules which are formed by
cells in the dermis called fibroblasts.

Nothing is known about the physical properties of the ground substance except that it exists in the form of a viscous gel. As it consists of long chain molecules and is amorphous at the highest levels of magnification in electron microscopy, these molecules must be in a contorted state. They will thus form a highly viscoelastic liquid somewhat similar to unvulcanised rubber.

I.3 The Mechanical Behaviour of Skin

The mechanical properties of human skin have been studied by a number of workers in the last three decades.

It is convenient to divide this work into three sections based on the general type of testing method used.

(i)   Uniaxial tensile tests
(ii) Biaxial tensile or membrane tests *in vitro*
(iii) *In vivo* tests

I.3.1 Uniaxial tests *in vitro*

Investigations of the mechanical properties of skin which have utilised uniaxial tensile test techniques have been carried out by Rollhauser (1950), Jansen and Rottier (1957, 1958 a, 1958 b), Ridge (1964) and Ridge and Wright (1964 a, 1964 b, 1965). Tests have also been carried out on guinea pig skin (Beckwith, Brody, Glaser, Prevenslik and White (1963), Glaser, Marangoni, Must, Beckwith, Brody, Walker and White (1964).

Work carried out in this field in the Bioengineering Unit at Strathclyde University has been reported by Kenedi and Gibson (1962), Kenedi (1963, 1964), Kenedi, Gibson and Abrahams (1963), Gibson and Kenedi (1963 a, 1963 b), Kenedi, Gibson and Daly (1965 a, 1965 b, 1965 c), Evans (1965), Kenedi, Gibson and Craik (1965), Craik and McNeil (1965) and Kenedi, Gibson, Daly and Abrahams (1966).
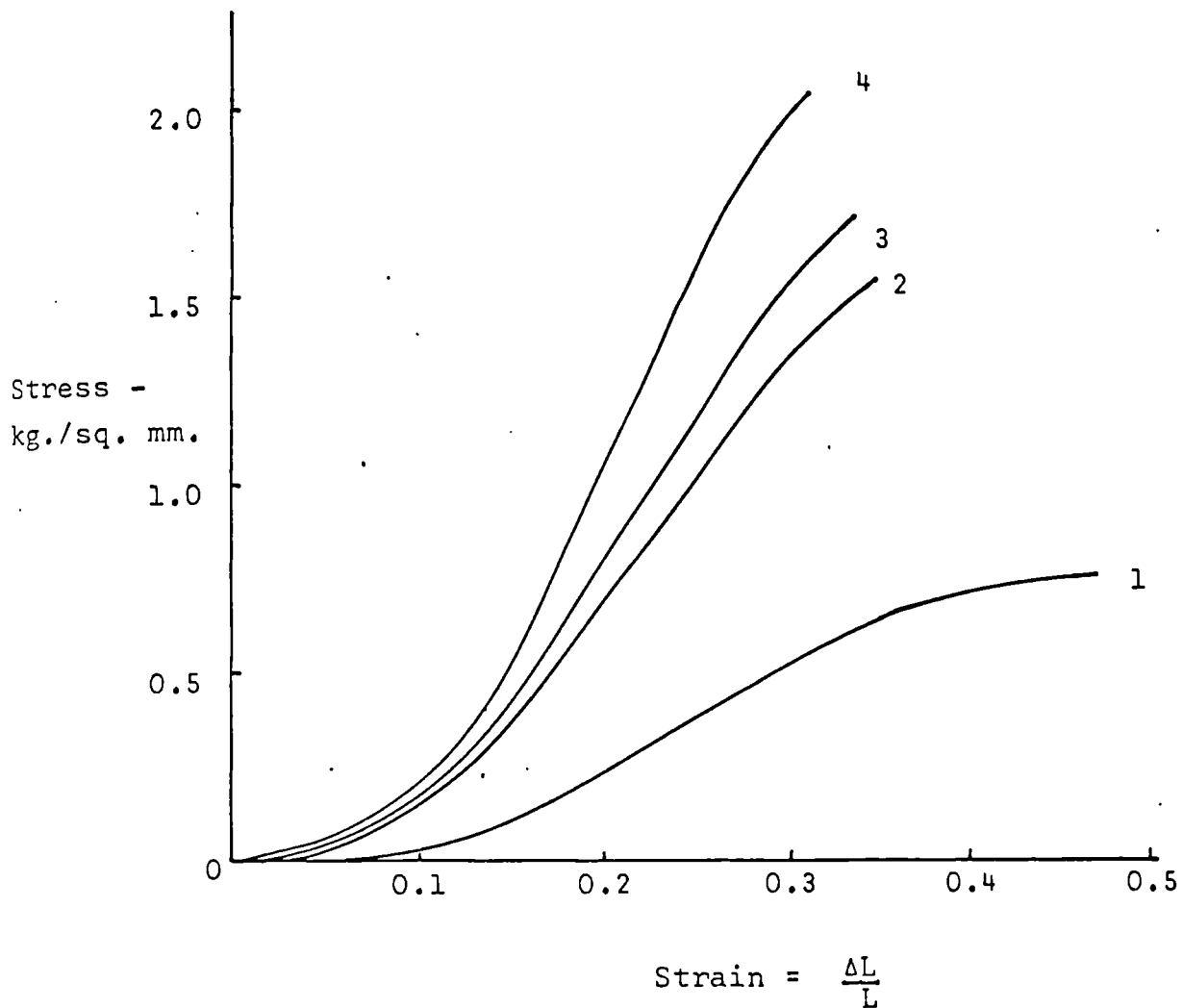
Fig I.23   Stress-strain curves for human skin.   Average
           results for different age groups.

1.   2 months premature to 3 years of age
2.   15-30 years
3.   30-50 years
4.   50-80 years

(Rollhauser 1950)

This work will not be reviewed here as it is fully discussed in subsequent chapters.

Rollhauser (1950) obtained stress-strain curves from samples of abdominal skin taken at autopsy. Few details of the testing technique used were given but at least one major criticism of this work is that the specimens were tested in air with no control of temperature or humidity. Also, the deformation of the specimen under its own weight must have introduced a considerable error in measuring the initial length of the specimen.

Typical results obtained by Rollhauser are shown in Fig I.23. These show an increase in skin stiffness with increasing age. Because of the above error, the values of strain are lower than those found by other workers.

Jansen and Rottier (1957) also tested 52 abdominal skin specimens obtained from cadavers.

A 10 cm. square was marked on the abdomen as shown in Fig I.24 and this square of skin was then excised. The subcutaneous fat was removed with scissors. The squares were then carefully adjusted to their original 10 x 10 cm. size, pinned down on a board and cut into parallel strips 0.5 cm. wide. The authors did not mention whether care was taken to avoid stretching the skin excessively both during removal from the cadaver and when removing the subcutaneous fat.

The testing technique used was very crude and was subject to the following major criticisms:

(i) Specimens were tested in air with no control of temperature or humidity
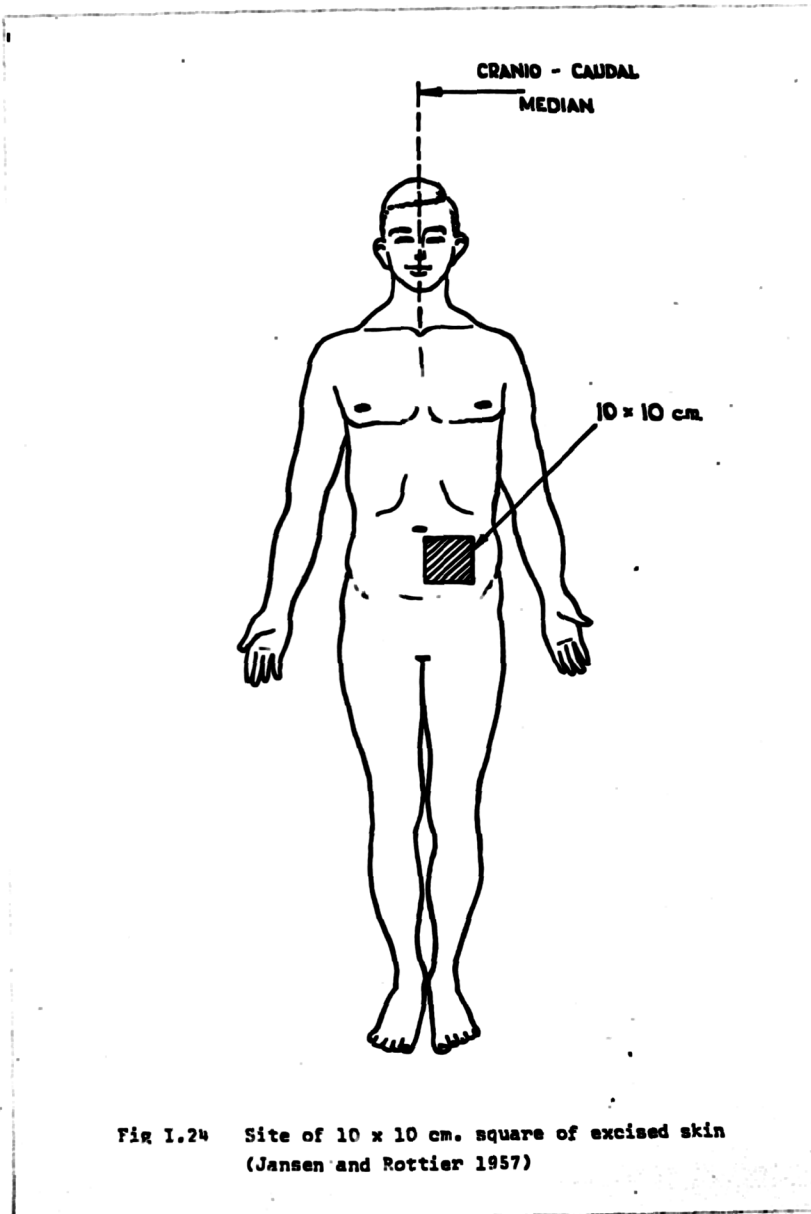
Fig I.24   Site of 10 x 10 cm. square of excised skin
            (Jansen and Rottier 1957)

(ii) A load of 10 gm. was applied to the specimen before the initial length was measured. This, together with the weight of the specimen, must have produced a large zero error in the strain measurements.

(iii) Strain measurements were calculated from grip movement and were therefore subject to errors due to stress concentration effects at the grips and to slippage of the specimen in the grips

As all of the test specimens were of the same length and width, the authors assumed that the thickness was proportional to the weight of the specimen. This implied the assumption that the specific gravity of human skin was constant. The error involved in this was probably small although it is interesting to compare the value of 1.1 quoted by Leider and Buncke (1954) with the value of 1.25 quoted by Rothman (1961).

However, in an attempt to compare results obtained from strips of different thickness, a serious error was introduced by the assumption that the extension of the specimen under a given load was inversely proportional to its thickness. This is not true for a non-linear material such as skin. It would have been more reasonable to assume that the tension in the specimen at a given extension was proportional to its thickness.

The authors concluded that they could find no relation between age and the mechanical properties of skin.

Jansen and Rottier (1958 a) realised the limitations of their simple testing equipment and, therefore, devised a more refined instrument. This was capable
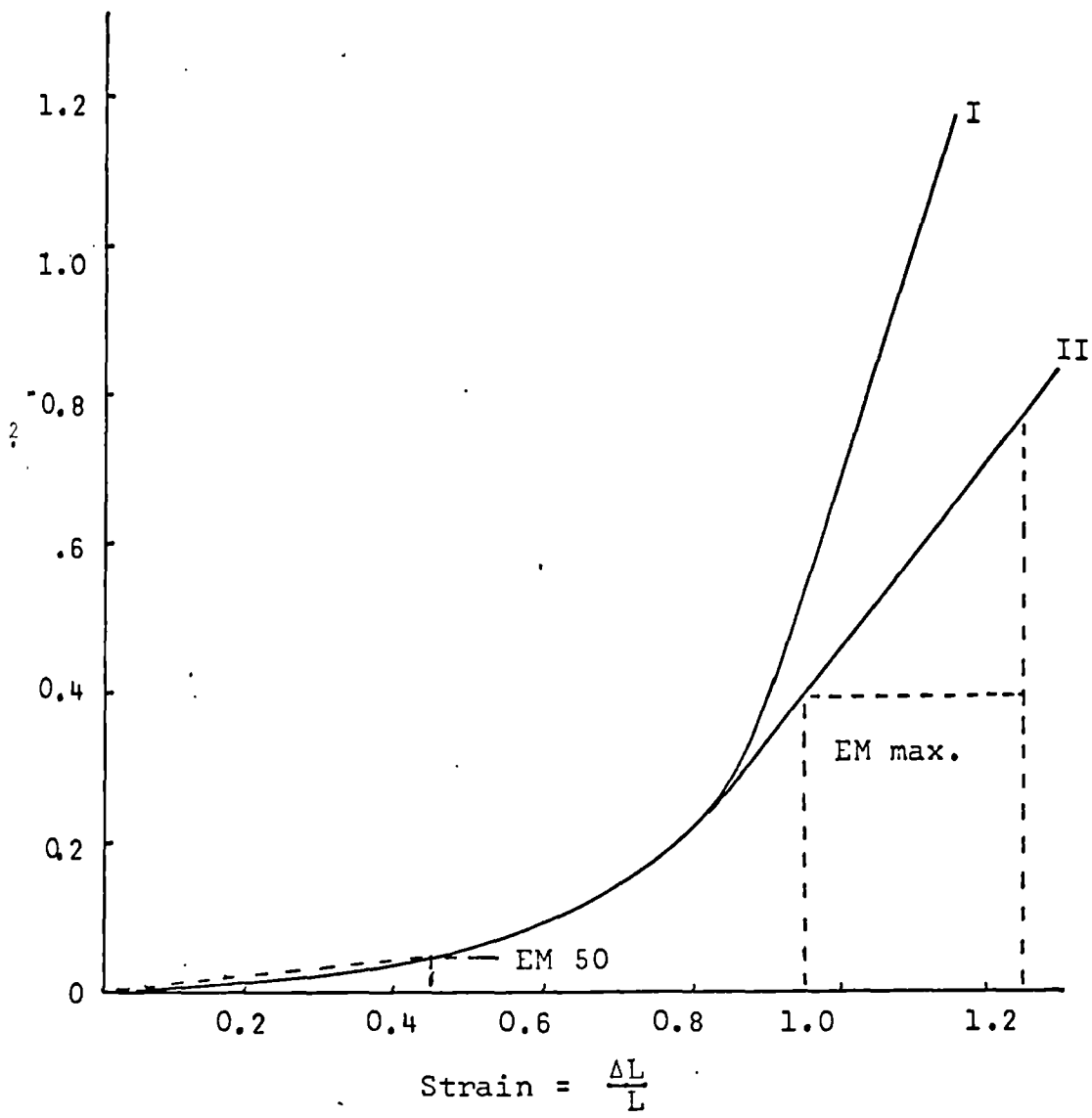
Fig I.25   Stress-strain curves for human skin
          (Jansen and Rottier 1958 a)

of loading skin to the point of rupture and was motor-
driven so that the load could be applied smoothly.
However, several features of this apparatus meant that their
data was of limited value for comparative purposes.

The specimens were again tested in air with no
control of temperature or humidity. The load weighing
part of the apparatus consisted of a coil spring, the
deflection of which gave the load. The deflection of this
spring was of the same order as the deflection of the
specimen. The spring was attached to one specimen grip,
the other grip being driven down at a constant rate.
Because of the highly non-linear nature of skin, this meant
that the specimen was neither tested at a constant strain
rate nor at a constant loading rate. In view of the
viscoelastic properties of skin which result in it being
sensitive to rate of strain and rate of loading, this
means that the results obtained cannot strictly be com-
pared with those of other workers or, indeed, among
themselves.

Extension measurement was again based on grip
separation and was therefore subject to the same error as
before. Also, the type of grip used, a straightforward
clamp, has been found to be prone to specimen slippage
at high loads. This may explain the fact that the
strains at rupture recorded by Jansen and Rottier were
much higher than those found by other workers.

Two typical stress-strain curves obtained
from this apparatus are shown in Fig I.25. The specimens
were obtained from the same 10 cm. square, No I being
excised close to the cranio-caudal median and No II being
excised 8 cm. further away from this median (see Fig I.
24). Because of the large difference in mechanical

properties between these relatively closely spaced strips, the authors concluded it would be unwise to compare results from skin specimens taken from different parts of the body.

A total of 267 specimens obtained from 89 cadavers were tested. In order to facilitate comparison of their results, each stress-strain curve was characterised by 4 parameters (see Fig I.25):

(i)   EM50: the "modulus" for the first 0.05 kg./sq. mm. of stress

i.e. $EM\ 50 = \dfrac{0.05}{\text{strain at 0.05 kg./sq. mm.}}$ kg./mm²

(ii) EM max: the "modulus" given by the slope of the final part of the stress-strain curve

(iii) The ultimate tensile stress based on the unstressed cross-sectional area

(iv) The strain at specimen rupture

The variation with age of each of these parameters was examined by separating the results into a series of age groups and averaging each parameter within each age group. The results were given with limits of 2 standard deviations to give an indication of spread. This resulted in some rather peculiar figures being quoted, e.g. EM max for females between 20 and 29 years was given as 3.0 ± 6.8 kg./sq. mm. which was obviously nonsensical and showed that the implied assumption of a Gaussian distribution was not justified.

The only one of these parameters which was age-dependent was the strain at rupture which showed a definite reduction with increasing age.

Figures were also obtained for the dry weight and hexosamine content of the skin. Neither of these quantities was found to be age-dependent.

The authors compared their results with those of Rollhauser (1950). There was a large discrepancy between the values which he had found for EM max, this being much higher than their own figures, and for the extension at rupture which was much lower. It was noted that Rollhauser had taken his specimens from the region of the abdomen above the umbilic, whereas their own skin had been excised from below the umbilic.

Jansen and Rottier (1958 b) therefore decided to compare the properties of specimens taken from above and below the umbilic. This was done in an identical manner to that described above using specimens taken from 15 cadavers. It was found that, although there were small differences between specimens taken from the two regions, these were not large enough to explain the discrepancy with Rollhauser's results.

Jansen and Rottier then investigated the effect of exsiccation on the mechanical properties of the specimens. Normally they had stored their specimens at 100% R.H. until just before test to minimise evaporation of fluid from the specimen. Three strips were taken from the same piece of skin, the first strip was tested immediately and the other two were tested after one hour and two hours respectively. During this time they were left hanging in the air. The weight of the second strip had decreased by 14% after one hour and that of the third strip by 27% after 2 hours. The changes in EM max and strain at rupture were as follows:

	1 Tested immed.	2 Exposed 1 hour	3 Exposed 2 hours
EM max kg./mm²	0.8	2.6	4.1
strain at rupture	1.32	1.13	0.88

The values of EM max found after exposure were comparable
with those found by Pollhauser but the values of strain at
rupture were still higher than Rollhauser's. The authors
therefore concluded that Rollhauser had allowed his
specimens to be exposed to air for some time before test
and that he had not started his load-extension curves from
a true load zero. While this may well have been true,
their values of strain at rupture are still much higher
than those found by other workers. This strongly suggests
that they must have suffered from specimen slippage in the
grips.

An investigation of the mechanical properties
of guinea pig skin has been reported by Beckwith et al.
(1963), Glaser et al. (1965), Must et al. (1965) and
Marangoni et al. (1965).

As the aim of this research was to develop a
standardised testing technique for a rational investigation
of the wound healing process, tests were carried out on
wounded and unwounded specimens.

The basic testing method used was described by
Beckwith et al. (1963). Using the machine described by
Must et al. (1965), a standard wound 1.5 ins. long by 0.1 in.
deep was made in the back of a guinea pig parallel to and
close to its spine. The machine automatically inserted a
series of sutures 0.1 in. apart and secured them in a
standard manner. After a suitable healing interval, the
scarred skin was removed and a standard test piece was
prepared. This consisted of a 0.25 in. wide strip cut
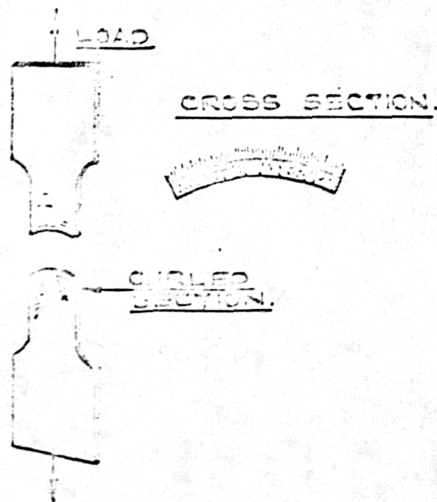
FIG. I.26 - SPECIMEN OF GUINEA PIG SKIN CURLS
WHEN UNDER UNIAXIAL TENSION (BECKWITH ET AL, 1965).
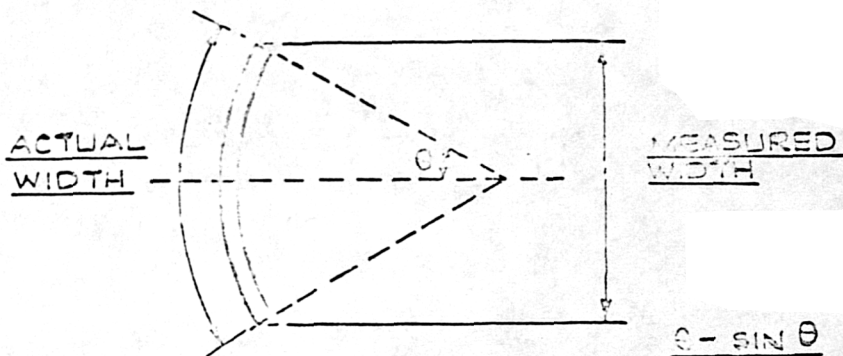
$$\text{PERCENTAGE ERROR IN WIDTH} = \frac{\theta - \sin\theta}{\theta} \times 100\%$$

∴ IF CURVATURE REMAINS CONSTANT, THE
ERROR IS REDUCED BY USING A
NARROW SPECIMEN (i.e. θ IS SMALL).

FIG. I.27. - WIDTH MEASUREMENT ERROR DUE TO
CURVATURE IS REDUCED BY USING NARROW
SPECIMEN.

perpendicular to the wound axis. A "waisted" specimen
was not necessary as failure always occurred at the scar.
For comparison purposes, specimens of unwounded skin were
also prepared. These were of "waisted" form, the test
section being 0.25 in. wide.

The specimens were tested in air with no control
over humidity and temperature. Testing was done as quickly
as possible to minimise exsiccation. A measure of strain
both in the direction of and transverse to the applied load
was obtained by taking a series of photographs of the
specimen as the test proceeded. A grid of 0.04 in. squares
was printed on the specimen to facilitate these measurements.
It was claimed that the results were not affected by strain
rate, provided that this lay between the limits 0.007 in./
in./sec. and 0.042 in./in./sec.

Various difficulties became apparent at an
early stage in this test programme.

The first of these manifested itself as a
peculiar "hump" on the stress-strain curve. This was found
to be caused by the panniculus, a layer of muscle attached
to the dermis. This layer is not present in human skin.
Removal of the panniculus overcame this problem.

The second problem was that the specimens were
found to curl under load in the manner shown in Fig I.26.
The authors suggested that this was due to the difference
between the elastic properties of the dermis and epidermis.
No attempt was made to investigate these properties to
substantiate this.

As this curling effect produced an error in
the measurement of width, Glaser et al. (1965) minimised
this error by reducing the width of the specimens to .064 in.
This will obviously reduce the error in width measurement
for the purely geometric reason shown in Fig I.27. The
authors stated that reducing the width of the specimen

reduced the tendency to curl but offered no explanation for this.

A very important effect, which must be considered when using very narrow specimens, is that, if the specimen width is comparable to the dimensions of the collagen network in the dermis, a fundamental change in the character of the tissue will occur. Those fibres which are oriented in directions appreciably different from the axis of the specimen will be cut short and will have no ability to carry load. Only those fibres oriented roughly along the specimen axis will carry the load and will thus determine the properties of the specimen. In theory, this would mean that, in the limit, a very narrow specimen would have the same properties as a single collagen fibre.

Glaser et al. stated that their specimens could be considered to be homogeneous as the width of their specimens (.064 in.) was 25,000 times the length of an average collagen fibre bundle. This is clearly nonsense as it implies a fibre bundle length of 640 Å. The length of a collagen molecule is 2,800 Å.

It was appreciated that testing the specimens in air would inevitably result in some degree of exsiccation. This was minimised by careful handling and rapid testing techniques (Marangoni et al. 1965). In view of the considerable lengths gone to to develop a standard testing technique, it is surprising that no attempt was made to control temperature and humidity during the actual test.

In spite of the high degree of test control achieved, a considerable variation in results was still found so that, in order to obtain meaningful results, each stress-strain curve was described by a series of parameters in a similar manner to that used by Jansen and Rottier. These results were then analysed by statistical methods. The parameters used were:
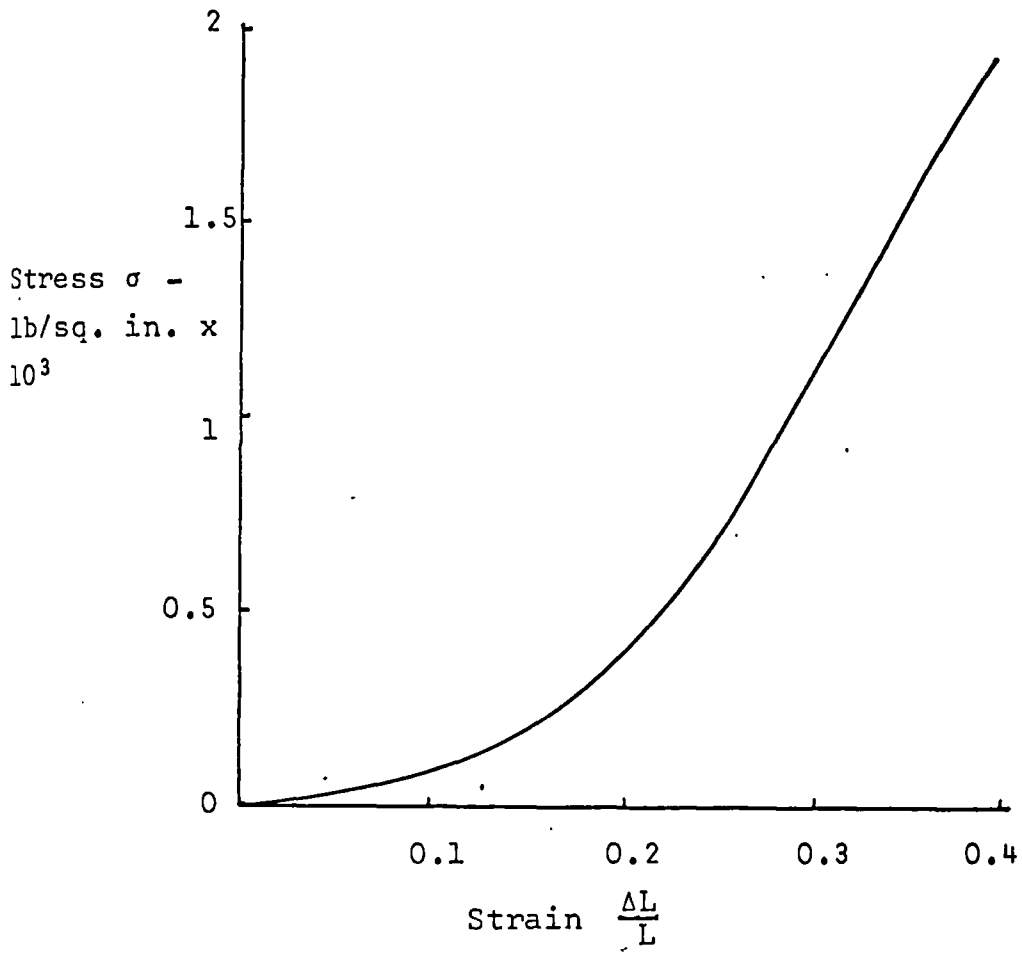
Fig I.28   Stress-strain curve for guinea pig
            skin (Glaser et al. 1965)

(i)   The ultimate tensile stress based on the cross-
       sectional area of the unstressed specimen
(ii)   The work input to the specimen to produce a
       stress of 500 lb/sq. in.   This was given by:

$$\frac{\text{area under stress-strain curve}}{\text{total volume of specimen}} \quad \text{in.lb/cub.in.}$$

(iii) The work input as shown but to a stress of
       1,000 lb/in?
(iv)   The "maximum stiffness".   This was equivalent
       to the EM max of Jansen and Rottier
(v)   The strain at specimen rupture

        In the case of the wounded skin specimens, the
work input to rupture was used instead of parameters (ii)
and (iii) as these specimens failed at stresses below
500 lb/sq.in.   It should also be noted that parameters (i)
and (v) were determined by measurements on the gauge length
of a reduced section specimen.   All other parameters were
found from parallel section specimens, the strain being
determined from the grip separation.   As the length to
width ratio of these specimens was about 15:1 the error
involved in this was probably small.
        A typical stress-strain curve for unwounded
guinea pig skin is shown in Fig I.28.   For strains greater
than about 0.3 it can be seen that the curve becomes almost
linear.
        For strains in the region 0 to 0.3 the curve
could be described fairly accurately by a simple power law
expression of the form:

$$\sigma = K\varepsilon^i$$

where σ = stress in specimen - lb/in^2

ε = strain

K, i are constants

Results obtained on unwounded guinea pig skin have shown that the measures taken to control the test conditions are reasonably effective in that the scatter of the values found for the various parameters is considerably lower than, for example, the equivalent figures found by Jansen and Rottier.

An intensive investigation of the mechanical properties of human skin has been described by Ridge (1964) and Ridge and Wright (1964 a, 1964 b, and 1965).

Both autopsy and biopsy skin specimens were used, these being obtained from standardised sites on the abdomen, back, forearm and thigh. Care was taken to subject the specimen to only minimal tension during removal. The specimens were oriented either parallel or perpendicular to the cleavage lines of the skin (Cox 1941, Langer 1861).

Ridge and Wright reduced all their skin specimens to the same thickness of 2 mm. by freezing the skin into a block of water and slicing the whole block down to size using a sledge microtome. In view of the variability found in skin thickness, some of their specimens must have had some of the dermis removed while others must have been left with a thin layer of subcutaneous fat under the dermis. No significant differences were found between specimens prepared by the above technique and specimens prepared by an unspecified method which did not involve freezing.

Standard shape, reduced section test specimens were prepared using a cutting die. The gauge length of these was 1 cm. long by 0.4 cm. wide.
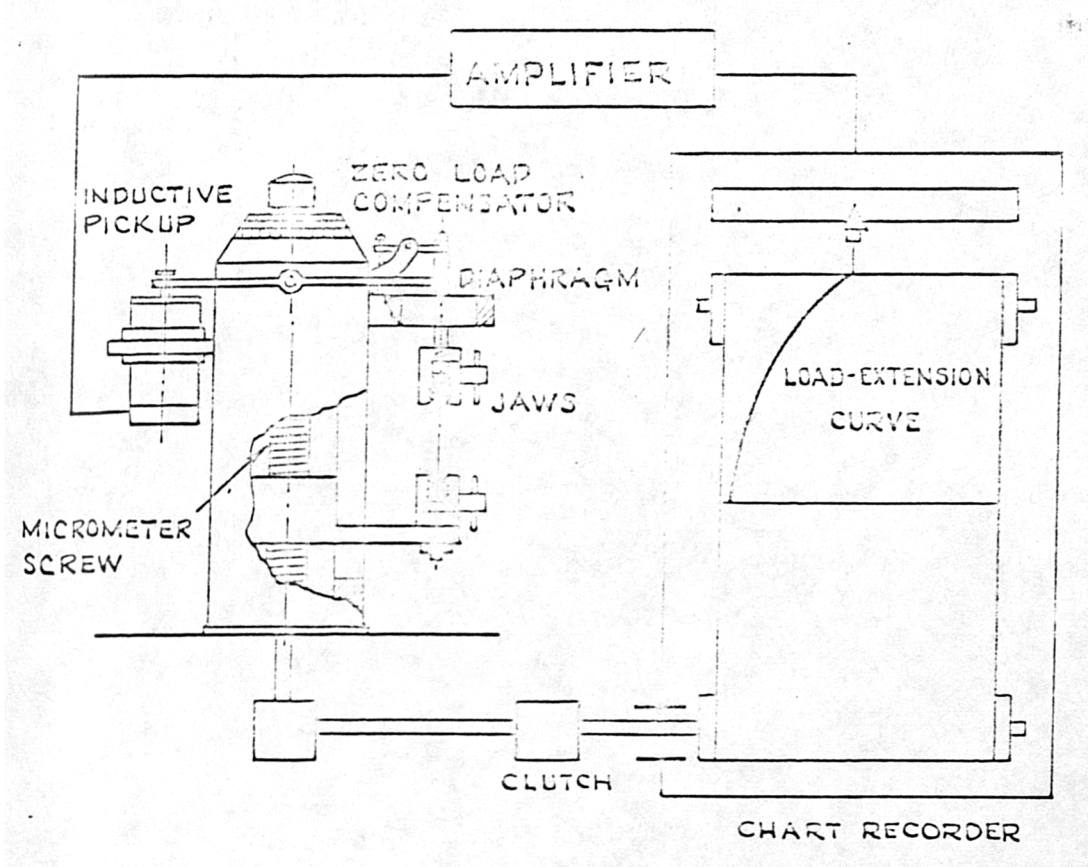
FIG. I. 29. TENSILE TESTING MACHINE
FOR SKIN SPECIMENS

(RIDGE 1964)

The initial tests were carried out using an
Instron testing machine. However, because of the
inconvenience of using this machine, the testing facility
shown in Fig I.29 was constructed. As the movement of the
chart was directly related to the jaw movement it was used
to give a measure of the specimen extension. In view of
the reduced section specimen which was used, this was an
obvious source of error. As the basic aim was to
develop a standard test for comparison purposes and not
to determine the absolute stress-strain relation for skin
this error was neglected because of the great simplification
of extension measurement.

The top jaw was supported by a spring system in
such a way that a load of 5 gm. had to be applied to the
jaw before any load was registered on the chart. This
meant that the initial length of the specimen was measured
with a load of 5 gm. on the specimen. This introduced
an appreciable zero error in strain measurement.

A typical load-extension curve obtained on
this apparatus is shown in Fig I.30. The extension given
was the actual jaw movement. As no details were given
of the initial jaw distance it was not possible to
calculate strain values.

For loads up to 150 gm. an equation of the form:

$$E = a + b \log L \quad \text{where} \quad E = \text{extension}$$
$$L = \text{load}$$
$$a, b = \text{constants}$$

was fitted to this curve.

This equation, however, gives a minus infinity
value for E at zero load so that it is difficult to see
how the curve fitting was done.
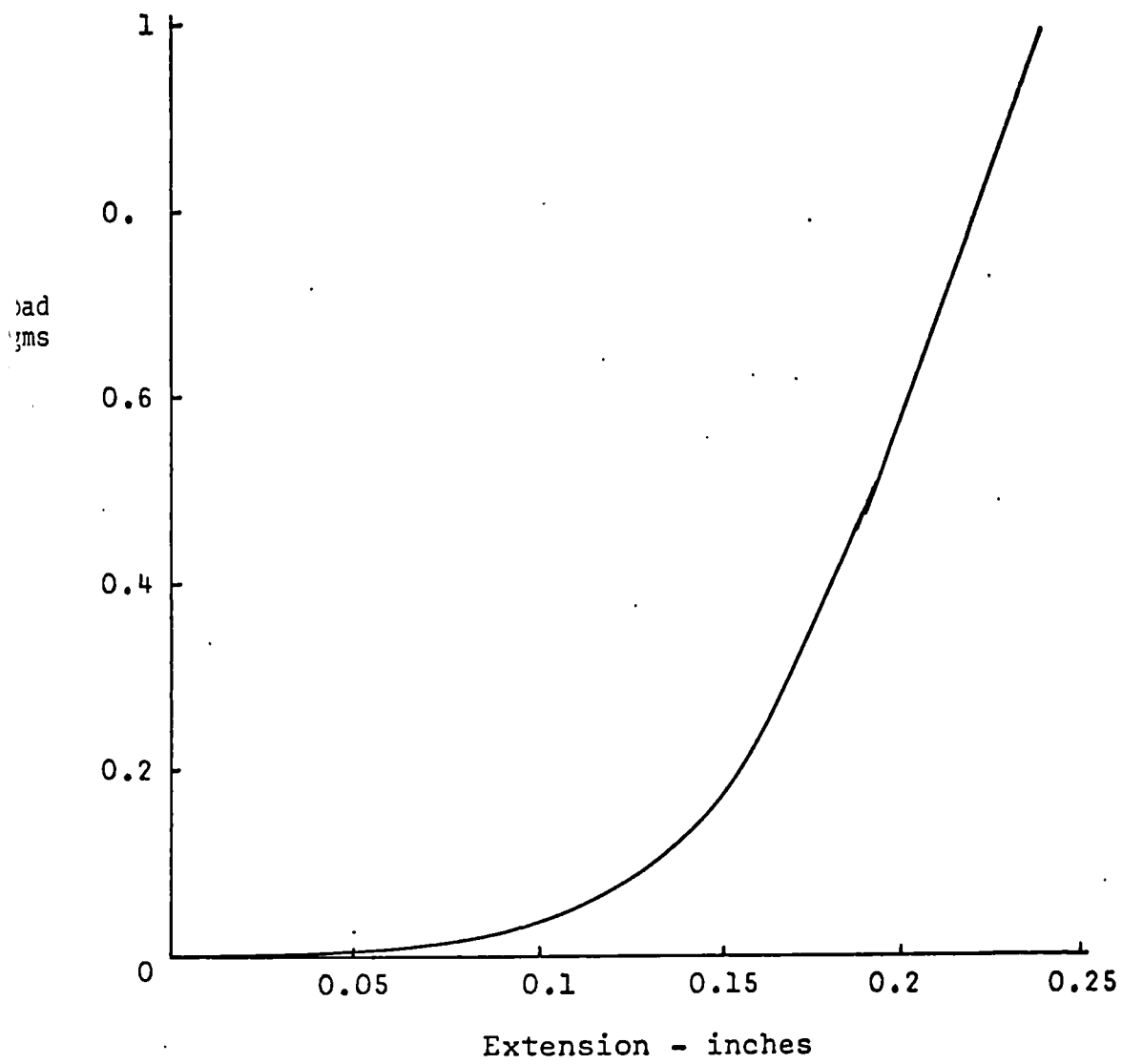
Fig I.30   Load v. extension curve for human skin
            (Ridge and Wright, 1964 b)

At loads above 150 gm. another expression was
fitted to the curve, *viz.*

$$E = i + kL^b$$

where E = extension
      L = load
 i, k, b = constants

As histological examination showed that most of
the collagen fibres were oriented in the direction of the
applied load during this phase of extension, then the load-
extension relation must have been primarily a measure of
collagen elasticity.   This part of the load-extension
curve was therefore subjected to a very detailed analysis
as the basic aim of this research was to determine the
effect of collagen diseases on the mechanical properties
of collagen.

Although this equation was purely empirical,
Ridge attempted to relate the various constants to
particular physical features of the skin.   The constant
k was assumed to give a measure of the number of fibres
oriented in the direction of the load and the index b was
thought to depend on the elasticity of the collagen.
Because of the difficulty of establishing a true zero
point for a material such as skin, the constant i was
introduced to correct the difference between the experimental
zero and the origin of the fitted curve.

The effects of changing several test conditions
on these constants were investigated.   Changes in the rate
of extension were found to have a very marked effect on the
index b.   A standard rate of 0.2 ins./min. was therefore
used for all further testing.

Tests on specimens oriented along and across
Langer's lines showed that the index b was not dependent
on orientation but that the constant k had consistently

higher values for specimens oriented across Langer's lines.

No significant difference was found between autopsy and biopsy material taken from similar sites.

The authors proposed a simple mechanism of skin deformation in which the part of the load-extension curve described by their first equation corresponded to a process of collagen fibre orientation within the viscous ground substance. The second equation was considered to describe the extension of the oriented fibres. Although histological evidence was produced to support this theory, sections were only made of unloaded and fully loaded specimens. No attempt was made to study the degree of fibre orientation at several points on the load-extension curve.

An appreciable variation with age was found with all of the constants. The index b in particular showed a definite decrease between 40 yrs. and 90 yrs. (the oldest specimen used). Insufficient data was obtained for specimens less than 40 years old to enable any definite conclusion to be reached. The other constants i and k were also found to decrease with age.

A certain amount of work was also done on the stress-relaxation behaviour of skin, but this was done in a rather haphazard manner and only served to show that skin does have viscoelastic properties.

The collagen content of all the specimens tested was found after test. No variation with age was found.

Although the testing methods developed by Ridge and Wright appear to be of some possible use within the aims of their research, their essentially empirical approach does not shed much light on the basic nature of skin elasticity.
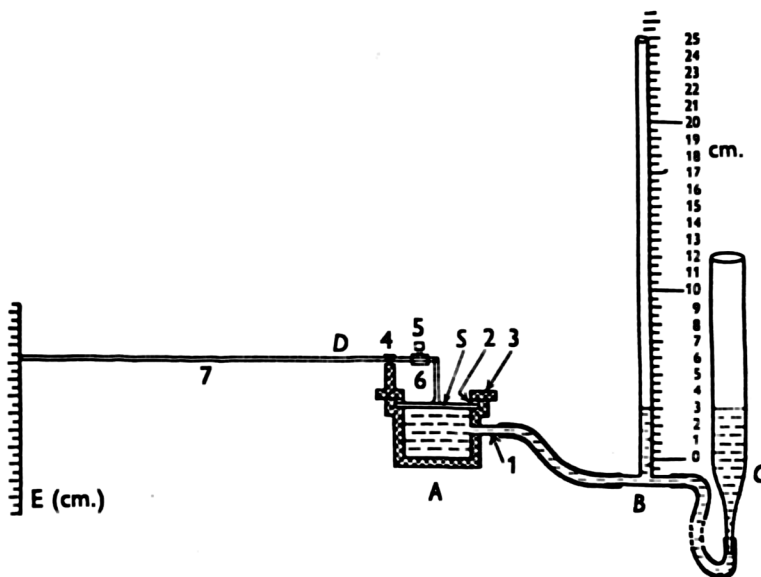
Diagram of apparatus for measuring the stretching of the skin (not drawn to scale). *A*, brass drum, with: 1, outlet to water manometer (*B*) and reservoir (*C*): 2, inner brass rings, holding skin (*S*) in position; 3, outer brass rings, holding skin (*S*) in position. *D*, lever, with: 4, knife edge on stand on outer ring of drum; 5, counter-balancing weight; 6, short arm, angled over centre of skin; 7, long arm, nine times the length of short arm. *E*, scale (cm.).

Fig 1.31   Apparatus used by Dick (1951)

I.3.2   _Biaxial and membrane tests in vitro_

As skin _in vivo_ is subjected to membrane stresses caused by the internal pressure of body fluids and tissues, various workers have attempted to simulate these conditions _in vitro_.   The only useful results of this type were obtained by Dick (1951) and Ragnell (1954).

Dick attempted to simulate the _in vivo_ conditions using the apparatus shown in Fig I.31.

The skin specimens were obtained from cadavers using a technique which was intended to maintain the existing tensions in the skin.   A circular ring of internal diameter 5 cm. with 8 sharp spikes projecting from one face was forced into the skin surface so that the points penetrated the skin.   The skin was then excised so that the spikes held the circular specimen at its original size and, it was assumed, at the same tension.   The number of spikes used seemed rather small to achieve this end and there was the possibility that a certain amount of stress relaxation could have occurred in the vicinity of the spikes.

Pressure deflection curves were obtained from 40 specimens.

In obtaining stress-strain relations from this data, Dick assumed that the deflected form of the specimen was a spherical cap.   In view of the anisotropic nature of skin and of the tensions maintained in the specimens, this would not be the case.

No details were given of the rate of loading although the author did note viscoelastic effects when he said that, at the higher pressures used, the skin was "slow to respond".

Dick presented his results in the form of graphs of stress v. pressure.   At the higher pressures,

these graphs were of straight line form. As the change of
deflection and hence of radius of curvature of the specimen
was found to be quite small for large pressure changes at
these pressures, one would expect this result.

At low pressures, however, the shape of the
curve was modified by the large changes of radius of
curvature which occurred and by the existing tension in
the specimen. By extrapolating the curves back to the
stress axis Dick obtained values of stress which he assumed
to be the stresses which normally existed in the specimens
when *in situ*. Although the accuracy of these values
cannot be very high, they are the only reasonable values
which have been quoted for these stresses.

Typical values obtained for skin specimens
taken from the lateral aspect of the thigh were from 7 gm./
cm. for a 14 year old female to 2 gm./cm. for a 65 year old
male. This reduction with age was found consistently.

By comparing the results of these tests with
a histological study of the structure of skin Dick (1947)
put forward an explanation for the widely differing
properties of young and old skin. He suggested that the
greater tensions found *in vivo* in young skin and the more
elastic nature of the response of young skin was due to the
existence of a well-formed elastin network and that the
loss of these properties with age was due to the degenerative
changes which take place in elastin with age.

Ragnell (1954) attempted to verify Langer's
hypothesis that human skin is more extensible in the
direction perpendicular to Langer's lines than in the
parallel direction.

Tests were carried out on 3 cm. diameter circular samples of human skin taken from cadavers. A circular grid was printed on the samples before excision. The specimen was placed, dermis down on a film of oil on a circular table and loads were applied in a radial direction by 32 equally spaced wires. The initial loads were such as to restore the grid on the specimen to its original size. Unfortunately, these loads, which would have given an indication of the value of the tensions existing *in vivo*, were not measured.

Superimposed on these initial loads was a uniaxial load pair either parallel or perpendicular to the direction of Langer's line. By measuring the change in diameter of the grid in the direction of this applied load, a form of load extension curve was obtained. From results obtained in this way Ragnell concluded that "the extensibility of human skin is one third greater at right angles to the lines of Langer than it is along them". However, as the stress-strain relation of skin is very non-linear, the statement has no meaning if the extension measurements are not made between the same absolute stress limits.

As no control of temperature or humidity was attempted and as no account at all was taken of the visco-elastic nature of skin, the results presented by Ragnell give no information of value on the mechanical properties of skin.

I.3.3   *In vivo* tests

Various workers have attempted to measure certain mechanical properties of skin *in vivo*.

Kirk and Kvorning (1949) carried out a large number of tests using an apparatus originally designed by

Schade (1912; 1921). A spherical indentor was pressed into
the skin by a known weight and the resulting movement of the
indentor was recorded against time. Although the results
obtained were reasonably consistent and showed definite
variations with age, the properties measured must have been
predominantly those of the subcutaneous tissue.

The same criticism can be made of the technique
used by Jochims (1934, 1948), who measured the force
necessary to compress a fold of skin. He also measured
the contraction of the skin between two parallel lines
drawn on the surface when these lines were pressed towards
each other until a fold just started to form. This
measurement would be expected to be related to the initial
tension in the skin but, again, it would be impossible to
account for the effect of the subcutaneous tissue.

Sodeman and Burch (1938) performed similar
tests using a calibrated, spring caliper instrument which
applied loads to a pair of cubes cemented to the skin surface.

I.2.4   Dynamic tests.

The term "dynamic" test is here taken to mean a
test in which some form of cyclic loading is used as distinct
from the static or quasi-static loading which was employed
in the tests described above. The load cycle is usually
of sinusoidal form because of the convenience of the
resulting mathematics.

Von Gierke, Oestreicher, Franke, Parrack and von
Wittern (1952) have described experiments of this type in
which sinusoidal loads were applied normal to the skin surface
over a small circular area, their measurements being made on
the thigh and on the upper arm. The results of these tests
were expressed in terms of the mechanical impedance Z
defined as the complex ratio of the periodic force F applied

to the area of the skin surface to the forced velocity u
of the area.   Z can be split into real and imaginary parts
thus:-

$$Z = \frac{F}{u} = R + iQ$$

.where   R = mechanical resistance
                                              Q = mechanical reactance
                                              i^2 = -1

The resistance R may be said to represent viscous friction
effects.   The reactance Q includes the effect of both the
mass and the elasticity of the material.   The results
showed that up to frequencies of the order of 5 kc/s. the
tissue behaved like an incompressible viscous fluid.
Above about 20 kc/s. the behaviour corresponded to a
frictionless, compressible fluid, i.e. normal acoustical
transmission.

It cannot be said that the above results
describe properties of the skin as the underlying tissues
must also have been involved.   However, they do give some
interesting information on the behaviour of soft tissue
under conditions which cannot be produced otherwise.   The
excellent agreement obtained between theoretical and
experimental results also suggested that linear, viscoelastic
theory is adequate to describe the behaviour of soft tissues
at small deformations.

I.3   Summary

Although no individual investigation among those
considered has given a complete description of the mechanical
behaviour of skin, an over-all picture does emerge,   In

particular the importance of the microscopic network concept
of skin structure was realised by several workers, although
there was no attempt made to carry this concept further.
The viscoelastic nature of skin was also well established,
although again this was not investigated in detail and the
importance of allowing for the effects of viscoelasticity
was not generally appreciated.

There is an obvious need for the development of
highly refined testing techniques in order to obtain more
meaningful results than those obtained in the work discussed
in this review.

Chapter II

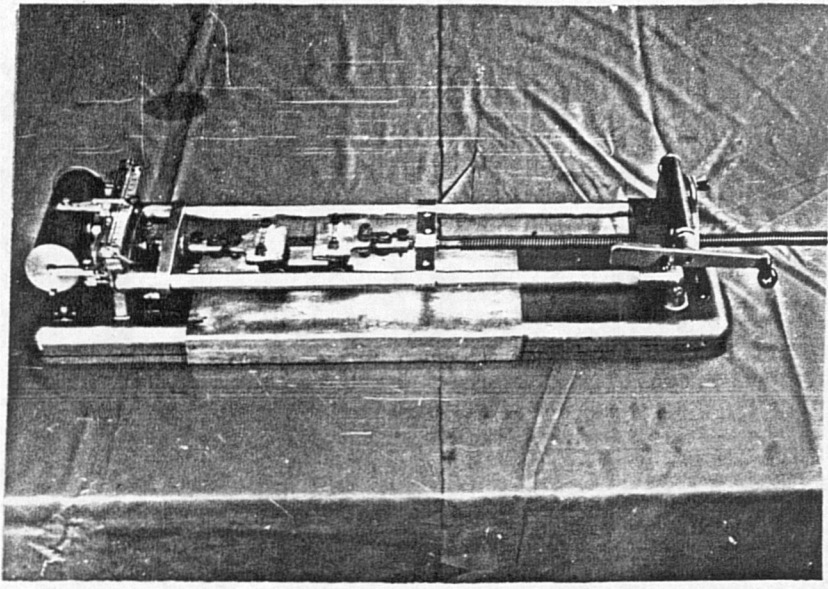# Pilot Experiments

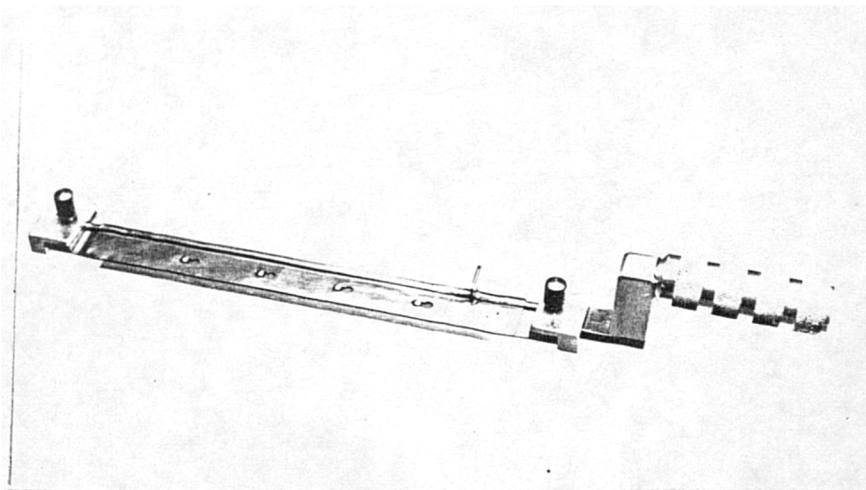Fig II.1   Hounsfield Tensometer

Fig II.2   Ground Glass Plate and Knife used for
            Fat Removal

At the start of this research programme, no information at all was available on the nature of the mechanical properties of skin. It was soon realised that, because of the lack of specialised journals in the field of bioengineering, the retrieval of information from the literature was likely to take a considerable time. It was therefore decided to carry out pilot experiments simultaneously with the literature search.

Simple testing techniques were used to define the problems involved in testing skin so that suitably refined testing equipment could be designed.

II.1 Uniaxial Tensile Tests *in vitro*

A number of tensile tests were carried out on specimens of post mortem skin using the Hounsfield Tensometer testing machine shown in Fig II.1.

Most of the specimens tested were obtained from the abdomen of cadavers immediately below the umbilicus and were oriented either parallel or perpendicular to the cranio-caudal median. The remaining specimens were obtained from infants at autopsy and were taken from the chest. All specimens were tested within 48 hours of death, being stored at $4^{\circ}C$ until tested.

The subcutaneous fat was removed using the knife shown in Fig II.2. The skin was stuck, epidermis down, on a ground glass plate using Evostick adhesive diluted with ether. The fat was then removed as shown in Fig II.3.

The specimens were tested in air at room temperature ($18-25^{\circ}C$). A waisted specimen (Fig II.4) was held in a horizontal position between simple clamp grips, the weight of the grips being supported by rollers (Fig II. 5). The grip jaws were lined with coarse glass paper to
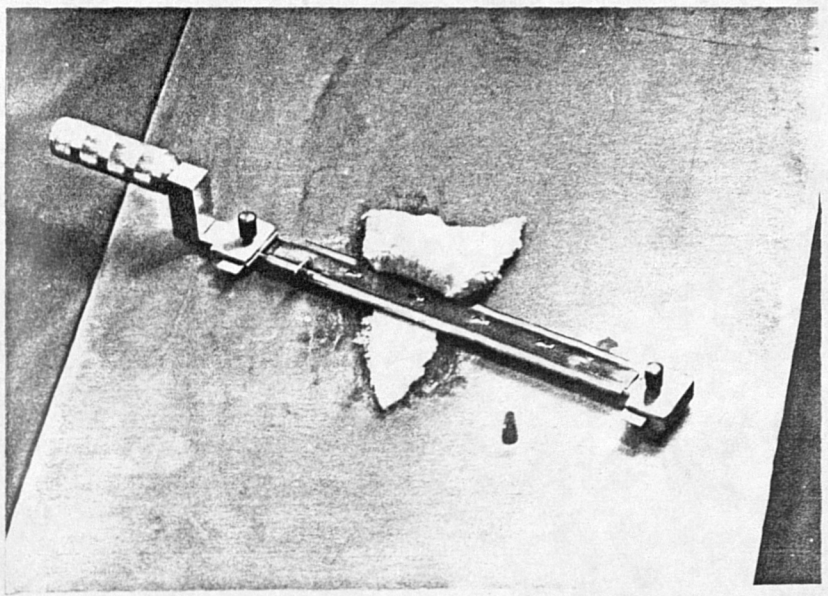
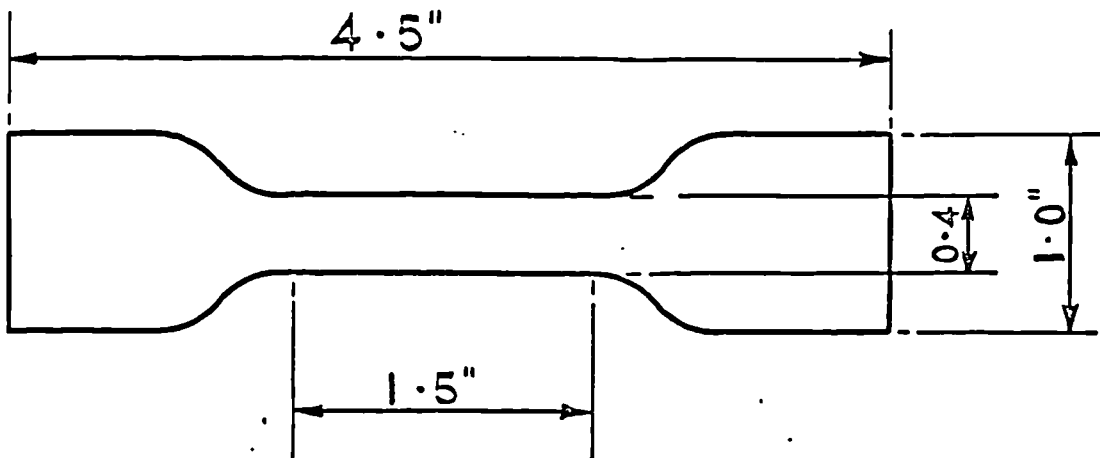FIG. II 3   REMOVAL   OF   SUBCUTANEOUS   FAT.

FIG. II 4   SPECIMEN   DIMENSIONS

minimise specimen slippage at high loads.

Load-extension curves were obtained by increasing
the load on the specimen in discrete increments and
measuring the length, width and thickness of a gauge
length at each increment, using the instruments shown in
Fig II.6. The gauge length was defined by attaching two
hairs to the specimen using Evostik impact adhesive.

Initial tests brought two major problems to
light:-

 (i) it was not possible to measure the
   unstressed size of the gauge length accurately
   because the specimen sagged under its own
   weight.

 (ii) skin was found to have very marked visco-
   elastic properties.

The first problem was partially overcome by
measuring the initial gauge length before the specimen was
mounted in the grips.

The effect of the viscoelasticity of skin was to
produce stress-relaxation effect at each loading increment
(i.e. with the specimen held at a fixed length, the load
decreased with time). A standard time of 5 minutes was
therefore allowed between each increment, the load being
measured at the end of this time.

Typical stress-strain curves obtained using this
technique are shown in Fig II.7. These curves may be
conveniently split into two parts:-

 (i) a primary extension in which a large
   deformation occurs at loading levels below
   the sensitivity of the machine (<0.25 lbs).

 (ii) a secondary extension characterised by
   rapidly increasing stiffness of the
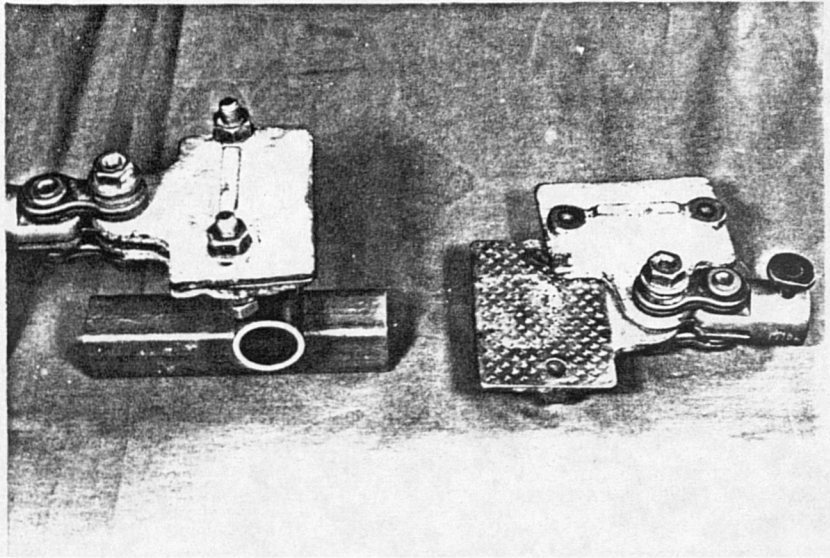
Fig II.5   Grips for Tensometer Showing Roller
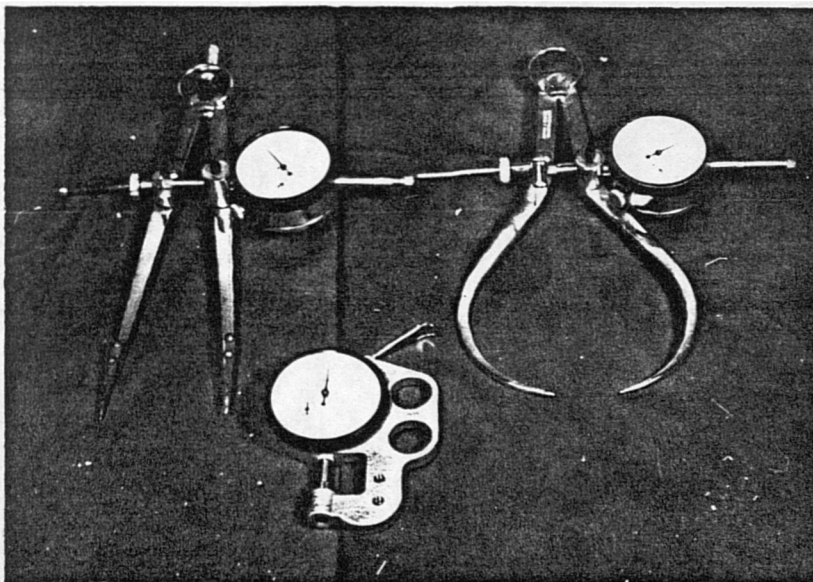   Supports

Fig II.6   Instruments for Measuring Specimen
           Deformations -

specimen.

The strain ϵ_2 measured perpendicular to the specimen axis is plotted in Fig II.8 in terms of the strain ratio k defined by

$$k = \frac{\epsilon_2}{\epsilon_1}$$

when
$$\epsilon_1 = \frac{x - x_0}{x_0}$$

$$\epsilon_2 = \frac{y_0 - y}{y_0}$$

x_0 = original unstressed gauge length

x = length of gauge length at stress σ

y_0 = original width of unstressed specimen

y = width at stress σ.

It was found that no measurable change occurred in the thickness of the specimen.

In spite of the somewhat crude testing techniques employed, the information obtained was very useful in defining the basic nature of skin as a material and in the design of the refined techniques required in performing mechanical tests on it.

Consideration of the volume changes occurring in the specimens shows that in all cases there was a very marked decrease in the volume with increasing stress. This was confirmed by the observation that a considerable quantity of fluid was expressed from the specimen during test. It is also interesting to compare the high values found for the strain ratio k (greater than unit in some cases) with the values of Poisson's Ratio for steel (0.3) and soft rubber (0.5). This evidence suggests that it is not possible to regard skin as a continuous material and that its highly unusual mechanical properties might best be explained by consideration of its microscopic architecture.
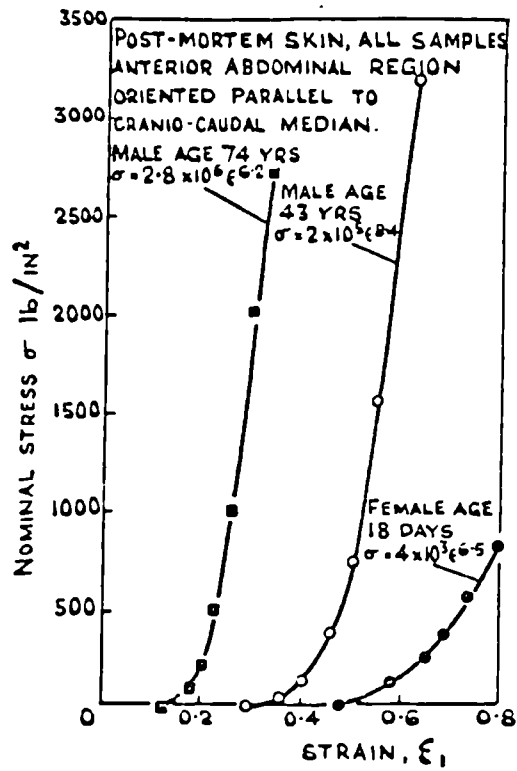
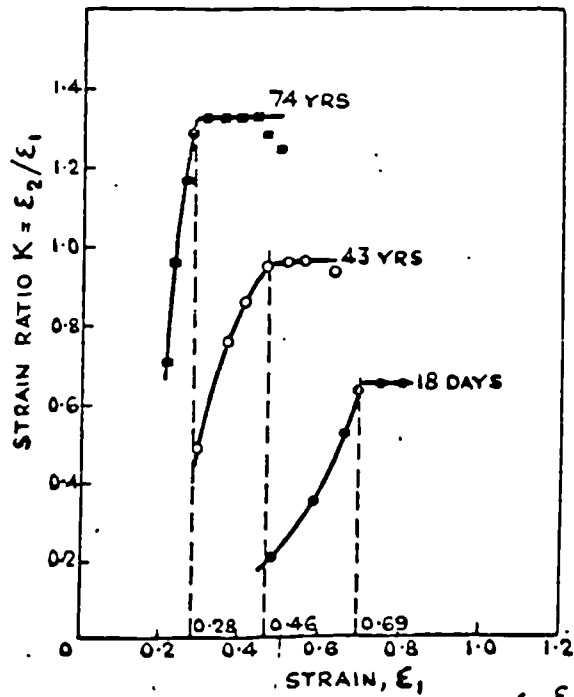FIG. II. 7   PILOT EXPERIMENTS - TYPICAL STRESS - STRAIN CURVES.

FIG. II. 8   VARIATION OF STRAIN RATIO k $\left(=\dfrac{\varepsilon_2}{\varepsilon_1}\right)$ WITH ε_1
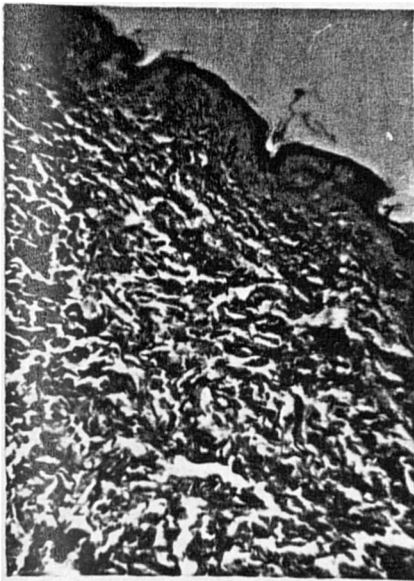
II.2   <u>Histology of Stressed Skin</u>

Fig II.9 shows the results of a histological investigation of skin specimens loaded to a range of stress values from zero to failure stress.   The specimens were loaded to the required stress and then held in the clamp shown in Fig II.10 so that the stress in the skin was maintained on removal from the Tensometer.   The specimen was then placed in a fixing solution for at least 7 days. The clamp could be removed as the specimen was by now quite rigid and in the configuration corresponding to the originally applied stress.

Sections were then prepared using the Mallory trichrome staining technique described in Appendix A.II.

In the section at zero stress, the collagen fibres in the dermis are shown stained green and are seen to form a randomly interwoven mesh with no apparent preferred orientation.   The spaces between the fibres are assumed to be filled with the amorphous ground substance.

When the skin is subjected to uniaxial stress, two major effects on the collagen fibres become apparent:-

(i)   as the stress is increased, the fibres are seen to straighten out and gradually take up positions oriented in the direction of the applied stress.   At first, only a few fibres are so oriented, but this number increases until all the fibres are fully oriented.   At this point, transverse fracture lines appear in the fibres, these increasing in number until failure obtains.

(ii) a change takes place in the staining reaction of those fibres which are fully oriented,

(a) Unstressed
    Skin: $\sigma = 0$
    $\varepsilon_1 = 0$

(b) Stressed Skin
    $\sigma = 10$ lb/in^2
    $\varepsilon_1 = 0.3$

(c) Stressed Skin
    $\sigma = 100$ lb/in^2
    $\varepsilon_1 = 0.55$

(d) Stressed Skin
    $\sigma = 1000$ lb/in^2
    $\varepsilon_1 = 0.65$

Fig II.9 Histology of Stressed Skin – the Effect of
        Uniaxial Tensile Stress (Mallory Trichrome
        Stain)

resulting in them taking up the acid fuchsin part of the stain and thus becoming red in colour. This change is apparently permanent in post mortem specimens, i.e. it is not reversible on release of stress. This is shown by Fig II.11.

The behaviour of the elastin fibres in stressed skin is shown in Fig II.12.

Under zero stress, the fine elastin fibres are randomly intertwined with the collagen fibres. Under increasing stress they behave in a similar manner to the collagen and become fully oriented and squeezed between the oriented collagen fibres.

II.3   Requirements for Refined Uniaxial Tensile Testing Techniques

As a result of the above tests, it was apparent that any attempt to obtain meaningful tensile test data on skin must take account of two major factors:

(i) The highly non-linear stress-strain characteristic

(ii) The marked viscoelastic properties

The first of these places certain requirements on the load measuring apparatus. This must have a high sensitivity so that the large primary extension exhibited by skin can be properly investigated. At the same time, however, it is required to be able to measure loads about 100 times greater than those involved in the primary extension. The apparatus must be "hard", i.e. the deflection of the load measuring device must be negligible
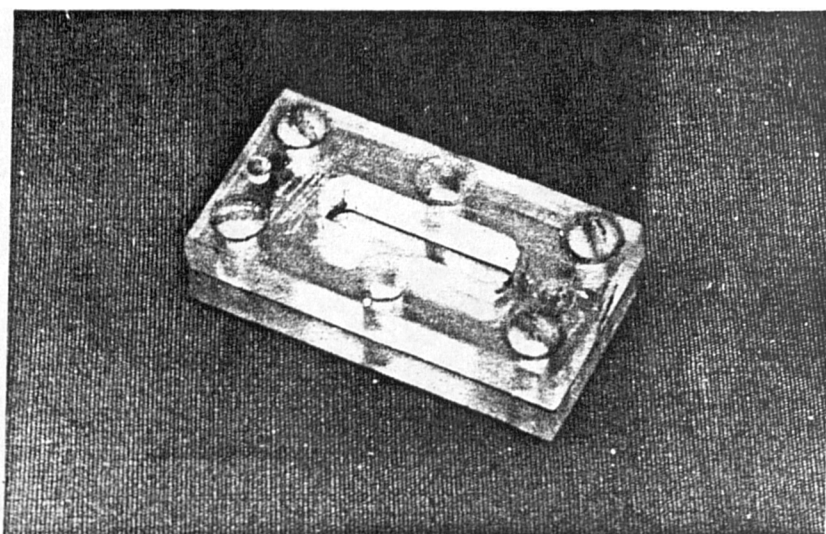
Fig II.10   Clamp for Maintaining Specimen at
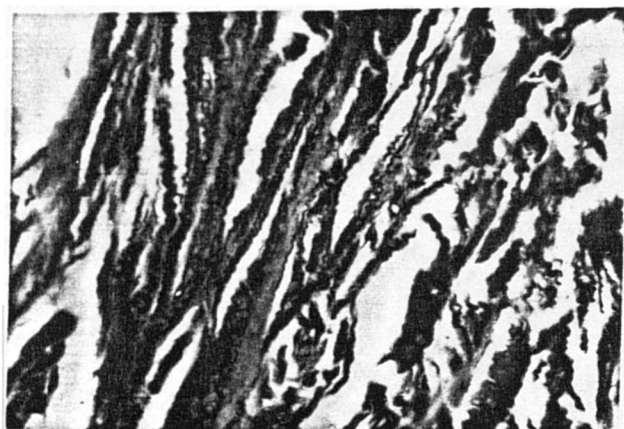   a Fixed Extension Whilst in Fixative

Fig II.11   Transverse Section of Skin Specimen which
             had been Stressed at 50 lb/in^2 and Allowed
             to Return to its Initial Length (Mallory
             Trichrome Stain)

in comparison with the accompanying deflection of the specimen. These requirements are best met by some form of electrical load cell.

Because of the viscoelasticity of skin, comparable results can only be obtained if all specimens are tested at either the same strain rate or the same loading rate. Specimens should also be tested at the same temperature as viscoelastic effects are temperature-dependent.

Because of the appreciable deformations of skin specimens caused by their own weight, it is essential to test skin specimens in a fluid of similar specific gravity to that of skin so that an accurate strain zero may be found. The most suitable medium is Ringer's solution.

It is impossible to use any mechanical means of strain measurement on skin because of its sensitivity to very small loads. Some form of optical strain measurement is therefore necessary. Further to this, it is relevant to consider whether the deformations of markings on the epidermal surface can be considered to represent the deformation of the skin as a whole.

A test was carried out in which the epidermis was carefully removed with a scalpel from a skin specimen which was under a tensile stress of 0.52 Kg/mm^2. There was no measurable fall in the load on the specimen. This implied that the stress in the epidermis was less than .025 Kg/mm^2 at a strain of 0.42 under these particular test conditions. The stress in the dermis was 0.58 Kg/mm^2.

Thus, as the stress required to deform the epidermis is very much smaller than that required to deform the dermis, the stress-strain properties of skin may be said to be primarily dictated by the dermis. Also, provided that there is no failure of the dermis-epidermis bond, the epidermis will strain with the dermis. Optical measurements
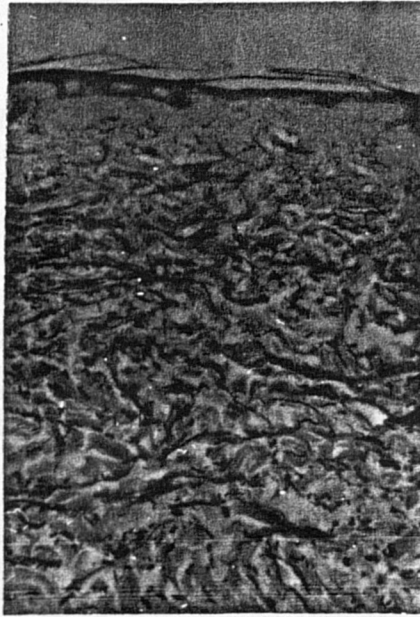
(a)   Unstressed Specimen
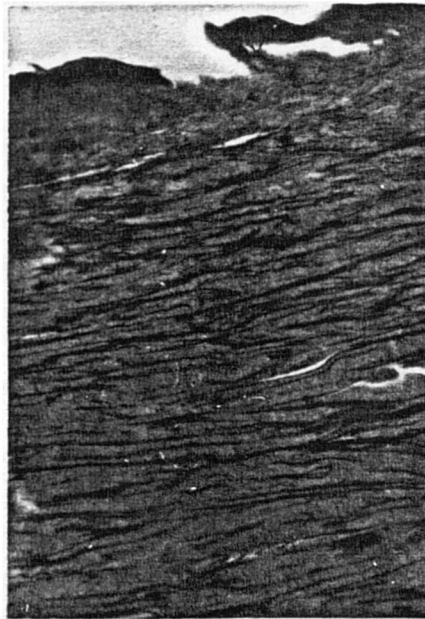
(b)   Specimen Stressed to 450 lb/in²

Fig II.12   Effect of Stressing on Elastin Fibres
(Lawson's Elastica Stain - the Elastin
Fibres are the Fine Black Filaments
among the Coarse Collagen Fibres)

of markings on the epidermal surface can, therefore, be assumed to give a measure of the strain of the specimen as a whole.

In addition to simple measurements of stress-strain properties, it is also essential to investigate further the viscoelastic properties of skin. This can best be done by stress-relaxation and creep tests. .

II.4   Summary

The pilot experiments described above have shown that human skin is a very complex material from an engineering point of view. Not only is its stress-strain response highly non-linear but it is further complicated by marked viscoelastic properties.

The requirements for testing such a material are as follows:

(i)   A wide range of load sensitivity must be available without interference with the specimens being required during the test.

(ii)   All specimens must be tested at a constant strain rate (this is much simpler to arrange than a constant loading rate).

(iii) Optical strain measurement is essential.

(iv)   All specimens must be tested in the same environment, i.e. constant temperature, humidity and pH. This may best be achieved by testing with the specimens immersed in a bath of Ringer's solution as this has a similar specific gravity to that of skin and will thus minimise errors caused by the deformation of the specimen under its own weight.

Chapter III

Theoretical Considerations

NOMINAL STRESS — LB/IN^2

NOMINAL STRESS — LB/IN^2

2500 2000 1500 1000 500

ε_1

0·1   0·2   0·3
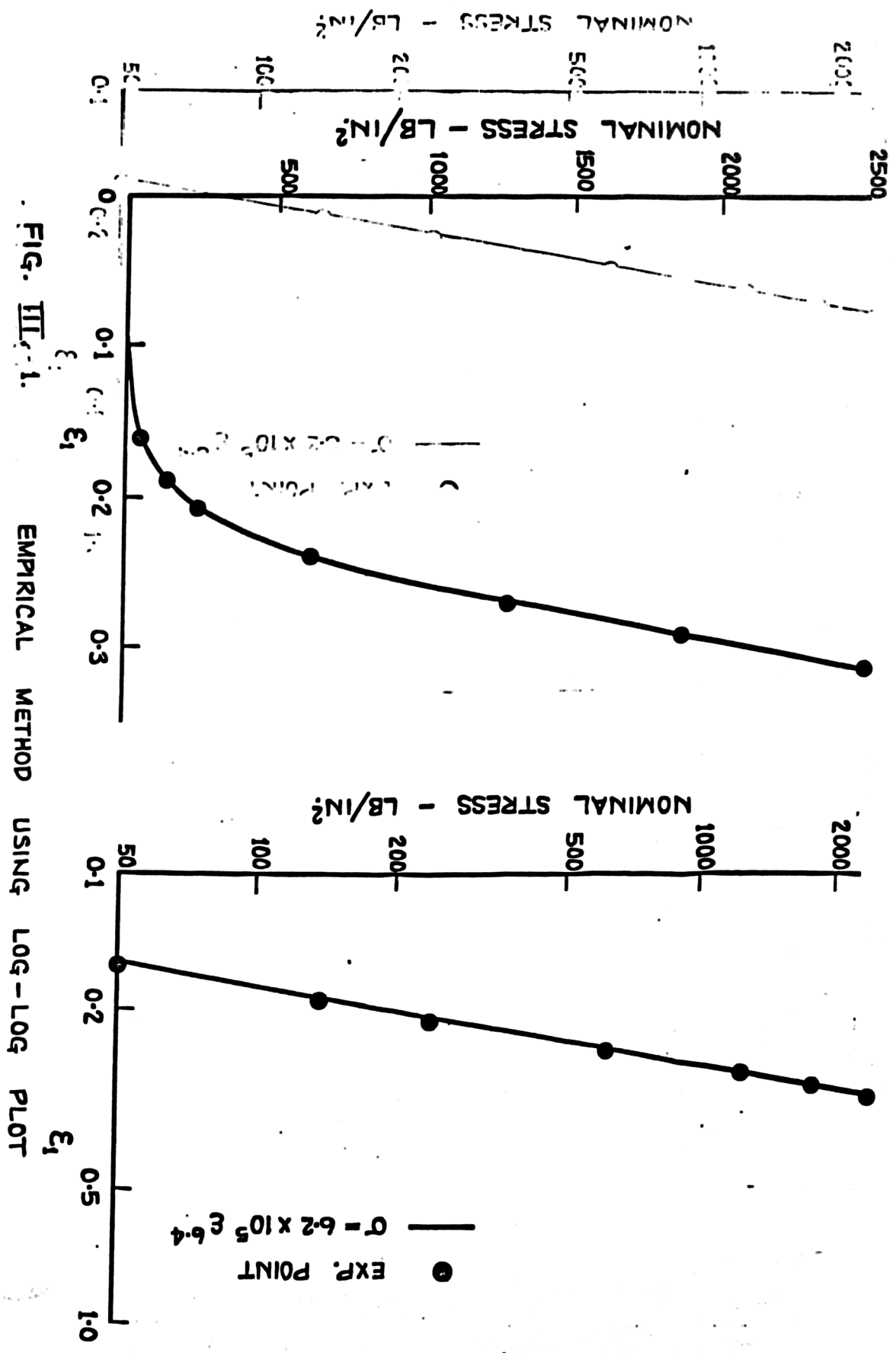
FIG. III-1.   EMPIRICAL METHOD USING LOG-LOG PLOT

NOMINAL STRESS — LB/IN^2

2000 1000 500 200 100 50

ε_1

0·1   0·2   0·5   1·0

● EXP. POINT

—— $\sigma = 6\cdot2 \times 10^5\ \varepsilon^{6\cdot4}$

There are, in general, three possible types of analytical treatment of the mechanical properties of a material such as skin:

(i) An empirical approach based on fitting mathematical expressions to the experimental data.

(ii) A semi-empirical approach involving the analysis of a physical model of skin based on its micro-architecture.

(iii) A rational approach using the techniques of statistical mechanics or continuum mechanics.

III.1 Empirical Method

This approach consists essentially of fitting a convenient mathematical expression to the experimental stress-strain curves. A basic failing of this approach is that it gives no information as to the physical nature of the stress-strain behaviour of skin.

The results of the pilot experiments described in Chapter II were plotted on log-log graph paper. In every case a good straight line was obtained (Fig III.1).

The following equation could be fitted to the experimental data:

$$\log \sigma = \log A + b \log \varepsilon$$
$$\sigma = A\varepsilon^b$$

where
σ = applied tensile stress

ε = strain in direction of σ

A, b = constants

The constants A and b were plotted against age. The index b showed a consistent decrease with increasing

1. FIBRES STRAIGHTEN OUT IN DIRECTION OF σ. BEHAVIOUR CONTROLLED BY ELASTIN AND/OR GROUND SUBSTANCE

2. INCREASING NUMBER OF FIBRES BECOME FULLY ORIENTED

3. ALL FIBRES FULLY ORIENTED. BEHAVIOUR IS SIMILAR TO THAT OF COLLAGEN FIBRES ALONE (DOTTED LINE)
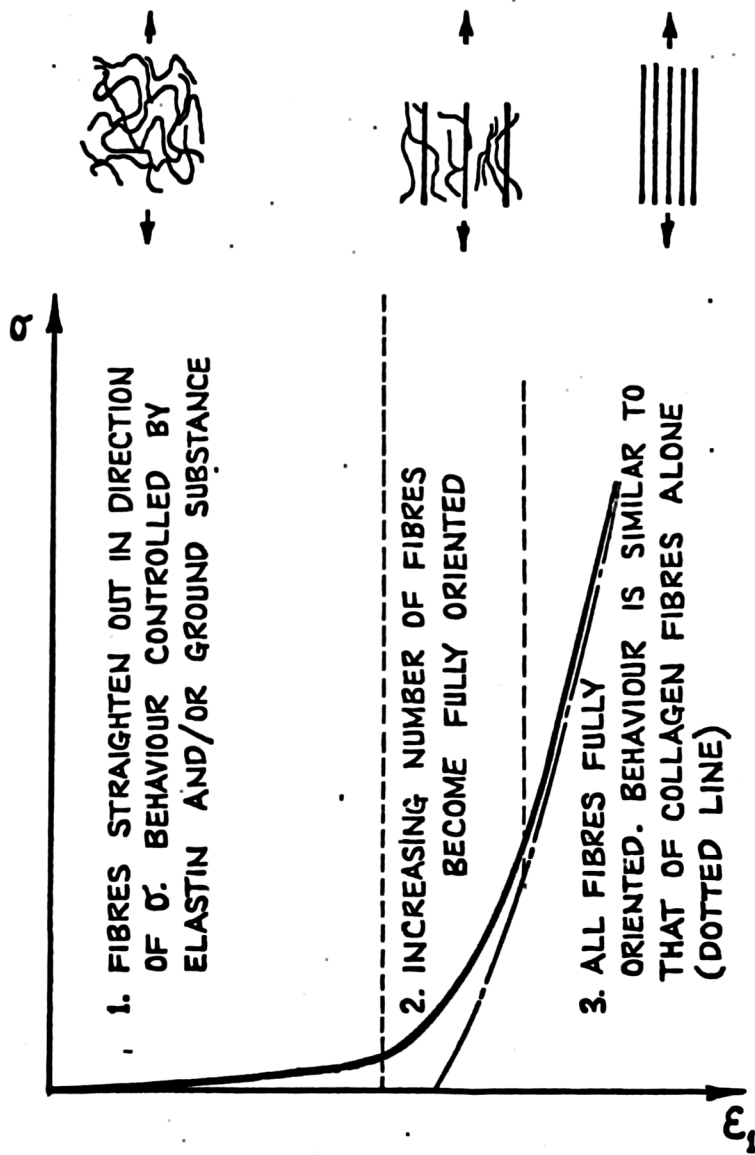
FIG. III. 2.   EXPLANATION OF STRESS—STRAIN BEHAVIOUR OF SKIN BASED ON HISTOLOGICAL DATA

age above 40 years.   Below this there was no apparent
dependence on age.   The coefficient A showed no dependence
on age.

These results agreed well with the data obtained
by Ridge (1964) who also fitted a power law expression of
this type to his data.   However, Ridge attempted to relate
the parameters A and b to various physical features of skin.
It should be emphasised that there is no rational basis for
this and that any consistent relations obtained in this way
are purely fortuitous.   For this reason, this type of
treatment was abandoned.

III.2   <u>Semi-Empirical Method - A Network Concept of Skin</u>
Histological investigation of skin has shown that
the dermis consists of three principal components which will
dominate its mechanical properties:

(i)   A dense, randomly interwoven mesh of
collagen fibres
(ii)   A similar mesh of very fine elastin
fibres
(iii) An apparently amorphous, viscoelastic
gel (ground substance) which permeates
the above fibre networks.

As the histology of skin subjected to uniaxial
stress has shown that the collagen fibres straighten out
and orient themselves in the direction of the stress, it
is reasonable to assume that the behaviour of the skin is
controlled by the specific mechanical properties of the
collagen fibres only once the fibres have thus oriented
themselves.   During the phase of extension corresponding
to the straightening and orientation of the collagen
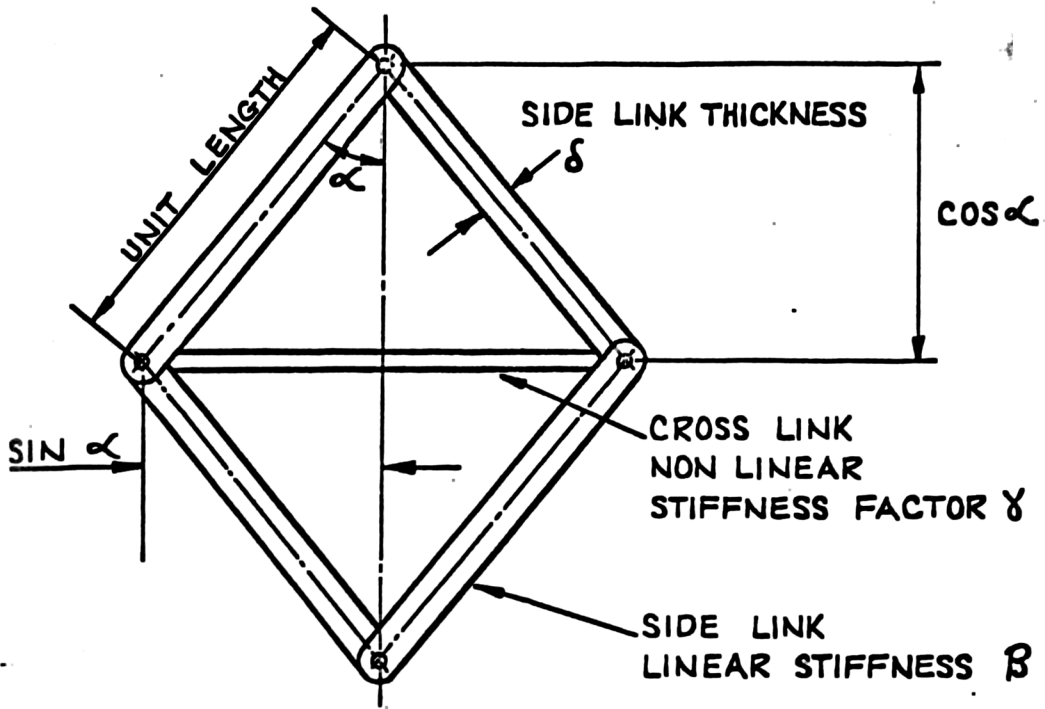fibres, the mechanical behaviour must be controlled by

FIG. Ⅲ. 3.   NETWORK UNIT
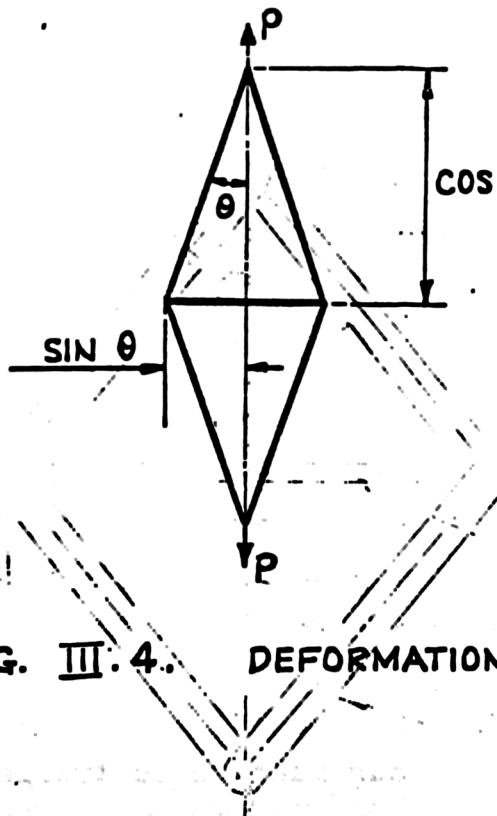

FIG. Ⅲ. 4.   DEFORMATION OF UNIT.

either the viscoelastic ground substance alone or by
the ground substance and elastin fibres. As more and
more collagen fibres become oriented, the stress-strain
curve approaches asymptotically to the stress-strain
curve of collagen. This process is shown diagrammatically
in Fig III.2.

III.2.1 <u>Network with perfectly elastic elements</u>

With this concept of the mechanical behaviour of
skin in mind, the load-extension behaviour of a very
simple network model was investigated. This was
conceived to consist of a large number of microscopic units
of the type shown in Fig III.3. The side links of this
unit consist of linear, perfectly elastic springs of
stiffness β. The cross link has non-linear viscoelastic
properties in general, but initially the viscous effects
will be neglected to simplify the analysis. In this form
the behaviour of the network is relevant to uniaxial tests
carried out at a constant strain rate. In the unloaded
condition, the network configuration is described by the
half angle α.

The application of a load p to this unit will
cause a deformation to the position described by half angle
θ as shown in Fig III.4. The deformation of the side
links is considered to represent the deformation of the
collagen fibres in skin and, because this is negligible
until the fibres are fully oriented, the side links are
assumed to be rigid until θ tends to zero.

Under these conditions, the force in the cross
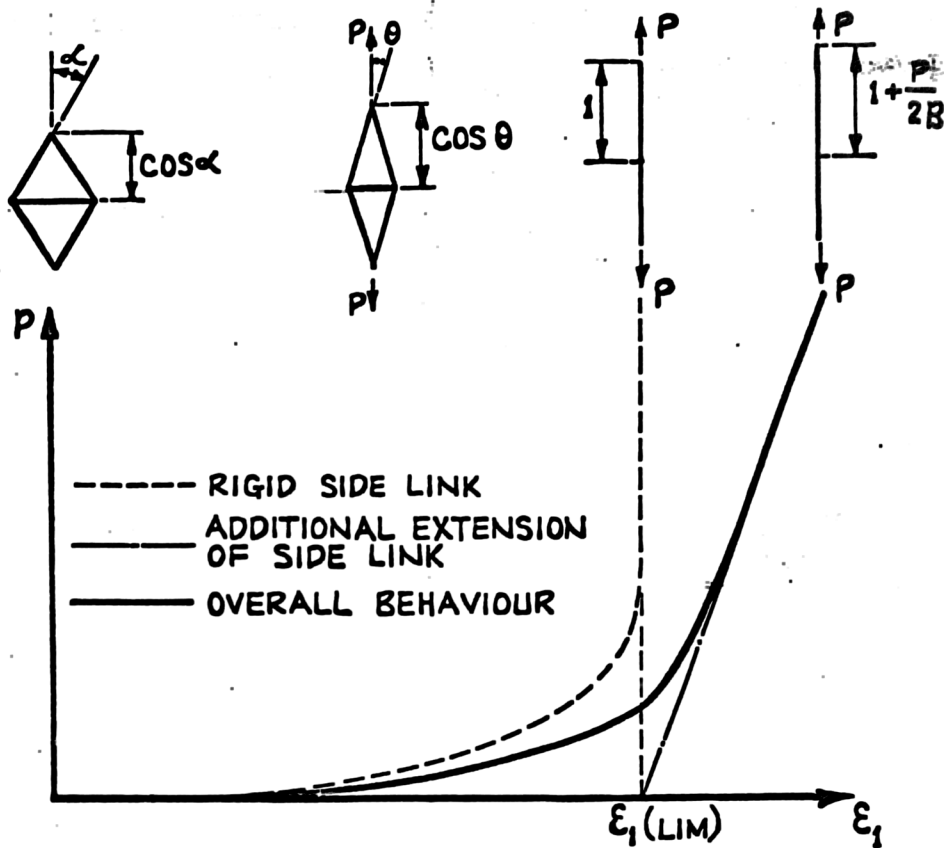link is given by:

FIG. III. 5. OVERALL EXTENSION OF UNIT IS OBTAINED BY ADDING THE SIDE LINK EXTENSION UNDER LOAD P TO THE EXTENSION OF A UNIT WITH RIGID SIDE LINKS UNDER THE SAME LOAD.
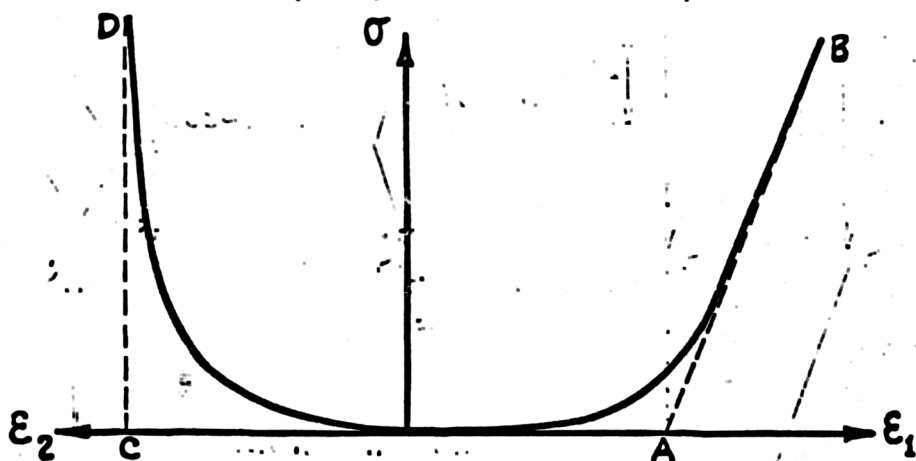

FIG. III. 6. TYPICAL STRESS STRAIN CURVE FOR SKIN (DIAGRAMMATIC)

$$p \tan \theta = f(\text{cross link deformation})$$
$$= f(\sin \alpha - \sin \theta) \qquad \text{III.1}$$

The form of the function $f(\sin \alpha - \sin \theta)$ depends on the physical properties of the ground substance. This function was therefore indirectly assessed by solving equation III.1 for various forms of the function by numerical procedures. The simplest function which gave a reasonable fit to the experimental data was:

$$p \tan \theta = 2\gamma (\sin \alpha - \sin \theta)^4 \qquad \text{III.2}$$

This equation in p and θ can readily be solved numerically by Newton's method.

The corresponding strain can then be calculated from:

$$\varepsilon_1 = \frac{\cos \theta - \cos \alpha}{\cos \alpha} \qquad \text{III.3}$$

where ε_1 = strain in direction of p.

In considering the effect of the side link stiffness, it has been assumed that no significant deformation of the side links occurs until θ is small. It will be a sufficiently good approximation to calculate the deformation of the side links under force p and add this directly to the strain calculated from equation III.3. This process is shown diagrammatically in Fig III.5.

The lateral contraction accompanying this extension can be found from:

$$\varepsilon_2 = \frac{\sin \alpha - \sin \theta}{\sin \alpha + \delta} \qquad \text{III.4}$$

where ε_2 = strain perpendicular to the direction of p
δ = thickness of side link

The mechanical behaviour of this model can therefore be defined in terms of the four parameters:

α = initial half angle of unit

β = side link stiffness

γ = cross link stiffness coefficient

δ = side link thickness

It is now possible to analyse the experimental stress-strain curves for skin in terms of these parameters as follows:

A typical stress-strain curve for skin is shown in Fig III.6.

The curve for σ v. ε_1 has the sloping asymptote AB and the curve for σ v. ε_2 has the vertical asymptote CD.

Comparison of the load-extension curve with Fig III.5 shows that the strain OA corresponds to the limiting strain of a network with rigid side links and is given by:

$$\varepsilon_1 \text{ (lim)} = \frac{1 - \cos \alpha}{\cos \alpha}$$

$$\alpha = \cos^{-1} \frac{1}{1 + \varepsilon_1 \text{ (lim)}} \qquad \text{III.5}$$

In calculating the side link stiffness β, account has to be taken of the effect of the change in the base from which strain is measured on the slope Δ of the asymptote AB. The additional extension of the unit resulting from replacing the rigid side links by elastic side links is:

$$\frac{P}{\beta}$$

the total length of the unit is:
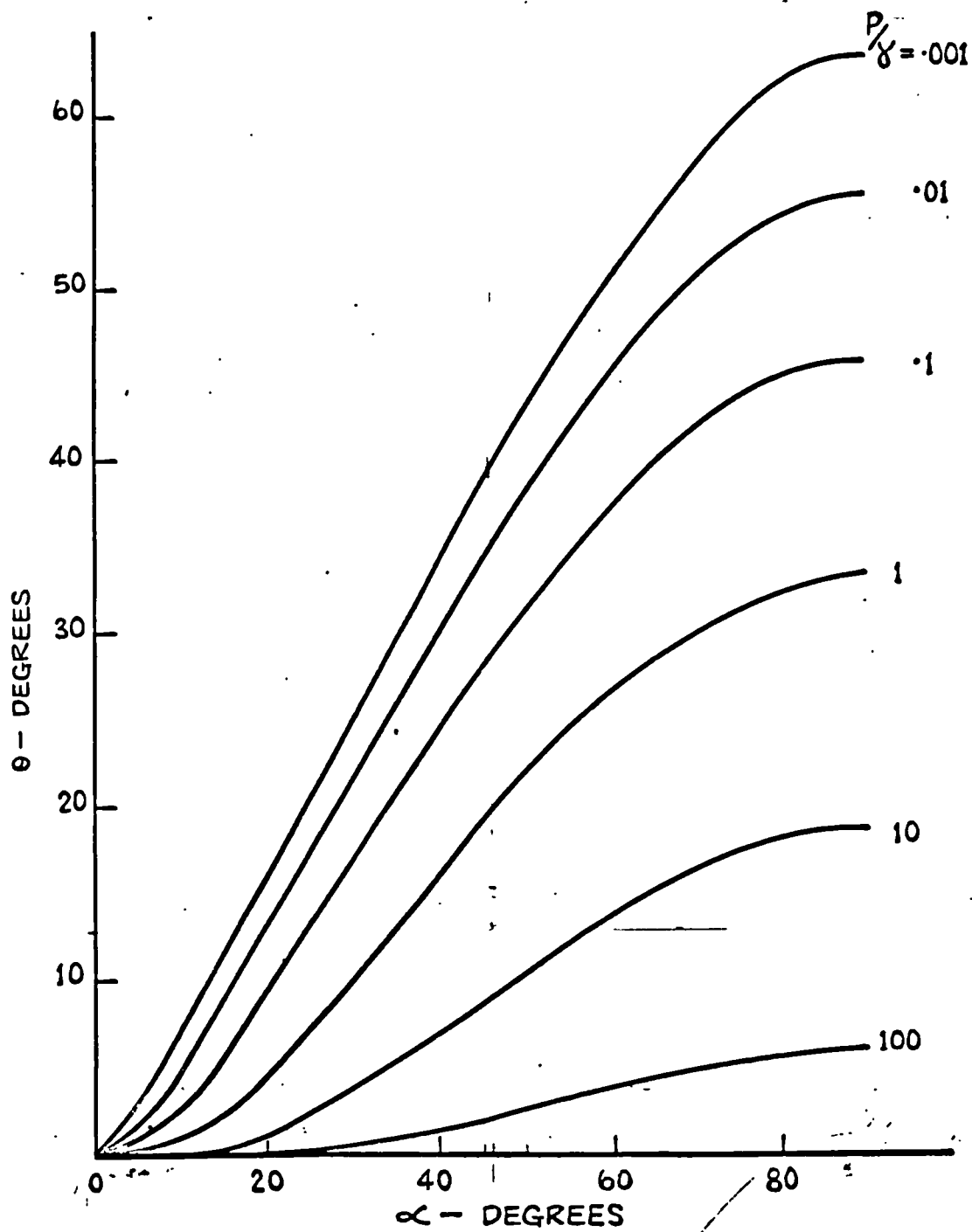
FIG. III. 7.   SOLUTION OF EQUATION III. 2.

$$\frac{P}{\gamma} = \frac{2}{TAN\ \theta} (SIN\ \alpha - SIN\ \theta)^4$$

$$2 + \frac{P}{\beta}$$

$$\varepsilon_1 = \frac{1 + \frac{P}{2\beta} - \cos\alpha}{\cos\alpha} \qquad \text{III.6}$$

However, from Fig III.6 it can also be seen that:

$$\varepsilon_1 = \frac{1}{\cos\alpha} - 1 + \frac{P}{\Delta}$$

Equating with III.6 gives:

$$\beta = \frac{\Delta}{2\cos\alpha} = \frac{\Delta}{2}\left[1 + \varepsilon_1 \text{ (lim)}\right] \qquad \text{III.7}$$

The cross link stiffness factor γ is found from the solution of equation III.2 shown in Fig III.7. The value of α is known from equation III.5. Therefore, from the value of ε_1 corresponding to any given value of p, a value of θ can be determined from equation III.3 and hence γ can be determined from Fig III.7.

The value of δ can be found by considering ε_2 (lim), the value of ε_2 given by the vertical asymptote of the σ v. ε_2 curve.

From equation III.4 as θ tends to zero:

$$\varepsilon_2 \text{ (lim)} = \frac{\sin\alpha}{\sin\alpha + \delta}$$

$$\delta = \sin\alpha \; \frac{1 - \varepsilon_2 \text{ (lim)}}{\varepsilon_2 \text{ (lim)}} \qquad \text{III.8}$$

FIG. III. 8. NETWORK ANALYSIS – ∝ Vs AGE
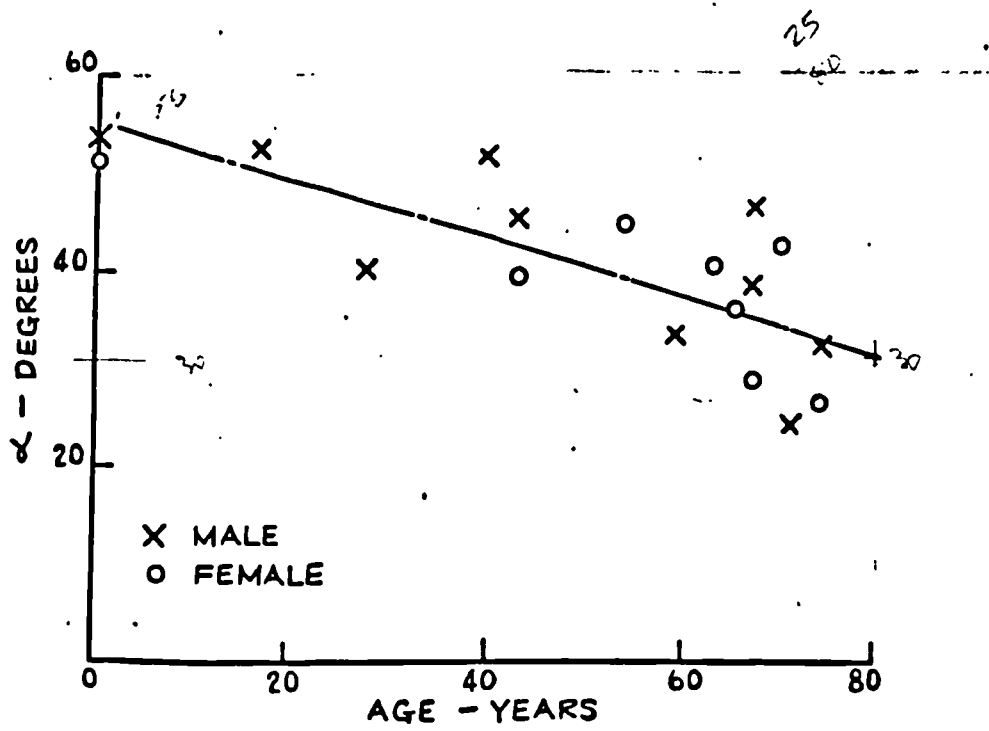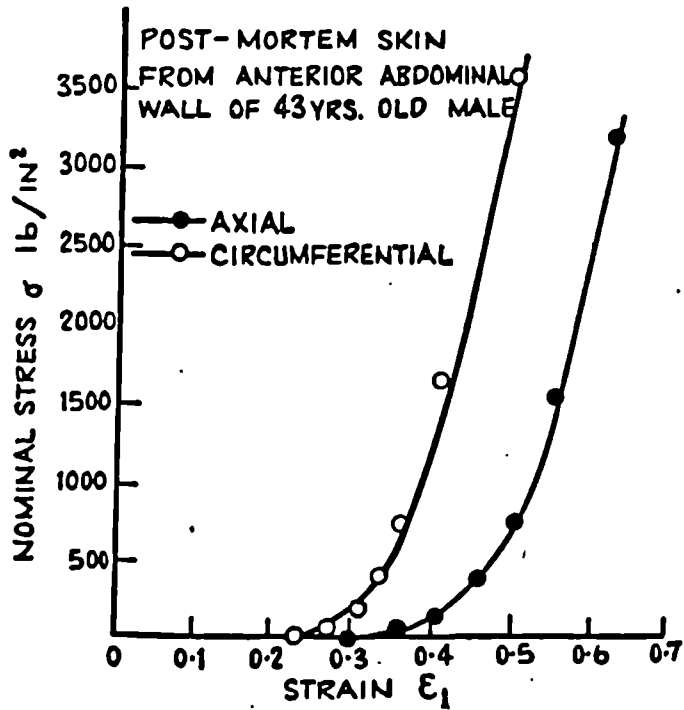(PILOT EXPERIMENTS)

FIG III. 9. PILOT EXPERIMENTS – VARIATION OF STRESS–STRAIN
CURVES WITH ORIENTATION

The results of the pilot experiments were analysed in terms of this model. The value of α was found to decrease with increasing age (Fig III.8). None of the other parameters was age-dependent. These results are fully discussed in Chapter V.

The network model in the above form is subject to two principal restrictions:

(i) It is essentially a uniaxial model

(ii It has no viscoelastic properties.

To overcome the first of these problems it is necessary to abandon the concept that the simple unit of the model corresponds to the fundamental microscopic unit of the collagen network in the dermis. Instead one can postulate that the model represents the average properties in a given direction of a large number of units of the collagen network and that the model parameters are a function of the direction in which the load is applied.

In several of the pilot experiments, specimens were tested which had been obtained from adjacent sites and which were oriented either parallel or perpendicular to the cranio-caudal median. The only parameter which showed a consistent variation with orientation was α, this being always smaller for the specimens oriented perpendicular to the cranio-caudal median (Fig III.9). These results are also discussed in Chapter V.

III.2.2 <u>Network with viscoelastic elements</u>

To take account of the viscoelastic properties of skin it is necessary to consider the behaviour of the network when the perfectly elastic members of the model are given time-dependent properties. Three possible

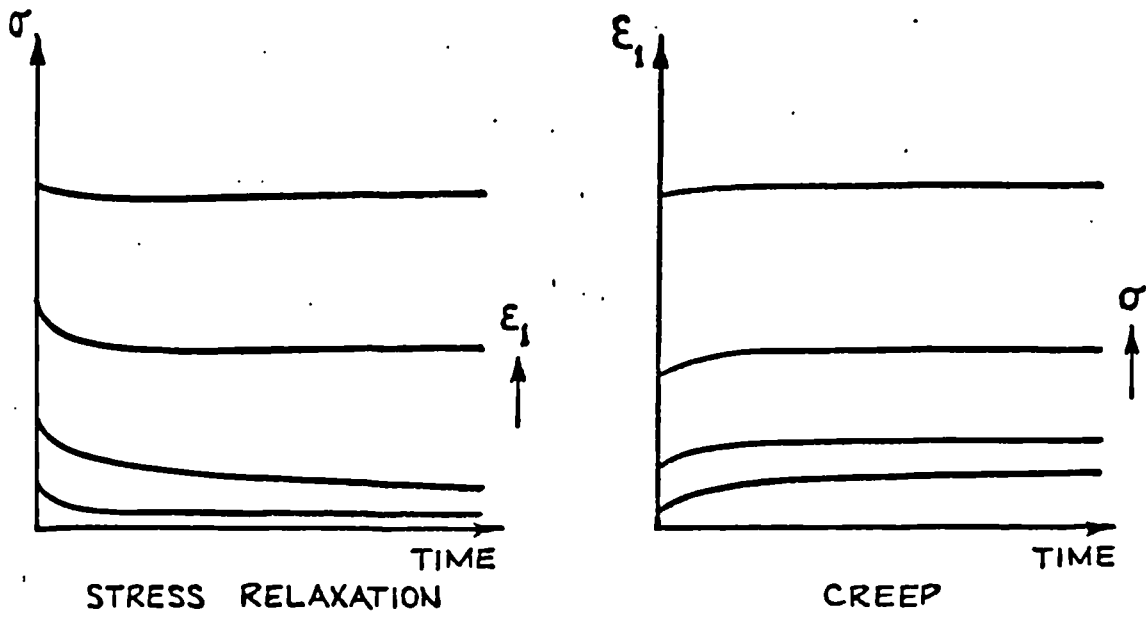STRESS RELAXATION

CREEP

FIG. III 10.   STRESS RELAXATION AND CREEP BEHAVIOUR
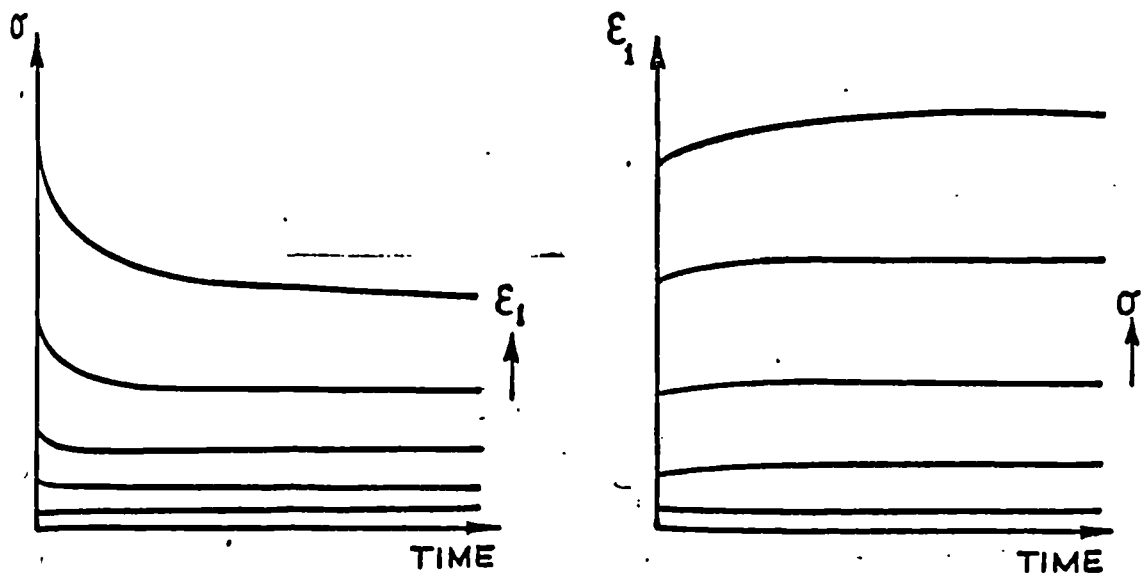OF MODEL WITH VISCOELASTIC CROSS MEMBER

FIG. III 11   STRESS RELAXATION AND CREEP BEHAVIOUR
OF MODEL WITH VISCOELASTIC SIDE MEMBERS

arrangements of the model can be considered:

(i)   side links elastic, cross member time-dependent

(ii) side links time-dependent, cross member elastic

(iii) all members time-dependent.

As the exact form of time-dependence found in skin has to be determined experimentally, it is only possible in this Chapter to consider the behaviour of these three systems in a qualitative manner.

Fig III.10 shows the type of behaviour which would obtain in stress-relaxation and creep tests with only the cross member being time-dependent.   At low stress levels, the deformation of the model is predominantly a function of the cross member.   Marked stress-relaxation and creep effects would therefore be found under these conditions. At high stress levels, the behaviour is controlled by the elastic side members and, therefore, the time effects would be reduced in magnitude.   As will be shown in Chapter V this model does not describe the results obtained experimentally.

Fig III.11 shows the effect of having only the side members time-dependent.   The behaviour is the converse of that described above, the viscoelastic effect becoming apparent only at the higher stress levels as the side members begin to carry load directly.   In Chapter V it will be shown that this is the type 'of behaviour exhibited by skin.

With all members time-dependent, viscoelastic effects are apparent throughout the stress range (Fig III. 12).   This type of behaviour was not found to be relevant to skin.
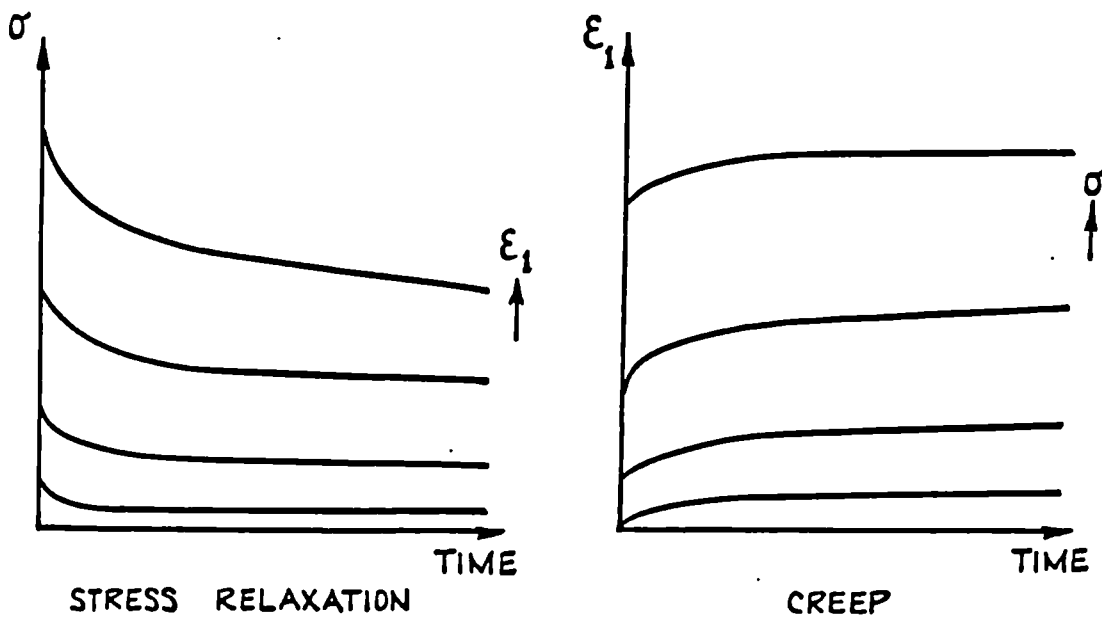
FIG. III. 12   STRESS RELAXATION .AND CREEP BEHAVIOUR
OF MODEL WITH VISCOELASTIC CROSS
MEMBER AND SIDE MEMBERS.

III.3   Rational Theories

There are two techniques whereby the behaviour
of materials subject to finite strains can be rationally
analysed:

(i)   Statistical Mechanics
(ii) Continuum Mechanics

III.3.1   Statistical mechanics

In the method of statistical mechanics, the
overall stress-strain properties of the gross material
are deduced by considering the effects of the applied
forces at the molecular level.   This type of approach
leads to useful stress-strain curves for the class of
materials known as elastomers in which strain energy is
not stored as internal energy in the material but results
in a decrease of the entropy of the material.   When
stress is removed the material reverts to its maximum
entropy (i.e. most probable) configuration.   The
derivation of the stress-strain relation for an ideal
elastomer is given in Appendix A.III.

This type of theory is not able to yield stress-
strain relations for materials in which strain energy is
stored as internal energy nor is it able to deal with
viscous effects.   As skin has very marked viscoelastic
properties and as its main fibrous constituent is collagen,
which Hall (1952) has shown does not exhibit an entropy
decrease on extension, this type of theory is not
relevant to skin.

III.3.2   Continuum mechanics

The methods of continuum mechanics may be used
to develop general stress-strain-time relations for
materials subject to finite deformation

Lockett (1965) outlined the derivation of such relations and has discussed the experimental work necessary to find them for a certain type of material. Two assumptions were made about this material.

(i) it is isotropic in the undeformed state

(ii) the stress at a given particle in the material at time t depends only on the displacement gradients at that particle at all times up to and including time t.

A deformation is considered in which a particle initially with coordinates X_i (i = 1, 2, 3) with respect to a fixed rectangular Cartesian coordinate system moves to a position $x_i(\tau)$ at some later time τ.

It is shown in Appendix A.IV that the constitutive relation (i.e. stress-strain-time relation) can, in general, be written in the matrix form:

$$Q = D(P)$$ III.9

when, either $Q = R^{\tau} \bar{\sigma} R$ $P = E$

or $Q = E$ $P = R^{\tau} \sigma R$

and D is a matrix functional of P

σ is the stress matrix at point x_i

E is the strain matrix at point x_i

and is defined by:

$$E = \left[E_{ij} \right]$$

$$2E_{ij} = \frac{\partial x_k}{\partial X_i} \frac{\partial x_k}{\partial X_j} - \delta_{ij}$$

$$\delta_{ij} = \begin{bmatrix} 1, & i = j \\ 0, & i \neq j \end{bmatrix}$$

If the deformation of the material is defined by $F = \begin{bmatrix} F_{ij} \end{bmatrix}$

$$F_{ij} = \frac{\partial x_i(\tau)}{\partial X_j}$$

this can be split into a rigid body rotation R and a pure, homogeneous strain M

thus F = RM

R^τ is the transpose of R.

It is further shown in Appendix A.IV that for the type of material considered, equation III.9 can be written in the form:

$$Q(t) = \int_0^t \{I\psi_1 T_1 + \psi_2 M_1\} d\tau_1$$

$$+ \int_0^t\!\!\int_0^t \{I\psi_3 T_1 T_2 + I\psi_4 T_{12} + \psi_5 T_1 M_2 + \psi_6 M_1 M_2\} d\tau_1 d\tau_2$$

$$+ \ldots\ldots\ldots\ldots \qquad\qquad III.10$$

where:

$$T_\alpha = \text{tr } \dot{p}(\tau_\alpha)$$

$$T_{\alpha\beta} = \text{tr } \dot{p}(\tau_\alpha)\, \dot{p}(\tau_\beta) \qquad etc$$

$$M_\alpha = \dot{p}(\tau_\alpha)$$

ψ_1; ψ_2 are functions of $t - \tau$
$\psi_3 - \psi_6$ are functions of $t - \tau_1$; $t - \tau_2$. etc. These functions characterise the mechanical properties of the material and have to be found experimentally using the test programme described by Lockett (1965). The practical difficulties involved in this would be very considerable

as several hundred tests would be required to determine
these functions for <u>one</u> specimen even if only the first
three terms of III.10 were considered. For this reason
it would be impractical to use this type of theoretical
approach to obtain a complete description of the
mechanical properties of skin.

III.3.3   Uniaxial experiments

However, it is still of interest to investigate
the viscoelastic properties of skin by means of stress-
relaxation and creep tests in which case one has to
analyse the experimental data in terms of the above theory.
If only uniaxial tests are considered, it is possible
greatly to simplify equation III.10 as the matrices P and
Q will only have one non-zero component, thus:

$$P = \sigma \qquad Q = E \text{ (creep test)}$$

$$\text{or} \quad P = E \qquad Q = \sigma \text{ (stress relaxation test)}.$$

In the case of a creep test (to obtain the
relations appropriate to a stress relaxation it is only
necessary to interchange σ and E). Equation III.10
becomes:

$$E(t) = \int_0^t J(t-\tau)\, \dot{\sigma}(\tau)d\tau$$

$$+ \int_0^t\int_0^t K(t-\tau_1;\, t-\tau_2)\, \dot{\sigma}(\tau_1)\, \dot{\sigma}(\tau_2)d\tau_1\, d\tau_2$$

$$+ \int_0^t\int_0^t\int_0^t L(t-\tau_1;\, t-\tau_2;\, t-\tau_3)\, \dot{\sigma}(\tau_1)\, \dot{\sigma}(\tau_2)\, \dot{\sigma}(\tau_3)\, d\tau_1\, d\tau_2\, d\tau_3$$

$$+ \ldots\ldots\ldots \qquad\qquad\qquad\qquad\qquad \text{III.11}$$
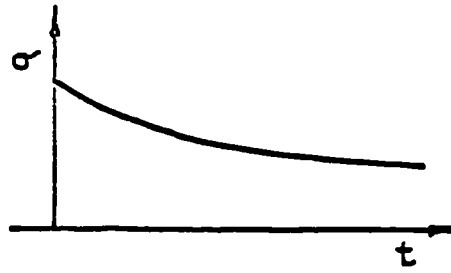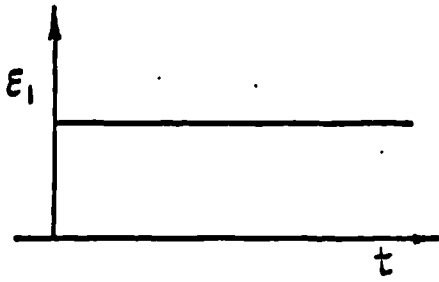
(a) SINGLE STEP TEST
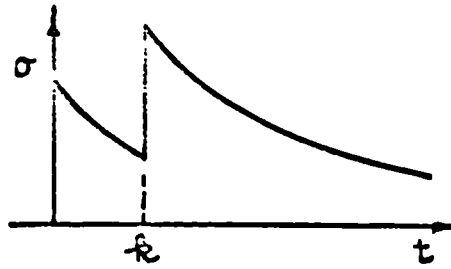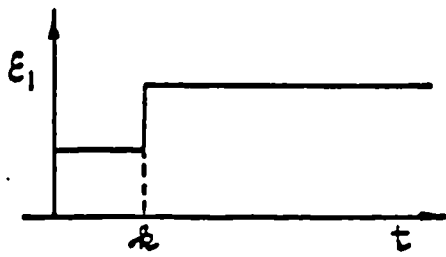
(b) TWO STEP TEST
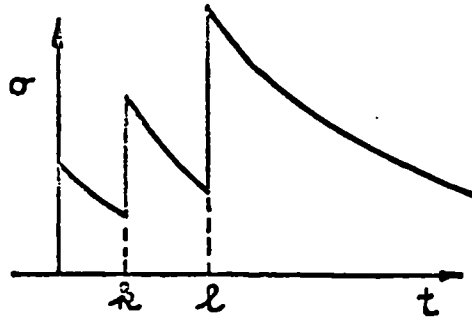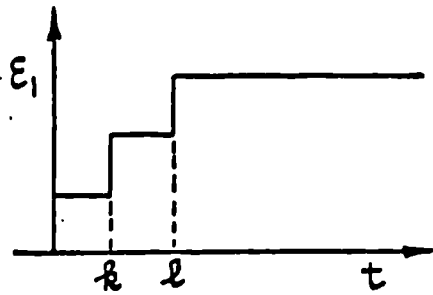
(c) THREE STEP TEST.

FIG. II 13 - MULTI-STEP STRESS RELAXATION TESTS.

Only the first three terms will be considered.   It
should be noted that:

$$2E = (\frac{\partial x}{\partial X})^2 - 1$$

and that if the material is homogeneous:

$$2E = (\frac{x}{X})^2 - 1$$

The classical strain component ε is defined by:

$$\varepsilon = \frac{x}{X} - 1$$

$$E = \varepsilon + \frac{\varepsilon^2}{2} \qquad \text{III.12}$$

It is shown in Appendix A.V that the functions
$J(t - \tau_1)$, $K(t - \tau_1; t - \tau_2)$, $L(t - \tau_1; t - \tau_2; t - \tau_3)$
can be completely determined by the test programme shown
in Table III.1 and Fig III.13.   It will be seen that,
even in the uniaxial case, a large number of tests is
still required.   For example, if n = 8 (i.e. 8 different
values of k and 8 different values of ℓ are considered),
a total of 59 tests will be required on <u>one</u> specimen.

Table III.1

Stress Relaxation Test Programme for
Non-linear Viscoelastic Material

Test No.	Straining Programme	Test Description	No. of Experiments
1	$E(t) = c_1 H(t)$	one step	1
2	$E(t) = c_2 H(t)$	" "	1
3	$E(t) = c_3 H(t)$	" "	1
4	$E(t) = a_1 H(t) + b_1 H(t-k)$	two step	n
5	$E(t) = a_1 H(t) + b_2 H(t-k)$	" "	n
6	$E(t) = a_3 H(t) + b_1 H(t-k)$	" "	n
7	$E(t) = aH(t) + bH(t-k) + cH(t-\ell)$	three step	$\frac{1}{2}n^2$

$$H(x) = \begin{bmatrix} 0, & x < 0 \\ 1, & x \geqslant 0 \end{bmatrix}$$

Tests 4, 5 and 6 have to be repeated for n values of k. Test 7 has to be repeated for n values of k and n values of ℓ in the range $0 < k < \ell$. n is the number of points required to define the functions in equation III.11 to the required accuracy.

The practical difficulties involved in attempting to approximate to a constant strain rate test by using a large number of discrete steps would render the use of this type of theory impossible for more than the crudest approximation. However, for the analysis of creep and stress relaxation tests it is the only rational approach.

Ward and Onat (1963) have shown that the method can be applied to the analysis of the creep behaviour of oriented polypropylene fibres.   They showed very clearly that the relations based on the assumption of linear viscoelastic behaviour were inadequate and that it is essential to use the more general expressions derived above.   It should be noted that in the case of small deformations and linear behaviour, equation III.11 reduces to:

$$\epsilon(t) = \int_0^t J(t - \tau) \; \dot{\sigma}(\tau) \; d\tau$$

which is the uniaxial constitutive relation for a linear viscoelastic material.

A test programme of the form given in Table III.1 was carried out on a specimen of skin.   The results of this test are analysed in Chapter V.   This practical application of the continuum mechanics theory makes much clearer many points which are not obvious from the inevitably somewhat abstruse matrix algebra presentation given above.

III.4   Summary

It is apparent that no single theoretical approach among those considered above is capable of adequately describing the whole of the mechanical properties of skin.

The network type of theory has the advantage that it gives some idea of the mechanism of deformation of skin but it is restricted in doing this more fully by the lack of knowledge of the viscoelastic properties of the ground
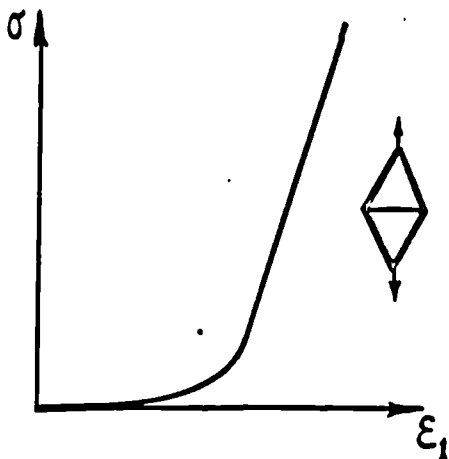
(a) STIFF SIDE LINK
WEAK CROSS LINK
LARGE α
eg. SKIN
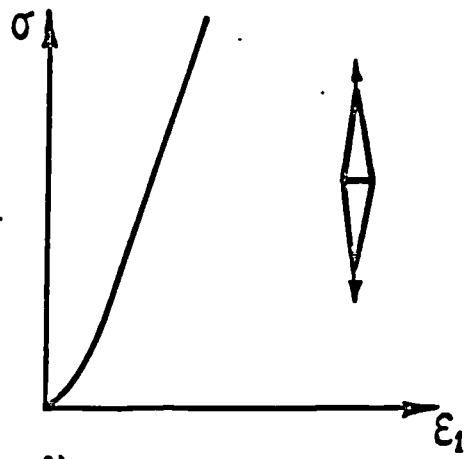
(b) STIFF SIDE LINK
WEAK CROSS LINK
SMALL α
eg. TENDON
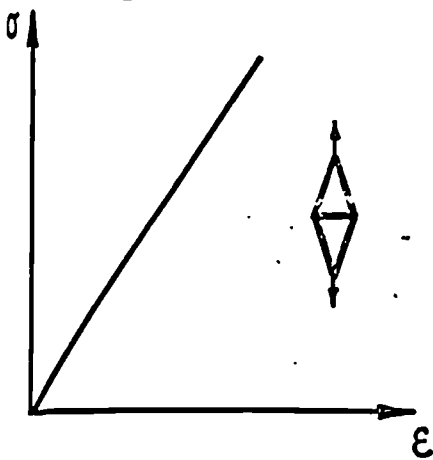
(c) STIFF SIDE LINK
STIFF CROSS LINK
LARGE α /
eg. CARTILAGE
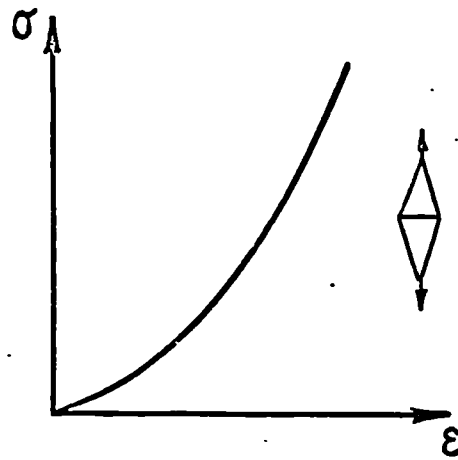
(d) WEAK/ SIDE LINK
WEAK CROSS LINK
LARGE α
eg. LIGAMENT

FIG. III. 14. BEHAVIOUR OF DIFFERENT NETWORK
CONFIGURATIONS REPRESENTING VARIOUS
TYPES OF CONNECTIVE TISSUE STRUCTURE

substance. It is, however, very useful in analysing the type of standardised, constant strain rate test which is the most convenient method for testing a reasonable number of specimens. Also, this type of theory is by no means restricted in application to skin but can, subject to simple modifications, be applied to a wide variety of connective tissue structures (Fig III.14).

Continuum mechanics theory is, in principle, capable of analysing any type of loading programme on a material such as skin. However, the practical difficulties involved in dealing with anything other than the very simplest cases render this method useless except for the analysis of simple creep and stress relaxation tests. This situation may improve as the whole field of continuum mechanics is at present the subject of intensive mathematical research.

Using the results of the pilot experiments
described in Chapter II as a basis, more refined testing
techniques were developed to investigate the mechanical
properties of skin *in vitro*.

IV.1   Uniaxial Tensile Tests

The classical engineering approach to
investigating the mechanical properties of any material
is the uniaxial tensile test.   This is a basically simple
technique with which large numbers of specimens can be
tested in a reasonable time.   In the case of skin, it
may be thought desirable to use a biaxial testing tech-
nique because skin *in vivo* is in a state of biaxial
tension.   However, because of the large number of para-
meters which have to be measured in such tests and the much
more complicated equipment required, it was decided to
restrict the investigation to the uniaxial technique.   It
was felt that this would provide more meaningful results
from a larger number of specimens.

IV.2   Design of Equipment

The requirements for uniaxial tensile tests of
skin outlined in Chapter II were used to draw up a
specification for the design of suitable equipment (Table
IV.1).   For clarity only a brief description of this
equipment in its fully developed form is given below.
Details of construction, technique and development
problems are given in various appendices at the end of
the thesis.

IV.2.1   Specimen loading apparatus

The testing frame is shown in Fig IV.1.   The
crosshead A was driven in the vertical direction by the
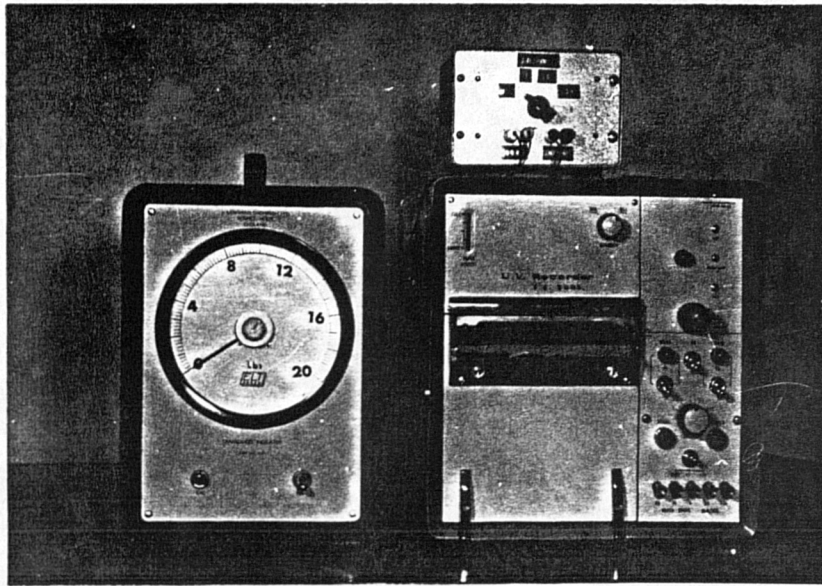hollow lead screw B.

Fig IV.2   Load Measuring and Recording Equipment
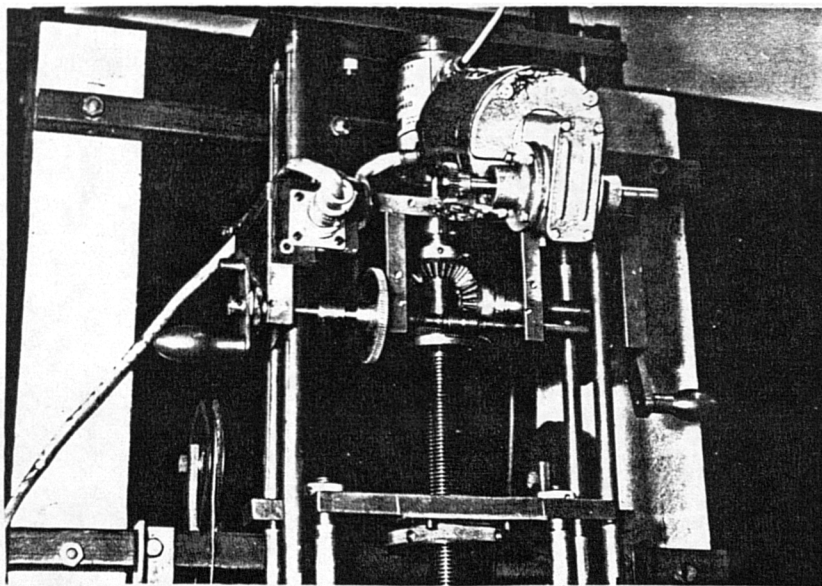
Fig IV.3   Crosshead Drive Motor and Gearing

The motor of this crosshead was transmitted by the push
rods CC to the lower crosshead D below the frame. Any
suitable type of specimen grip E could be mounted on this
crosshead. The upper grip F was suspended directly from
the load cell G by means of a rod passing through the
hollow lead screw. This arrangement ensured that the
tension in the specimen was measured accurately with no
possibility of error due to friction effects. Load cell
output was displayed on the Transducer Indicator (A in
Fig IV.2) and was simultaneously recorded on the Southern
Electrics Ultra Violet Recorder, type 2005 (B in Fig IV.2).
The attenuator box C allowed the effective sensitivity of
the system to be varied during the test. Therefore, a
high sensitivity could be used during the initial large
extension at very small loads which is characteristic of
skin. The sensitivity could then be reduced as the load
increased towards specimen failure.

The crosshead driving facilities are shown in
detail in Fig IV.3. Rapid traverse of the crosshead was
achieved by the handle A driving *via* the bevel gears B.
The worm gear drive C could be operated either manually
or by the reversible induction motor D, the gearing being
such that the crosshead speed was 0.667 in./min.

Environmental control of the specimen was obtained
using the tank and temperature control equipment shown in
Fig IV.4. The tank was mounted on vertical runners and
was counterbalanced so that it could easily be lowered to
facilitate specimen loading. The liquid used in the tank
was Ringer's solution. The temperature of this solutinn
could be maintained at any desired value above ambient to
within $\pm 0.5^\circ C$ by means of two 1 kw heaters and the
Fielden temperature controller. A small pump was used to
maintain a gentle circulation of the solution through the
tank.
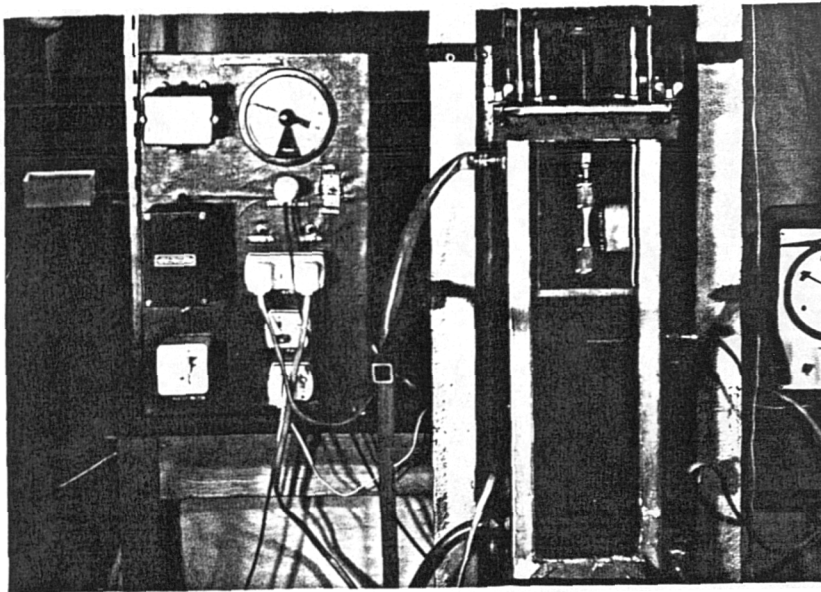
Fig IV.4   Immersion Tank and Temperature Control
            Equipment

Chapter IV

Systematic Experimental Work *in Vitro*
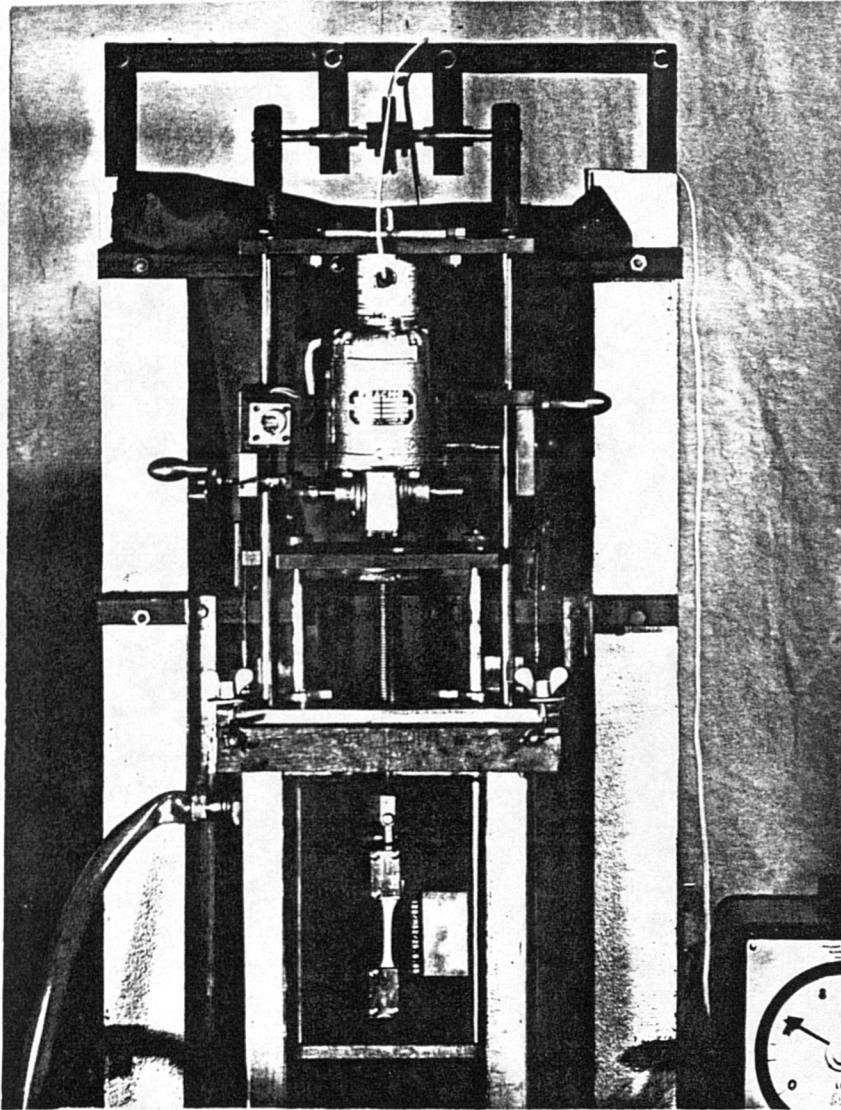
Fig IV.1   Tensile Testing Machine Designed and
            Built in the BioEngineering Unit
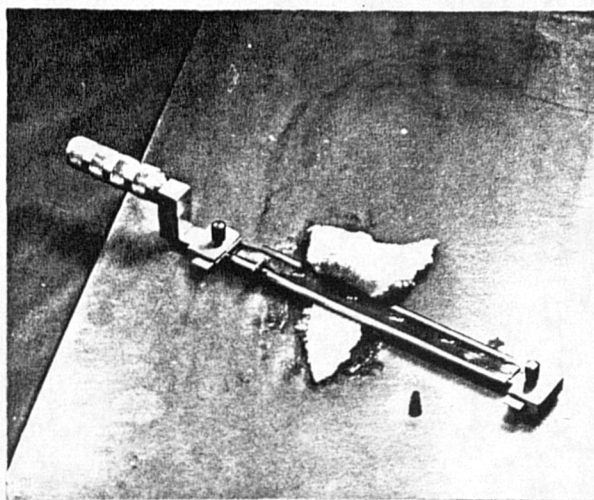
(a) removal of
    subcutaneous
    fat
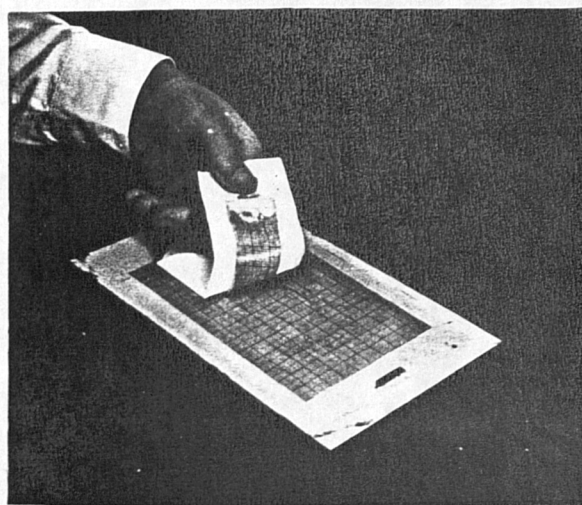
(b) a grid is printed
    on the epidermal
    surface
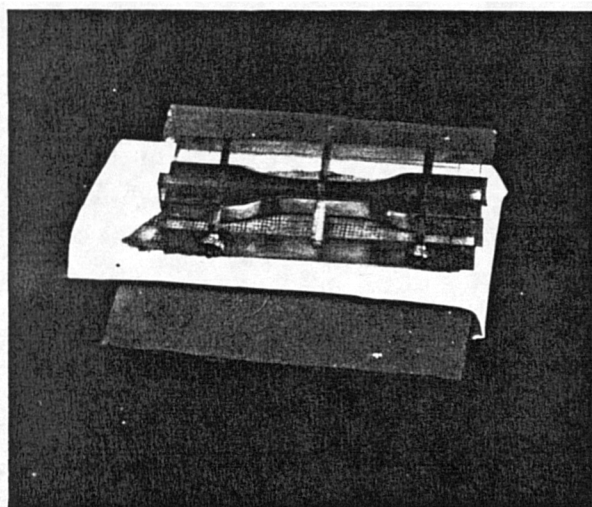
(c) a waisted specimen
    is made with this
    "pastry cutter"
    type punch
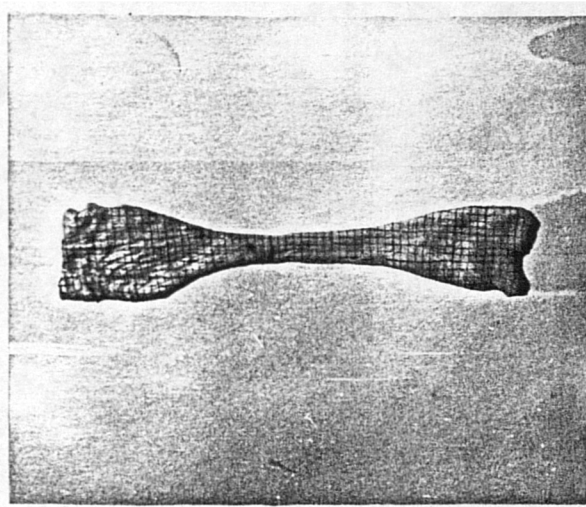
(d) the finished specimen

Fig IV.5   Preparation of Specimen
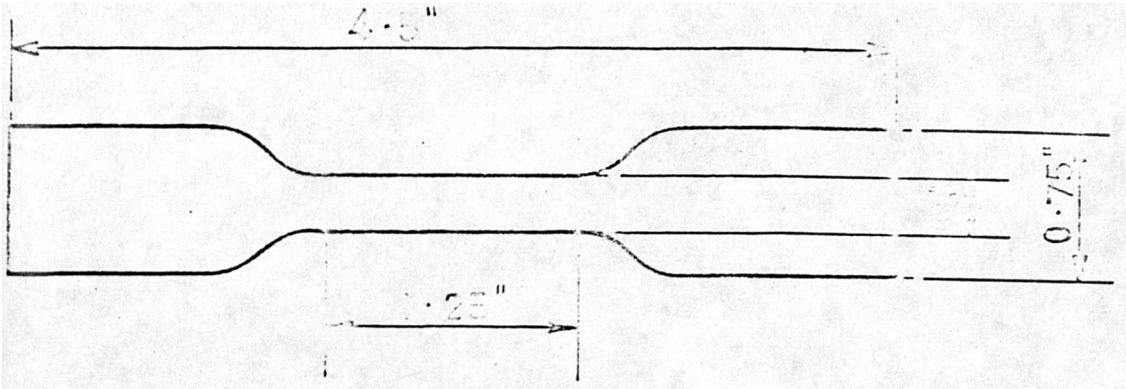
FIG. IV 6.   SPECIMEN DIMENSIONS
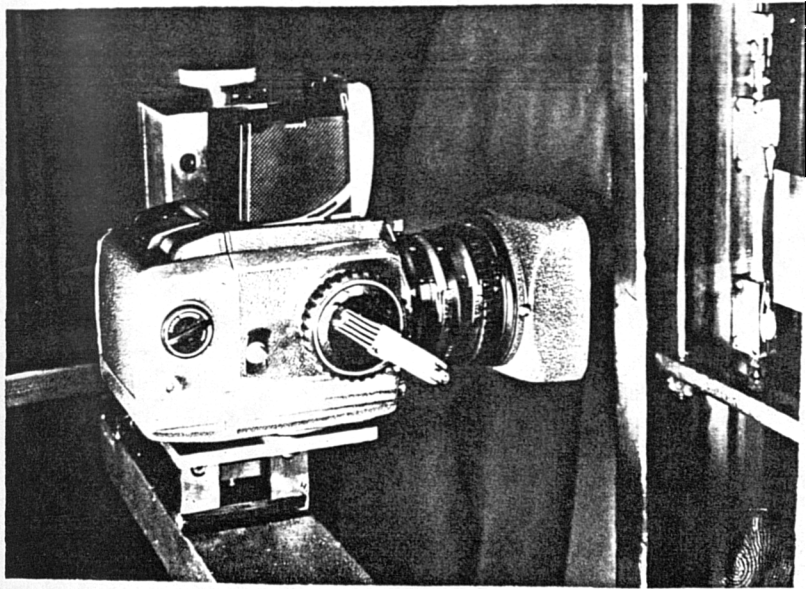
FIG. IV 7.   PHOTOGRAPHIC STRAIN
              MEASURING EQUIPMENT.

IV.2.2   Specimen preparation

Skin samples were obtained from cadavers at
autopsy.   Abdominal skin was excised from the area below
the umbilicus except in the case of infants, when skin
from the whole length of the chest was excised. Various
stages in the preparation of the specimens are shown in
Fig IV.5.   The grid printed on the specimen was used for
strain measurement as described below.   The dimensions
of the specimen are given in Fig IV.6.   All specimens were
tested within 48 hours of death, being stored in Ringer's
solution at $4^{\circ}C$ until required for test.

IV.2.3   Strain measurement

Because skin is subject to appreciable deformations
under very small stresses, it was impossible to use any
form of mechanical device contacting the specimen to measure
the deformation during test.   An optical strain measuring
technique was therefore necessary.

A photographic method was used, the deformations of
a grid printed on the epidermal surface of the specimen
being recorded at short time intervals by the equipment
shown in Fig IV.7.   Because of the large extensions
obtaining in skin, it was necessary for the camera to be
moved down during the test to keep its optical axis in
line with the centre of the specimen.   For this reason,
the camera was mounted on a screw operated vertical slide.

The negatives obtained by the above technique (Fig
IV.8) were measured using a Watson stereomicroscope (Fig
IV.9), the table of which was equipped with a dial gauge
and micrometer drive.

The specimen was illuminated by an electronic
flash gun giving an effective exposure time of 1 m.sec.
The flash gun also provided a very convenient pulse which
was recorded on the u.v. Recorder so that the strain
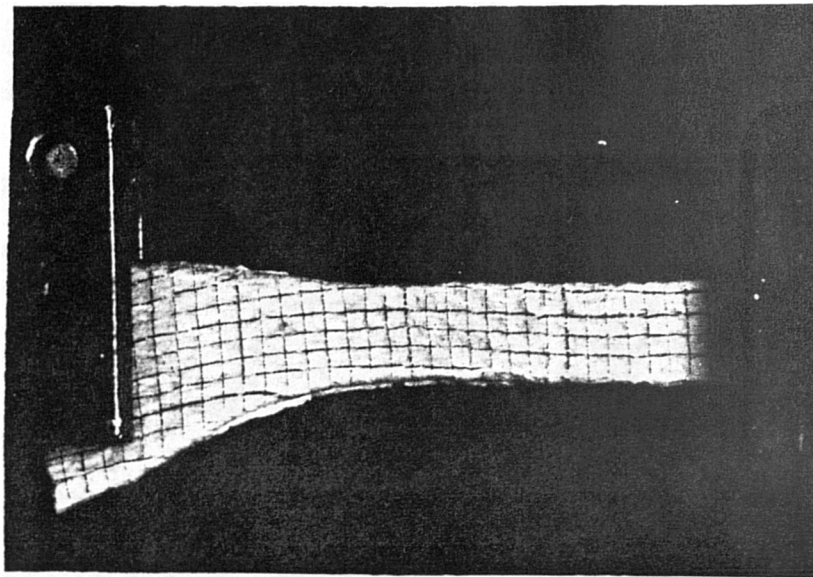
(a)   Grid on Unstressed Specimen
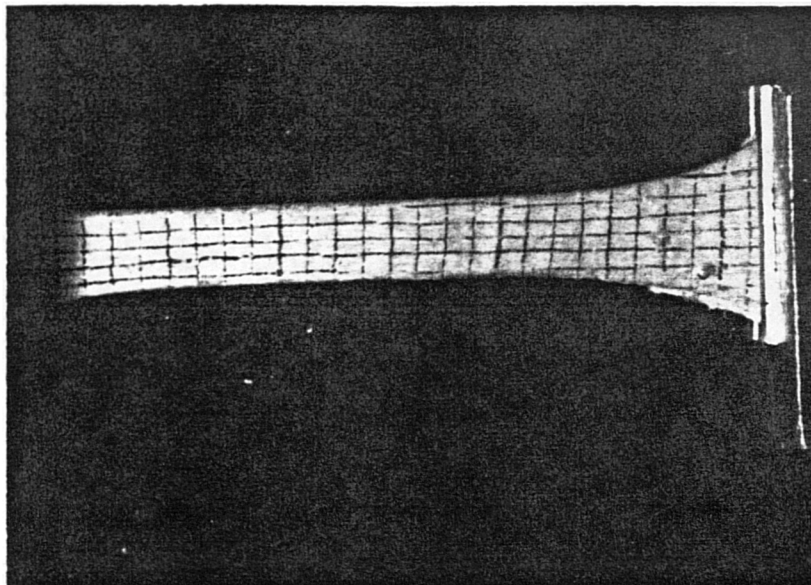
(b) Grid on Stressed Specimen

Fig IV.8   Photographic Strain Measurement - Typical
Results
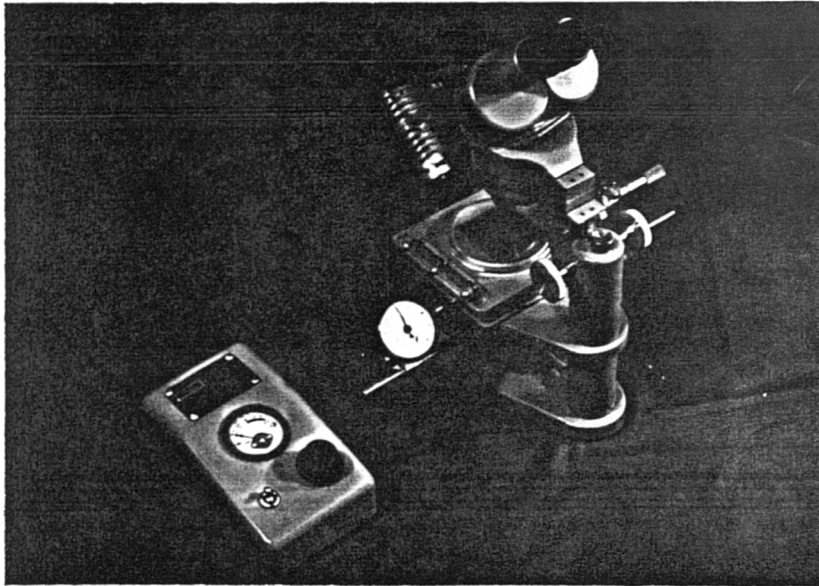
Fig IV.9   Watson's Stereomicroscope used for
Measurement of Negatives
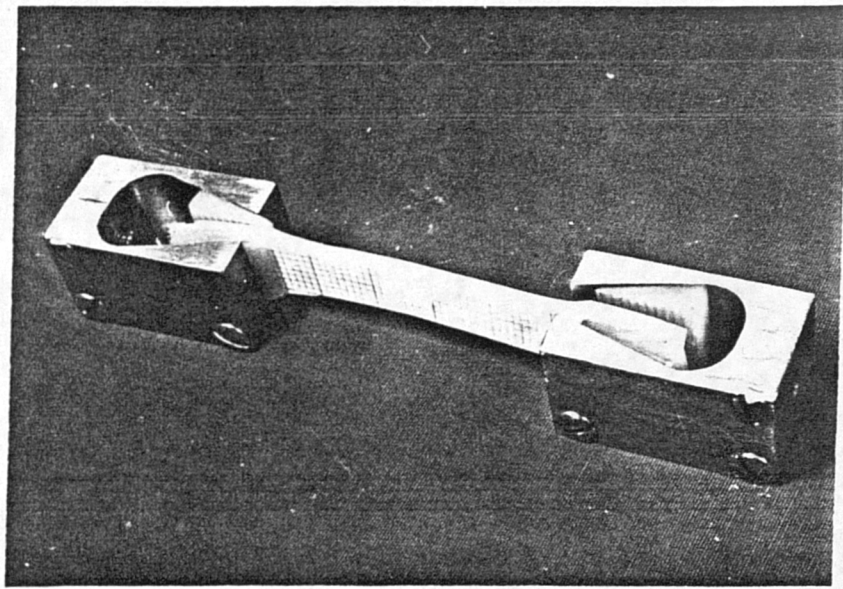
Fig IV.10   Wedge Action Grips

values could be correlated with the load at the instant of exposure.

IV.2.4   Specimen grips

The grips used were of the self-tightening wedge action type shown in Fig IV.10. With this design, the clamping force between the surfaces of the wedge-shaped jaws is proportional to the force applied along the axis of the specimen. This feature combined with the serrated jaw faces was found to give a very satisfactory gripping action, no trouble being experienced with specimen slippage.

IV.2.5   Test techniques

As the pilot experiments described in Chapter II had shown that the ultimate strength of apparently identical specimens varied over wide limits and appeared to be sensitive to artefacts on the specimen such as small irregularities along the edges of the gauge length, it was decided   not to attempt to measure this parameter.

The majority of tests were therefore carried out using a load cell with a maximum load capability of 20 lb, this load being much lower than the expected failure load for most specimens (around 100 lb).   This cell had the further advantage of giving a higher sensitivity (.05 lb) for investigating the initial large extension of the specimen.   However, as this was found inadequate for a full investigation of this region, a number of tests was also carried out using a 2 lb cell to give greater sensitivity (.005 lb).

The actual test was very quick and simple to carry out.   With the specimen mounted in the grips and the tank

raised, a photograph was taken to establish the initial
dimensions of the specimen. The motor was then started
causing the grips to separate at 0.67 in./min. As the
load increased, ·photographs were taken at convenient
intervals until the maximum load was reached. Analysis of
the negatives and the load-time record from the u.v.
recorder allowed a stress-strain curve to be obtained.

IV.3   Test Programme with Refined Equipment
          The aims of the test programme carried out with
this machine were to investigate the possible variation with
age and sex of the parameters of the network theory
described in Chapter III, and to investigate more fully
the initial large extension at low stress levels which is
such a marked feature of the stress-strain properties of
skin.   A total of 37 tests was performed, 24 of these
being with the 20 lb load cell and the remaining 13
being with the 2 lb cell.
          Further tests were carried out to determine the
effect of varying several test parameters:

(i)   Changing the width of the specimen to
       determine the possible effect of this
       being comparable to the effective size
       of the collagen network of the dermis.
(ii)   The orientation of the specimen with
       respect to Langer's lines.
(iii) The introduction of stress concentration
       in the form of puncture patterns, small
       circular holes, etc. on the specimen.

Fig IV.11   The Instron TT-CM Tensile Testing Machine

Details of all of these tests are summarised in
Table IV.3 at the end of this Chapter. The results of
these and all subsequent tests are discussed fully in
Chapter V.

IV.4   Instron Tensile Testing Machine

At a later stage in the testing programme, an
Instron Floor Model TT-C (Fig IV.11) became available.
This machine represented a very considerable improvement
over the existing equipment from the point of view of
accuracy, long-term stability, range of testing speeds and
load sensitivity range available from each load cell. A
brief specification of this instrument is given in Table
IV.2.

The specimen preparation technique used with this
machine was identical to that used previously.

IV.4.1   Photographic strain measurement

A similar type of photographic strain measuring
technique to that employed on the original equipment was
used. In order to increase the number of shots available
it was decided to use a precision 35 mm camera giving 36
exposures per film. Also, the whole technique was
automated by using an electrical motor drive on the camera,
this being triggered by an external timing device. The
camera was mounted on a pantograph arrangement (Fig IV.12)
so that its optical axis automatically followed the centre
of the specimen. The Camera Timer Unit (Fig IV.13)
allowed the interval between shots to be varied between 1
second and 1 hour. The device also produced pips on the
load recorder, thus allowing the correlation of load and
strain readings.
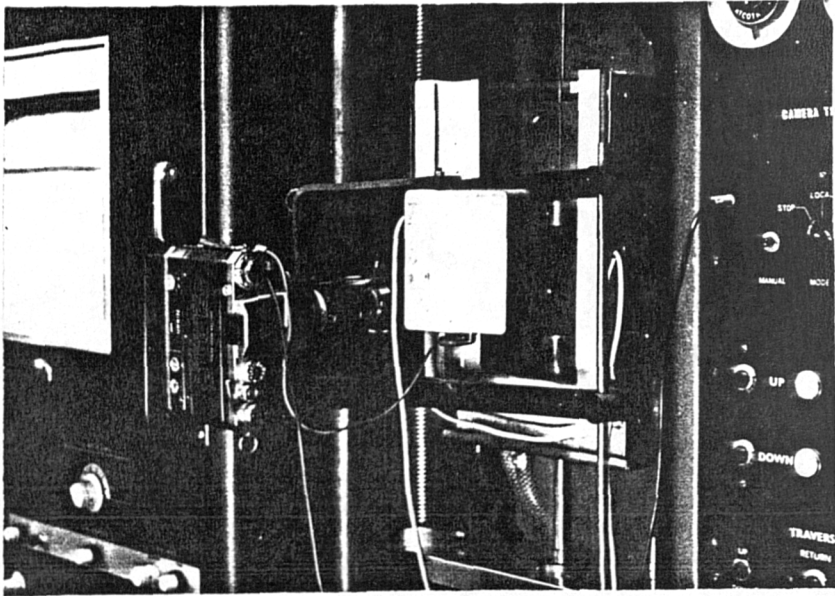
Fig IV.12   Photographic strain measuring
              equipment on Instron
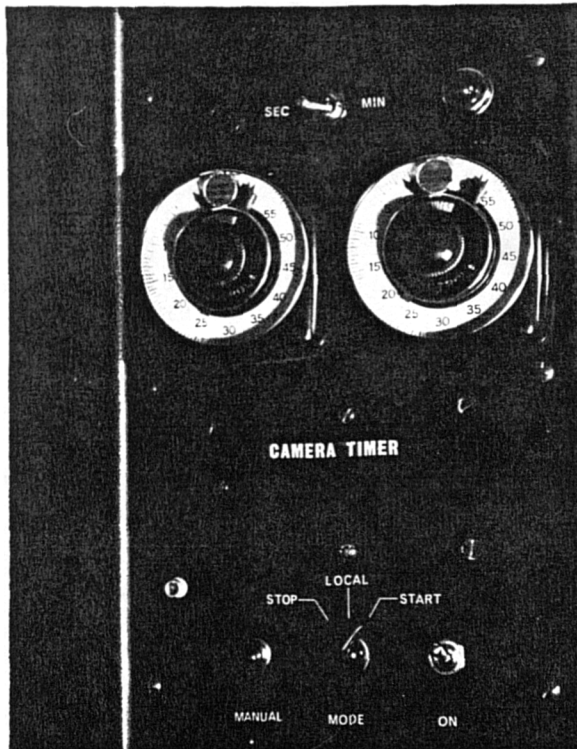
Fig IV.13   Camera timer unit
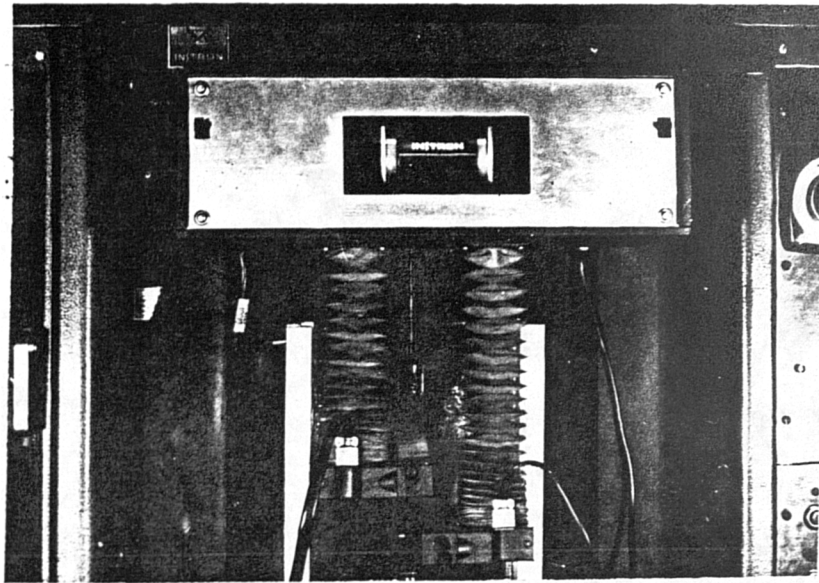
FIG. Ⅳ. 14. INSTRON OPTICAL EXTENSOMETER.
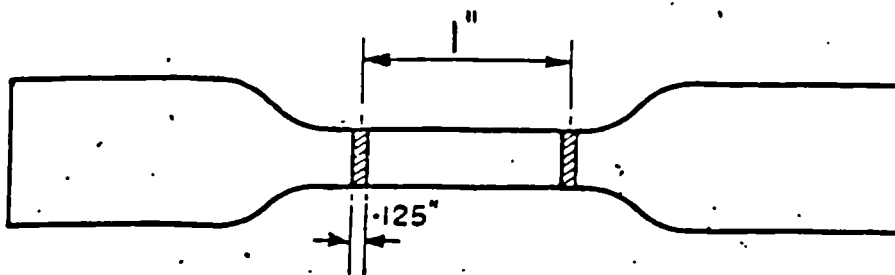
FIG. Ⅳ 15 SPECIMEN MARKING FOR USE WITH OPTICAL EXTENSOMETER
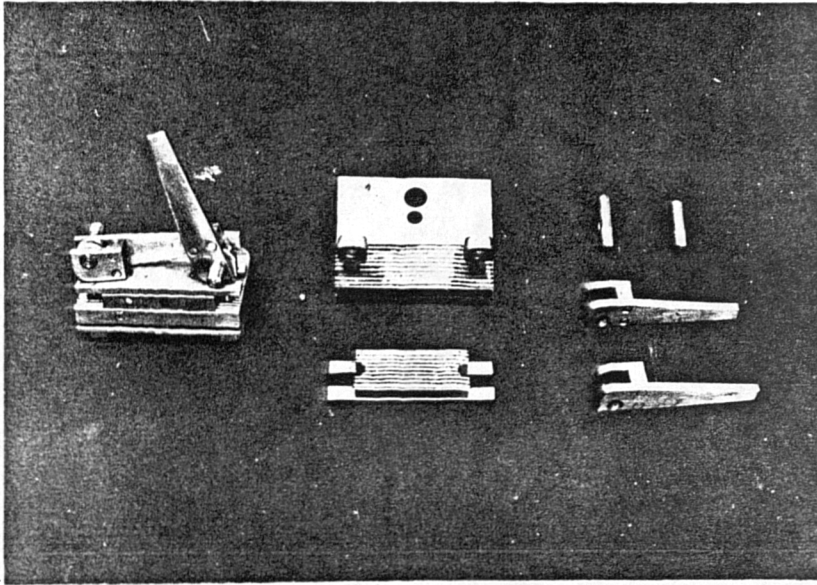
Fig IV.16   Toggle Action Grips for Instron
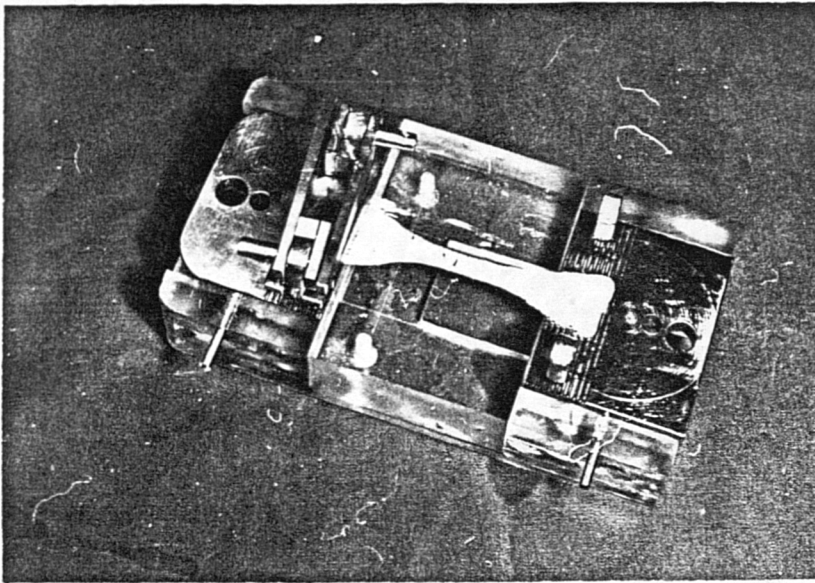
Fig IV.17   Specimen Loading Jig

IV.4.2   Instron optical extensometer

A second method of measuring uniaxial strain became available at a late stage in the test programme in the form of an Instron Optical Extensometer.   This device offered a very considerable saving in analysis time over the photographic method as it produced a continuous record of load v. extension of the specimen gauge length.

The extensometer is shown in Fig IV.14.   The specimen used with the device was similar to that used previously except that instead of a grid, it was marked as shown in Fig IV.15.   A servo system operated by photocells in the optical heads AA allowed these heads to "lock on" to the gauge length marks, and to follow the movements of these marks.   A further servo system drove the chart of the load recorder by an amount proportional to the difference in the head movements and thus to the specimen extension.

IV.4.3   Grips and specimen loading jig

The grips used are shown in Fig IV.16.   These were of serrated jaw, straight clamp action type.   The beam spring mounted on the back of the grips provided the "take up" necessary when gripping a soft, viscoelastic material such as skin.   The jaw pressure was applied quickly and simply by the toggle levers.

To load a specimen, the grips were mounted in the jig shown in Fig IV.17 and the assembly was immersed in Ringer's solutinn at the same temperature as that used in the test.   The skin specimen was then laid horizontally across the jaws.   In this position,it practically floated and therefore any forces in the horizontal direction were negligible.   The top jaws were then assembled to the grips and clamped in place.   The whole jig was then mounted on the Instron through the opening door on the back of the
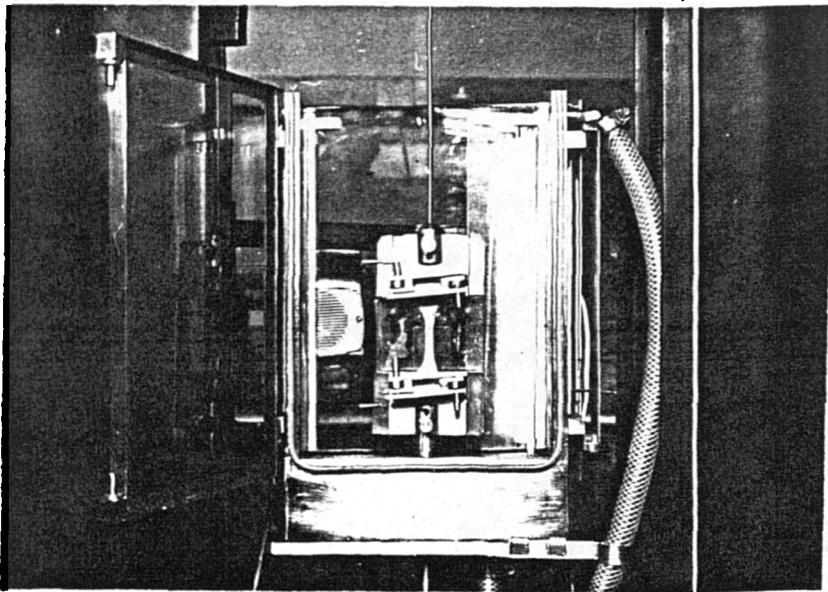
Fig IV.18   Loading Jig Mounted on Instron.   When
            the Jig is Removed the Specimen and
            Grips are Left Mounted on the Machine
            at the True Zero Load Length.

immersion tank (Fig IV.18). By this means the specimen was maintained at the same length as it had when lying horizontally.

IV.4.4   Immersion tank

The Ringer's solution required for the immersion tank was contained in a large tank equipped with temperature control facilities mounted behind the machine and below the level of the crosshead. The Ringer's solution could be pumped up into the bottom of the immersion tank so that this tank filled up until the level of an overflow pipe was reached. The solution returned by the overflow to the main tank thus maintaining a constant circulation. At the end of a test, a valve allowed the solution to return to the main tank *via* the supply pipe. The tank door could then be opened to allow access to the specimen.

IV.4.5   Test technique

The actual test procedure used with the Instron was simple in the extreme because of the high degree of automation achieved. A crosshead speed of 2 cm./mm. (0.79 in./min.) was used as this was the closest speed available to that used on the BioEngineering Unit machine. The load cell used for the majority of tests had a maximum load capability of 2 Kg. (4.4 lb) but, with the wide range of amplifier gain settings available, a sensitivity of 0.1 gm. (.00022 lb) was available. Another load cell of 50 Kg. (110 lb) maximum capability was used for some tests to allow the behaviour at higher loads to be investigated.

IV.5   Test Programme with Instron

A total of 18 uniaxial tensile tests was performed with the Instron. Of these 12 were carried out using the photographic strain measurement technique, the remainder
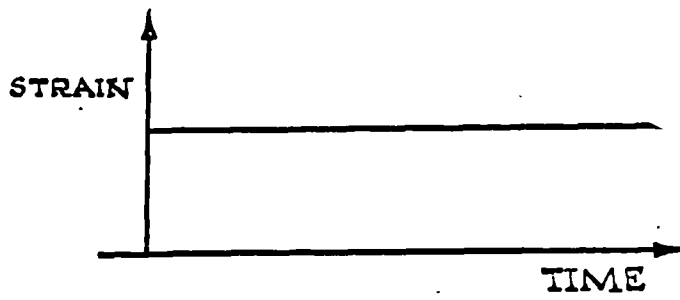
FIG. IV. 19.   STRESS   RELAXATION   TEST.
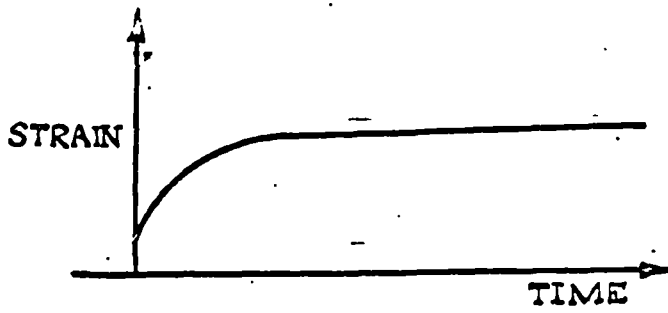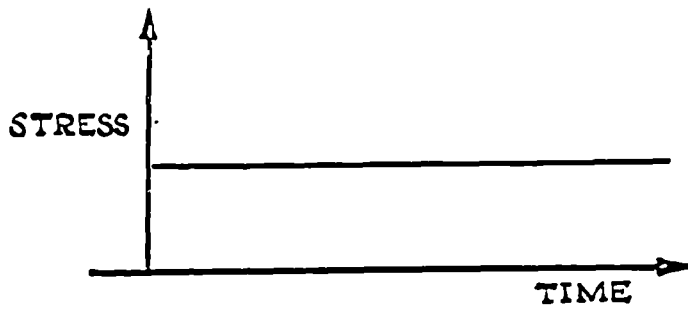
FIG. IV. 20.   CREEP TEST.

being done with the optical extensometer.   In 7 tests the
specimen was loaded until failure occurred.

Details of these tests are summarised in Table
IV.3 at the end of this Chapter.

IV.6   Viscoelastic Behaviour

Further to the theory of non-linear viscoelastic
behaviour, discussed in Chapter III, it was decided to
carry out a limited number of stress-relaxation and creep
experiments.

In a stress relaxation test the specimen is
suddenly extended to a given strain and is then held in
this position.   The variation of the load in the specimen
with time is then recorded (Fig IV.19).

In a creep test a given load is suddenly applied
to the specimen and then maintained.   The resulting
variation of specimen extension with time is then recorded
(Fig IV.20).

The above tests are single step tests, i.e. there
is only one sudden increase in extension (or load).   It
was also required to perform more complicated two step and
three step tests (Fig IV.21) these being of only stress
relaxation type. .

IV.6.1.   Modifications to apparatus

The original method of driving the crosshead by
means of a lead screw was not suitable for applying precise,
rapid crosshead movements.   The crosshead was, therefore,
disconnected from the lead screw so that it was free to
fall under its own weight, this movement being controlled by
the device shown in Fig IV.22.   The pins were pushed
through the holes in the plate and engaged with the under-
side of the crosshead.   Thus, if the uppermost pin is
removed, the crosshead will drop until it is stopped by
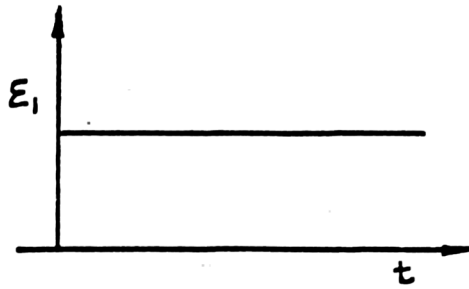
(a) SINGLE STEP TEST.
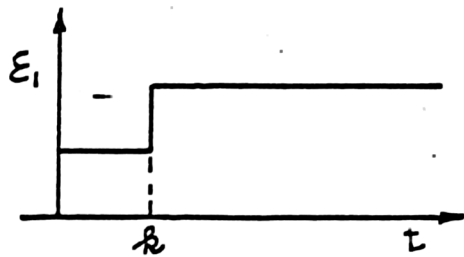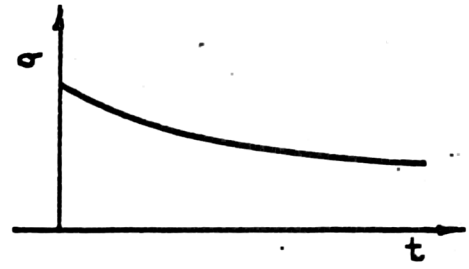
(b) TWO STEP TEST.
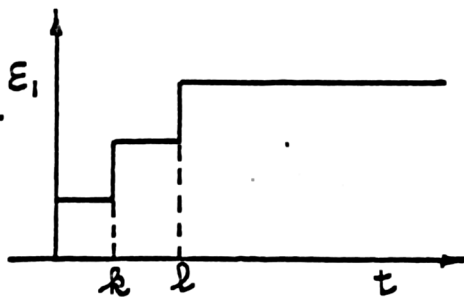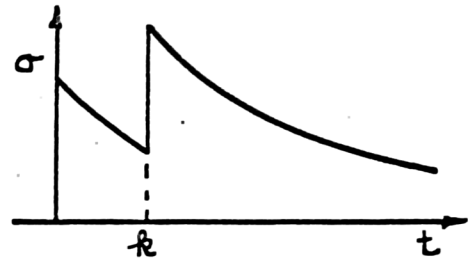
(c) THREE STEP TEST.
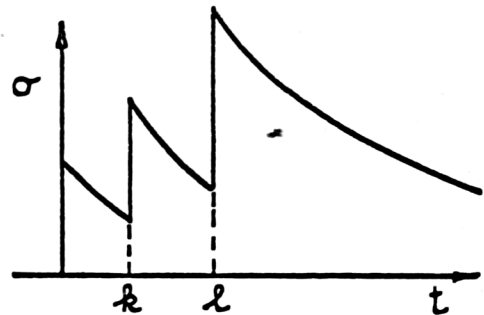
FIG. IV.21. - MULTI-STEP STRESS RELAXATION TESTS.
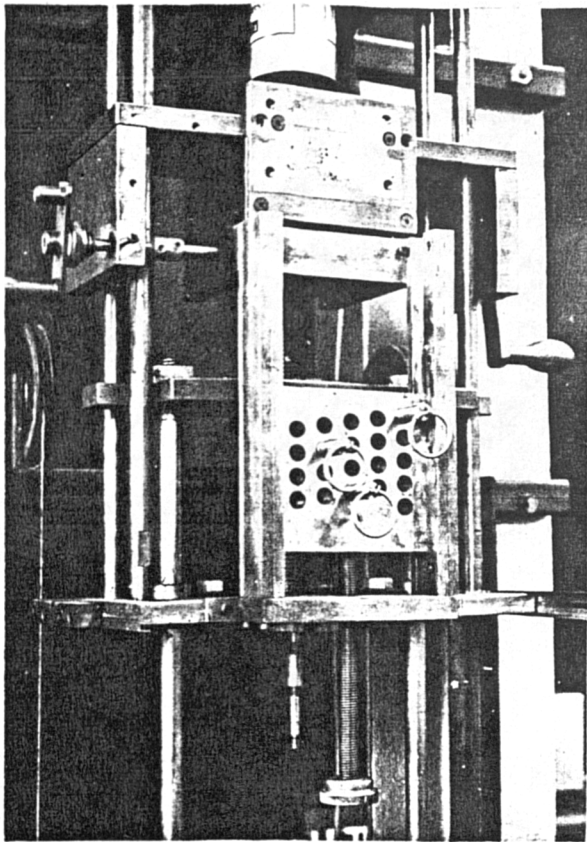
Fig IV.22   Modification to Testing Machine for
            Stress-Relaxation Tests

the next pin.   The screw adjustment allowed the initial
length of the specimen to be adjusted.

Some stress-relaxation experiments were also carried
out on the Instron.   In this case the crosshead was
traversed at maximum speed (50 cm./min.) until the desired
extension was obtained.   Although this resulted in a
poorer approximation to the theoretical instantaneous
extension step than the method described above, this was
compensated for by the greater accuracy and better quality
of the load v. time record obtained from the Instron.

Creep tests were performed on the Instron using
a limit switch device on the load recorder which allowed
the machine to maintain a constant load on the specimen.
Strain measurements were made photographically as in the
uniaxial tensile tests.

IV.7   Stress Relaxation and Creep Test Programme

A total of 12 single step stress-relaxation tests
was performed.   The details of these tests (and all other
stress-relaxation and creep tests) are given in Table IV.4
at the end of the Chapter.

Because of the long, complicated test programme
involved, only one complete experiment, consisting of one,
two and three step tests, was carried out.   The details of
this test are given in Table IV.4 and it is also fully
discussed in Chapter V.

Eight single step creep tests were performed
with various loads and test durations.

IV.7.1   Load cycling tests

Because the experiments involving multi-step tests
required a number of tests on the same specimen, it was
decided to investigate the effect of repeated load cycles
on a specimen.   The result of such a load cycling test is
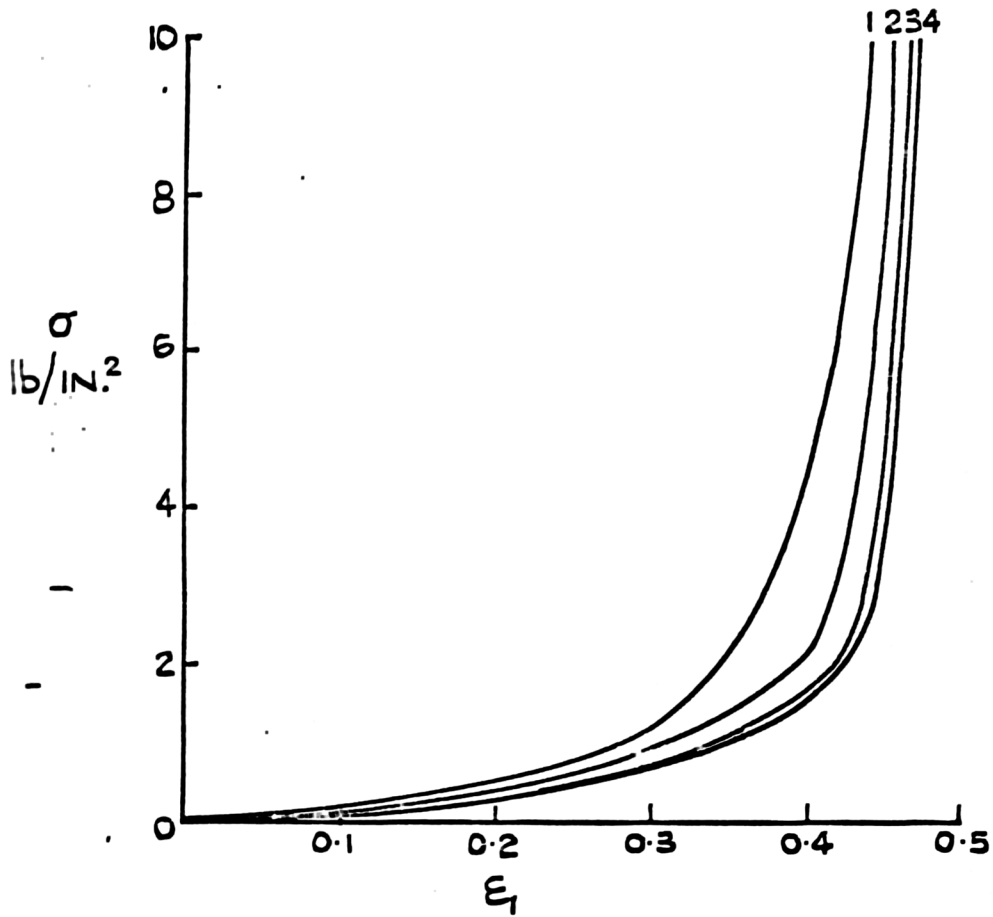
FIG. $\overline{V}$. 25. - LOAD CYCLING TEST.

shown in Fig IV.23. It can be seen that after four cycles, the stress strain curve settled down to a fixed pattern. All specimens used in the stress-relaxation and creep experiment were therefore subjected to five such load cycles before test.

IV.8   Summary

The specifications of the testing equipment used in these investigations and details of the testing programme carried out are given in Tables IV.1 to IV.4 below.

Table IV.1

Specification of Uniaxial Tensile Testing Machine
Designed and Built in the BioEngineering Unit

Load Measurement	Electrical Load Cells (Interchangeable)
Maximum Load Capacity	200 lb
Sensitivity	.01 lb
Accuracy	±1% of Full Scale Load
Load Recording	Continuous Record on u-v Recorder
Crosshead Drive	Constant Speed Drive; Speed Selected by Change Gears. Rapid Traverse and Fine Manual Positioning Facilities
Strain Measurement	Photographic
Environmental Control	Specimen to be Immersed in a Constant Temperature bath of Ringer's Solution during Test. Temperature $37^{\circ}C$ $±0.5^{\circ}C$; pH=7.0. Immersion Tank to be easily Removed to Facilitate Specimen Handling

TABLE IV.2

Specification of Instron Floor Model TT-CM

ad cell ranges:-

ell A   0-2, 0-10, 0-20, 0-50 gms.

ell B   0-100, 0-200, 0-500, 0-1000, 0-2000 gms.

ell CM   0-1, 0-2, 0-5, 0-10, 0-20, 0-50 Kg.

ell DM   0-10, 0-20, 0-50, 0-100, 0-200, 0-500 Kg.

ell FM   0-100, 0-200, 0-500, 0-1000, 0-2000, 01500 Kg.

Crosshead Speeds:-   0.005 to 50 cm./min.

Chart Speeds:-   0.2 to 50 cm./min.

oad recorder system:-

Maximum pen response speed:- 0.25 secs. for full
                              scale (10 in.)

Accuracy:-   ±1% of full scale at pen speed of
          0.75 sec. for full scale

Maximum accuracy:-   ±$\frac{1}{2}$% of indicated load or
               ±$\frac{1}{4}$% of recorder full scale
               whichever is the greater

81

TABLE IV.3

Test Programme - Uniaxial Tensile Tests at Constant Strain Rate

Testing Machine	No. of Tests	Sex	Age Range (years)	Specimen Orientation (Note 1)	Maximum Load Applied (lb)	Grip Separation Rate in./min.
	16	M	0-89	∥	20	.67
	8	F	16-85	=	20	.67
Bioengineering	4	M	18-80	⊥	20	.67
Unit Machine	2	F	44-82	⊥	20	.67
	5	M	53-78	=	2	.67
	8	F	39-80	≡	2	.67
	4	M	26-72	∥	failure load	.79
Instron	3	F	52-76	∥	failure load	.79
	7	M	37-79	=	4.4	.79
	4	F	26-73	∥	4.4	.79

Note 1: ∥ = parallel to cranio-caudal median
⊥ = perpendicular to cranio-caudal median

All specimens were obtained at post mortem from the anterior abdominal wall.

Table IV.4

Stress Relaxation and Creep Tests

Type of Test	Testing Machine	Initial Strain or Stress	Relaxation or Creep Time (seconds)	Age (years) and Sex	Comments
Single Step Stress Relaxation	Bioengineering Unit Machine	$\varepsilon_1 = 0.45$	10,000	43 M	
		0.39	10,000	52 M	
		0.53	10,000	39 F	
		0.27	10,000	85 M	
		0.35	1,000	73 M	
		0.44	1,000	56 F	
		0.47	1,000	61 F	
	Instron	-	100	48 M	Several
		-	100	57 M	Tests
		-	100	63 F	Carried
		-	100	45 F	out on Each
		-	100	77 M	Specimen

Table IV.4 (continued)

Type of Test	Testing Machine	Initial Strain or Stress	Relaxation or Creep Time (seconds)	Age (years) and Sex	Comments
Multi-Step Stress Relaxation	Bioeng-ineering Unit Machine	-	500	45 F	Complete Prog-ramme of 1,2 & 3 Step Tests
Single Step Creep	Instron	1 lb/in^2	100	48 M	4 Tests were Perfor-med in Order of Inc-reasing Stress
		2 "	"	"	
		5 "	"	"	
		10 "	"	"	
		1 "	"	57 M	
		2 "	"	"	do
		5 "	"	"	
		10 "	"	"	

Chapter V

Analysis of Experimental Results
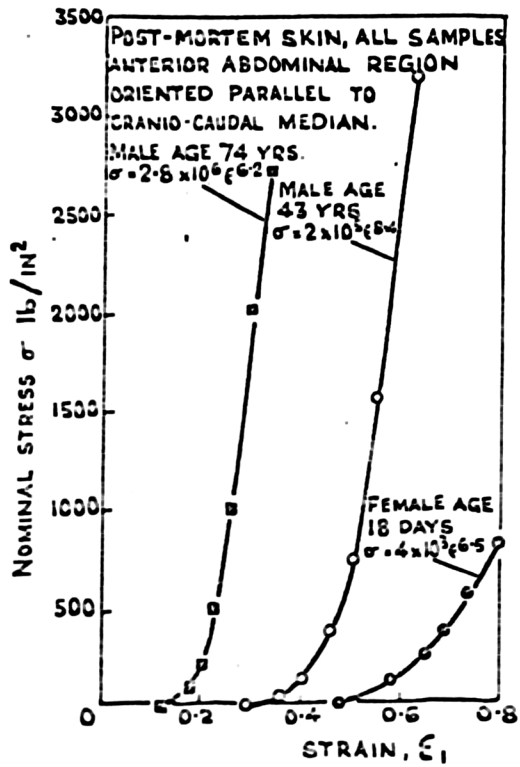
FIG. Ⅴ. 1   TYPICAL STRESS-STRAIN CURVES FOR
HUMAN SKIN - PILOT EXPERIMENTS
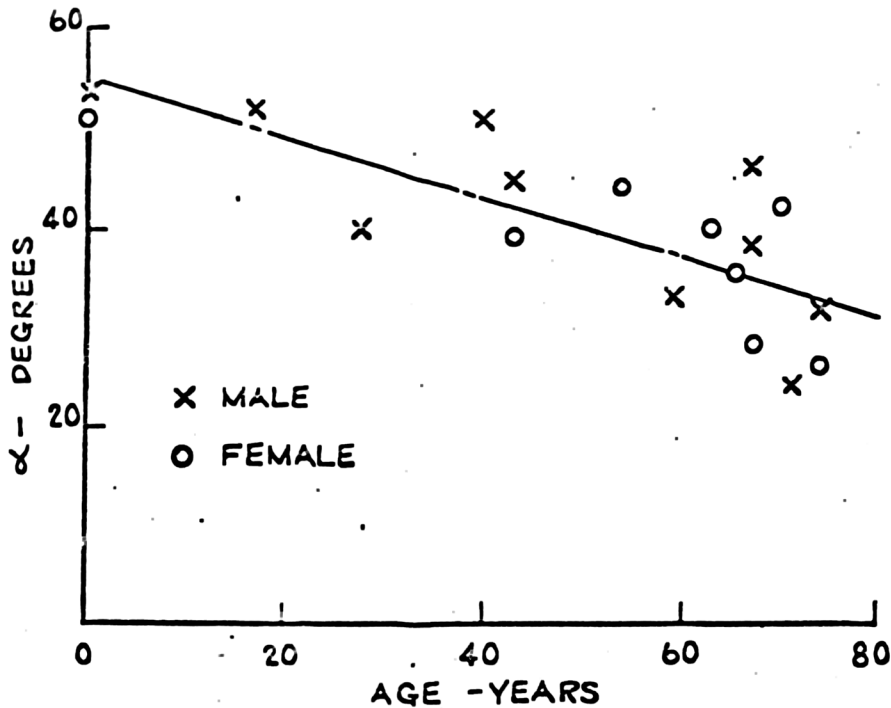
FIG. Ⅴ. 2.   NETWORK ANALYSIS - α Vs AGE
(PILOT EXPERIMENTS)

V.1   Uniaxial Tensile Tests at Constant Strain Rate

The results of the uniaxial tensile tests described in the previous chapter and of the pilot experiments described in Chapter II were analysed in terms of the network theory outlined in Chapter III.   This analysis produced four parameters from each test:

(i) α - this angle defines the unstressed configuration of the model

(ii) β - the linear stiffness of the side links of the model.   In skin β represents a a linear approximation to the slightly non-linear stiffness of the collagen fibres.

(iii) γ - the non-linear stiffness factor of the network cross link.   The force p in the cross link is given by:

$$p = \gamma(\text{cross link deformation})^4.$$

(iv) δ - the width of the network side links.

V.1.1   Pilot experiments

Fig V.1 shows some typical stress-strain curves obtained from the pilot experiments described in Chapter II.   The results were analysed in terms of the network theory, but, because of the poor accuracy of the data and the low sensitivity of the testing machine used it was not possible to obtain reliable values for the parameters γ and δ.   The values obtained for α and β were plotted against age (Figs V.2 and V.3 respectively).   Although there was a considerable scatter in the results, it is seen that the value of α tended to decrease with age.
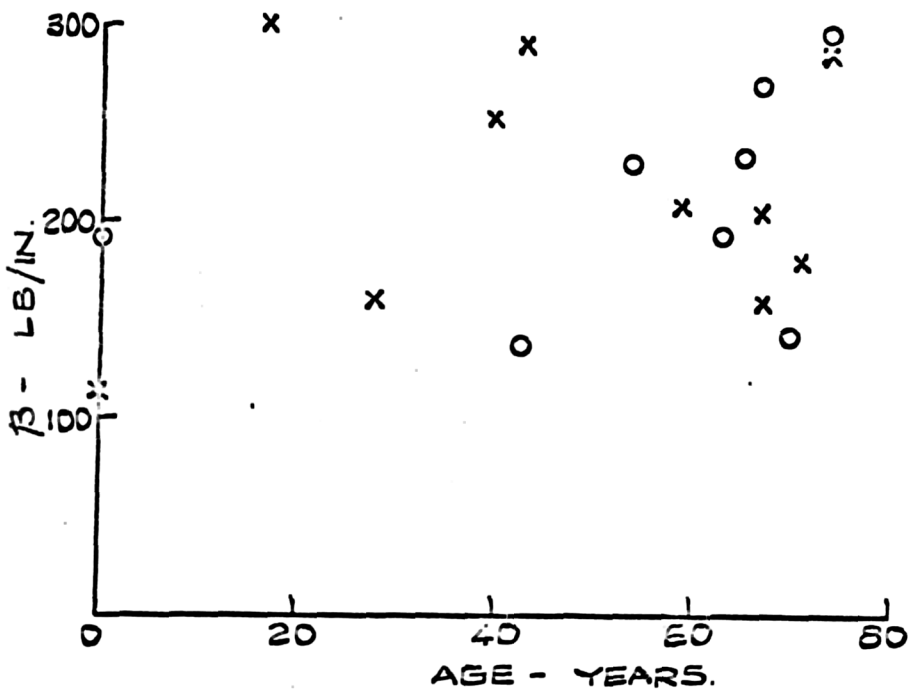
FIG. $\underline{\text{V}}$. 3. — NETWORK ANALYSIS — β Vs AGE
(PILOT EXPERIMENTS).
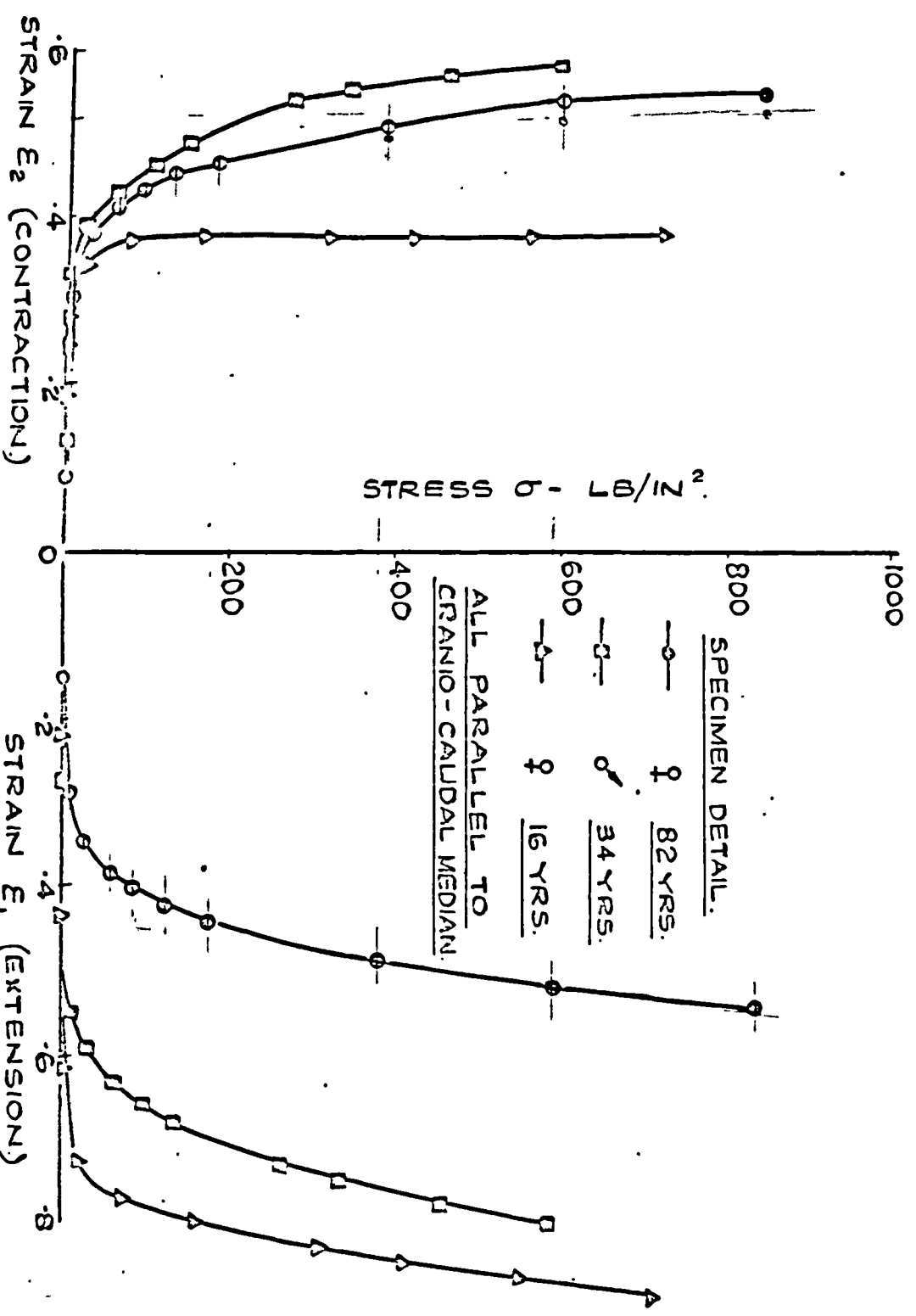
FIG. V. 4. — TYPICAL STRESS - STRAIN CURVES FOR HUMAN SKIN
OBTAINED USING BIOENGINEERING UNIT MACHINE.

STRAIN ε_2 (CONTRACTION)

STRESS σ - LB/IN^2

STRAIN ε_1 (EXTENSION)

SPECIMEN DETAIL.

♀   82 YRS.

♂   34 YRS.

♀   16 YRS.

ALL PARALLEL TO
CRANIO- CAUDAL MEDIAN.

ALL SPECIMENS TESTED TO 20 LB MAX LOAD ON
BIOENGINEERING UNIT MACHINE.
STRAIN RATE 0·20⁺·02 IN/IN/SEC.

X   MALE.

O   FEMALE.
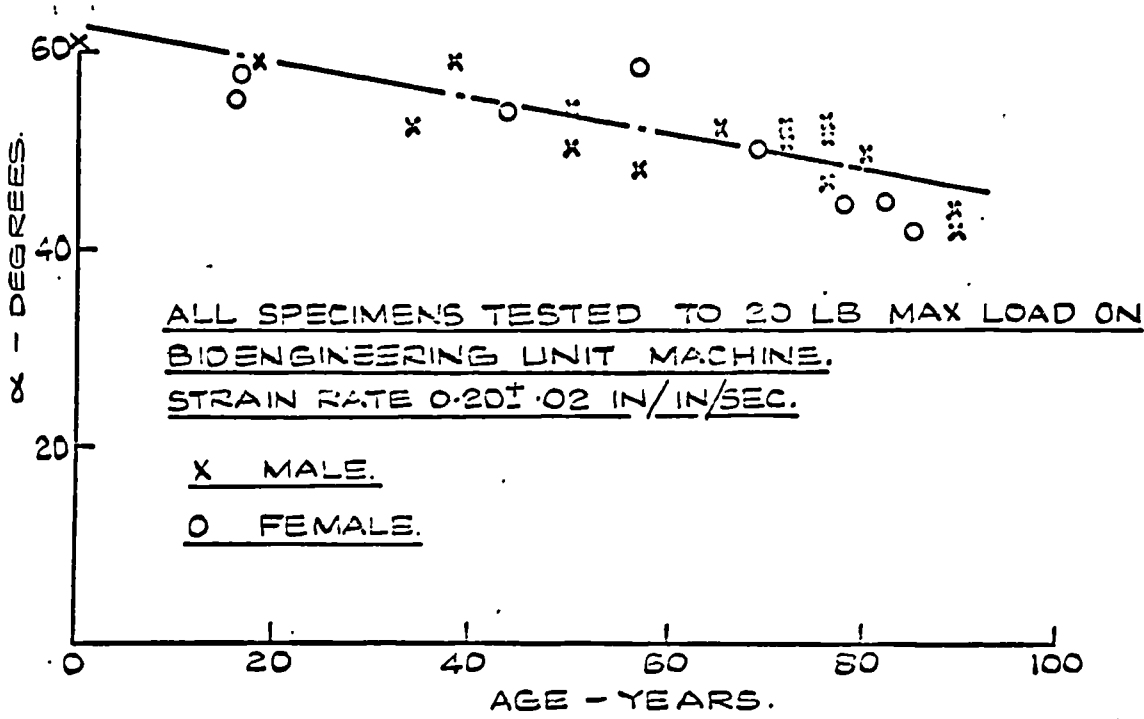
FIG V. 5.- NETWORK ANALYSIS ∝ Vₛ AGE.
(BIOENGINEERING MACHINE)
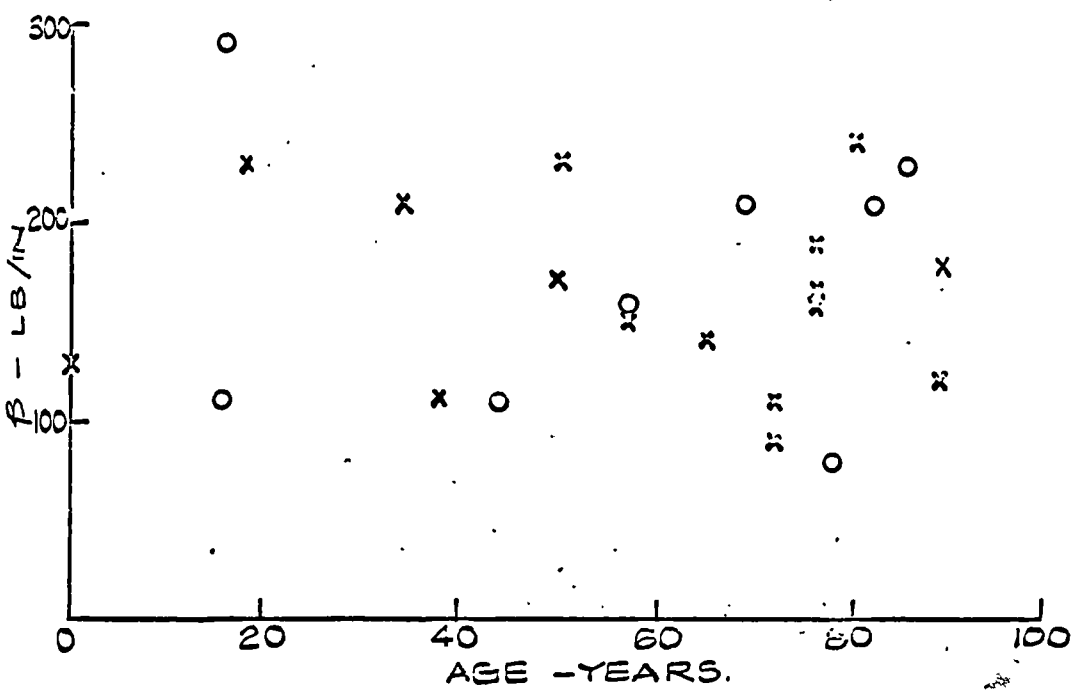
FIG V. 6.- NETWORK ANALYSIS β Vₛ AGE.
(BIOENGINEERING MACHINE.)

β showed no age-dependence and neither parameter varied significantly between the sexes.

V.1.2   Tests on bioengineering unit machine

Fig V.4 shows some typical results of uniaxial tensile tests carried out on the machine designed and built in the BioEngineering Unit.   These tests were carried out under standardised conditions:-

Grip separation rate = 0.67 in./min.
Specimens immersed in Ringer's solution
Temperature 37°C
pH 7.0
Maximum load at end of test = 20 lb

The general shape of these curves is similar to those obtained in the pilot experiments.   Because of the much better control achieved over the test conditions, the results were found to be more consistent and more accurate than the pilot experiments.   A total of 24 tests of this type were carried out and were analys d in terms of the network theory.   The results of this analysis are shown in Figs V.5 to V.8.

The parameter α (Fig V.5) was found to have the most consistent values and showed a definite decrease with age.

Comparison of Figs V.5 and V.2 shows clearly the improvement in accuracy of the refined testing technique over that of the pilot experiments.   There is a much reduced scatter of the values of α. Also, the values obtained by the new technique are consistently some 5-10 degrees greater than the pilot results throughout the age range.   This is due to the improved accuracy of the zero strain measurement.
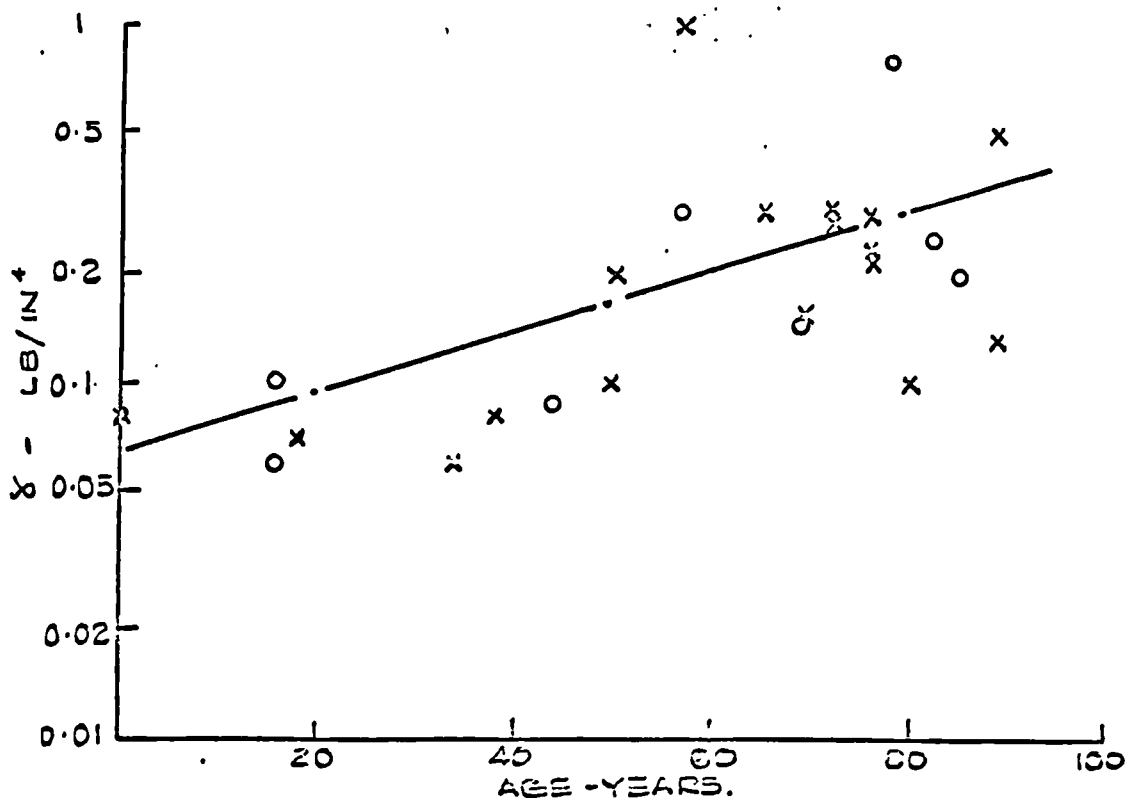
FIG. V. 7. — NETWORK ANALYSIS — Ɣ Vs AGE
(BIOENGINEERING MACHINE.)

FIG V 8. — NETWORK ANALYSIS — δ Vs AGE.
(BIOENGINEERING MACHINE.)

The side link stiffness β (Fig V.6) showed considerable variations but no relation was found with age.

The cross link stiffness factor γ, although showing large variations, tended to increase with age (Fig V.7, note logarithmic ordinate scale).

The side link thickness δ showed a reasonably consistent decrease with age (Fig V.8).

None of the four parameters showed any significant variation with sex.

Because of the small number of tests involved, no attempt was made to apply statistical techniques to the above data to obtain quantitative estimates of the trends shown in the figures.

The interpolation of these results (and the results of all other tests) is discussed in the final section of this chapter.

A further 13 tests were carried out on this machine, these being identical in all respects to the tests discussed above except that the maximum load applied was only 2 lb. Because of this feature it was impossible to analyse the results of these tests in terms of the network theory as it was not possible to obtain values for the parameters α and β from the curves obtained. The purpose of these tests was to obtain data on the initial phase of large extension at very low stress levels which is a characteristic of skin.

Typical results of these tests are shown in Fig V.9. It can be seen that there is still a considerable extension of the specimen occurring at very low stress levels below the sensitivity of the load cell in use. As it was not possible to use this cell at a higher sensitivity setting, any further investigation of the

X MALE AGE 63
+ MALE AGE 49
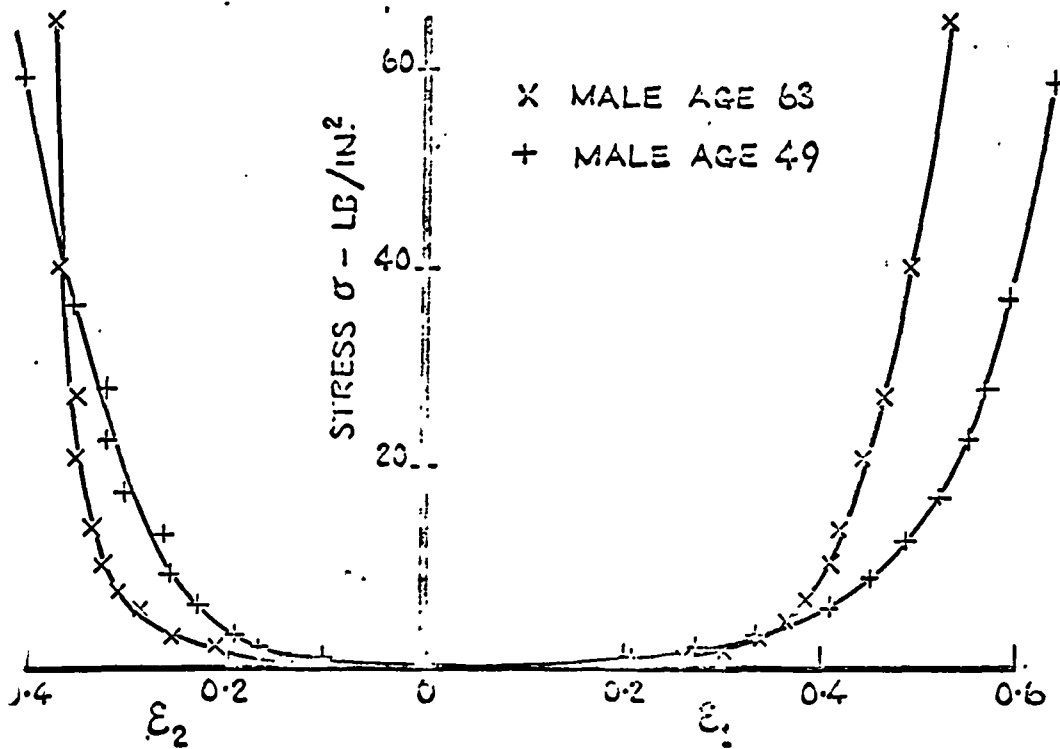
FIG. V. 9. TYPICAL STRESS-STRAIN CURVES FOR HUMAN SKIN AT LOW STRESS LEVELS.

O PARALLEL TO CRANIO-CAUDAL MEDIAN
□ PERPENDICULAR TO CRANIO-CAUDAL MEDIAN

FEMALE 82 YRS.
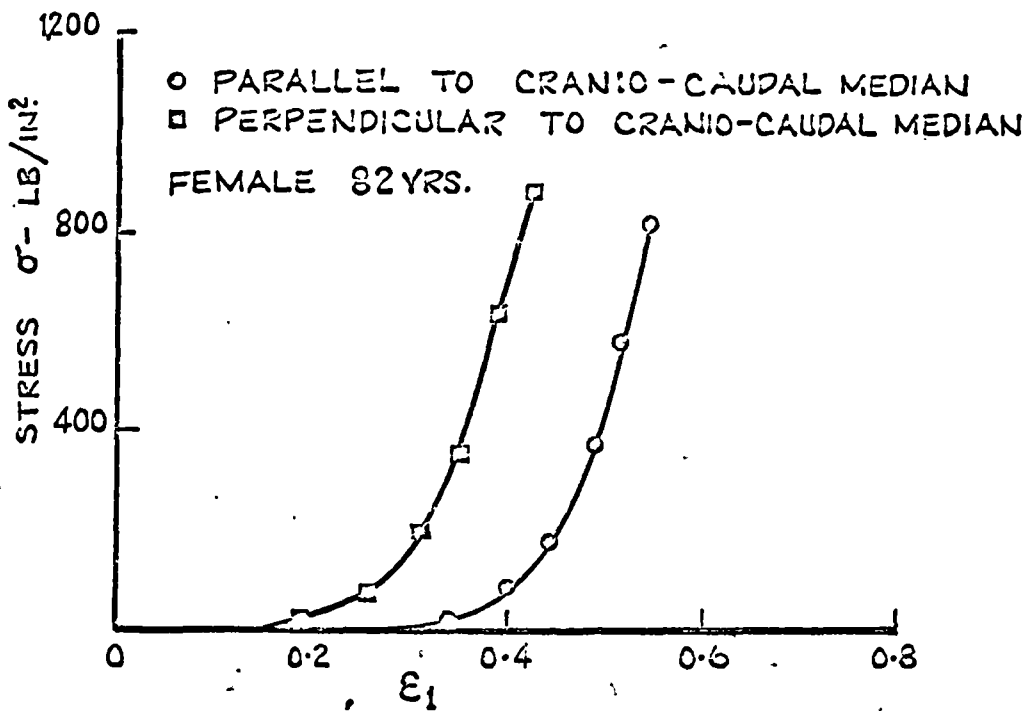
FIG. V. 10. EFFECT OF SPECIMEN ORIENTATION

behaviour at low stress levels was deferred until the much more sensitive Instron machine became available.

V.1.3   Variation of stress-strain properties with specimen orientation

In six of the tests described above using the 20 lb load cell specimens of skin were also obtained in which the long axis was oriented perpendicular to the cranio-caudal median as well as the normal specimens oriented parallel to the median.   These specimens were all tested in the normal way using the 20 lb load cell. Fig V.10 shows a typical comparison of the behaviour of specimens oriented parallel and perpendicular to the cranio-caudal median.   The results of all six tests were analysed in terms of the network theory, the results being given in Table V.1.

Table V.1

Network Analysis - Variation with Orientation

Age & Sex	α		β		γ		δ	
	∥	⊥	∥	⊥	∥	⊥	∥	⊥
82 F	45	40	210	200	0.25	0.15	2.0	2.2
80 M	50	42	240	220	0.1	0.15	2.3	2.0
57 M	48	43	150	180	1.0	0.7	2.0	2.4
44 F	54	45	110	120	0.09	0.1	2.6	2.0
34 M	52	48	210	190	0.06	0.05	2.2	2.5
18 M	59	51	230	240	0.07	0.07	2.5	2.6

∥   parallel to cranio-caudal median
⊥   perpendicular to cranio-caudal median

The only parameter which was significantly altered by the change of orientation was α, this being consistently lower for specimens perpendicular to the median.

Several tests of this type were included in the pilot experiments. Analysis of these tests also showed that α was consistently lower for specimens oriented perpendicular to the cranio caudal median (Table V.2).

Table V.2

Net work Analysis - Variation with Orientation
(Pilot Experiments)

Age & Sex	α		β	
	‖	⊥	‖	⊥
43 M	45	40	290	220
54 F	44	41	230	240
67 M	38	33	160	200
71 M	24	21	180	180

V.I.4   The effect of specimen width

In considering a network theory of the type proposed one has to take account of the effects produced at the edge of the network where the presence of free ends of the network links will affect the behaviour of the network. These effects are only negligible if the total width of the network is large compared to the size of network unit. If not negligible, this effect would result in a variation in the stress-strain curve for specimens of different widths. Tests were therefore

$2\frac{1}{2}''$

BLANK
GAUGE LENGTH

GAUGE LENGTH
WITH DISCONTINUITY
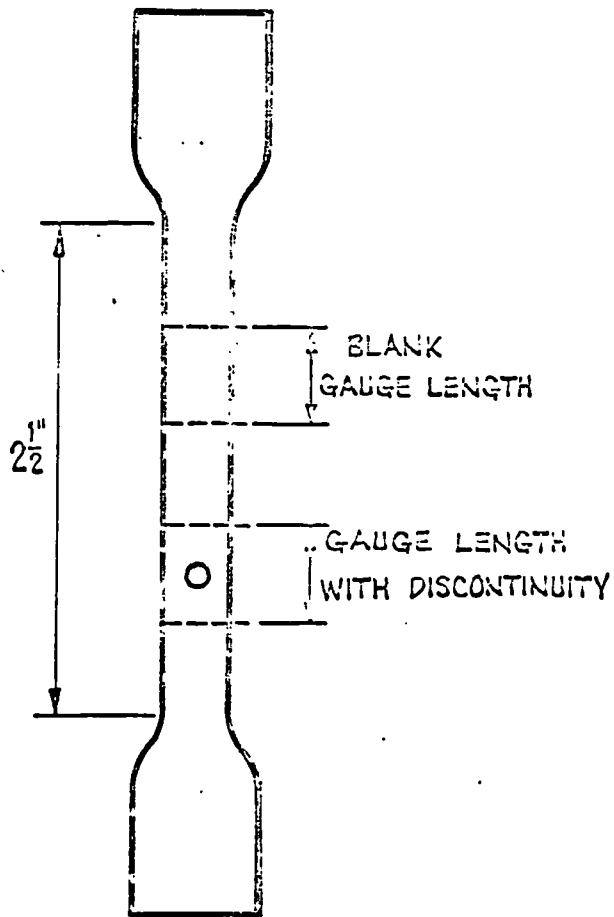
FIG. V. 11.   LONG SPECIMEN WITH TWO GAUGE
LENGTHS USED TO OBTAIN COMPARITIVE
EFFECT OF A DISCONTINUITY IN THE
SPECIMEN.
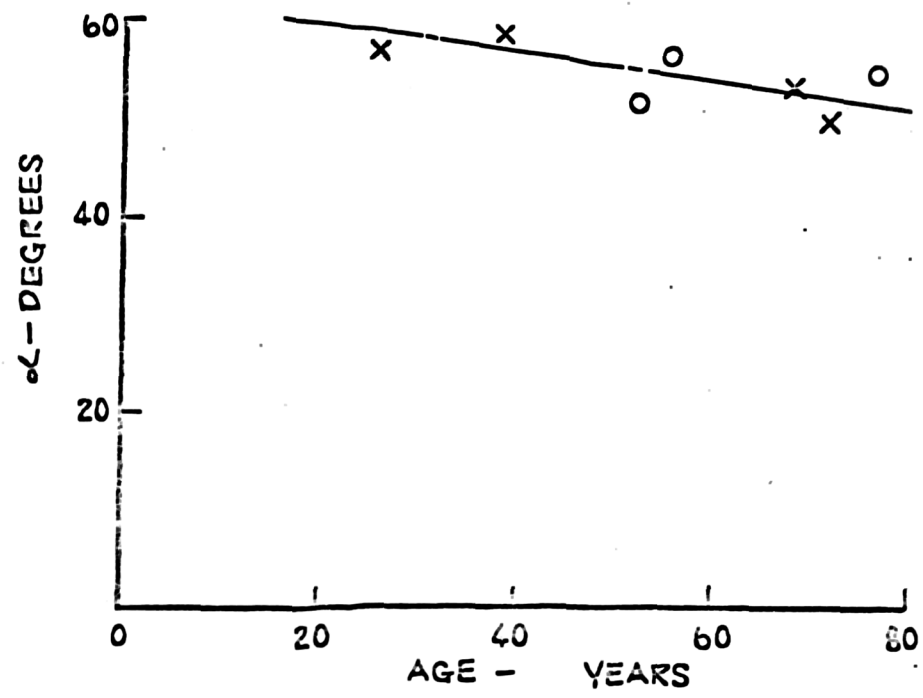
FIG. $\underline{V}$ 12.   NETWORK ANALYSIS $-$ $\propto$ VS AGE
(INSTRON)
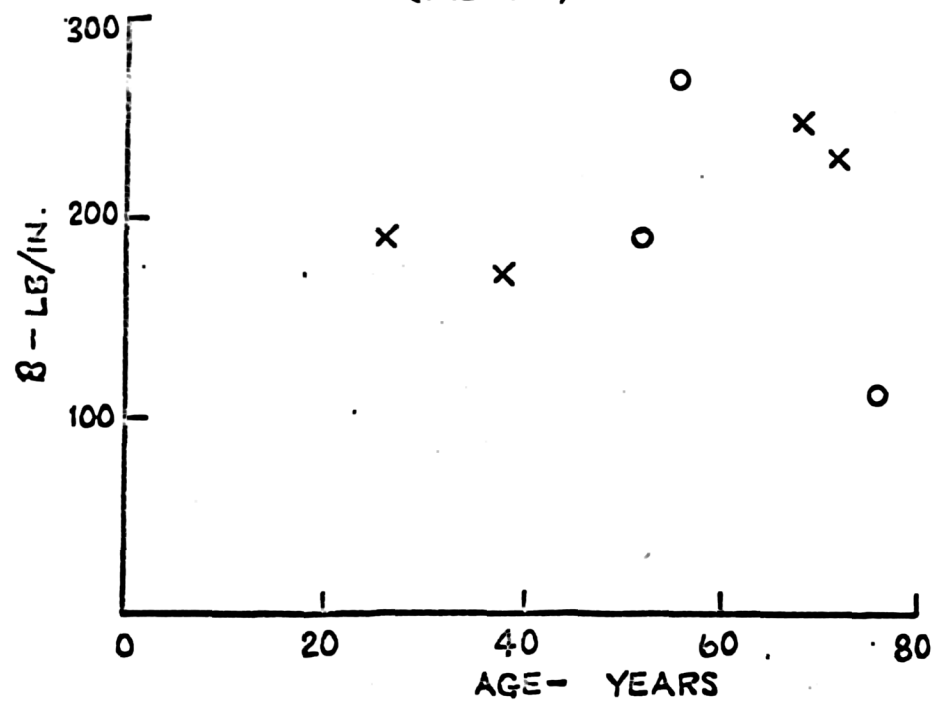
FIG. $\underline{V}$ 13.   NETWORK ANALYSIS $-$ β VS AGE
(INSTRON)
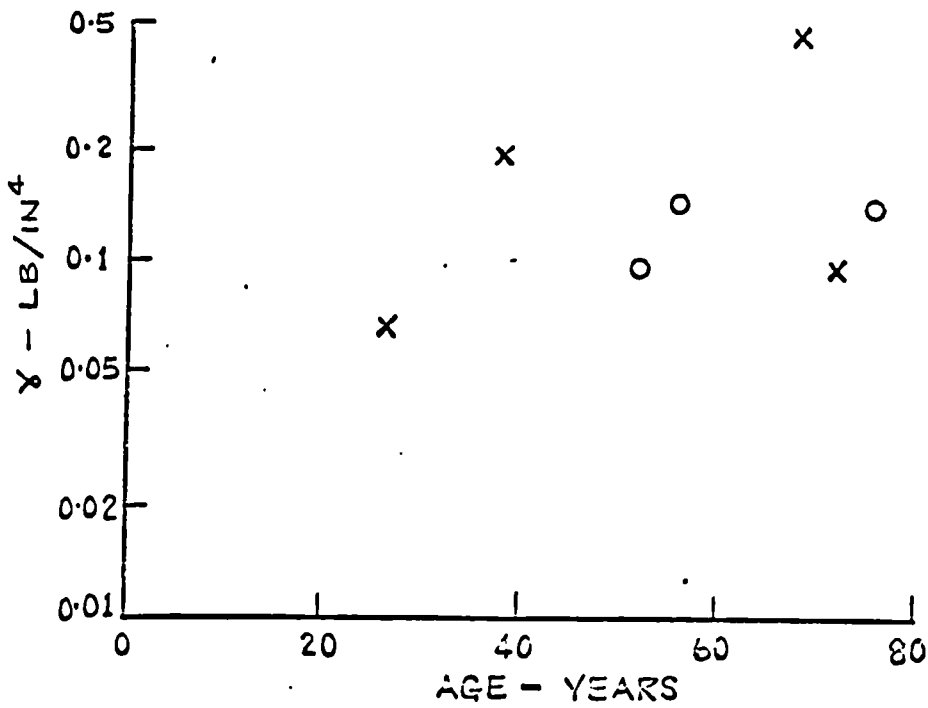
FIG. $\underline{V}$. 14. NETWORK ANALYSIS - γ VS AGE
(INSTRON)
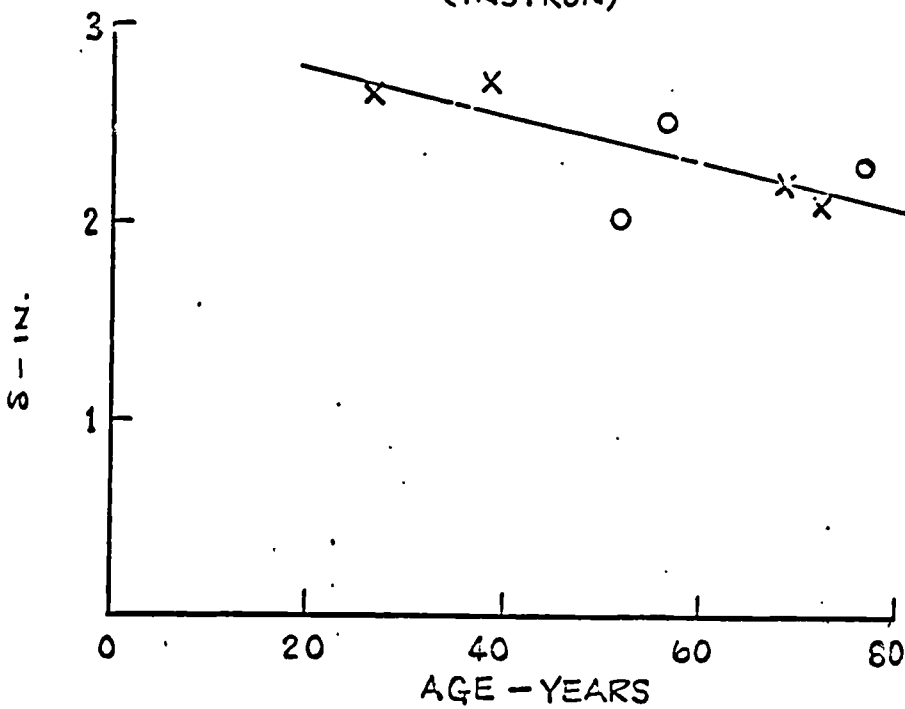
FIG. $\underline{V}$. 15. NETWORK ANALYSIS - δ VS AGE
(INSTRON)
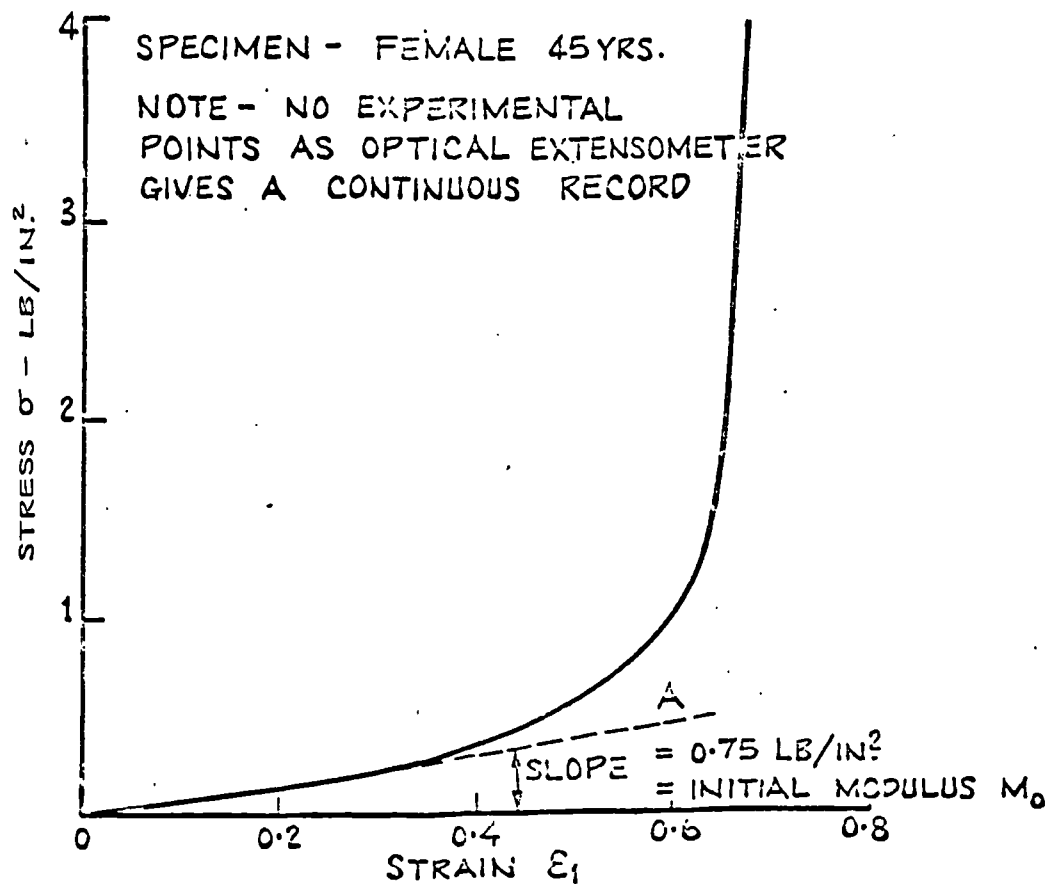
FIG. <u>V</u>. 16 STRESS-STRAIN BEHAVIOUR AT LOW
STRESS LEVELS (INSTRON)
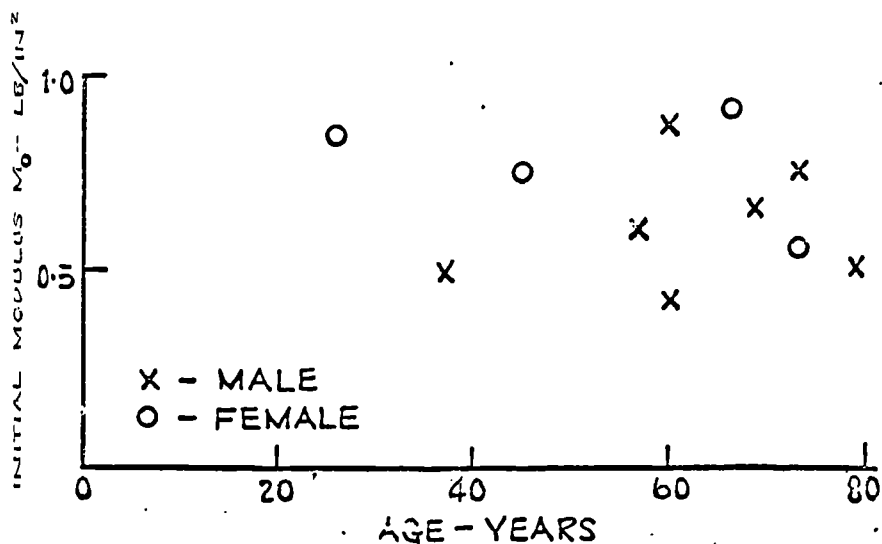
FIG. <u>V</u>. 17. INITIAL MODULUS M_o VS AGE.

A further 11 tests were carried out using a more sensitive load cell in order to extend the investigation of the behaviour of skin at very low stress levels. The first 5 of these tests were performed with the photographic strain measuring technique, the remaining 6 tests involving the use of the Instron optical extensometer. A typical result is shown in Fig V.16. The most important feature of this is the initially linear extension of the specimen, in this case with an effective "Young's Modulus" of 0.75 lb/in². This initial linear extension of skin was found consistently in these tests, although the continuous record obtained with the optical extensometer showed the effect more clearly. The values obtained for this initial modulus (termed M_o) were plotted against age (Fig V.17). There was no significant age- or sex-dependence.

V.1.7 Load cycling tests

For the reasons given in Chapter IV, the specimens used in the creep and stress relaxation tests described later in this chapter were subjected to 5 load cycles from zero load to the maximum load to be used in the test proper before commencing the creep or stress relaxation programme. A large amount of data on the effect of repeated load cycles was therefore made available. A typical result is shown in Fig V.18. It is seen that, after a small number of cycles, the stress-strain curve settles down to a steady pattern. This effect was found in all of the specimens considered.

V.1.8 Tests at different strain rates

Three tests were carried out in which the specimen was first subjected to a number of load cycles at the usual strain rate (0.25 in./in./min.) until the stress-strain
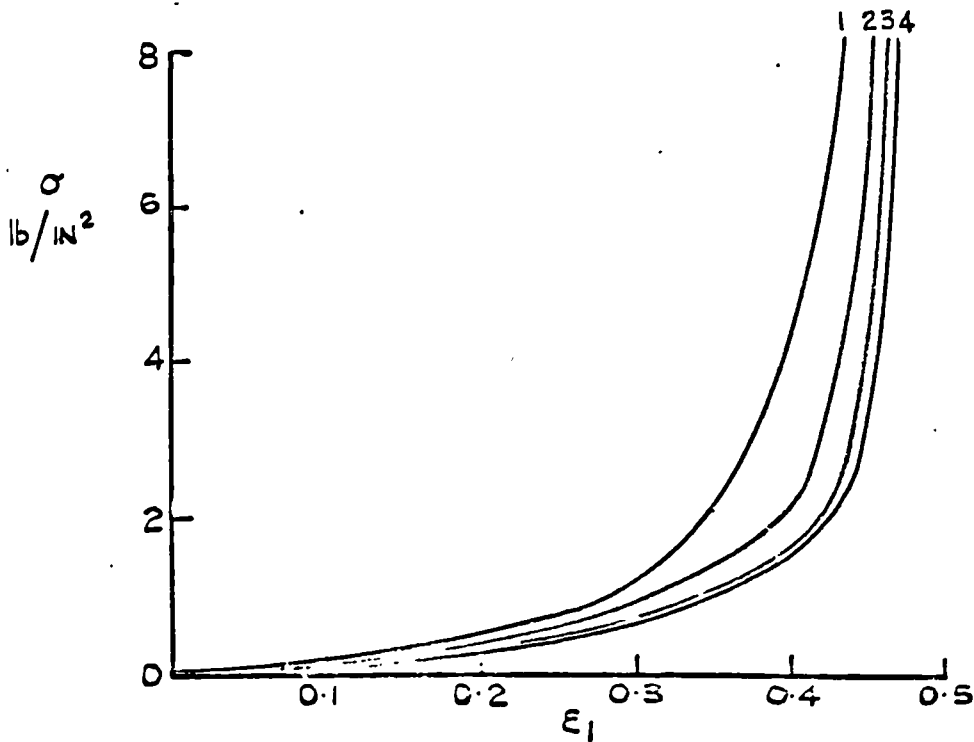
FIG. Ⅴ. 18.- LOAD CYCLING TEST.
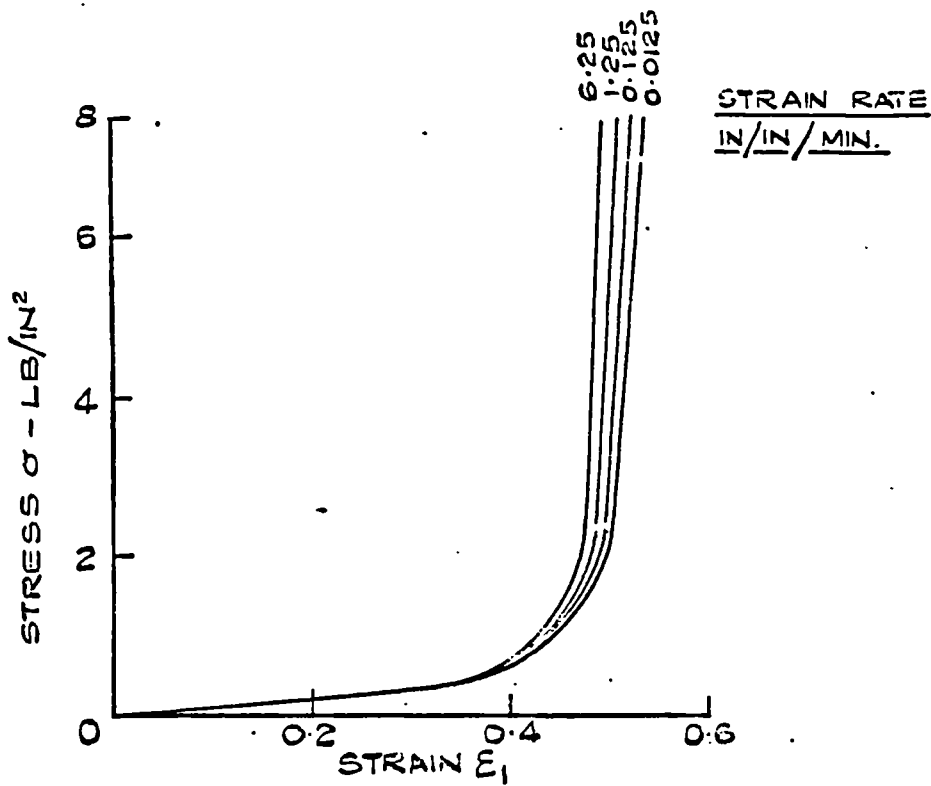
FIG. Ⅴ 19.- EFFECT OF CHANGING STRAIN RATE.

curve had stabilised. The maximum stress applied was restricted to 10 lb/in? to avoid any possibility of causing a permanent extension in the specimen. With this stress, the specimen would always return to its original length when the stress was removed.

A further series of load cycles to the same maximum stress was then applied to the specimen using a different strain rate for each cycle. The strain rate was varied in the range 6.25 in./in./min. to 0.0125 in./in. min. A typical result is shown in Fig V.19. The effect of changing the strain rate was very small at the stress levels in question. It is not possible to carry out this type of test at higher stress levels because of the permanent set which would occur.

V.2   Stress Relaxation and Creep Tests

The viscoelastic properties of skin were investigated by means of a variety of stress relaxation and creep tests.

V.2.1   Single step stress relaxation tests

In this type of test the skin specimen was suddenly extended by a predetermined amount and then held at this extension. The load in the specimen was then recorded against time. Fig V.20 shows some typical results of such tests. After some three hours, the stress in the specimens is seen to decay to approximately 10% of its initial value. Using the method described by the British Rheologists Club (1944) the stress relaxation curves were fitted graphically to exponential decay functions of the form:

$$\sigma(t) = a_0 + a_1 \exp(-t/\tau_1) + a_2 \exp(-t/\tau_2) + \ldots\ldots \quad V.1$$
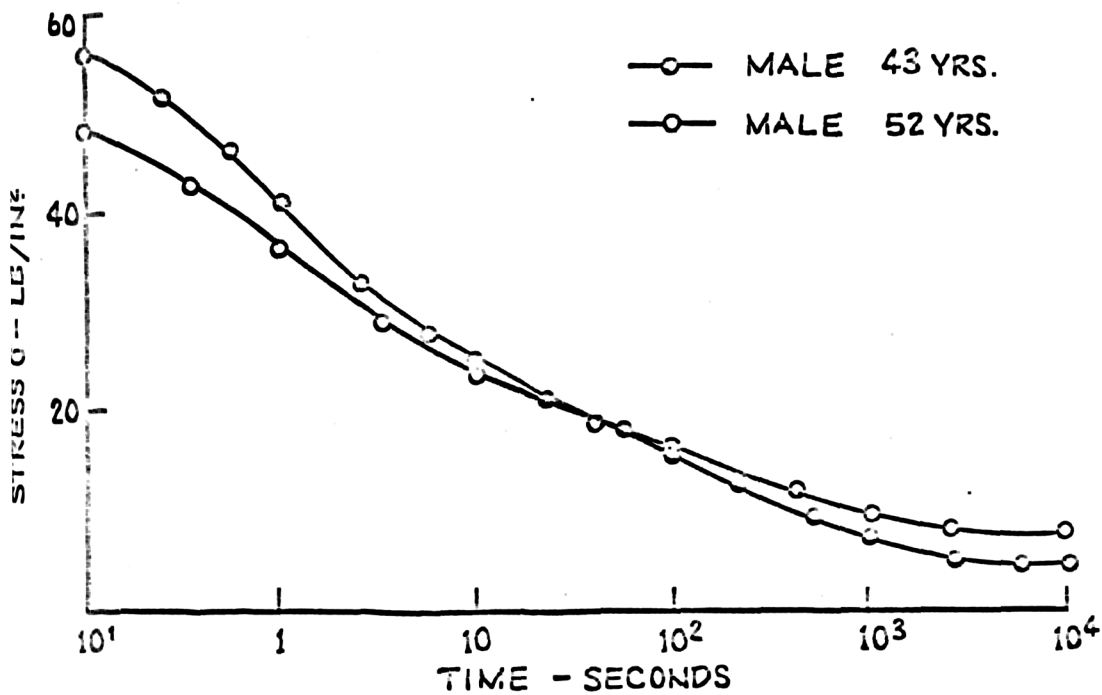
EXPONENTIAL DECAY EQUATIONS FOR THE ABOVE CURVES WERE -

MALE AGE 43 YRS.
$$\sigma(t) = 3.9 + 5.1\, \varepsilon^{-t/1700} + 10\, \varepsilon^{-t/250}$$
$$+ 12\, \varepsilon^{-t/17} + 17.5\, \varepsilon^{-t/2.1} + 12.5\, \varepsilon^{-t/0.29}$$

MALE AGE 52 YRS.
$$\sigma(t) = 7 + 4.05\, \varepsilon^{-t/1950} + 5.4\, \varepsilon^{-t/240}$$
$$+ 8.7\, \varepsilon^{-t/34} + 13.0\, \varepsilon^{-t/4.1} + 12.0\, \varepsilon^{-t/0.55}$$

FIG. V. 20. SINGLE STEP STRESS-RELAXATION TESTS.

Fig V.20 also includes the equations of this type found for the given stress relaxation curves. The curve fitting method is described in Appendix A.IX.

As these stress relaxation equations are derived empirically it is not possible to make any deductions as to the physical interpretation of the stress relaxation phenomana observed in skin.

V.2.2   Stress relaxation tests - network theory

Using the Instron machine it was possible to perform stress relaxation experiments at very low stress levels. Also, a number of tests with different initial extensions could be performed on one specimen provided that the stresses involved did not cause any permanent deformation of the specimen. A typical result of this type of test is shown in Fig V.21. It will be seen that at very low stresses, no stress relaxation effect is present in the time scale of the experiment. As the initial stress is increased the stress relaxation effect becomes more marked. Comparison with Fig III.11 shows that this type of stress relaxation behaviour can be described in terms of the network theory if the side members of the network have viscoelastic properties. The results of the stress relaxation tests carried out at low stress levels were therefore analysed in terms of a net-work model of this type. As this analysis was rather complex it is illustrated below in the form of a sample calculation using the results of the test shown in Fig V.21. To obtain values for the network parameters at time t = 0, the stresses at t = 0 were plotted against the appropriate strains to give a form of stress-strain curve. The appropriate network parameters were:
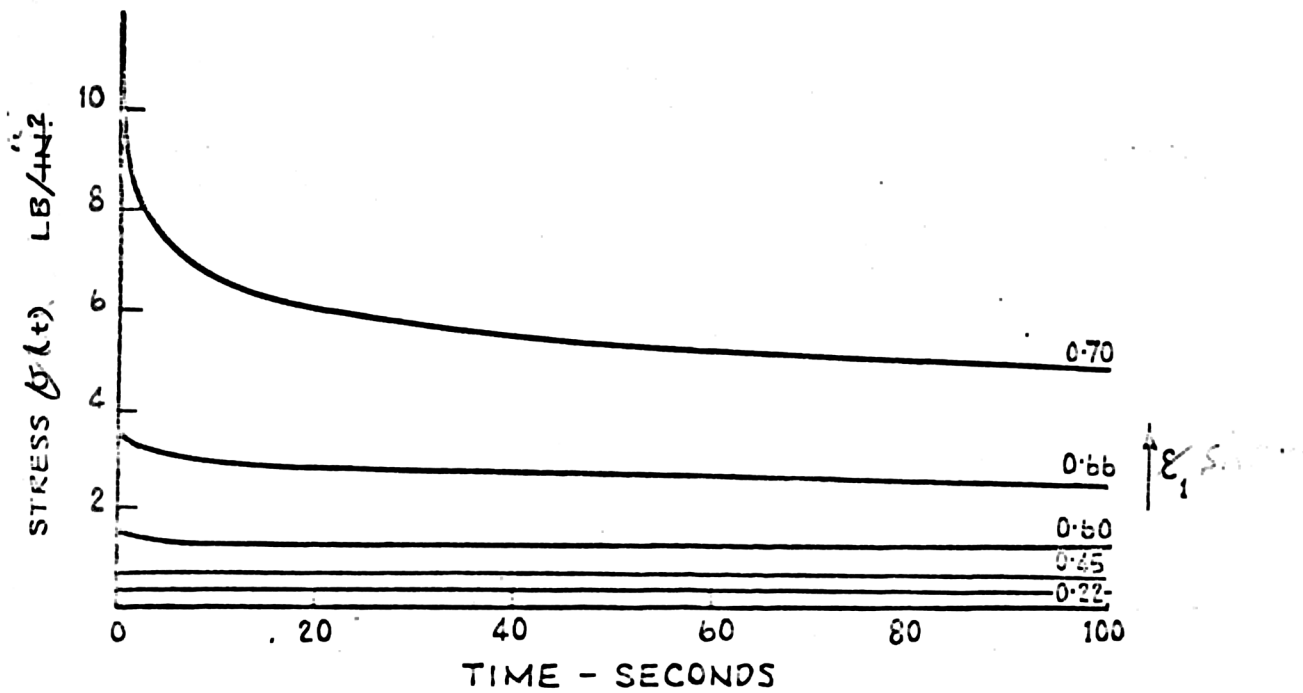
FIG. V 21. STRESS-RELAXATION TESTS AT LOW STRESS LEVELS
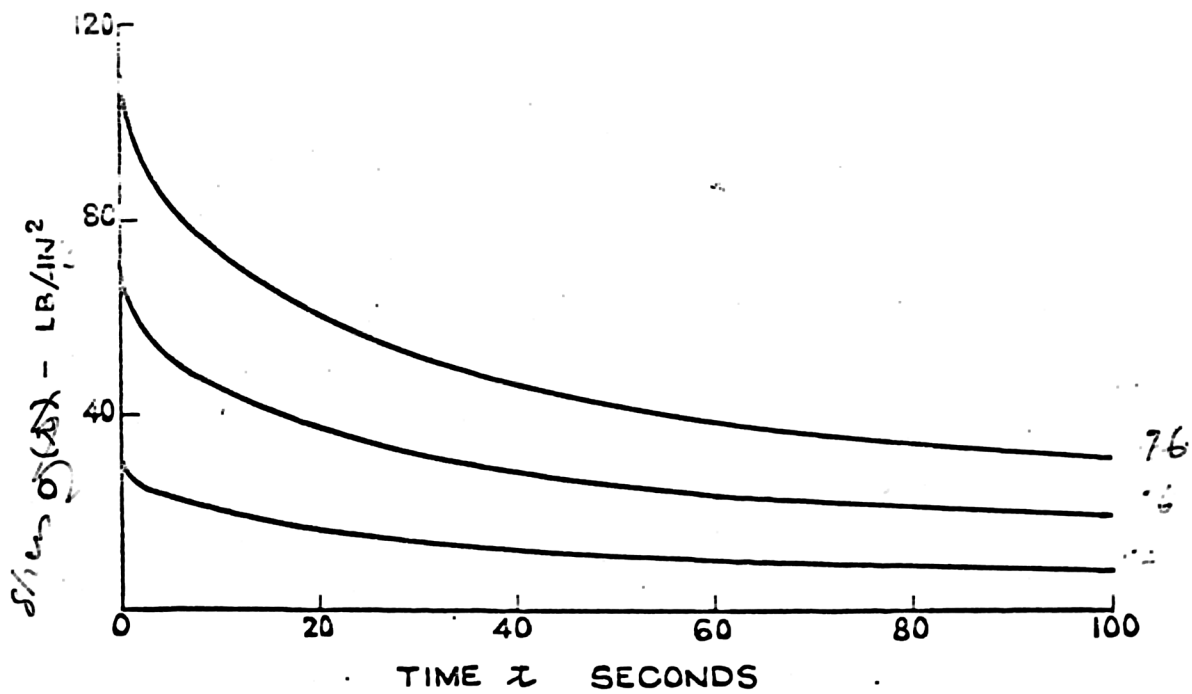
FIG. V 22 EXPERIMENTAL STRESS RELAXATION CURVES
AT HIGH STRESS LEVELS

$$\alpha = 53^{\circ} \qquad \beta(0) = 130 \text{ lb/in}^2$$

$$\gamma = 0.4 \text{ lb/in}^6$$

In order to define the viscoelastic properties of the side links, it was assumed that, when the network was in the fully oriented configuration, i.e. θ was small, the mechanical properties of the network were determined only by the mechanical properties of the side members as these were directly in line with the applied stress.

A further justification for this assumption, Fig V.22 shows the result of a series of stress relaxation tests carried out at higher stress levels on the same specimen. It can be seen that the form of the stress relaxation curves is identical, the only difference being a factor of proportionality.

Thus, in the example being considered, the value of θ corresponding to σ(0) = 10 lb/in² was 2°. It was assumed that the stress relaxation properties of the side links were defined by the result of this test. These properties were expressed in terms of a stress relaxation modulus β(t), the variation of this with time t being given in Table V.3.

Table V.3

Stress Relaxation Modulus β(t)

t - sec.	1	2	5	10	20	50	100
β(t) - lb/in²	117	107	96	87.5	79.5	67.5	62.5

As the network model was now fully defined, its stress relaxation behaviour was investigated, i.e. the
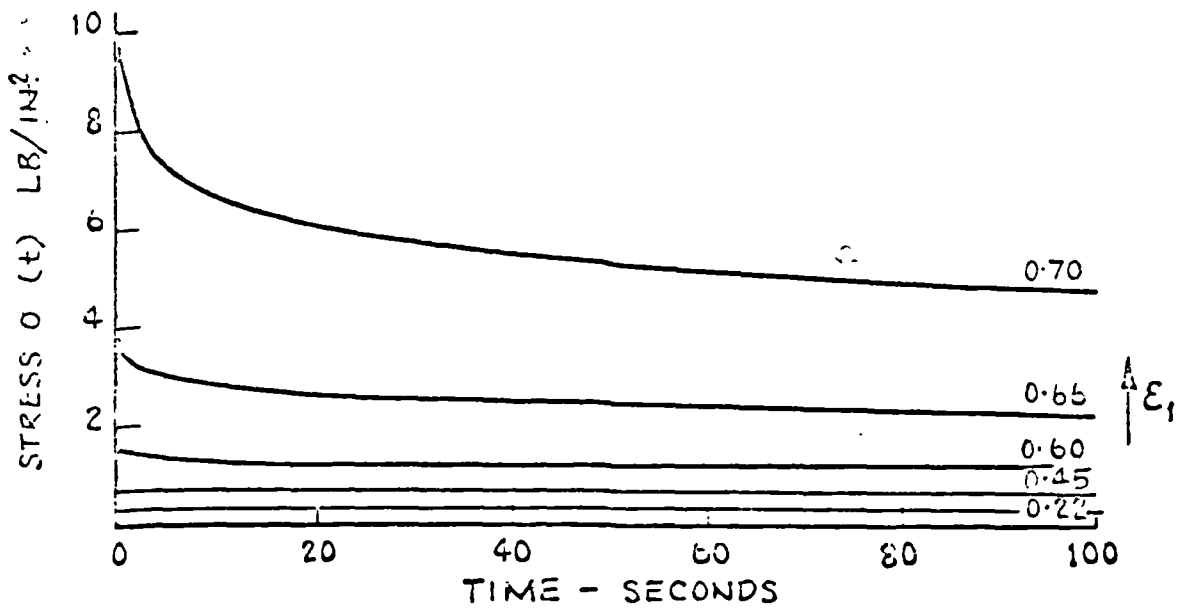
FIG. V. 23 NETWORK THEORY — PREDICTED STRESS
                                RELAXATION BEHAVIOUR

model was suddenly extended by a known amount and held
at this extension.   The variation with time of the form
required to maintain this extension was then calculated.
This calculation was performed for extensions corresponding
to the strains used experimentally, i.e. $\epsilon_1 = 0.22$, 0.45, 0.60,
0.66, 0.70.   The result is shown in Fig V.23.

It was found that the model behaviour could be
split into three phases:

(i)   for $\epsilon_1 < 0.6$, there was no apparent stress
         relaxation effect in the time scale ($0 < t < 100$ secs.)
         being considered.

(ii)   for $0.60 < \epsilon_1 < 0.70$ the model exhibited a more
         complex behaviour.   The time-dependent
         deformation of the side links was sufficient to
         cause an appreciable change in the model geometry
         with a consequent time-dependent change in the
         forces in the model.

(iii)   for $\epsilon_1 > 0.70$, the network was nearly fully
         oriented and the side elements were almost
         directly in line with the applied stress.   The
         stress relaxation properties of the network were
         thus defined by the properties of the side
         members.

Sample calculations given in Appendix A.IX show
clearly how the three types of behaviour discussed above
arise.

Very good agreement was obtained between the
theoretical and experimental results, the only appreciable
discrepancies being in the second phase of network
behaviour, i.e. $0.60 < \epsilon_1 < 0.70$.   This was the result
of the assumption of linear viscoelastic behaviour of the
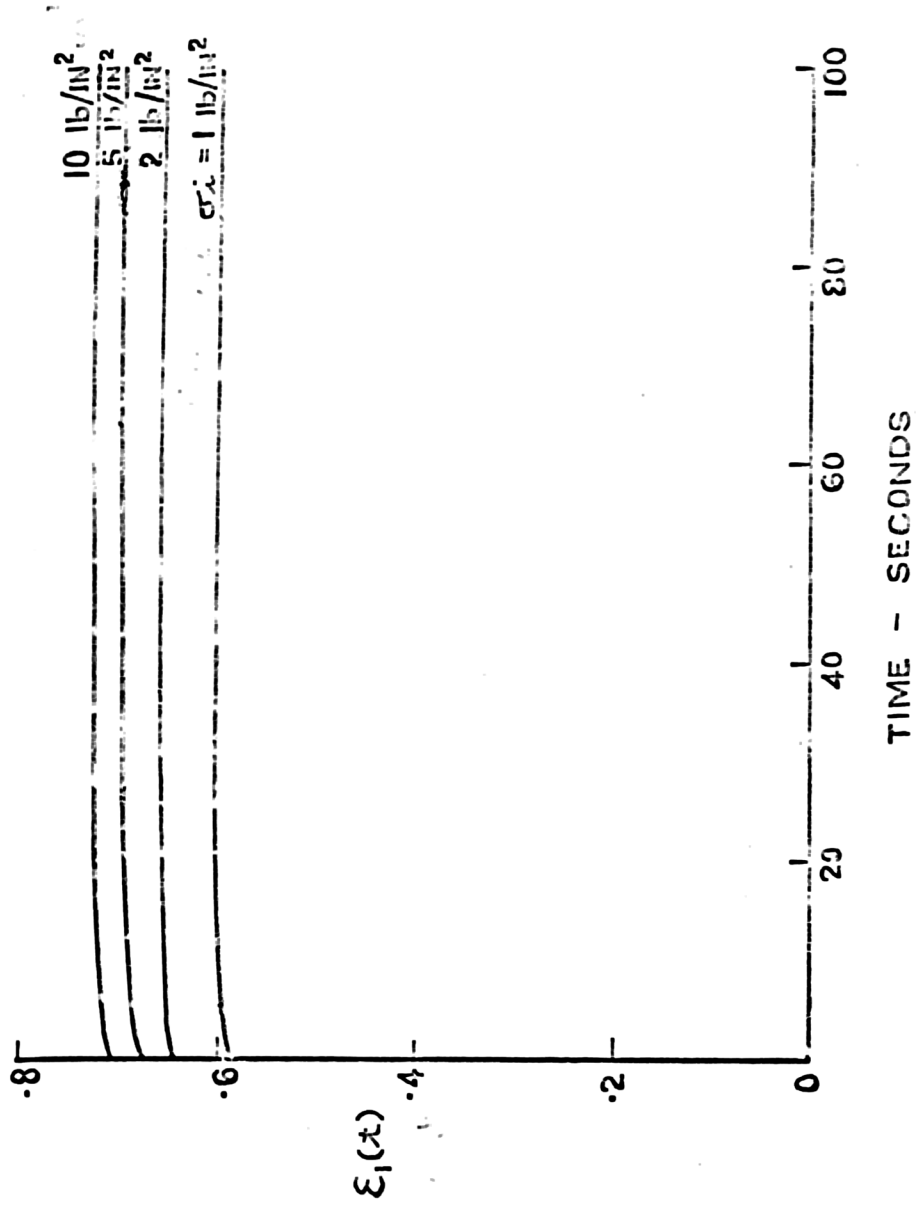
FIG. $\underline{V}$ 24 TYPICAL CREEP TEST RESULT AT
LOW STRESS LEVELS.

side members which was necessary in the calculations.
The stress-strain behaviour of collagen is known to be
slightly non-linear (Morgan 1960) so that this assumption
is only an approximation to the true conditions.

V.2.3   Single step creep tests

Concurrently with the single step stress
relaxation tests discussed in the previous section, a series
of creep tests at low stress levels was performed. This
was done immediately after the stress relaxation tests on
a given specimen.

Using the same data as was used to predict the
stress relaxation curves from the network model, the
creep behaviour of the model was calculated and compared
with the experimental data. These calculations were
simpler than for the stress relaxation case as, because
the creep deformations of the network occurring after
the initial sudden extension were always small, the forces
in the network could be assumed constant throughout the
creep deformation.

As the actual creep deformations were very
small, it is not satisfactory to produce the results of
these experiments in graphical form (Fig V.24). The
experimental and theoretical creep deformations at various
loads after a time of 100 seconds are given in Table V.3·
for the same specimen which was used for the stress
relaxation test discussed in the previous section.

Table V.3

Experimental and Theoretical Creep Deformation

Stress σ lb/in?		1	2	5	10
Strain ε_1 at t = 0		.593	.645	.688	.710
Strain ε_1 at t = 100 secs.	Experimental	.602	.660	.697	.726
	Theoretical	.600	.659	.712	.767

It will be seen that the theoretical results were in close agreement with the experimental data at the lower stress levels but that there was an appreciable difference at a stress of 10 lb/in? This again indicates that the assumption of linear viscoelastic behaviour for the network side members is not strictly permissible. The creep behaviour of the side members predicted from the stress relaxation data on the basis of this assumption represented the true behaviour of the material only to a first order approximation.

V.2.4   Stress relaxation cycling tests

In the stress relaxation and creep tests described above, the specimens were subjected to at least five loading cycles up to the maximum load to be used during the test proper. Under these conditions it was found that if a given test was repeated, the same result was obtained within the limits of accuracy of the test.

To investigate the effect of repeated stress relaxation cycles, tests were carried out using the Instron machine on specimens which had no previous loading history.
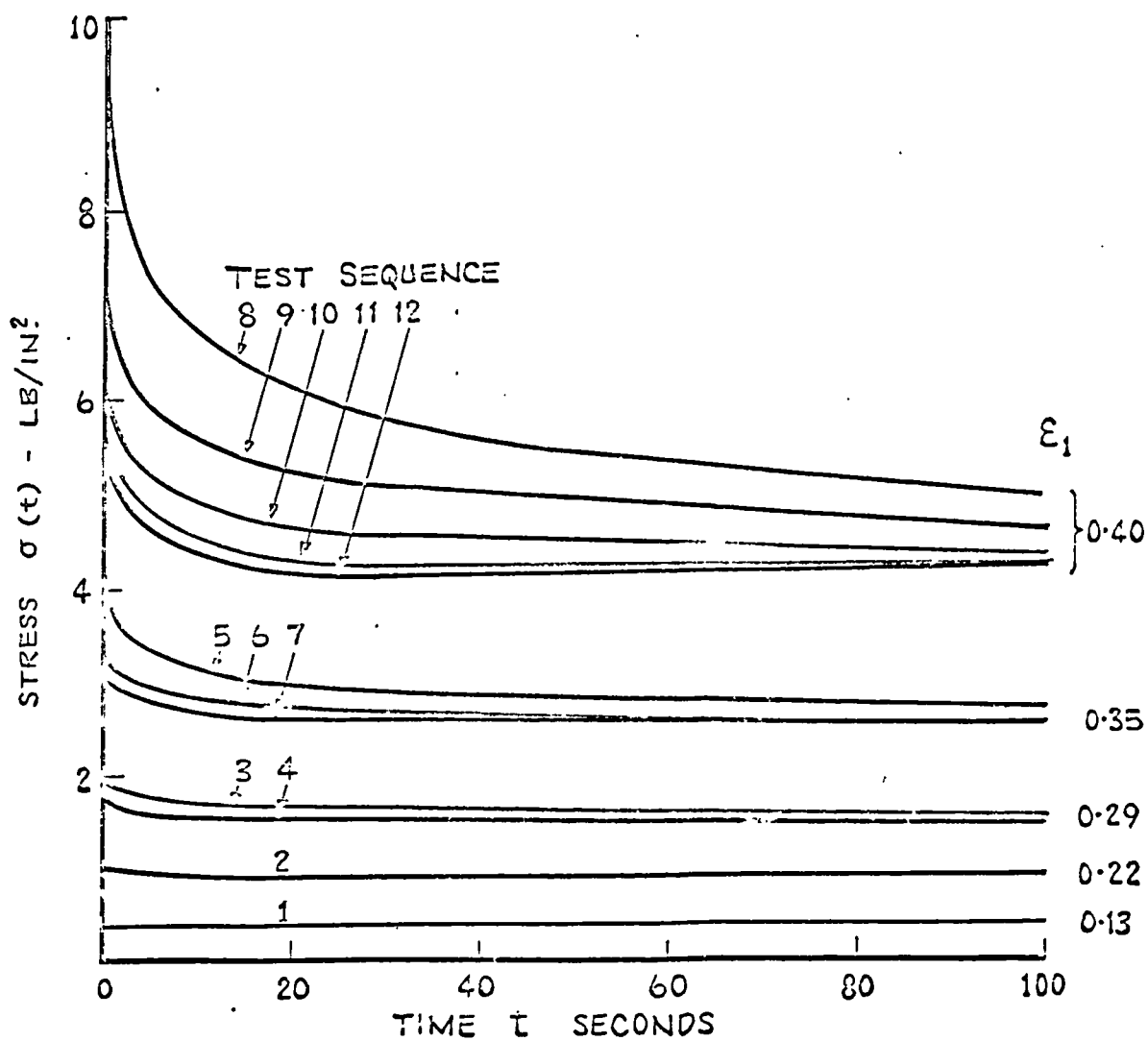
FIG. V. 25.   REPEATED STRESS RELAXATION EXPERIMENTS ON SPECIMEN WITH NO PREVIOUS LOADING HISTORY. EACH GROUP OF TESTS IS CARRIED OUT AT THE SAME STRAIN.

The test procedure was as follows:-

(i) specimen extended at constant rate to a
suitable value of <u>strain</u> and then held
at this strain

(ii) stress relaxation for a period of 100 seconds

(iii) specimen returned to original length and
allowed to rest for five minutes

(iv) extension at same constant rate to the
same <u>strain</u> then stress relaxation for
100 seconds

(v) returned to original length, rested for
five minutes then cycle repeated several
times at same <u>strain</u>

(vi) the above procedure was repeated for a
series of increased <u>strains</u>.

The result of such a test is shown in Fig V.25. It is
seen that at any given strain, the initial stress is
reduced on successive cycles and that the magnitude of
the stress relaxation effect is also reduced. At any
given strain, the value of $\sigma(t)$ as t increases is seen to
approach the same value for each successive stress
relaxation at that strain although the values of $\sigma(0)$ at
t = 0 are markedly different. Also after several cycles
the form of the stress relaxation curve at a given strain
becomes constant.

Fig V.26 shows the result of a similar type of
test. In this case the successive stress relaxations
were started at the same <u>stress</u> instead of the same
strain. Again the magnitude of the stress relaxation
effect is seen to diminish with successive cycles, the
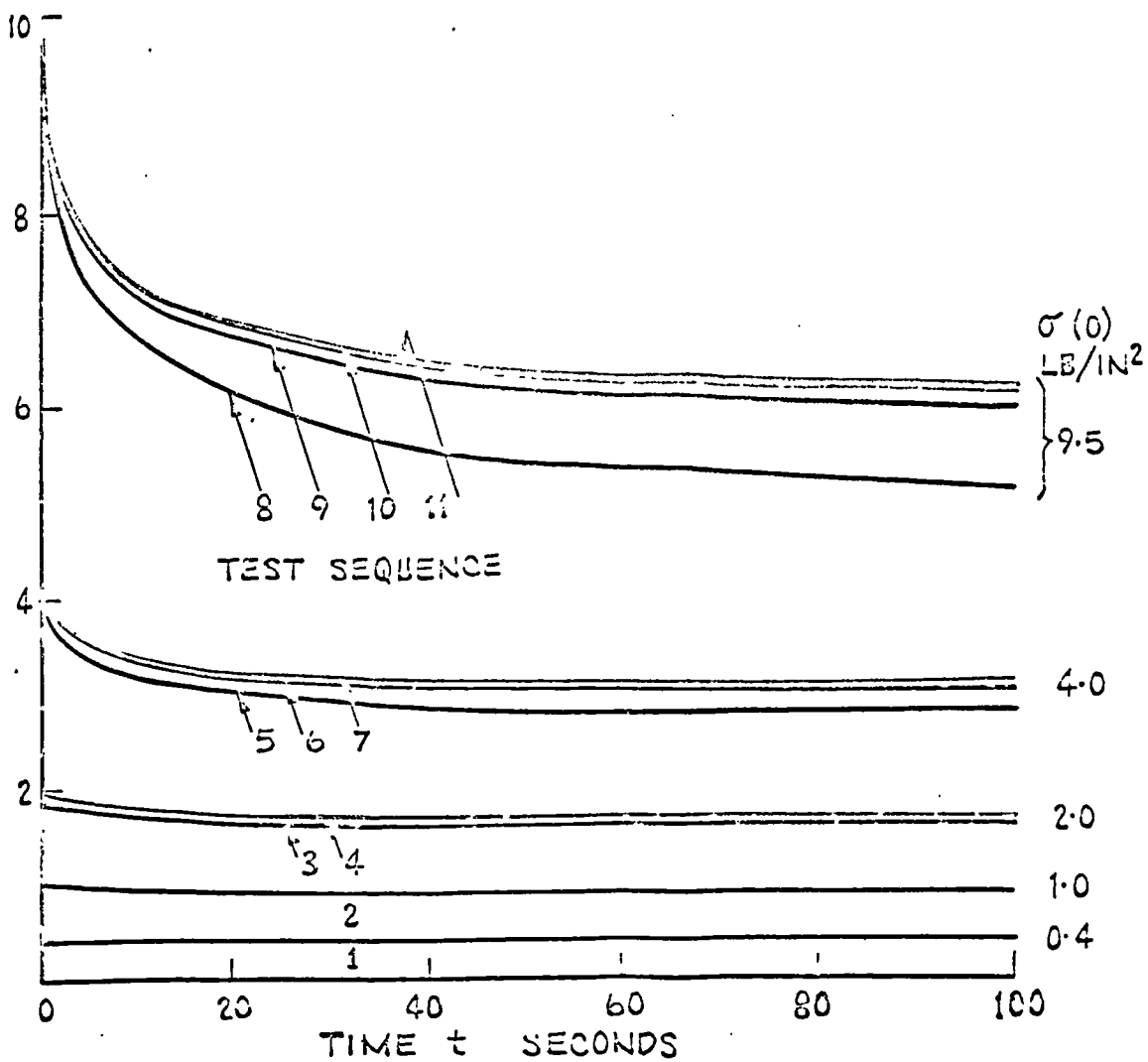
G. V. 26. REPEATED STRESS RELAXATION EXPERIMENTS ON SPECIMEN WITH NO PREVIOUS LOADING HISTORY. EACH GROUP OF TESTS IS CARRIED OUT AT THE SAME INITIAL STRESS.

form of the curve obtained becoming constant after some
four cycles.

V.3   Multi Step Stress Relaxation Test
         In order to assess the possibility of applying
the general theory of non-linear viscoelastic materials
presented in Chapter III to assessing the behaviour of
human skin, one specimen of skin was subjected to the
uniaxial test programme suggested by Lockett (1965).

V.3.1   Test programme
         The specimen was subjected to 20 loading cycles
to a maximum stress of twice the maximum stress to be used
in the succeeding test programme.   There was no discernible
difference between successive cycles after this treatment.
         The test programme proper was split up into three
main types of test:-

(i)   single step tests, in which the specimen
         was suddenly extended to a preset strain
         c_i at time $t = 0$ and then held at this
         strain.   The stress in the specimen
         was recorded with time.   Six such tests
         were performed with different strains
         on the same specimen

(ii)   two step tests in which the specimen
         was given a strain a_i at $t = 0$, held at
         this strain until $t = k$ and then given a
         further strain b_j.   This strain was
         maintained and the stress in the specimen
         was recorded with time.   Three tests of
         this type were performed with the same
         value of k and different values for a_i
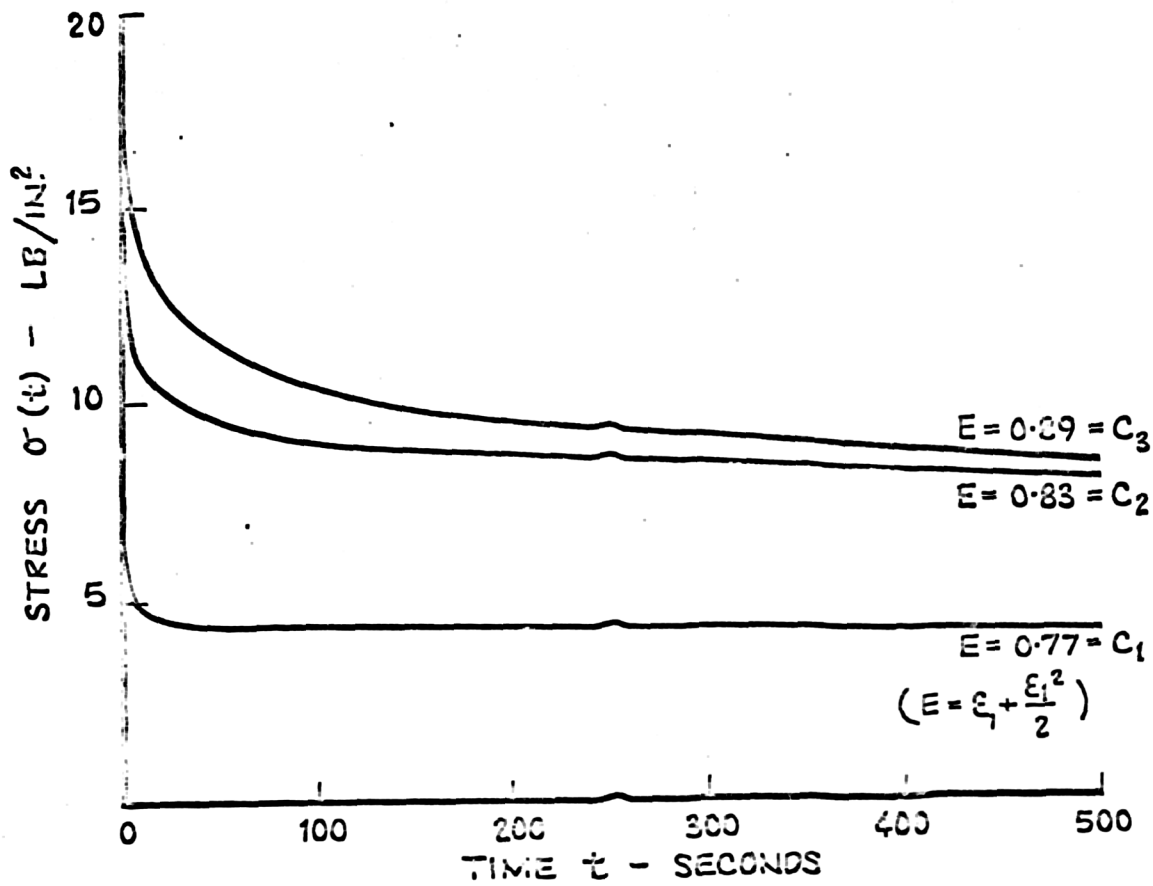
FIG. V 27. SINGLE STEP STRESS RELAXATION TESTS.
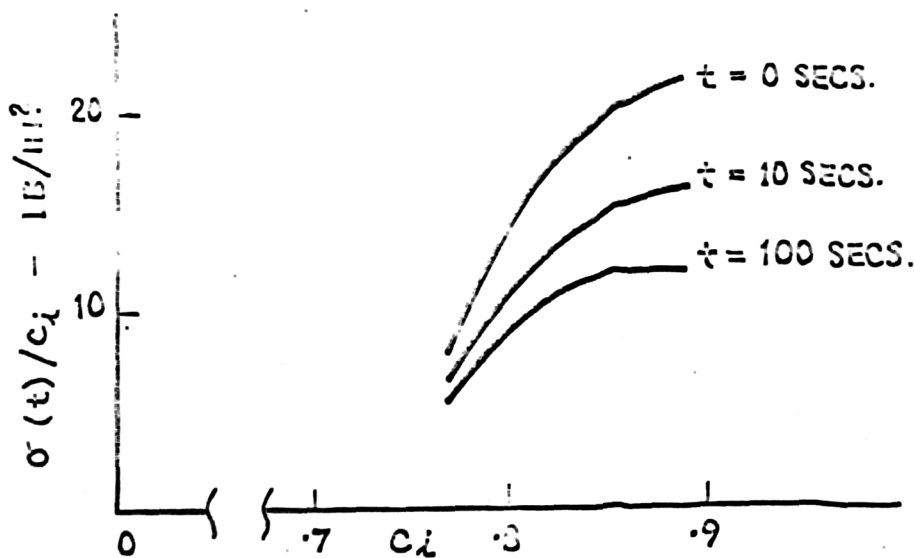
FIG. V. 28 $\sigma(t)/c_i$ Vs c_i PLOT SHOWING NON LINEAR
VISCOELASTIC BEHAVIOUR.
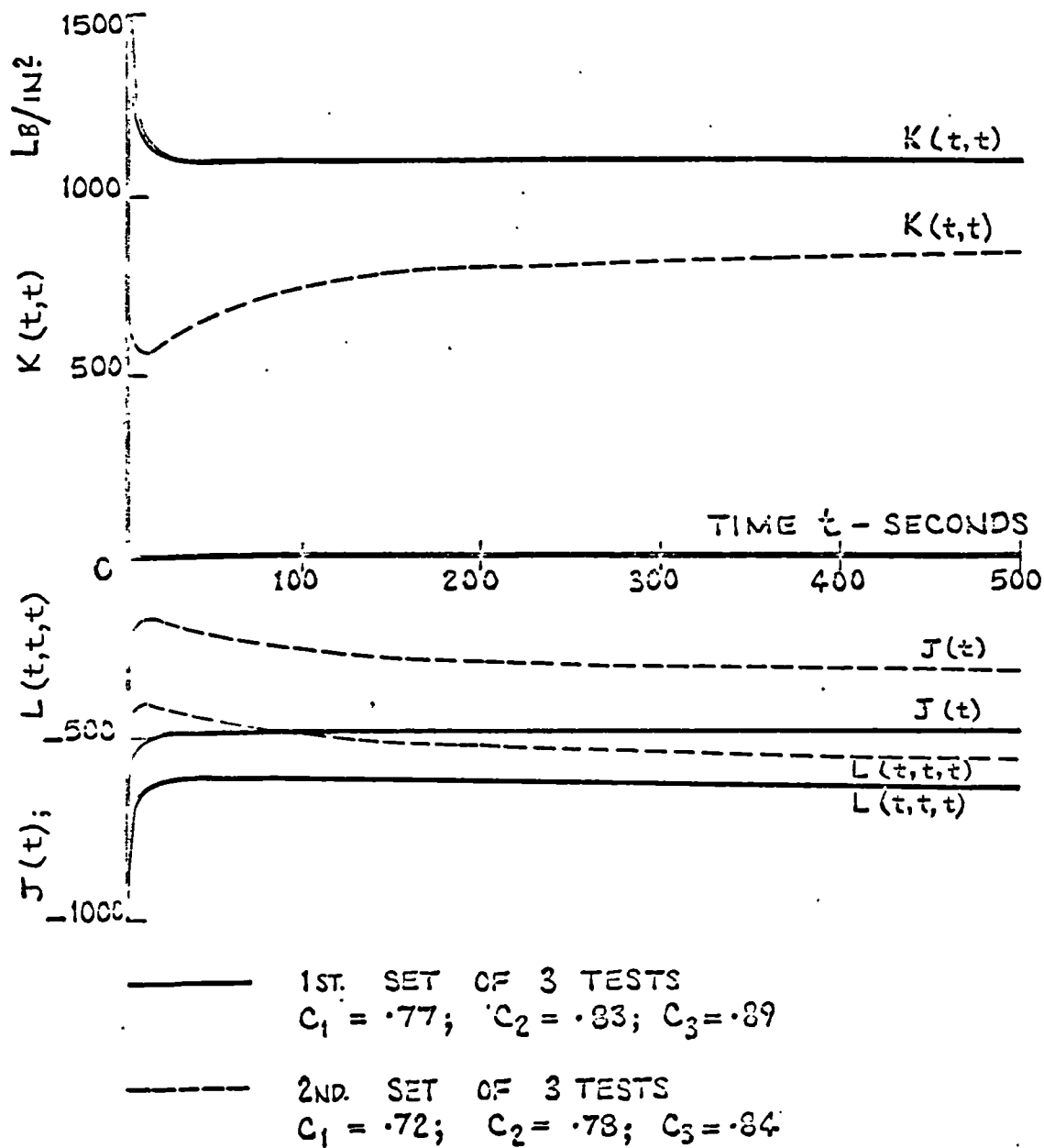
FIG. $\underline{V}$. 29. NON-LINEAR VISCOELASTIC THEORY-
ANALYSIS OF SINGLE STEP TEST RESULTS.

and b_j. These were selected in a
manner which much simplified the analysis
of the results, *viz.*

1st test	a_1	,	b_1
2nd test	a_1	,	b_2
3rd test	a_3	,	b_1

This whole procedure was repeated for a
number of different values of k.

(iii) three step tests in which a strain a was
applied at $t = 0$ and held constant until
$t = k$. A further strain b was then
applied and held constant until $t = \ell$
and then a final strain c was applied and
held constant, the stress in the specimen
then being recorded with time. This
test was repeated with the same values of
a, b and c for a number of different
values of k and ℓ in the range $0 < k < \ell$.

V.3.2   Analysis of results

The results of three of the single step tests
are shown in Fig V.27 and are seen to be of the usual form
for such tests.

The functions $J(t)$, $K(t, t)$, $L(t, t, t)$ were
obtained from these curves by the methods of analysis
described in Chapter III and Appendix A.V. The
variation of stress $\sigma(t)$ with time t is given by:

$$\sigma(t) = c_i^1 \, J(t) + c_i^2 \, K(t, t) + c_i^3 \, L(t, t, t) \qquad \text{V.2}$$

and b .   These were selected in a
manner which much simplified the analysis
of the results, *viz.*

1st test	a_1	,	b_1
2nd test	a_1	,	b_2
3rd test	a_3	,	b_1

This whole procedure was repeated for a
number of different values of k.

(iii) three step tests in which a strain a was
applied at t = 0 and held constant until
t = k. A further strain b was then
applied and held constant until t = ℓ
and then a final strain c was applied and
held constant, the stress in the specimen
then being recorded with time.   This
test was repeated with the same values of
a, b and c for a number of different
values of k and ℓ in the range 0 < k < ℓ.

V.3.2   Analysis of results

The results of three of the single step tests
are shown in Fig V.27 and are seen to be of the usual form
for such tests.

The functions J(t), K(t, t), L(t, t, t) were
obtained from these curves by the methods of analysis
described in Chapter III and Appendix A.V.   The
variation of stress σ(t) with time t is given by:

$$\sigma(t) = c_1 J(t) + c_1^2 K(t, t) + c_1^3 L(t, t, t) \qquad\qquad V.2$$

where c_i is the constant strain in the material. For
c_i $\ll 1$ the terms in c_i^2 and c_i^3 can be neglected and
equation V.2 reduces to:

$$\sigma(t) = c_i J(t) \qquad\qquad V.3$$

which is the equivalent expression from linear visco-
elastic theory. That equation V.3 does not describe the
behaviour of skin is readily shown by plotting $\sigma(t)/c_i$
against c_i (Fig V.28). If equation V.3 was correct
this would result in a series of horizontal lines each
representing a given time t. This is seen to be not the
case. It is therefore necessary to consider equation V.2.
Although only three terms are given in this equation,
it should be appreciated that further terms might be
needed adequately to describe the material. However, it
is not practical to consider such terms because of the
much greater complexity of the analysis and, more
significant, the experimental accuracy is unlikely to be
high enough to allow such terms to be resolved.

The functions J(t), K(t, t) and L(t, t, t)
obtained from the experimental data are shown in Fig V.
29. Before proceeding with the analysis of the two step
and three step tests, a similar analysis was performed on
the results of the remaining three single step tests.
The functions obtained from these tests are also shown in
Fig V.29. It is seen that there was a considerable
difference between the functions obtained from the two sets
of results. Also, if the behaviour of the skin at small
deformations is considered (i.e. equation V.3 holds) it is
seen that as the function J(t) has a negative value, the
specimen would have a negative modulus, i.e. its length

would reduce under tensile stress.   This is clearly non-
sense as this does not occur in practice.

These results indicate clearly that the
presently available concepts of non-linear viscoelastic
theory are not applicable to skin in the form considered.
Two possible reasons for this are:-

(i)   the basic assumptions of the theory do not
apply to skin, in particular it is definitely
known that skin is not a continuous material
but has a complex multi-phase network structure.

(ii) the three terms considered in the equations of
the theory are not sufficient to describe the
behaviour of skin

Although this type of theory is not at present a
practical approach to the problems presented by skin, it
should be appreciated that future mathematical developments
in this field may radically alter this situation.

V.4   Discussion of Results

The analysis of the results of the uniaxial tests
at constant strain rate in terms of the network theory
shows that even this very simple approach gives a good
approximation to the actual behaviour of skin *in vitro* and
lends further support to the histological evidence which
originally suggested the three-phase network concept of
skin.

Of the four network parameters, only α gave
consistent values and showed a definite age-dependence.
This parameter gives a measure of the amount by which the

collagen fibres have to straighten out and orient themselves
in the direction of the applied stress.   The reduction in
this with increasing age suggests that the number of
"linkages" between the collagen fibre bundles increases
with age as this would result in a restriction of the net-
work movement involved in the orientation of the fibres.

The parameter β varied within wide limits but
showed no dependence on age or sex.   It is obviously
necessary to consider other variables such as the disease
history of the donor to find the reasons for this
variation in β which in turn implies a variation in the
mechanical properties of the collagen fibres.

As γ is a purely empirical factor it is not
possible to give any physical interpretation of its apparent
increase with age other than to say that it indicates a
change in the ground substance and elastin network with
increasing age.

The apparent reduction with age of the parameter
δ suggests that the collagen fibre bundles become either
fewer or narrower with increasing age.

The extension of the network theory to include
viscoelastic effects resulted in good agreement with the
experimental data, the only significant error being due
to the assumption of linear viscoelastic behaviour of the
collagen fibres. In marked contrast, the general theory
of continuum mechanics was not able to describe the visco-
elastic behaviour of skin when used in a simplified form.
Although, in principle, the continuum mechanics approach
is capable of producing a correct solution, the
difficulties involved in considering more than three terms

in the equations of this theory render its use impractical at present.

The load cycling and repeated stress relaxation tests showed that even at very low stress levels, permanent effects are produced in skin *in vitro* by mechanical stress. This could possibly imply that some form of consolidation of the "linkages" between collagen fibre bundles takes place. For example, if these linkages are in the form of mechanical entanglements between adjacent fibres, the "knot" so formed could be pulled tighter. It has not yet been possible to demonstrate any form of connection between the fibre bundles histologically.

V.5   Summary

Taken as a whole, the results presented give very strong support to the concept of skin as a three-phase network consisting of:-

(i)   a dense collagen fibre network which acts as a very strong limit stop to the extension of skin and provides a supporting framework for the ground substance

(ii)   a fine network of elastin fibres which may or may not contribute to the initial large extension at low stress of skin

(iii)   an apparently amorphous ground substance which permeates the above networks. This would be expected to have appreciable viscoelastic properties but the apparently perfectly elastic behaviour shown by skin in the initial extension

region shows that the elastic properties
predominate. This implies that the
viscosity of the ground substance is
either so low that stress relaxation
and creep effects occur in too short
a time to be measured or so great that
these effects occur too slowly to show
up in the time scale of the experiments.

Chapter VI

Experimental Work *in Vivo*

—————————————————
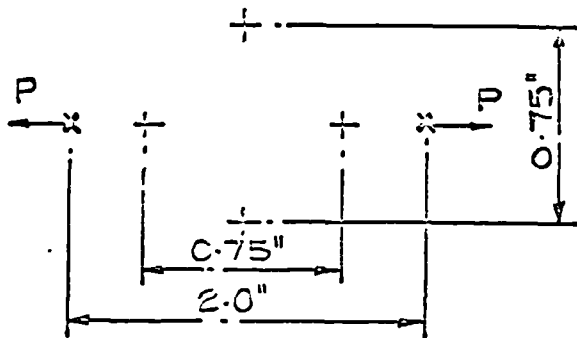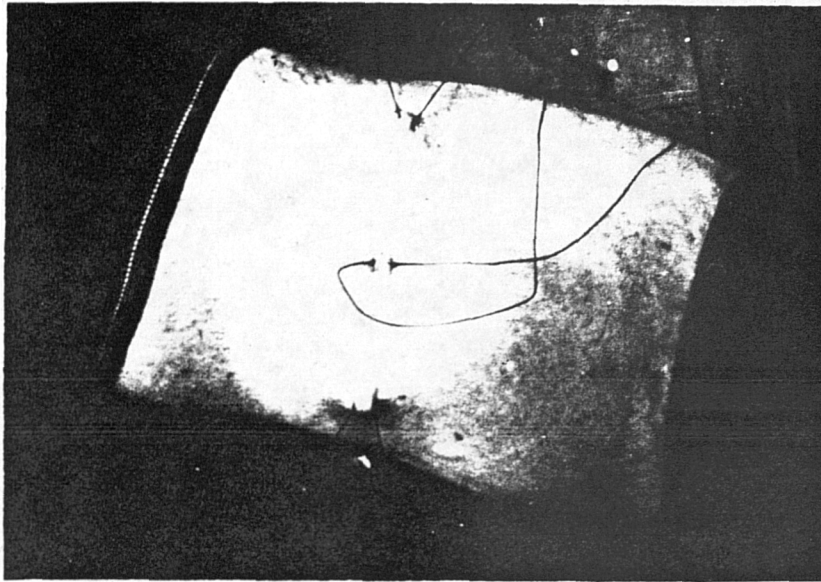
FIG. VI 1-LOAD PAIR ATTACHMENT POINTS AND
GAUGE LENGTH MARKINGS USED FOR IN VIVO TESTS.

Concurrently with the programme of *in vitro* tests described in the previous chapters, an investigation of the mechanical porperties of skin *in vivo* was carried out. The aims of this were twofold:-

(i)   to determine the basic mechanical character-
      istics of skin *in vivo* and, if possible, to
      relate these to *in vitro* results.

(ii) to examine the possibility of applying
      knowledge of the mechanical properties of
      skin to a variety of clinical problems.
      This topic is discussed in Chapter VII.

VI.1   Uniaxial Tensile Tests *in Vivo*

Human skin *in vivo* can be regarded as a membrane which is normally subject to a biaxial tensile stress system and a traverse pressure. The magnitude of these stresses and pressure varies in a complex manner over the surface of the body. The method of uniaxial test employed was to apply a load pair to the skin surface and to measure the resulting extension of a gauge length marked between the points of load application (Fig VI.1). When possible, the dimensions given in the Fig were ahhered to,but in some cases this could not be done because of the size of the test site or difficulty of access by the instrumentation to the site.

VI.1.1   *In vivo* loading apparatus

Various pieces of apparatus were built for applying loads to the skin. The first of these is shown in Fig VI.2. This consisted of a simple tubular frame A with two screw operated slides BB carrying the load measuring beams CC. The loads were applied to the skin *via* sutures on light strings attached to the hooks D on
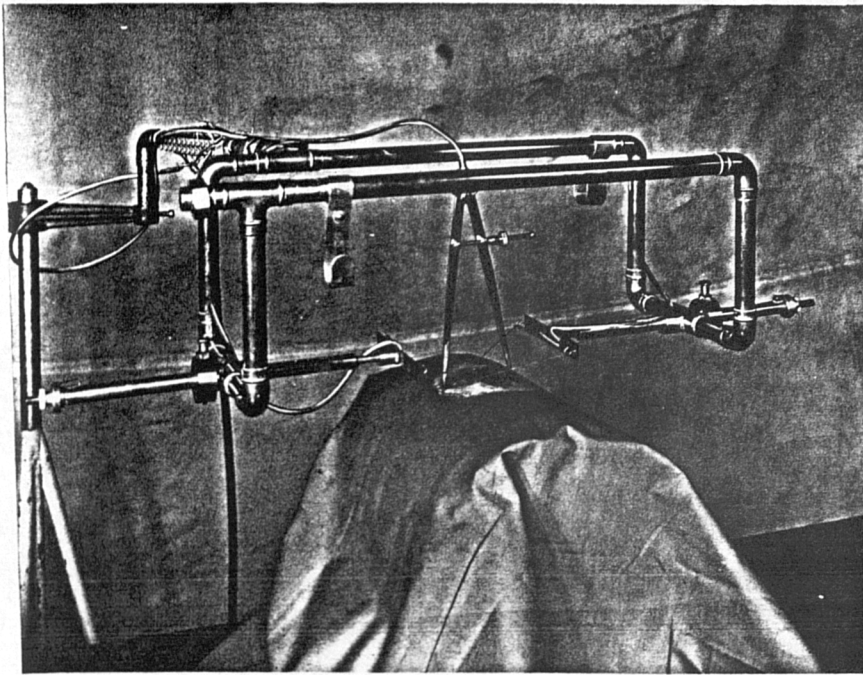
FIG. VI.2. - SKIN DYNAMOMETER MK.1.
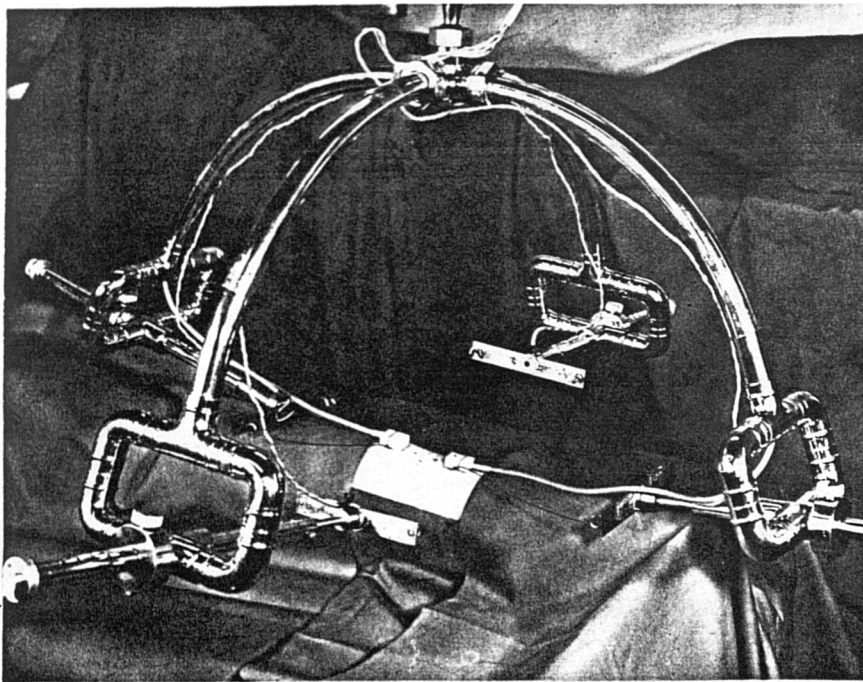
FIG. VI.3. SKIN DYNAMOMETER MK.2.

the beams.   The method of load application to the skin
surface is discussed below.   The applied loads were
measured by means of foil strain gauges on the beams and
a suitable strain bridge.   The whole arrangement was
mounted by means of a universal joint on a suitable
stand.

      This equipment was superseded by the Mark II
instrument, shown in Fig VI.3.   This had four arms so
that two load pairs could be applied perpendicular to
each other.   The load measuring beams were identical
to those used on the Mark I dynamometer.   One pair of
arms could be removed if only one load pair was required.
This instrument was mounted on a more complicated stand
giving a much wider range of adjustment.

      As both of the above instruments were often
used under sterile conditions in the operating theatre,
they were designed to be readily sterilisable, this being
achieved by exposure to paraformaldehyde vapour for a
minimum period of 36 hours.

VI.1.2   Load application to skin

      When tests were performed in the operating
theatre on an anaesthetised subject, the loads were applied
by means of sutures embedded deep in the dermis.   The
free ends of the sutures were attached to the load
measuring beams and the load applied by moving the beams
apart using the screw operated slides.

      Because of the obviously limited opportunities
for working on anaesthetised subjects, it was necessary
to develop means of applying loads to the skin surface of
conscious subjects.   Initially, this was done by means
of tabs bonded to the skin by Eastman 910 adhesive, this
being a very powerful contact adhesive which only required
a few seconds to cure.   However, although this adhesive
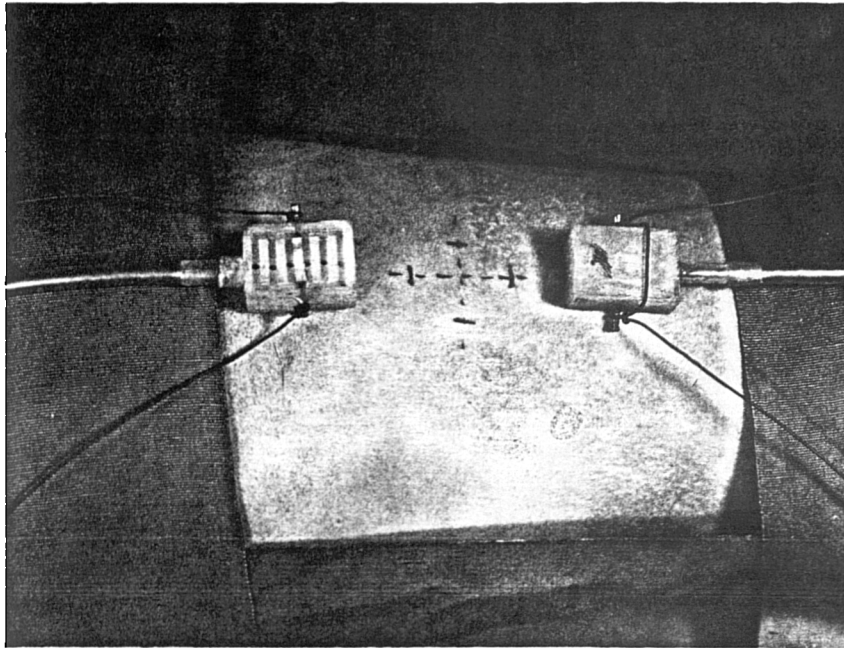
FIG. Ⅵ.4. SUCTION TABS.
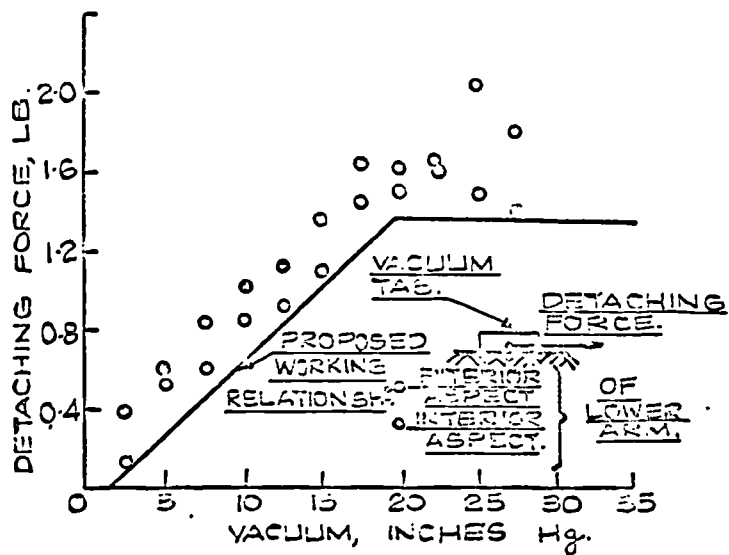
FIG. Ⅵ.5.—VARIATION OF SUCTION TAB DETACHING
FORCE WITH APPLIED VACUUM.

was itself satisfactory, it was found that the tabs
would come adrift at loads of the order of 0.25 lb due to
a failure of the skin itself.   The outermost layer of
the strateum corneum of the epidermis failed in shear
and came away with the tab.   Repeated application of
the tab to the same site merely resulted in the removal
of further layers of the epidermis and was, to say the
least, uncomfortable to the subject.

Because of the above, the adhesive tabs were
replaced by the suction tabs shown in Fig VI.4.   The
variation of the force required to detach the tab with
applied vacuum is shown in Fig VI.5.

IV.1.3   <u>Strain measurement</u>

Measurements of strain in these experiments were
based on the deformation of a gauge length marked between
the load application points.   This was measured by means
of the dial gauge calipers shown in Fig VI.6.

VI.1.4   <u>Experimental technique</u>

The technique was essentially the same as that
used for the pilot *in vitro* experiments.   As stress
relaxation effects were found to occur *in vivo*, it was
necessary to allow the load to stabilise at each increment
for a period of 5 minutes before load and strain were
measured.   This was the major disadvantage of the
technique as it meant that:-

  (i) in the operating theatre, the time available for
       the test was too short to allow for more than a
       few large loading increments.
  (ii) on conscious subjects, the suction tabs could
       not be tolerated for more than approximately
       15 minutes so that again only a few loading
       increments were possible.
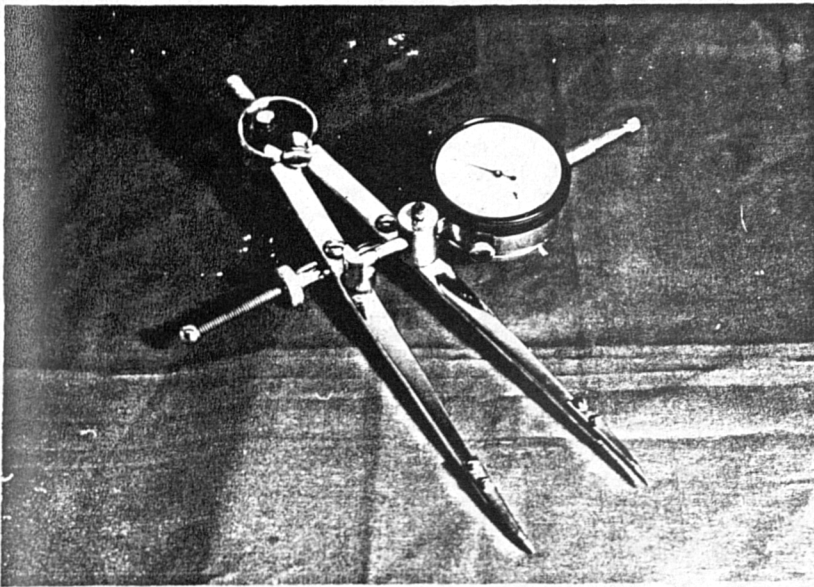
FIG. VI. 6.—DIAL GAUGE CALIPERS USED FOR IN
VIVO STRAIN MEASUREMENT.
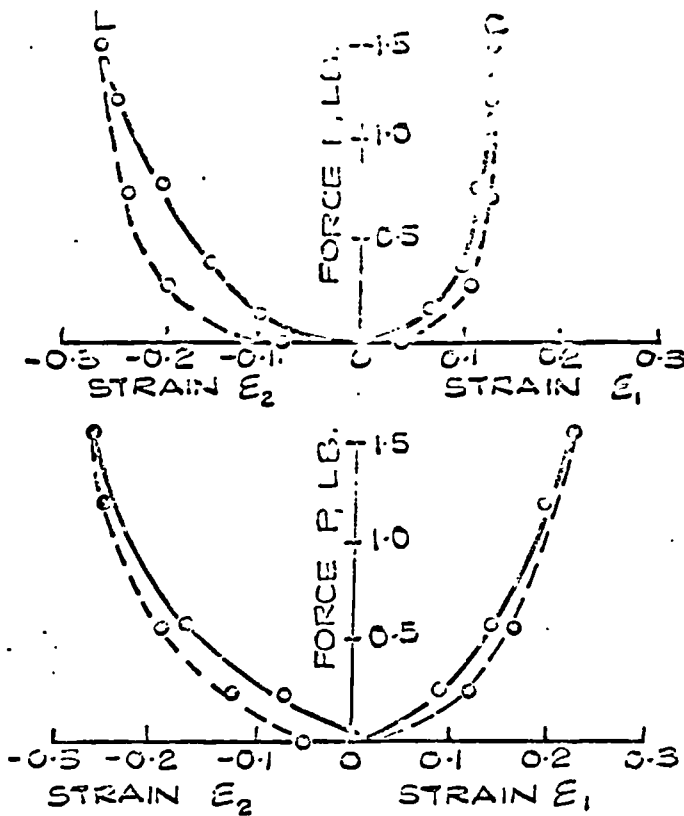
FIG. VI. 7. — IN VIVO TEST — TYPICAL LOAD-EXTENSION
RELATIONS.

As a result of these restrictions, the accuracy of the uniaxial experiments was not as high as the precision of the test equipment would have suggested. Also, it was not possible to carry out a proposed biaxial testing programme using the Mark II dynamometer as the effect of the above limitations combined with the more complicated nature of the test rendered this type of experiment impracticable.

VI.2   Uniaxial Test Results

In spite of the above difficulties a considerable number of tests of this type were carried out and brought to light some important results.

VI.2.1   Load v. strain properties

Fig VI.7 shows a typical load v. strain relation obtained from a uniaxial test. As in the *in vitro* test, strain was measured both along and perpendicular to the axis of the applied load pair. The load v. strain curves are of similar form to the stress v. strain curves obtained *in vitro* except that the initial large extension at very low load levels is not present to the same extent. This is to be expected because the pre-existing biaxial stress field in skin *in vivo* must cause considerable deformation of the skin from the absolute zero stress condition.

The magnitude of strain ε_2 perpendicular to the loading axis is seen to be of the same order as the strain ε_1 in the direction of the load. It most cases it was found to be the greater of the two measurements. This effect is much more marked than in the *in vitro* results, in which the ratio $\varepsilon_2/\varepsilon_1$ only exceeded unity at much higher stress levels than those produced in the *in vivo* tests.
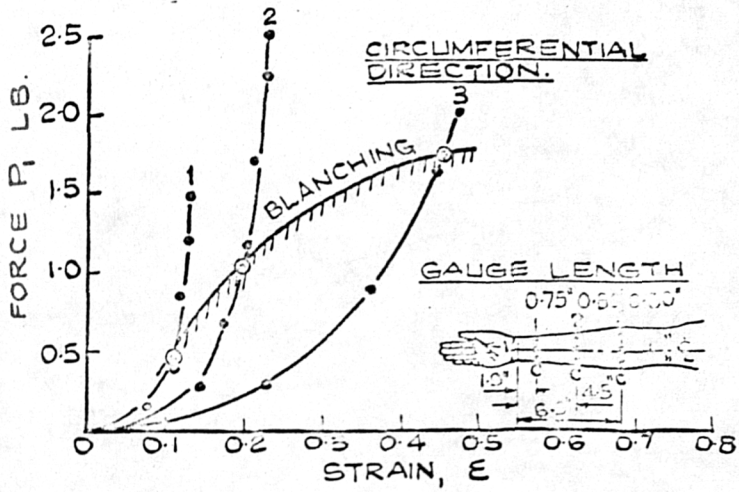
FIG. VI. 8. — VARIATION OF BLANCHING TENSION WITH SITE.
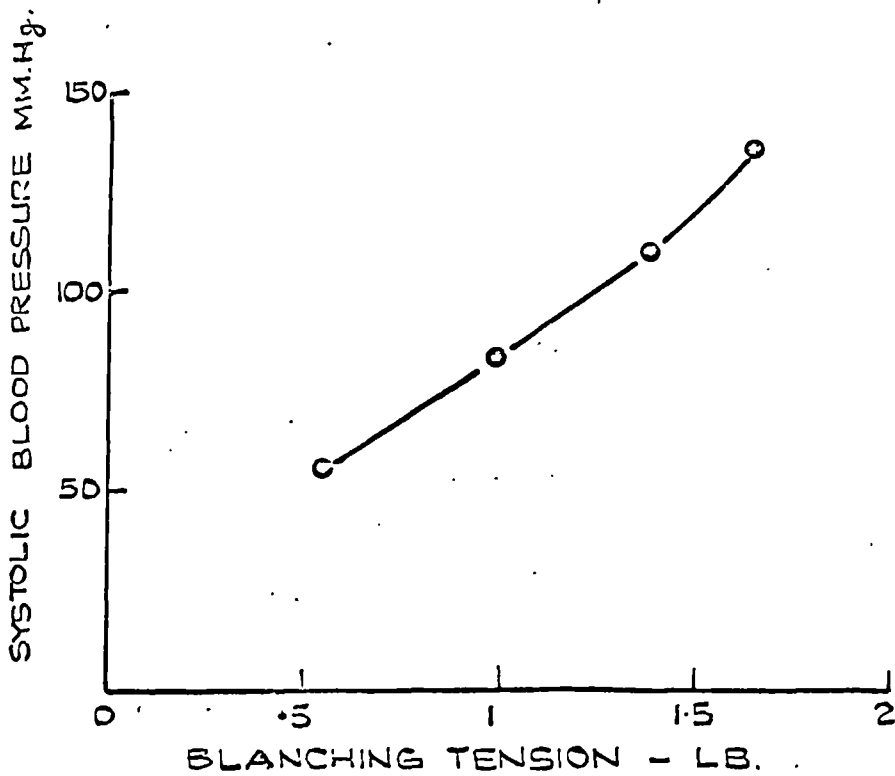
FIG. VI. 9. — VARIATION OF BLANCHING TENSION WITH SYSTOLIC BLOOD PRESSURE.

It is not possible to draw any conclusions from this because of the pre-existing stresses and the complex nature of the stress field produced by the load pair.

In view of the general similarity between the *in vivo* and *in vitro* results, it is reasonable to conclude that the deformation mechanism of skin under both conditions is one of straightening and orientation of the collagen fibre bundles of the dermis in the direction of the applied load in the manner discussed in the previous chapter.

VI.2.2   <u>Blanching tension</u>

In the course of the experiments described above, a phenomenon of considerable importance in clinical practice was investigated. As the load was increased during test a point was reached at which the area of skin between the load application points lost its natural pink colour and became white. This effect is called blanching and the load required to produce it was termed the blanching tension. This load was found to be well defined in most cases, the blanching effect developing fully within a small range of load. The effect is produced by the occlusion of the capillaries supplying blood to the area under tension. This can be explained in terms of the network concept of skin deformation as being the result of the capillaries being collapsed during the compaction of the collagen fibre network associated with the deformation of the skin.

The value of blanching tension was found to vary considerably over the body surface. Fig VI.8 shows a typical variation along the interior aspect of the forearm. Blanching tension also varied with blood pressure as one would expect (Fig VI.9).

At a given site the blanching tension was found to vary with orientation but the strain associated with
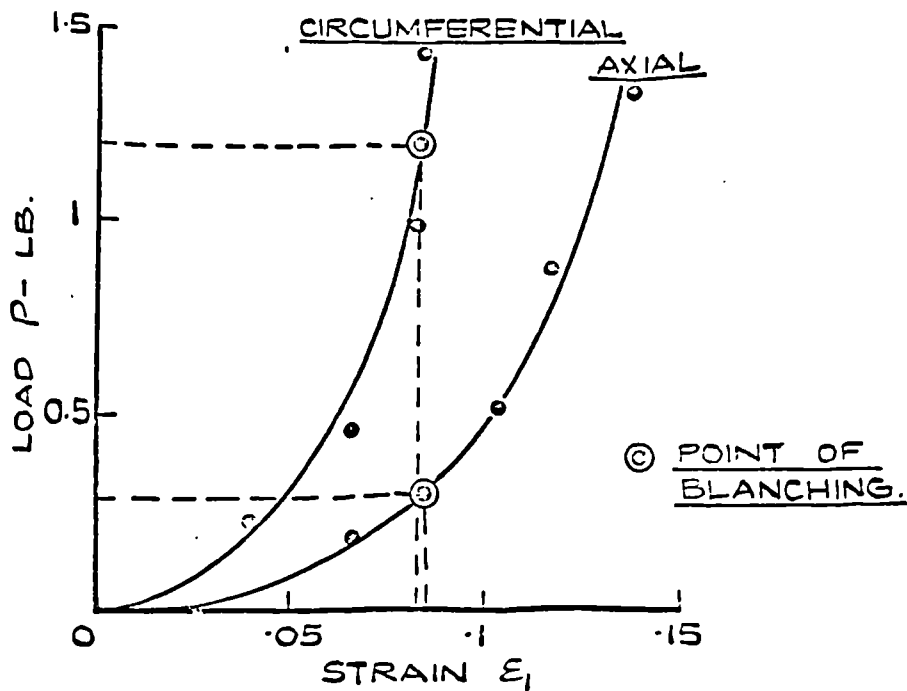
FIG. VI 10. – VARIATION OF BLANCHING TENSION WITH ORIENTATION. BLANCHING STRAIN IS NOT AFFECTED.

DETAILS OF OPERATION	UNCUT SKIN RL. L.L.	FLAP CUT ON 3 SIDES & STITCHED BACK.	AFTER DELAY BEFORE LIFTING	FLAP LIFTED & STITCHED TO HOST SITE.	FLAP HEALED
TIME FROM FIRST TEST.	0	20 MINS	34 DYS	55 DYS	62 DYS
BLANCHING TENSION-LB	1·5	0·5	2·6	1·8	1·4
BLANCHING STRAIN.	0·09	0·04	0·09	0·10	0·09

FIG. VI 11. – VARIATION OF BLANCHING TENSION AND BLANCHING STRAIN DURING CROSS LEG FLAP OPERATION.

the occurrence of blanching was constant within the limits
of accuracy of the test (Fig VI.10).   This effect was
also found in blanching measurements made during a cross
leg flap operation.   The details of this operation and
of the values obtained for blanching tension and the
associated blanching strain are given in Fig VI.11.   It
is seen that although wide variations occurred in the
blanching tension, the blanching strain remained
substantially constant except for the first operation in
which the rectangular flap of skin was raised along three
edges and undercut so that its blood supply only came
through the base of the flap.   In this condition the
flap had a poor blood supply and would thus be expected to
show blanching effects at a lower strain than when the
blood supply was normal.

The blanching effect is of vital importance in
clinical practice.   If the tensions produced in the skin
during the closure of a wound or incision are sufficient
to produce localised blanching, then the area of skin
affected is deprived of its blood supply and will eventually
necrose.   Blanching tension therefore represents the
physiological load limit of skin.   This phenomenon is one
example of a purely mechanical measurement being used to
define a factor of clinical significance.

VI.3   Constant Strain Rate Tests *in Vivo*
Because of the problems caused by the viscoelastic
properties of skin it was decided to attempt to carry out
a form of constant strain rate test *in vivo*.

VI.3.1   Loading apparatus
The loads were applied to the skin by the
instrument shown in Fig VI.12.   This was developed in
collaboration with Mr J.H. Evans of the BioEngineering
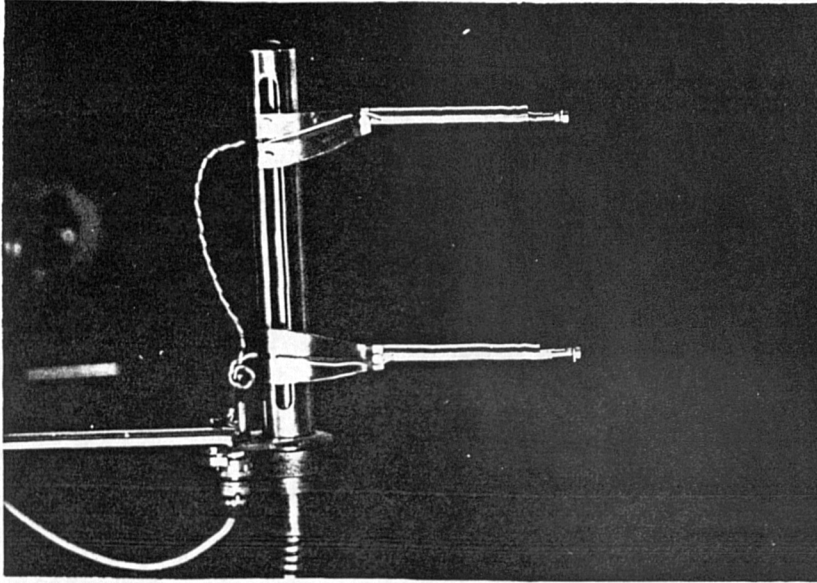
FIG. VI.12.- APARATUS FOR IN VIVO LOADING
AT CONSTANT STRAIN RATE.
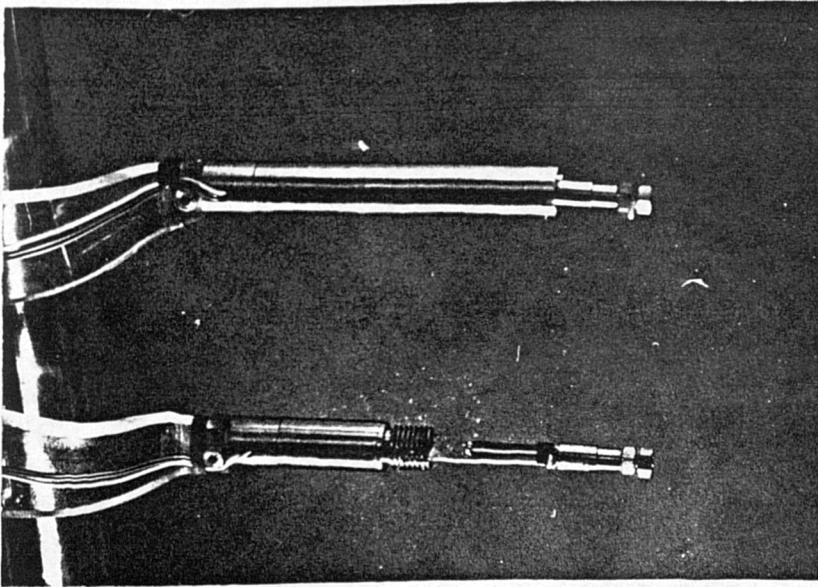
FIG. VI.13.- LOAD MEASURING HEADS.

Unit.   The two load measuring heads AA were mounted on
nuts driven by a lead screw mounted within the barrel B.
One nut had a right hand thread and the other a left hand
thread so that by turning the lead screw the loading heads
could be driven apart or together as required.   The lead
screw was driven *via* a flexible drive shaft by an electric
motor equipped with an infinitely variable and reversible
gear drive.   The load measuring heads are shown in detail
in Fig VI.13.   These consisted of a simple cantilever A
suitably strain gauged.   The sleeve B fitted around the
cantilever and acted as an overload stop.   The output from
the strain gauges was fed to the Ether Langham Thomson
Transducer Indicator, attenuator box and u-v Recorder
which were used with BioEngineering Unit tensile testing
machine described in Chapter IV.

VI.3.2   Strain measurement

Because of the continuously increasing extension
of a gauge length marked on the surface of skin which was
produced by the apparatus described above, some form of
automatic strain recording technique was necessary.   The
Instron Optical Extensometer described in Chapter IV was
found to be suited for this purpose.   As the strain out-
put was recorded on the Instron recorder and the load
output was recorded on the u-v recorder, the two measure-
ments were correlated by time markers on both charts.

IV.3.3   Testing technique

As the equipment described above did not become
available until a very late stage of the research programme,
the testing technique is still very much in the development
stage as can be seen from Fig VI.14; which shows a general
view of the temporary set-up used at present.   A number of
problems were encountered during the only test which has
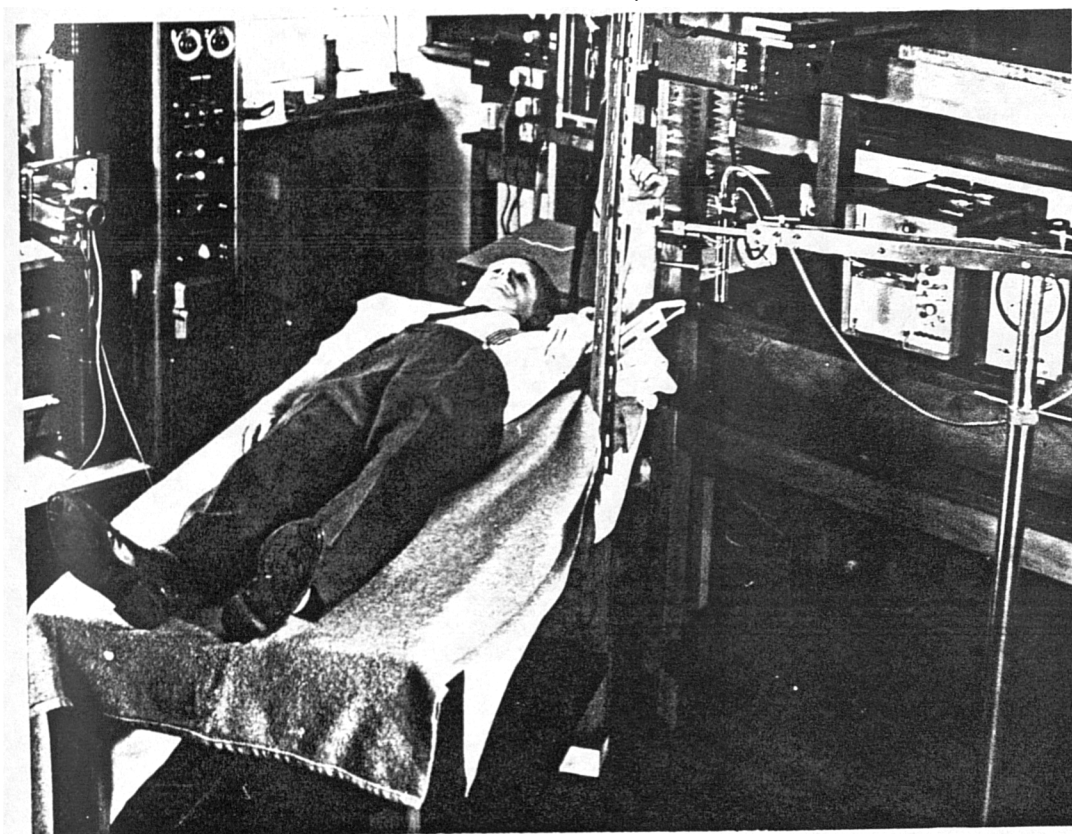
FIG. VI. 14. — TEMPORARY ARRANGEMENT FOR
IN VIVO TESTING WITH CONSTANT STRAIN
RATE APPARATUS.

been carried out with this equipment. These are discussed further in Appendix A.X.

The test was performed on the exterior aspect of the forearm, this being strapped to a rigid vertical support. The loads were applied by means of stitches, this being made possible by a local block anaesthetic. This method was completely reliable and proved to be much more comfortable than the suction tabs which would have produced very painful blisters if they have been left on one site for the one-hour duration of this test. The stitches were placed approximately $2\frac{1}{2}$ inches apart and a one-inch gauge length was marked centrally between them with black ink so that the optical extensometer could readily lock on to the marks and follow the extension.

The loading programme was as follows:-

(i)   load increased at constant extension rate to 0.2 lb

(ii)   extension held constant and load relaxation was recorded

(iii)   load reduced to zero at same constant rate

(iv)   three cycles of load to 0.2 lb and immediately back to zero were carried out at constant extension rate

(v)   steps (i), (ii) and (iii) were repeated then the site was allowed to rest for 5 minutes

(vi)   the above loading programme was repeated for maximum loads of 0.4, 0.6, 0.8, 1.0 and 1.5 lb.

VI.3.4   <u>Results of constant strain rate tests</u>

The successive load-extension curves obtained during each group of tests are shown in Fig VI.15. The unloading parts of the cycles have been omitted for
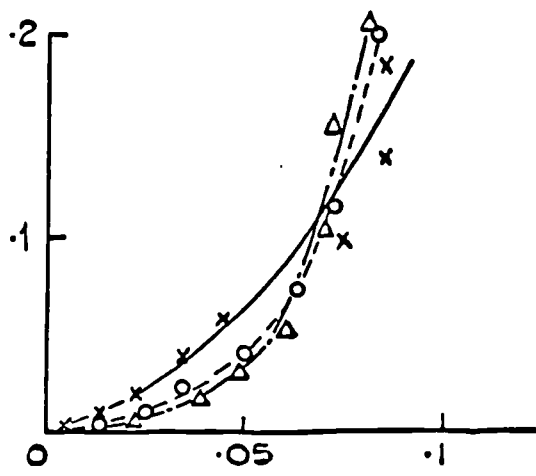
(a) MAX. LOAD = 0·2 LB.

(b). MAX. LOAD = 0·4 LB.

——X—— FIRST CYCLE
——O—— SECOND CYCLE
——Δ——— THIRD CYCLE.
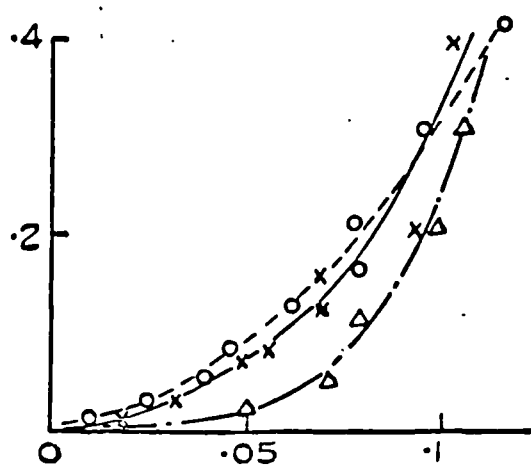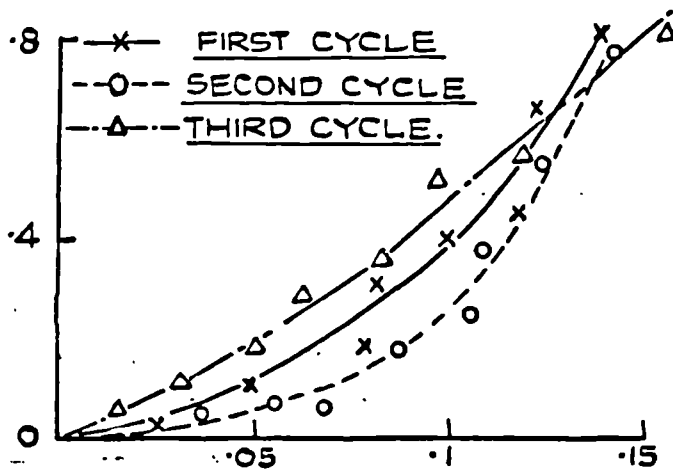
(c). MAX. LOAD = 0·8 LB.

FIG. VI. 15. - LOAD CYCLING TESTS IN VIVO
(THE UNLOADING PARTS OF THE CYCLES IS OMITTED
FOR CLARITY)..

clarity. It is seen that there are considerable differences between successive cycles but that there is no trend similar to that shown by load cycling tests *in vitro*.

However, it cannot be concluded that this does not occur as there was a greater scatter in the results caused by inaccuracies in the strain measurement. These are further discussed in Appendix X.

Fig VI.16 shows the results of the load relaxation parts of the loading programme. These are much more satisfactory showing that the load measuring part of the apparatus needs no further development. It is seen that in every case, the magnitude of the load relaxation effect was less in the test carried out after several loading cycles than in the initial load relaxation test. Comparison with the *in vitro* result (Fig V.25) from a similar test shows that, in this respect, the behaviour is similar.

This equipment shows considerable promise and, when fully developed, it will be a very valuable tool for use in the wide variety of *in vivo* tests which are obviously necessary and which will be the subject of a research project by Mr Evans.

VI.4   Mechanical Impedance Measurements

In addition to the static or quasi-static testing methods described above, a radically different method of measuring certain mechanical properties of skin *in vivo* has been developed by Mr T.C. Duggan of the BioEngineering Unit. Although the author has not been closely concerned with the development of this technique, for the sake of completeness, a brief account is given below of the equipment used and of some pilot results.

FIRST TEST.

TEST AFTER 4 LOAD CYCLES.
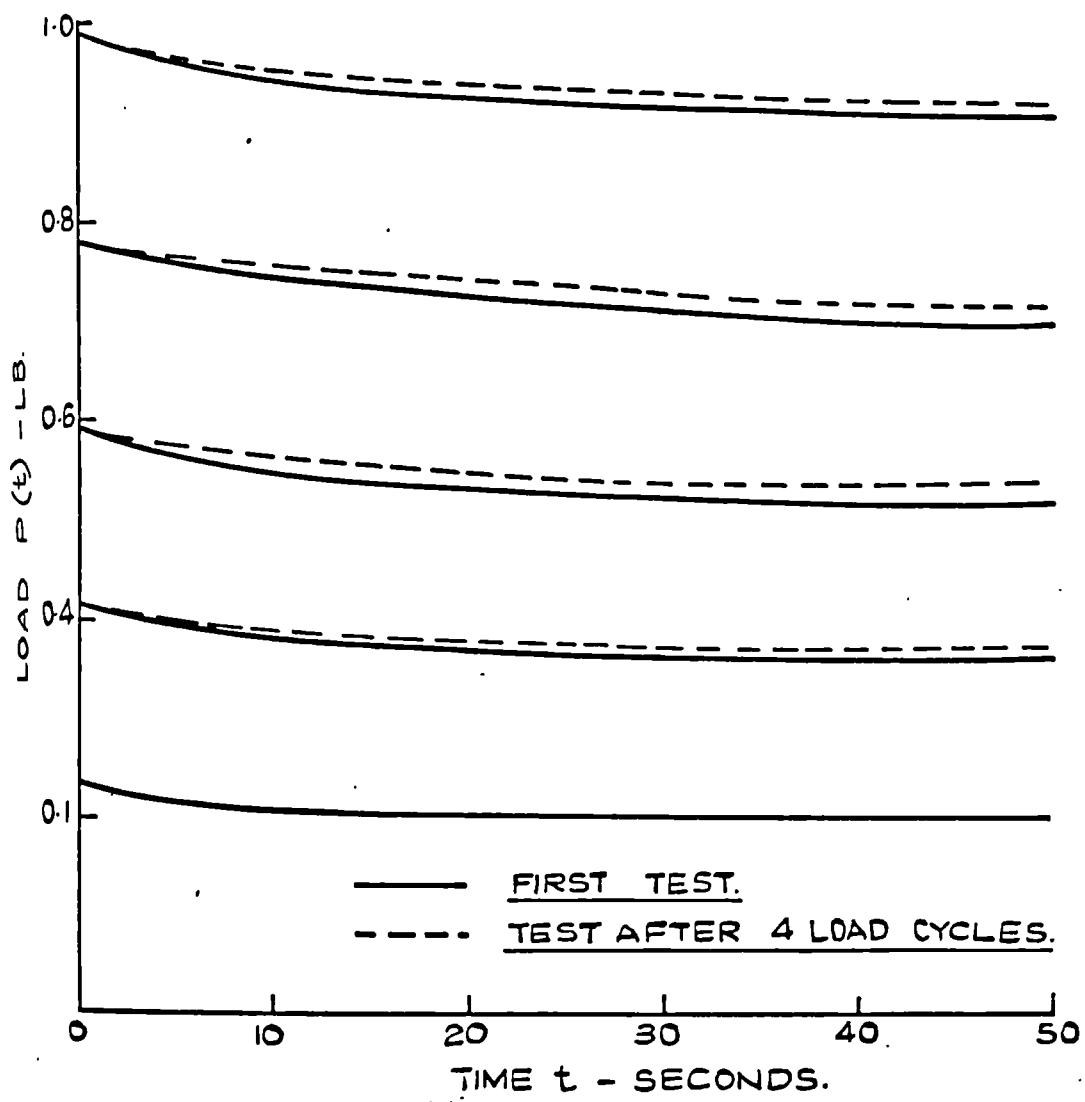
FIG VI. 16 - STRESS RELAXATION TESTS IN VIVO.

VI.4.1   <u>Theory</u>

The type of test to be considered measures a
quantity called the mechanical impedance. If a
sinusoidally varying force P is applied to the surface of
the skin and the resulting velocity of the surface is
measured, then the mechanical impedance Z is defined by:

$$Z = \frac{F}{U}$$
      VI.1

If the system behaves in a linear manner, then
the velocity U will also vary sinusoidally but will, in
general, differ in phase from the force P. The velocity
can be split into the components u, in phase with P and
v in quadrature with P (i.e. leading or lagging P by 90°).

$$U = u + jv \quad (j^2 = -1)$$

Z is therefore also split into two similar components:

$$Z = R + jQ$$
      VI.2

The component R in phase with P is termed the mechanical
resistance and the component Q in quadrature with P is
termed the mechanical reactance.

VI.4.2   <u>Apparatus</u>

A general view of the apparatus used for these
tests is shown in Fig VI.17. Again it will be readily
appreciated that this technique is still in the development
stage. The load applied to the skin surface was in the
form of a sinusoidally varying torque supplied by the
torque motor A in Fig VI.18. This torque was applied
via the strain gauged torque tube B. The angular

FIG. VI. 17. MECHANICAL IMPEDANCE INSTRUMENTATION.
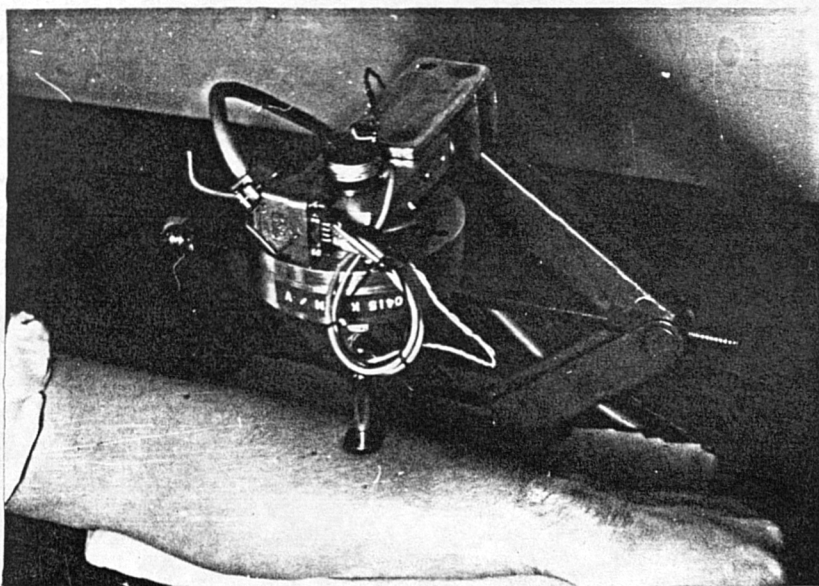
FIG. VI. 18. TORQUE MOTOR.

displacement produced at the skin surface was sensed by
the precision potentiometer C mounted on the motor shaft.

The disc D was cemented to the skin surface
with Evostick impact adhesive to prevent slipping.

The outputs from the torque tube and potentio-
meter were suitably amplified, then the angular
displacement signal was electronically resolved into
components in phase and in quadrature with the torque.
The mechanical impedance Z could then be calculated.

VI.4.3   Pilot measurements

At present only a few pilot experiments have
been carried out with this equipment.   The test site used
was the exterior aspect of the forearm.   At the low
torque levels being used the response was found to be
slightly non-linear (Fig VI.19).   Measurements of the
mechanical impedance were therefore made using torques at
the lower end of this curve when the deviation from
linearity was small.   The variation of the mechanical
impedance with frequency f was measured and is presented
in Figs VI.20 and VI.21.in terms of the amplitude Z of
the impedance and the phase angle ϕ of the velocity
relative to the torque.   The quantities are found from:

$$Z = R + j Q$$

$$Z = \sqrt{R^2 + Q^2}$$

$$\phi = \tan^{-1} (Q/R)$$

The variation of Z with frequency indicates
that, in the frequency range considered, the response is
predominantly an elastic effect.   However, the small
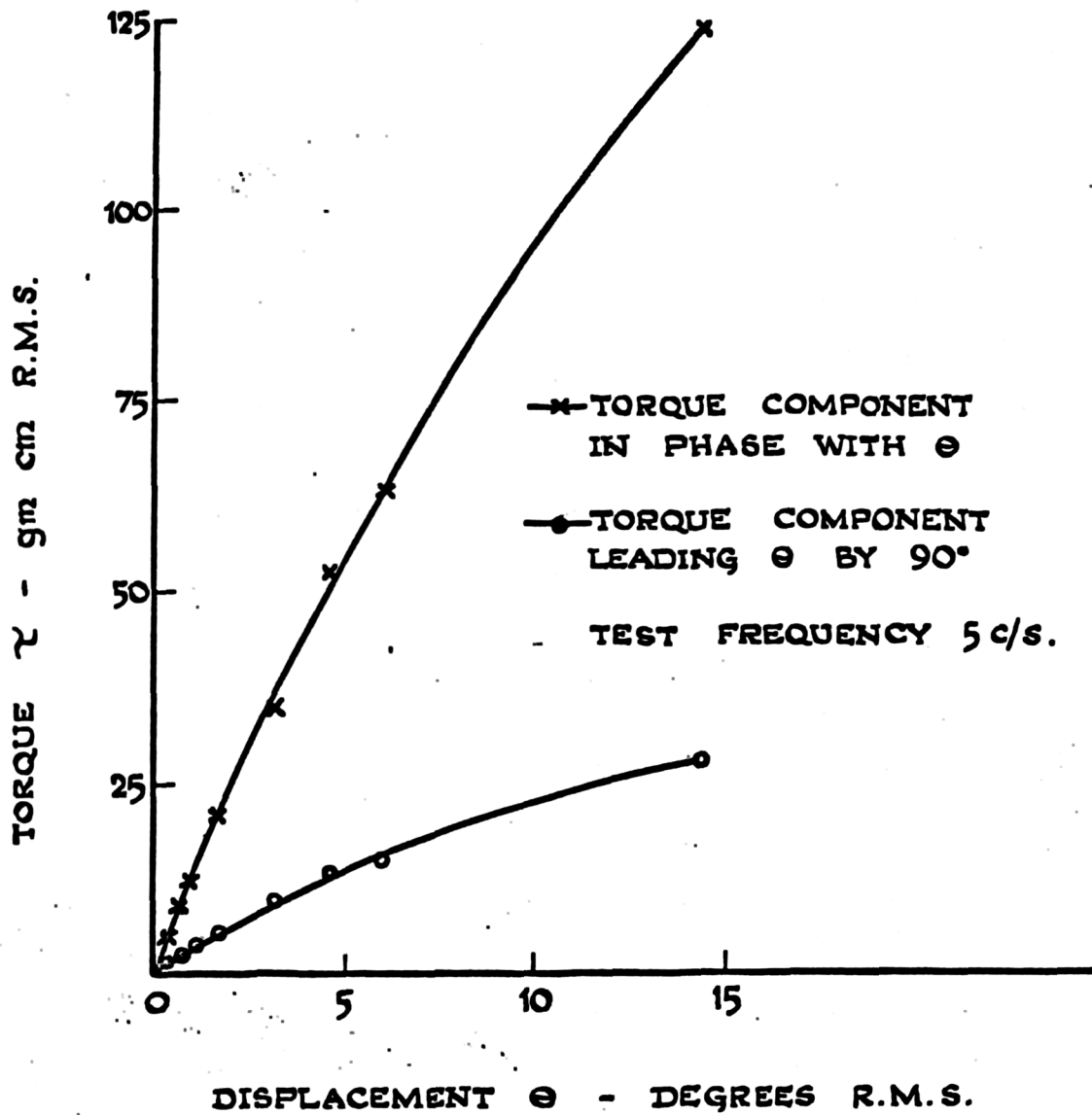
FIG. VI.19. MECHANICAL IMPEDANCE MEASUREMENT - TORQUE V DISPLACEMENT AT CONSTANT FREQUENCY.

change in ϕ over the same frequency range is not readily explained in these terms.

The additional stresses being developed in the skin by the low torques used in these tests are very small and are certainly within the initial linearly elastic region found in the *in vitro* uniaxial experiments. However, the effect of the pre-existing biaxial stress field and the involvement of the subcutaneous tissues in the deformation makes it difficult to assess the overall effect.

VI.5   Summary

The *in vivo* tests described have shown that there is a broad similarity between the mechanical behaviour of skin *in vitro* and *in vivo*. The development of refined *in vivo* testing techniques has been hindered by the many difficulties which do not arise in the *in vitro* case. The instruments which have now been developed show considerable promise both in further elucidating the basic characteristics of skin *in vivo* and also as possible clinical tools to be used in diagnosis and for the assessment of the progress of therapy in conditions which result in change in the mechanical characteristics of connective tissue.
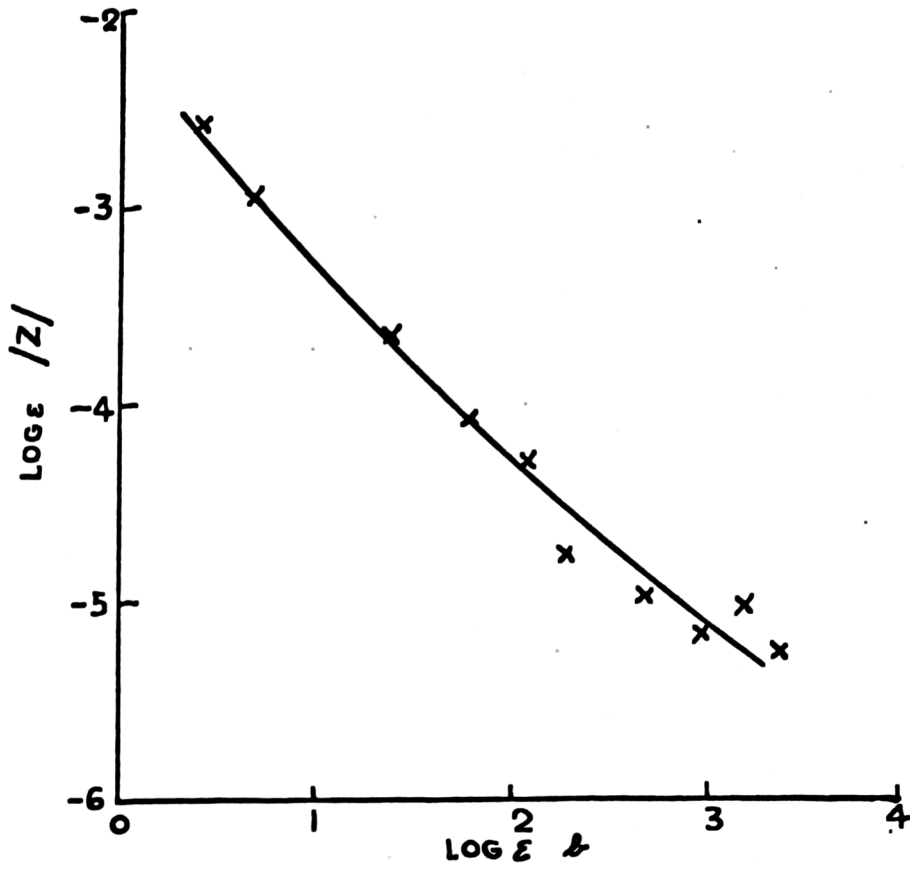
FIG. VI - 20 MECHANICAL IMPEDANCE Vs FREQUENCY
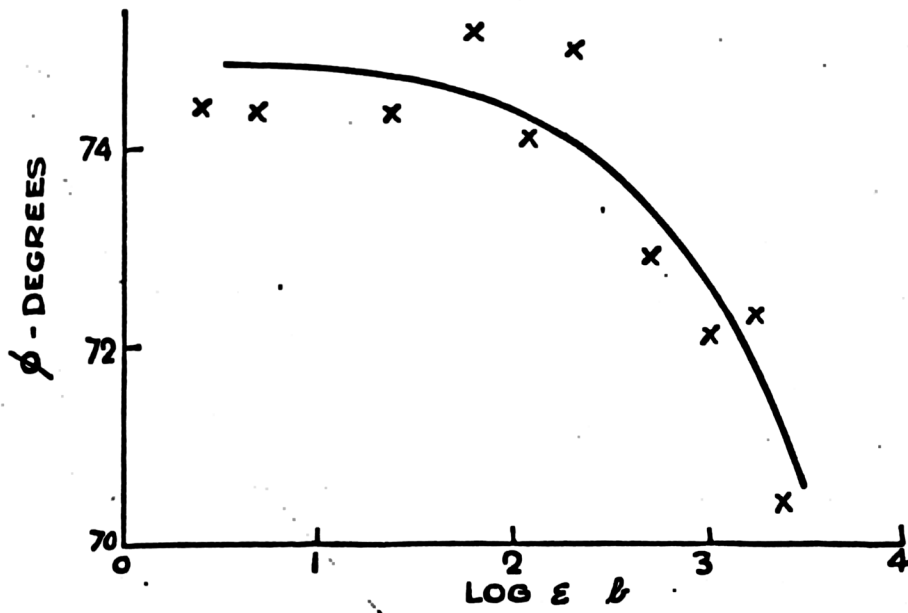
FIG VI 21. IMPEDANCE PHASE ANGLE ϕ
Vs FREQUENCY

Chapter VII

Clinical Applications
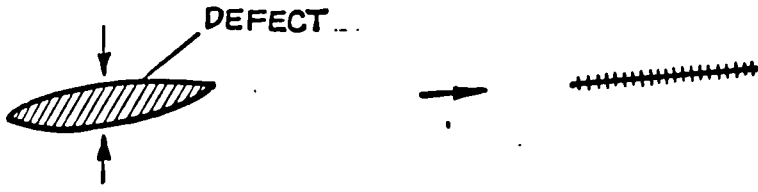
(i)   SLIDING FLAP
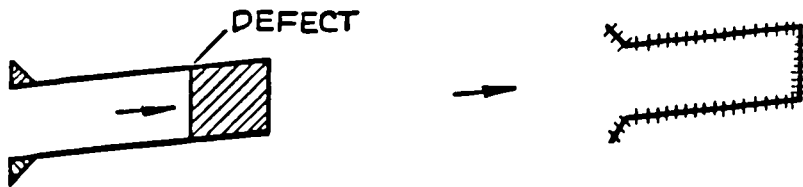
(ii)   ADVANCEMENT FLAP
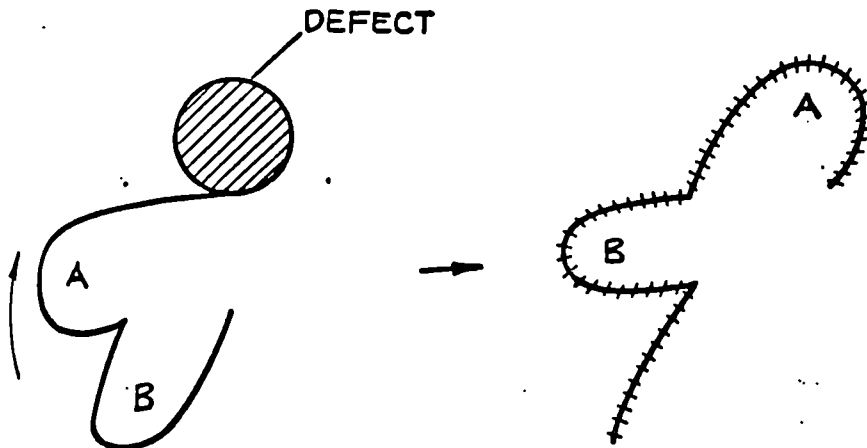
(iii)   BILOBED FLAP

FIG. VII. I. VARIOUS DESIGNS FOR LOCAL FLAPS

In the repair of skin defects two distinct
techniques are used by plastic surgeons:

(i)   free skin grafts
(ii) local skin flaps

A free skin graft consists of a piece of skin cut to the
size of the defect to be repaired, this skin being obtained
from some other site on the body. This technique
obviously involves surgery at two separate sites. This is
undesirable and has led to the development of a very wide
variety of local flap operations. In these, the skin in
the region of the defect is rearranged by the transposition
of various flaps so as to cover the area of the defect.
In this way the extensibility of the skin adjacent to the
defect is made use of to provide the extra area of skin
required. Fig VII.1 shows various designs of such flaps.
This type of flap is used to repair defects caused by the
removal of an ulcer, birthmark, etc. and which thus leaves
an area of the underlying tissue uncovered.

Another commonly found type of defect is the
scar contracture (Fig VII.2), this usually resulting from
a burn injury. As this matures with time it contracts
and, if the injury is in the region of a joint, the band
of scar tissue acts as a limit stop and restricts the
joint movement. This type of defect is also repaired by
a flap type of operation. The design of operation used
most commonly in this condition is the Z-plasty. Because
of the simple geometrical layout of this operation, it
has been subjected to a considerable amount of mathematical
analysis.
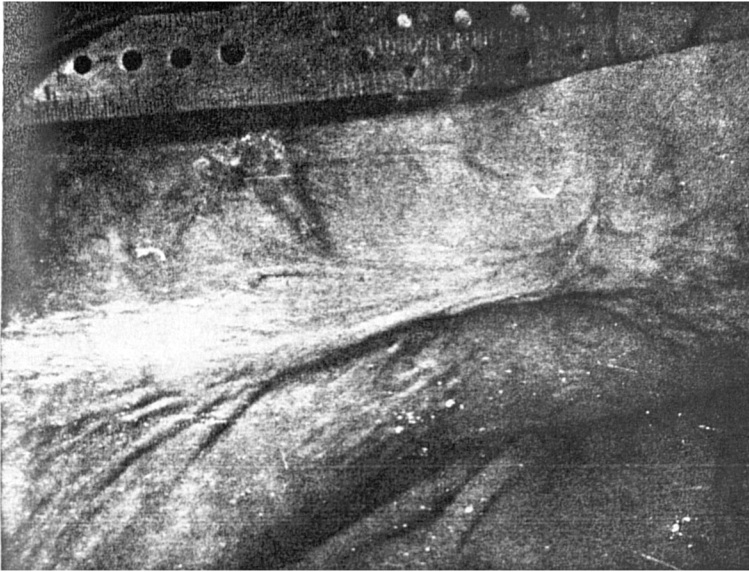
G. $\overline{VII}$. 2.   TYPICAL SCAR CONTRACTION RESULTING
FROM A BURN INJURY.

AB = BC = CD

INITIAL LINES OF INCISION   (ii) AFTER FLAP TRANSPOSITION
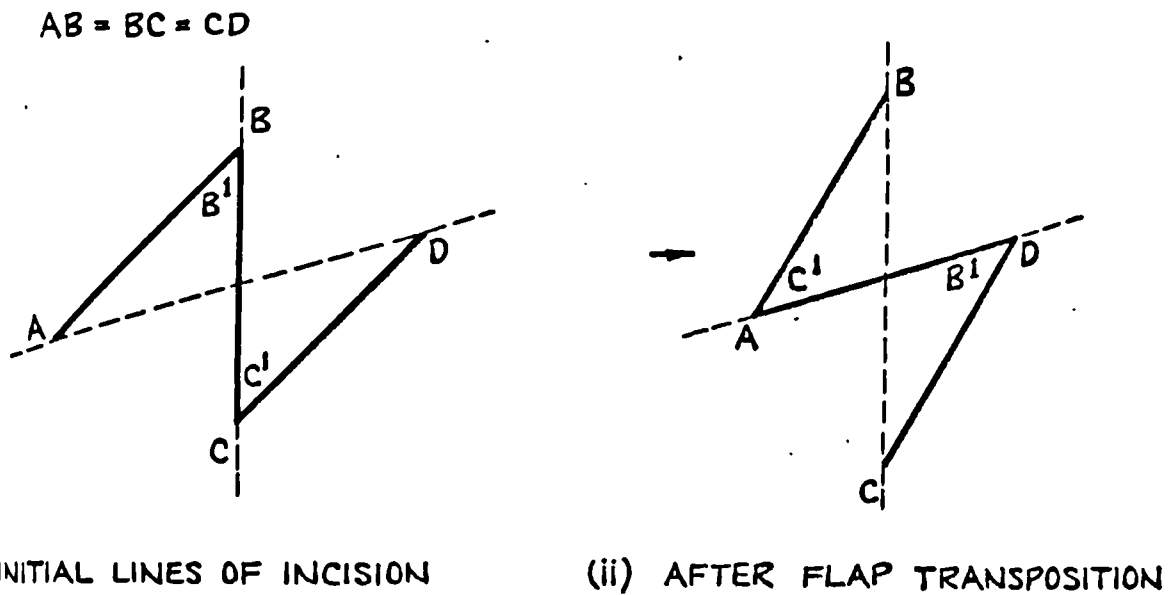
IG. $\overline{VII}$. 3.   THE PLANE Z — PLASTY

VII.1   The Z-plasty

In this operation, the tension in the direction
of the contracted scar is relieved by replacing the scar
with normal skin.   This is achieved by the transposition
of two triangular flaps.   The whole process is shown in
Fig VII.3.   This shows how the original markings made to
define the flaps define a parallelogram on the skin
surface and that transposing the flaps has the effect of
interchanging the diagonals of this parallelogram.   The
longer diagonal is transposed to lie in the direction of
the tension field produced by the scar contraction so that
the tension in this direction is relieved.   There is a
corresponding reduction in the width of the area enclosed
by the flaps so that there is an increase in the tension
in this direction.   For the operation to be successful,
the tension produced must not be such as to give rise to
the blanching effect discussed in the previous chapter.
For this reason it would be desirable for the surgeon to
have some method of predicting the magnitude of the tension
field that would be produced by the operation.   In view
of the number of variables involved in the assessment of
a given Z-plasty it is remarkable that, by purely
intuitive methods, an experienced plastic surgeon can obtain
excellent results in a large percentage of such operations.

Because of the geometrical simplicity of the Z-
plasty, various attempts have been made to predict the
effects of changes in the geometry of the flaps on the
relief of tension obtained and on the disturbance to the
surrounding skin (Limberg 1929; Davis and Kitlowski 1939;
MacGregor 1957; Woodruff 1960; Devlin 1965).

In all of these theoretical treatments, the
assumption was made that the flaps were rigid, i.e. the
shape of the flaps was unaltered by the transposition

AXIS OF Z-PLASTY

(a)
FLAP OUTLINE

(b)
ROTATION

(c)
TRANSLATION
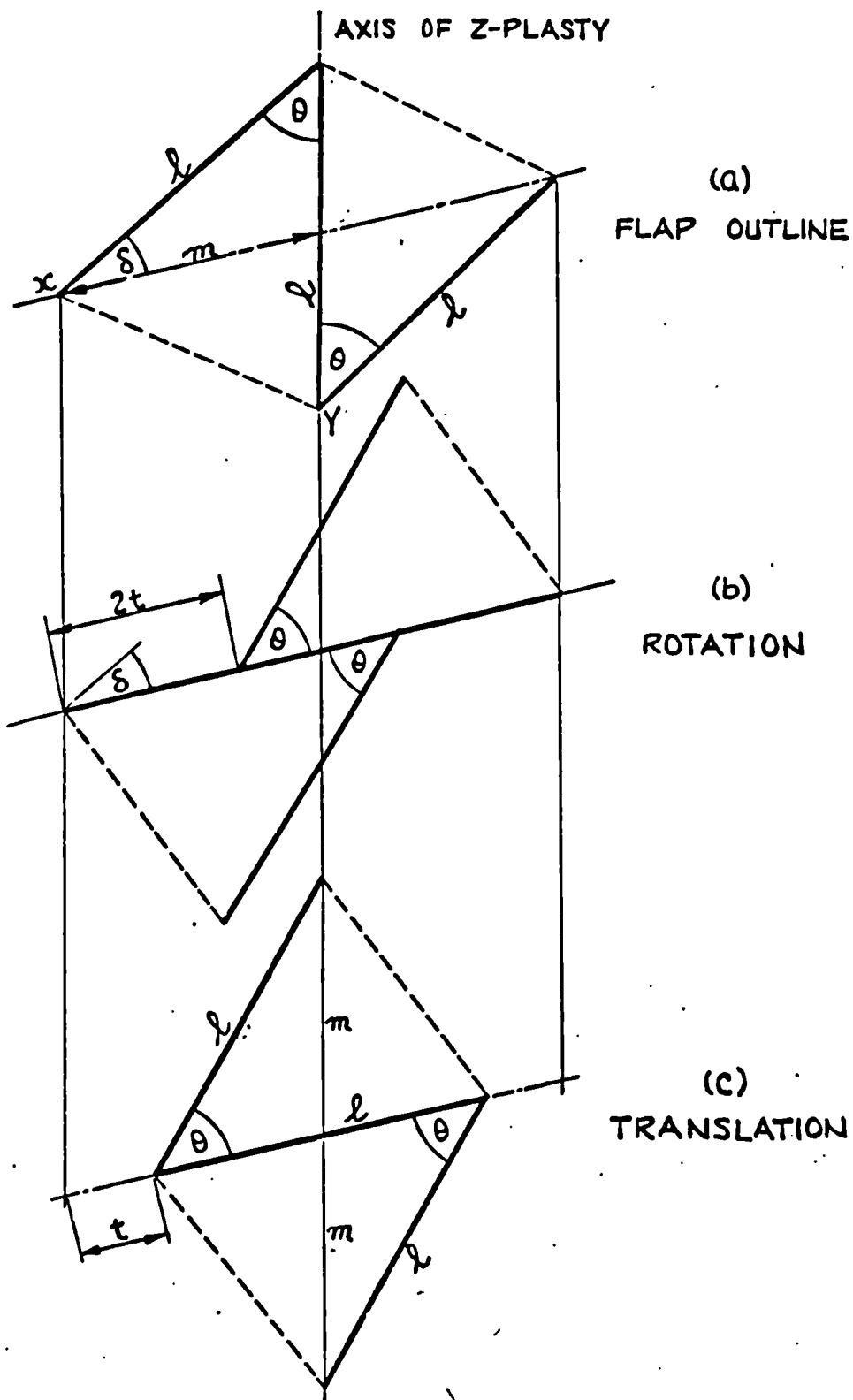
FIG. VII. 4.   Z- PLASTY FLAP TRANSPOSITION CAN BE
SPLIT UP INTO A ROTATION AND A TRANSLATION.

process and that all of the deformation occurred in the surrounding skin.

VII.2   <u>Rigid Flap Theory Applied to the Plane Z-plasty</u>

In this discussion the term "plane Z-plasty" implies that the skin involved in the operation is contained within a flat plane surface or rather that it approximates to this condition. Considering first the case of the Z-plasty with equal flap tip angles; Fig VII.4 shows how the transposition of the flaps can be split up into two distinct movements:

(i)   a rotation of the two flaps by the angle δ about the extreme ends of the limb

(ii)   a translation t of the two flaps along the transverse diagonal to bring them into line.

It is seen that this process has the effect of interchanging the diagonals of the parallelogram. The fractional increase in length R_ℓ along the axis of the Z-plasty is given by:

$$R_\ell = \frac{2m - \ell}{\ell} \qquad\qquad \text{VII.1}$$

from Fig VII.4:

$$m^2 = 4\ell^2(5 - 4\cos\theta)$$

substituting in VII.1 gives:

$$R_\ell = \sqrt{5 - 4\cos\theta} - 1 \qquad\qquad \text{VII.2}$$
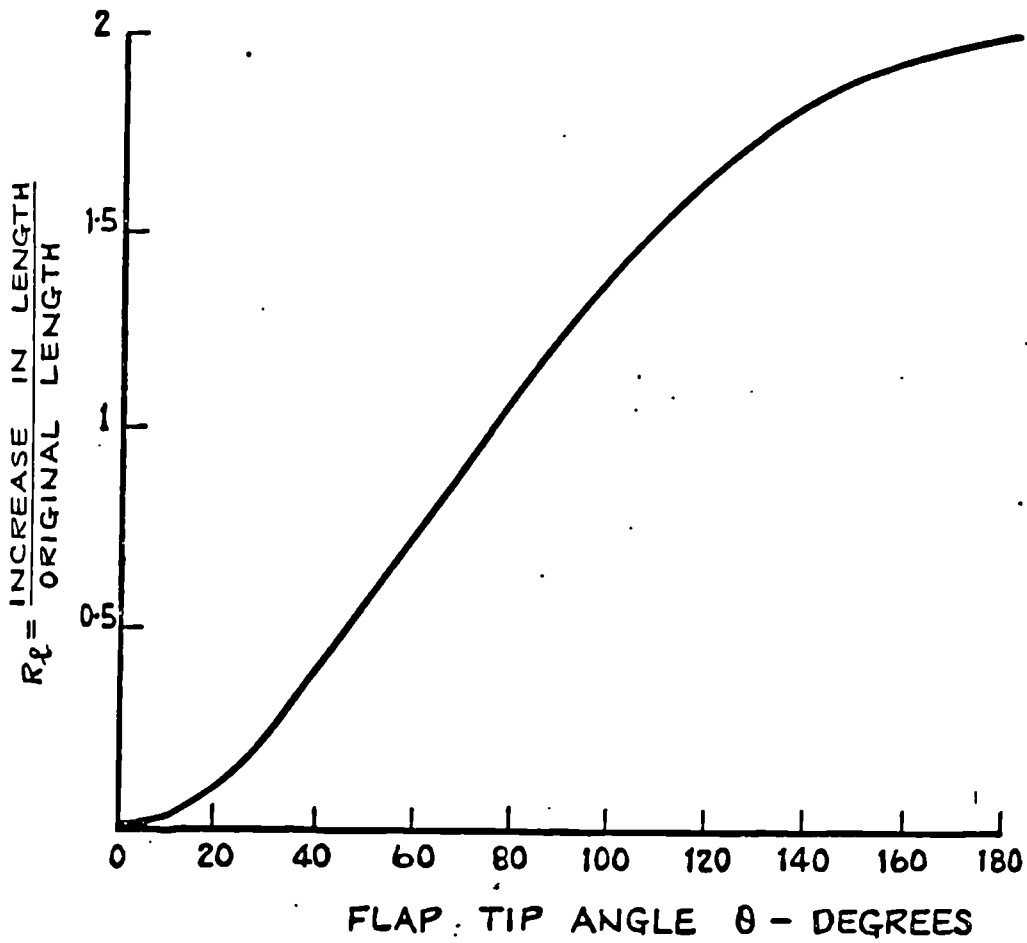
FIG. VII 5. RIGID FLAP THEORY - INCREASE IN LENGTH · Vs-FLAP TIP ANGLE FOR .PLANE Z PLASTY

This variation of R_ℓ with θ is shown in Fig VII.5.

It is also of interest to consider the variation of δ and t with θ.

From Fig VII.4:

$$\frac{2 \sin\delta}{\ell} = \frac{\sin\theta}{m}$$

from which:

$$\delta = \sin^{-1} \left(\frac{\sin\theta}{\sqrt{5 - 4 \cos\theta}} \right) \qquad \text{VII.3}$$

also:

$$2t = 2m - \ell$$

$$\frac{t}{\ell} = R_t = \frac{R_\ell}{2} \qquad \text{VII.4}$$

The resulting variations of δ and R_t with θ are shown in Figs VII.6 and VII.7 respectively. It can be seen that δ has a maximum value at $\theta = 60^\circ$. Because plastic surgeons have found by purely subjective assessment that the best results are obtained with Z-plasty flap angles of approximately 60° there have been some speculative attempts to give some meaning to this apparent significance of the maximum value of δ. However, it must be remembered that this technique of splitting the flap transposition into a rotation δ and a translation t is only used for mathematical convenience and bears little relation to the actual changes occurring during flap transposition in an operation.

It is more likely that $\theta = 60^\circ$ represents a
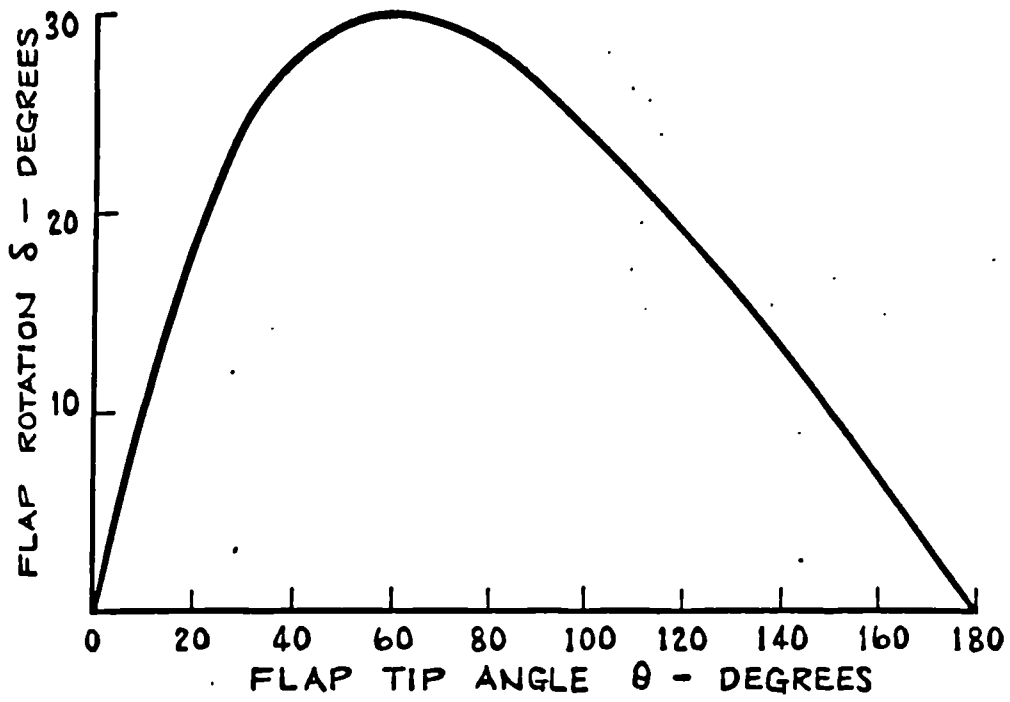
FIG. VII. 6.   FLAP ROTATION Vs TIP. ANGLE
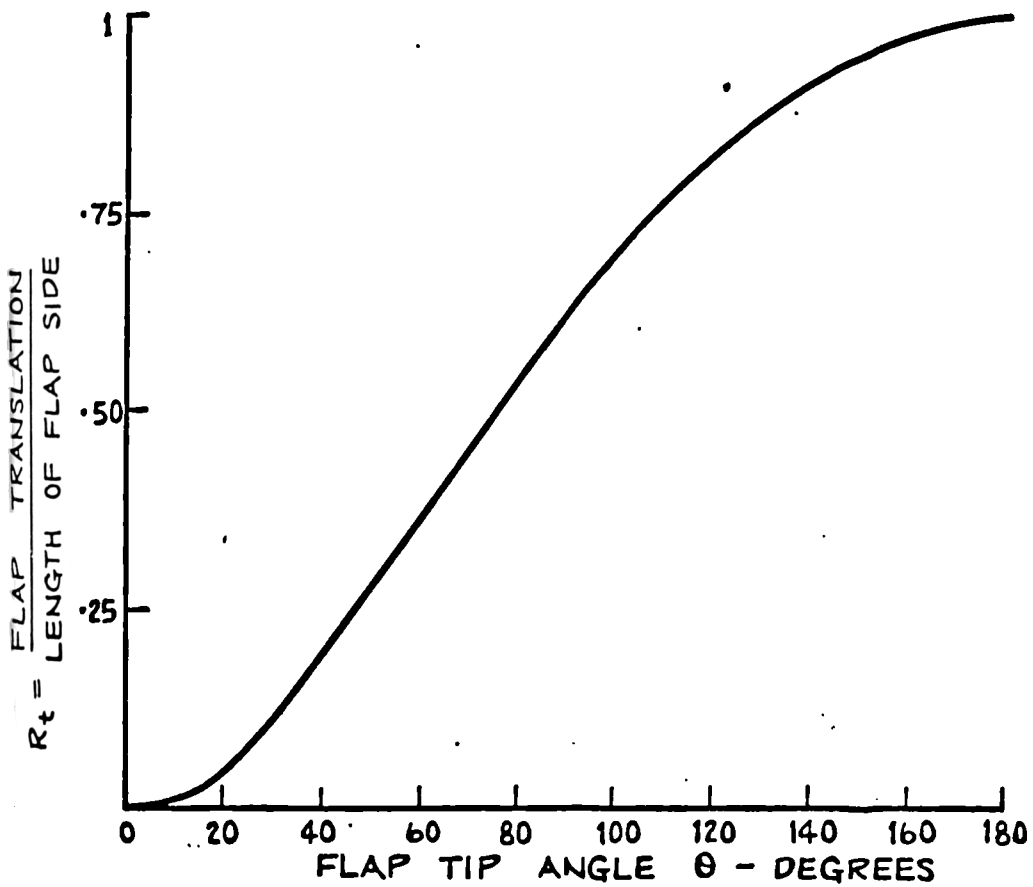
FIG. VII. 7.   FLAP TRANSLATION Vs TIP ANGLE

good compromise between the amount of extension obtained
and the occurrence of blanching due to the tension field
produced in the surrounding skin by the lateral contraction
of the Z-plasty.

VII.2.1 The effect of extensibility of the flaps

In the above theory, the assumption is made that
the shape of the flaps is unaltered by the transposition.
It is found in practice that this is not the case and that,
as a result, the actual extension produced may differ
considerably from the theoretical result.   Table VII.1
gives some typical comparisons between the actual
extension and lateral contractions found in practice with
those predicted on the basis of the rigid flap theory.

TABLE VII.1

Comparison of Actual and Theoretical Z-plasty
Extensions and Contractions

Actual		Theoretical	
Extensions	Contractions	Extensions	Contractions
0.56	0.28	0.70	0.35
0.56	0.34	0.29	0.15
0.65	0.30	0.81	0.40
0.72	0.32	0.65	0.33

It is obvious from these results that the rigid flap theory
does not give satisfactory predictions of the deformations

produced by the Z-plasty operations.   Still more
important, it gives no information at all as to the
tension field which will result from this operation.
The prediction of this would require:-

(i)   knowledge of the biaxial mechanical properties
of the actual area of skin involved in the
operation

(ii)   measurement of the tension field existing
prior to the operation

(iii) the development of an approximate method of
analysis as the use of exact theories of
finite elasticity would be impracticable.

VII.3   More Complex Flaps

The above analysis has been concerned only with
the simple plane Z-plasty.   The rigid flap theory has
also been applied to more complex flap designs such as
the split Z-plasty devised by Limberg (Fig VII.8).   In
an attempt to overcome one limitation of the plane Z-
plasty theory, Furnas (1965) has extended this theory to
three dimensions by means of his tetrahedral Z-plasty
concept (Fig VII.9).   In many cases, this is a much
better approximation to the actual geometry involved than
the plane Z-plasty.

As the rigid flap theory has been shown to be of
little value in the case of the simple plane Z-plasty, it
is very unlikely that its application to these more
complex designs will produce meaningful results.

VII.4   Summary

Present theories of surgical flap design have
been shown to be of little value and offer no assistance
to the plastic surgeon.   From an engineering standpoint,

the design of such flaps presents a problem of considerable magnitude.   A high degree of refinement would be required if the results produced were to be appreciably better than those obtained in practice by experienced surgeons. When this situation is considered against the background of the investigations of the mechanical properties of skin described in previous chapters, it is very apparent that a great deal of work is still required in this field of flap design.

Chapter VIII

General Summary
_____

The orientation of the investigation described was twofold:-

(i) to elucidate the basic mechanical characteristics of human skin and to arrive at a hypothesis permitting the description of such behaviour in analytic terms

(ii) to explore the potential significance of the application of these characteristics in the clinical practice of medicine and surgery.

A comprehensive review of literature and some simple pilot experiments established that skin was a non-linear viscoelastic material and that very refined testing techniques would be required to obtain meaningful results. These techniques have been developed. From the results obtained the following basic characteristics of human skin are considered to have been established.

(a) It is not possible to consider skin as being a homogeneous material. From a biomechanical point of view, skin is a multi-phase material, consisting of collagen and elastin fibre networks permeated by an apparently amorphous ground substance.

(b) The collagen network consists of long unbranched filaments which are disposed in a random manner in unstressed skin. On stressing, the fibres are oriented into the direction of the applied stress and in so doing develop random mechanical interconnections. The stability of these interconnections appears to be increased with stress cycling. This action obtains

irrespective of the direction of the stress,
although there appear to be quantitative
differences in characteristics depending on stress
orientation.

(c)   The much finer elastin network behaves in a
similar manner, although in this case histologically
identifiable positive interconnections exist among
the fibres.   The contribution of this network to
supporting the applied stress appears very small
and may or may not be significant in the initial
large extension under low stress which is a
characteristic of skin.   It is probable, however,
that this elastin network contributes to recovery
on stress removal.

(d)   The ground substance is displaced from the fibre
networks during stressing.

(e)   The character of the overall behaviour of skin
changes considerably as the applied stress is
increased.   At low stresses very large extensions
obtain with no significant time-dependent effects.
As the stress is increased and the collagen fibres
are further oriented in the direction of the stress,
the behaviour of the skin becomes more a function
of the characteristics of the collagen itself.
The time-dependent mechanical properties of the
collagen fibres result in the skin showing non-
linear viscoelastic behaviour, this effect becoming
more marked as the stress is increased.

(f)   A network model with non time-dependent elements
has been developed.   This provides an acceptable
first approximation for describing the overall
behaviour of skin when it is extended at a constant

rate. By giving linear viscoelastic properties to the elements of the network which correspond to the collagen fibre network in skin, the model is able to predict accurately the effects of stress relaxation and creep in skin.

(g)   The multi-phase network concept is not restricted in application to skin only. Similar network systems can be derived for other tissues, the overall characteristic being determined by the relative significance of the various network components.

(h)   *In vivo* testing techniques have been developed and results obtained to date indicate behaviour consistent with the concepts evolved from the results of the *in vitro* testing programme.

Further development of the investigations reported is visualised as follows:-

(i)   The highly refined *in vitro* testing techniques which have been developed permit rapid and accurate assessment of biomechanical characteristics. It is now practical to consider a test programme of considerably enlarged scope to permit statistical assessment of the significance in normalcy and disease of these characteristics.

(ii)   The *in vivo* testing techniques which have been developed give promise of permitting an effective assessment of biomechanical characteristics *in vivo*.

This is essential from the point of view of clinical application in fields of local flap design,

diagnosis and the "measurement" of the progress
of therapy.

BIBLIOGRAPHY

BIBLIOGRAPHY

ABRAHAMS, M.
1965

"The Mechanical Properties of Costal Cartilage". PhD Thesis, University of Strathclyde.

ABRAHAMS, M. and DUGGAN, T.C.
1965

"The Mechanical Characteristics of Rib Cartilage". Proc. Symposium on "Biomechanics and Related Bio-engineering Topics". p.285-300. Ed. R.M. Kenedi, Pergamon Press.

AYER, J.P.
1964

"Elastic Tissue". Int. Review of Connective Tissue Research. 2: 33. Ed. D.A. Hall, Academic Press.

BANGA, I. and BALO, J.
1961

"Elasticity of the Vascular Wall". Acta Physiologica - Acad. Sci. Hung. 20: Part 3, 237-247.

BECKWITH, T.G., BRODY, G.S., GLASER, A.A., PREVENSLIK, T. and WHITE, W.L.
1963

"Standardisation of Methods for Measuring the Mechanical Properties of Wounds". A.S.M.E. Publication, No. 63-WA-276.

BERGEL, D.H.
1960

"The Static Elastic Properties of the Arterial Wall". J. Physiol. 156: 445.

BRITISH RHEOLOGISTS CLUB
1944

"Essays in Rheology".

CARTON, R.W., DAINAUSKAS, J. and CLARK, J.W.
1962

"Elastic Properties of Single Elastic Fibres". J. Appl. Physiol. 17: No. 3, 547-551.

COX, H.T.
1941

"The Cleavage Lines of the Skin". Brit. J. of Surg. 29: 234.

CRAIK, J.E. and McNEILL, I.R.R.
1965

"Histological Studies of Stressed Skin". Proc. Symposium on "Biomechanics and Related Bioengineering Topics". p. 159-164. Ed. R.M. Kenedi, Pergamon Press.

CRONKITE, A.E.
1936

"The Tensile Strength of Human Tendons". Anat. Rec. 64: 173.

DAVIS, J.S. and
KITLOWSKI, E.A.
1939

"The Theory and Practical Use of Z Incisions for the Relief of Scar Contractures". Ann. Surg. 109: 1001.

DELAUNAY, A. and BAZIN,
S.
1964

"Mucopolysaccharides, Collagen and Nonfibrillar Proteins in Inflammation". Internat. Review of Connective Tissue Research. 2: 301 Ed. D.A. Hall, Academic Press.

DEVLIN, P.
1965

"Biomechanical Aspects of Flap Design in Plastic Surgery". BSc Thesis. University of Strathclyde.

DICK, J.C.
1947

"Observations on the Elastic Tissue of the Skin with a Note on the Reticular Layer at the Junction of the Dermis and Epidermis". J. of Anat. 81: Part 3, 201-211.

DICK, J.C.
1951

"The Tension and Resistance to Stretching of Human Skin and Other Membranes, with Results from a Series of Normal and Oedematous Cases". J. of Physiol. 112: 102-113.

EVANS, J.H.
1965

"The Mechanical Characteristics of Human Skin". MSc Thesis. University of Strathclyde.

FERRY, J.D.
1961

"Viscoelastic Properties of Polymers". Wiley, New York.

FRANKE, E.K.
1951

"Mechanical Impedance Measurements of the Human Body Surface". USAF Technical Report No. 6469. p.1.

FURNAS, D.W.
1965

"The Tetrahedral Z-plasty". Plastic and Reconstructive Surg. 35: 291.

GIBSON, T.
1965

"Biomechanics in Plastic Surgery". Proc. Symposium on "Biomechanics & Related Bioengineering Topics". p. 129-134. Ed. R.M. Kenedi, Pergamon Press.

GIBSON, T. and KENEDI, R.M. 1963a — "The Significance and Measurement of Skin Tension in Man". Proc. Third Internat. Cong. on Plastic Surg. Washington.

GIBSON, T. and KENEDI, R.M. 1963b — "Biomechanics in Plastic Surgery". Surgical Forum, Amer. Coll. of Surgeons. 14: 478.

GIBSON, T., KENEDI, R.M. and CRAIK, J.E. 1965 — "Micro-architecture of Dermal Collagen: a Bioengineering Study". J. Plastic Surg. (in press)

GLASER, A.A., MARANGONI, R.D., MUST, J.S., BECKWITH, T.G., BRODY, G.S., WALKER, G.R. and WHITE, W.L. — "Refinements in the Methods for the Measurement of the Mechanical Properties of Unwounded and Wounded Skin". Med. Elec. and Biol. Eng. 3: No. 4, 411.

GRATZ, C.M. 1931 — "Tensile Strength and Elasticity Tests on Human Fascia Lata". J. of Bone and Joint Surg. 13: 334.

GREEN, A.E. and RIVLIN, R.S. 1957 — "The Mechanics of Non-linear Materials with Memory". Part I. Arch. Rat. Mech. Anal. 1: 1.

GREEN, A.E., RIVLIN, R.S. and SPENCER, A.J.M. 1959 — "The Mechanics of Non-linear Materials with Memory". Part 2. Arch. Rat. Mech. Anal. 3: 82.

GROSS, J. 1961 — "Collagen". Scientific American.

GROSS, J. and SCHMITT, F.O. 1948 — "The Structure of Human Skin Collagen as Studied with the Electron Microscope". J. of Exp. Med. 88: 555.

HALL, R.H. 1951a — "Changes in Length of Stressed Collagen Fibres with Time". J. of Society of Leather Trades' Chemists. 35: No. 1, 11-17.

HALL, R.H. 1951b — "Variations with pH of the Tensile Properties of Collagen Fibres". J. of Society of Leather Trades' Chemists. 35: No. 6, 195-210.

HALL, R.H.
1952
"Energy and Entropy Effects on the Elasticity of Collagen Fibres". J. of the Society of Leather Trades' Chemists. 36: No. 5, 137-138.

HALLOCK, P. and BENSON, J.C.
1937
"Studies on Elastic Properties of Human Isolated Aorta". J. Clinical Investigation. 16: 595.

HARKNESS, R.D.
1961
"Biological Functions of Collagen" Biol. Reviews. 36: 399.

JAMES, H.M. and GUTH, E.
1941
"Theoretical Stress-Strain Curve for Rubberlike Materials. Physical Review. 59: 111.

JAMES, H.M. and GUTH, E.
1943
"Theory of Elastic Properties of Rubber". J. of Chemical Physics. 11:455.

JAMES, H.M. and GUTH, E.
1944
"Theory of Elasticity of Rubber". J. of Applied Physics. 15: 294.

JAMES, H.M. and GUTH, E.
1947
"Theory of Elastic Properties of Rubber". J. of Chemical Physics. 15: 682.

JANSEN, L.H. and ROTTIER, P.B.
1957
"Elasticity of Human Skin Related to Age". Dermatologica. 115: 106-111.

JANSEN, L.H. and ROTTIER, P.B.
1958a
"Some Mechanical Properties of Human Abdominal Skin Measured of Excised Strips". Dermatologica. 117: 65.

JANSEN, L.H. and ROTTIER, P.B.
1958b
"Comparison of the Mechanical Properties of Strips of Human Abdominal Skin Excised from below and above the Umbilic". Dermatologica. 117: 252-258.

JOCHIMS, J.
1934
"Untersuchungen des mechanischen Verhaltens der Hautgewehe (Cutis und Subcutis) mit einer neuen Methode". Z. f. Kinderheilk. 56: 81.

JOCHIMS, J.
1948
"Elastometrie an Kindern bei wechselnder Hautdehnung". Arch. f. Kinderheilk. 135: 228.

KANAGY and WALLACE
1943

J.A.L.C.A. 38: 314.

KELLY, A. and DAVIES, G.J.
1965

"The Principles of the Fibre Reinforcement of Metals". Metallurg. Reviews. 10: No. 37, p.1.

KENEDI, R.M.
1963

"Studies in Biological Engineering - a Confluence of Many Disciplines". Research and Development. No.26.p.16-25.

KENEDI, R.M.
1964

"Bioengineering Studies of the Structural Components of the Human Body". The Structural Engineer. 42: 101-109.

KENEDI, R.M. and GIBSON, T.
1962

"The Experimental Study of Skin Tensions in the Human Body - a Force Measuring Device and Typical Results". Revue Francaise de Mécanique. 4: 121.

KENEDI, R.M., GIBSON, T. and ABRAHAMS, M.
1963

"Mechanical Characteristics of Skin and Cartilage.". J. of the Human Factors Society. p. 525.

KENEDI, R.M., GIBSON, T. and DALY, C.H.
1965a

"Bioengineering Studies of the Human Skin - I". NATO Advanced Study Course on Connective Tissue, St Andrews, June 1964. Butterworths.

KENEDI, R.M., GIBSON, T. and DALY, C.H.
1965b

"Bioengineering Studies of the Human Skin - II". Proc. Symposium on "Biomechanics and Related Bioengineering Topics". p.147. Ed. R.M. Kenedi, Pergamon Press.

KENEDI, R.M., GIBSON, T. and DALY, C.H.
1965c

"The Determination, Significance and Application of the Biomechanical Characteristics of Human Skin". Digest of the 6th Internat. Conf. on Med. Elec. and Biol. Eng., Tokyo. p.531-534.

KENEDI, R.M., GIBSON, T., DALY, C.H. and ABRAHAMS, M. 1966
"Biomechanical Characteristics of Human Skin and Costal Cartilage". Federation Proc. 25: No. 3, p.1084-1087.

KING, A.L. and LAWTON, R.W. 1950
"Elasticity of Body Tissues". Med. Phys. 2: 303-316. Ed. O. Glaser, Year Book Publishers.

KING, A.L. and LAWTON, R.W. 1951
"Free Longitudinal Vibrations of Rubber and Tissue Strips". J. of Appl. Phys. 22: No. 11, p. 1340-1343.

KING, A.L. and LAWTON, R.W. 1960
"Elasticity of Body Tissues". Med. Phys. 3: 234. Ed. O. Glaser, Year Book Publishers.

KIRK, E. and KVORNING, S.A. 1949
"Quantitative Measurements of the Elastic Properties of the Skin and Subcutaneous Tissue in Young and Old Individuals". J.of Gerontology. 4: No. 4, p. 273.

LABAN, M.M. 1962
"Collagen Tissue: Implications of its Response to Stress *in Vitro*". Archives of Phys. Med. and Rehabil. 43: No. 9, p. 461-466.

LANGER, A.K. 1861
"Zur Anatomie und Physiologie der Haut". Sitzurgeber Wissenach D.K. Akad. D. 19: 179.

LEIDER, M. and BUNCKE, C.M. 1954
"Physical Dimensions of the Skin". Arch. Derm. 69: 563.

LIMBERG, A.A. 1929
"Skin Plasty with Shifting Triangular Flaps". Leningrad Tech. Inst.

LOCKETT, F.J. 1965
"Creep and Stress Relaxation Experiments for Non-linear Materials". Inst. J. Eng. Sci. 3: 59.

LOWTHER, D.A. 1963
"Chemical Aspects of Collagen Fibrillo-genesis". Int. Review of Connective Tissue Res. 1: 63. Ed. D.A. Hall, Academic Press.

MacGREGOR, I.A.
1957
"The Theoretical Basis of the Z-plasty". Brit. J. Plast.Surg. 9: 256.

MARANGONI, R.D.,
GLASER, A.A., MUST,
J.S., BRODY, G.S.,
BECKWITH, T.G.,
WALKER, G.R. and
WHITE, W.L.
1965
"Effect of Storage and Handling Techniques on Skin Tissue Properties". Annals of the N.Y. Acad. of Sci.

MILCH, R.A.
1965
"Matrix Properties of the Ageing Arterial Wall". Monographs in the Surgical Sciences. 2: 261.

MITTON, R.L. and
MORGAN, F.R.
1960
"The Mechanical Properties of Vegetable Tanned Collagen Fibres". J. of Society of Leather Trades' Chemists. 44: 58.

MONTAGNA, W.
1956
"The Structure and Function of Skin". Academic Press.

MORGAN, F.R.
1960a
"Apparatus for the Measurement of the Mechanical Properties of Fibres". J. of Sci. Instruments. 37: No. 1, p. 25-27.

MORGAN, F.R. and
MITTON, R.L.
1960
"Mechanical Properties of Raw Collagen Fibres". J. of Society of Leather Trades' Chemists. 44: 2.

MUIR, H.
1964
"Chemistry and Metabolism of Connective Tissue Glycosaminoglycans". Internat. Review of Connective Tissue Res. 2: 101. Ed. D.A. Hall, Academic Press.

MUST, J.S., BRODY, G.
S., PREVENSLIK, T.,
BECKWITH, T.G., GLASER,
A.A. and MARANGONI,
R.D.
1965
"Apparatus Designed to Produce Uniform Experimental Wounds". Med. Elec. and Biol. Eng. 3: No. 4, p. 407.

NEUMAN, R.E. and
LOGAN, M.A.
1950
"The Determination of Hydroxy-proline". J. Biol. Chem. 184: 299.

PARTINGTON, F.R. and   "The Rôle of Non-Collagen Components
WOOD, G.C.   in the Mechanical Behaviour of Tendon
1963   Fibres". Biophys. Aca. 69: 485.

RAGNELL, A.   "The Tensibility of the Skin: an
1954   Experimental Investigation". Plastic
                             and Reconstructive Surg. 14: No. 5,
                             p.317.

RAMACHANDRAN, G.N.   "Molecular Structure of Collagen".
1963   Int. Reviews of Connective Tissue
                             Res. 1: 127. Ed. D.A. Hall, Academic
                             Press.

RAMACHANDRAN, G.N. and Proc. Indian Acad. Sci. A45: 124.
SANTHANAM, M.S.
1957

RICH, A. and CRICK, F. J. Med. Biol. 3: 71.
H.C.
1961

RIDGE, M.D.   "The Rheology of Skin". PhD Thesis,
1964   Dept of Med., University of Leeds.

RIDGE, M.D. and   "The Description of Skin Stiffness".
WRIGHT, V.   Biorheol. 2: 67.
1964a

RIDGE, M.D. and   "A Rheological Study of Skin".
WRIGHT, V.   Proc. Symposium on "Biomechanics &
1964b   Related Bioengineering Topics". p.
                             165-175. Ed. R.M. Kenedi, Pergamon
                             Press.

RIDGE, M.D. and   "An Engineering Study of Human Skin".
WRIGHT, V.   Engineering. 199: No. 5161, p.363.
1965

ROLLHAUSER, H.   "Die Zungfestigkeit der Menschlichen
1950   Haut". Gegenbaurs Morphol. 90: 249.

ROTHMAN, S.   "Physiology and Biochemistry of the
1954   Skin". University of Chicago Press.

SCHADE, H.
1912

"Untersuchungen zur Organfunktion des Bindegewebes." Z. f. Exper. Path. u. Therap. 11: 369.

SCHADE, H.
1921

"Die physikelische Chemie in der inneren Medizin". T. Steinkopft, Dresden and Leipzig.

SIMEONE, F.A. and
LAMPSON, R.S.
1937

"Cystometric Study of Function of Urinary Bladder". Annals of Surg. 106: 413.

SODEMANN, W.A. and
BURCH, G.E.
1938

J. Clinical Invest. 17: 785.

STEGEMANN, H.
1958

"Microhistimmung von Hydroxyprolin mit Chloramin-T und p-Demethylamino bengaldehyd". Hofpe-Senl Z. 311: 41.

TREGEAR, R.T. and
DIRNHUBER, P.
1965

"Viscous Flow in Compressed Human and Rat Skin". J. of Investigative Dermatology. 45: No. 2, p.119.

TRELOAR, L.R.L.
1943

"Elasticity of Network of Long Chain Molecules". Tr. Farad. Soc. 39: 36.

von GIERKE, H.E.,
OESTREICHER, H.L.;
FRANKE, E.J., PARRACK,
H.O. and von WITTERN,
W.W.
1952

"Physics of Vibration in Living Tissues". J. Appl. Physiol. 4: 886.

WALKER, L.B., HARRIS,
E.H. and BENEDICT, J.
V.
1964

"Stress-Strain Relationship in Human Cadaveric Plantaris Tendon: A Preliminary Study". Med. Elec. and Biol. Eng. 2: 31.

WALL, F.T.
1942a

"Statistical Thermodynamics of Rubber Part I". J. Chem. Phys. 10: 132.

WALL, F.T.
1942b

"Statistical Thermodynamics of Rubber Part II". J. Chem. Phys. 10: 485.

WALL, F.T.
1943

"Statistical Thermodynamics of Rubber Part III". J. Chem. Phys. 11: 527.

WARD, I.M. and ONAT, E.T.
1963
"Non-linear Mechanical Behaviour of Oriented Polypropylene". J. Mech. Phys. Solids. 11: 217.

WIEGAND and SNYDER
1934
Trans. Inst. Rubber Ind. 10: 234.

WOOD, G.C.
1954
"Some Tensile Properties of Elastic Tissue". Biochim. Biophys. Acta 15: 311.

WOOD, G.C.
1964
"The Precipitation of Collagen Fibres from Solution". Inter. Review of Connective Tissue Res. 2: 1. Ed. D.A. Hall, Academic Press.

WOOD, G.C. and CHAMBERLAIN, N.H.
1954
"The Relaxation of Stretched Animal Fibres". J. Textile Inst. 45: T.147.

WOODRUFF, M.F.A.
1960
"The Transplantation of Tissues and Organs". Thomas, Springfield, Ill.

Appendix A.I

Derivation of the Wiegand-Snyder equation.

Let T = absolute temperature

F = tensile force

ℓ = length of material in tension

q = heat absorbed during extension

E = internal energy

dw = work done by material during extension

= $-Fd\ell$

s = entropy

ds = $\dfrac{dq}{T}$

From the first law of thermodynamics:

$$dq = dE + dw$$

and from the second law:

$$Tds = dE + dw$$
$$= dE - Fd\ell \qquad\qquad\qquad \text{A.I.1}$$

therefore, at constant temperature,

$$F = - T\frac{\partial s}{\partial \ell} + \frac{\partial E}{\partial \ell} \qquad\qquad\qquad \text{A.I.2}$$

Differentiating with respect to T, we have:

$$\frac{\partial F}{\partial T} = - T\frac{\partial^2 s}{\partial T\partial \ell} - \frac{\partial s}{\partial \ell} + \frac{\partial^2 E}{\partial T\partial \ell} \qquad\qquad \text{A.I.3}$$

Similarly, from A.I.1, we have, at constant length:

$$\partial s = \frac{\partial E}{T}$$

$$\frac{\partial s}{\partial T} = \frac{1}{T} \ \frac{\partial E}{\partial T}$$

$$\frac{\partial^2 s}{\partial T\partial \ell} = \frac{1}{T} \ \frac{\partial^2 E}{\partial T\partial \ell}$$

Combined with A.I.3:

$$\frac{\partial F}{\partial T} = - \frac{\partial s}{\partial \ell} \qquad\qquad\qquad \text{A.I.4}$$

Combined with A.I.2:

$$F = \frac{\partial E}{\partial \ell} \qquad + \qquad T\frac{\partial F}{\partial T} \qquad \text{A.I.5}$$

$$\underset{\text{internal}}{} \qquad \qquad \underset{\text{entropy}}{}$$
$$\text{energy}$$

      This equation gives only the rates of change of energy and entropy. To find the actual changes produced by a given extension from ℓ_1 to ℓ_2 we proceed as follows:

      Multiplying A.I.4 by T:

$$T\left(\frac{\partial F}{\partial T}\right) = - T\left(\frac{\partial S}{\partial \ell}\right)$$

$$= - \frac{\partial q}{\partial \ell}$$

substituting in A.I.5 gives:

$$\frac{\partial E}{\partial \ell} = F + \frac{\partial q}{\partial \ell}$$

integrating between ℓ_1 and ℓ_2 gives:

$$\int_{\ell_1}^{\ell_2} \frac{\partial E}{\partial \ell}\, d\ell = \int_{\ell_1}^{\ell_2} F d\ell + \int_{\ell_1}^{\ell_2} \frac{\partial q}{\partial \ell}\, d\ell$$

Appendix A.II

MALLORY TRICHROME (Modified)

Staining Solutions:

A.	Ponceau 2R	0.2 gm.
	Acid fuchsin	0.1 gm.
	Orange G.	0.1 gm.
	0.2% Acetic acid in Aq. dest.	300 cc.
B.	Light green	0.5 gm.
	0.2% Acetic acid in Aq. dest.	100 cc.

Method:

1. Section to water. Treat artefact if necessary.
2. Celestin blue   5 mins.
3. Rinse water
4. Haemalum   7 mins.
5. Rinse water
6. Ponceau mixture (Soln. A)   5 mins.
7. Rinse water
8. 0.2% Acetic acid   5 mins.
9. Rinse water
10. 5% Phosphotungstic acid in water   5 mins.
11. Light green mixture (Soln. B)   5 mins.
12. Rinse water
13. 0.2% Acetic acid   5 mins.
14. Dehydrate, clear and mount.

Results:

Epithelial cells, Muscle, Fibroblasts	Red
Collagen and Basement membranes	Green
Erythrocytes	Orange
Nuclei	Purple to Red

Appendix A.III

Derivation of Elastomer Stress-strain Relations

Consider a block of elastomer idealised as consisting of a network of chains extending between the 3 pairs of parallel faces.

The chains joining a given pair of parallel faces are all of the same lengths but are in highly contorted configurations which are constantly changing because of thermal agitation. The stress-strain behaviour of such a system can be derived by the techniques of statistical mechanics.

Consider a chain consisting of N links each of length ℓ. Let the mean distance between the ends of the chain be x_o. If a force F stretches the chain by an amount Δx, let the number of possible configurations of the chain which result in an end separation between x and x + dx be:

$$dC = C(x)\ dx$$

where $x = x_o + \Delta x$.

Then the probability that the chain will have an end separation between x and x + dx is given by:

$$dp = p\ dx = \varepsilon^{F\Delta x/kT}\ dC$$

$$= \varepsilon^{F\Delta x/kT}\ C(x)\ dx$$

when k = Boltzman's Constant

T = absolute temperature.

The probability function p has a maximum value p_{max} when $\Delta x = e$, the most probable extension associated with force F.

$$p_{max} = \varepsilon^{F_\ell / kT} C_{(x)}.$$

$$\log P_{(max)} = \frac{F_\ell}{kT} + \log C_{(x)}$$

$$\frac{\partial}{\partial F}\left[\log (P_{max})\right] = \frac{\ell}{kT}$$

$$x = x_o + \ell$$

$$= x_o + kT \frac{\partial}{\partial F}\left[\log (P_{max})\right] \qquad A.II.1.$$

<div align="right">A.II.1</div>

Consider the link length ℓ to be a vector which may assume all orientations in space with equal probability. Because N is large we may consider the mean contribution of each link to the extension e. Let the rth link with component x_r in the x direction make a contribution e_r to e. i.e.

$$\ell = \ell_1 + \ell_2 + \cdots + \ell_r + \cdots + \ell_N .$$

$$\varepsilon^{F_\ell / kT} = \varepsilon^{F_{\ell_1} / kT} \cdot \varepsilon^{F_{\ell_2} / kT} \cdots \varepsilon^{F_{\ell_N} / kT}$$

$$= \prod_{r=1}^{N} \varepsilon^{F_{\ell_r} / kT}$$

e_r may assume values between $-\ell - x_r$ and $\ell - x_r$

$$\left[\varepsilon^{F_{\ell_r} / kT} \right]_{MEAN} = \frac{1}{2\ell} \int_{-\ell - x_r}^{\ell - x_r} \varepsilon^{F_{\ell_r} / kT} \, d\ell_r$$

$$= \frac{kT}{2\ell F} \left[\varepsilon^{F(\ell - x_r)/kT} - \varepsilon^{F(-\ell - x_r)/kT} \right]$$

$$= \frac{kT}{\ell F} \sinh\left(\frac{F\ell}{kT}\right) \cdot \varepsilon^{-Fx_r / kT}$$

$$= \frac{\sinh u}{u} \varepsilon^{-Fx_r / kT} \quad \text{WHEN } u = \frac{F\ell}{kT}$$

substituting in A.II.2 gives:

$$\varepsilon^{F_\ell / kT} = \left[\frac{\sinh u}{u} \right]^N \prod_{r=1}^{N} \varepsilon^{-Fx_r / kT}$$

and, since $x_0 = x_1 + x_2 + x_3 + \ldots\ldots \text{to } x_N$

$$\varepsilon^{F_\ell / kT} = \left[\frac{\sinh u}{u} \right]^N \varepsilon^{-Fx_0 / kT}$$

$$p_{max} = \left[\frac{\sinh u}{u} \right]^N \varepsilon^{-Fx_0 / kT} \, C_{(x)}$$

$$\log (p_{max}) = N \log \left(\frac{\sinh u}{u} \right) - \frac{F x_0}{kT} + \log C_{(x)}$$

$$\frac{\partial}{\partial F} \left[\log (p_{max}) \right] = \frac{N u}{\sinh u} \left[\frac{\cosh u}{u} - \frac{\sinh u}{u_2} \right] \frac{\ell}{kT} - \frac{x_0}{kT}$$

$$= \frac{N \ell}{kT} \left[\coth u - \frac{1}{u} \right] - \frac{x_0}{kT}$$

substituting in A.II.1 gives:

$$x = N \ell \left[\coth u - \frac{1}{u} \right]$$

$$x = N \ell \; \mathcal{L} \, (u) \qquad\qquad\qquad \text{A.II.3}$$

$\mathcal{L}(u) = \coth u - \frac{1}{u}$ is called a Langevin function.

let $q = \frac{1}{N \ell}$

$$= \qquad \mathcal{L} \left(\frac{F \ell}{kT} \right) = q \, x$$

$$= \qquad F = \frac{kT}{\ell} \; \mathcal{L}^{-1} (q \, x) \qquad\qquad \text{A.II.4}$$

$\mathcal{L}^{-1}$ is the inverse Langevin function.

This is the force extension relation for a single molecule.

<u>Uniaxial stress-strain relation for elastomer block</u>

Assume that the extension is isovolumetric:

i.e. $x_0 \, y_0 \, z_0 = x \, y \, z$ A.II.5

Let M be the number of chain ends per unit area of the surface of the unstretched block. Equation A.II.4 shows that a force F is required to maintain an end separation x for each chain where x > 0. There is therefore a force acting inwards on each face of the block which must be in equilibrium with an internal hydrostatic pressure P in the absence of external forces. The pressure may be considered to arise from the thermal agitation of the chain links in the same manner as the pressure in a gas arises from the thermal agitation of the gas molecules.

Consider a tensile force X applied to the yz surfaces so as to extend the block in the x direction. Then, at the yz surface:

$$X = MFy_0 z_0 - Pyz \quad\quad\quad \text{A.II.5}$$

To evaluate P, consider the force equilibrium at the xy (or yz) surface:

$$P = MF \, \frac{x_0 \, y_0}{x \, y}$$

where $= M \cdot kT \; \mathcal{L}^{-1} (\mathcal{V}_z \, \gamma) \cdot \frac{x_0 \, y_0}{x \, y}$

$\mathcal{V}_z = \frac{1}{N_z l}$

and $N_z l$ = total length of chain in z direction.

As the material is assumed isotropic:

from A.II.5:

$$\frac{y_o}{y} = \frac{z_o}{z} = \left(\frac{x}{x_o}\right)^{\frac{1}{2}}$$

The number of links per chain is assumed proportional to the distance between the ends in the unstressed block.

$$\mathcal{V}_z = \mathcal{V}_x \left(\frac{x_o}{y_o}\right)$$

$$P = \frac{MkT}{\ell} \mathcal{L}^{-1}\left[\mathcal{V}_x \, x_o \left(\frac{x_o}{x}\right)^{\frac{1}{2}}\right] \left(\frac{x_o}{x}\right)^{\frac{1}{2}}$$

in A.II.6

$$X = \frac{MkT}{\ell} \, y_o \, z_o \left[\mathcal{L}^{-1}(\mathcal{V}_x \, x) - \left(\frac{x_o}{x}\right)^{\frac{3}{2}} \mathcal{L}^{-1}\left[\mathcal{V}_x \, x_o \left(\frac{x_o}{x}\right)^{\frac{1}{2}}\right] \right]$$

This is the force-extension relation for an elastomer block.

Appendix A.IV

Derivation of General Constitutive Relations for Non-linear Viscoelastic Material

Consider a deformation in which a particle initially with coordinates X_i (i = 1, 2, 3) with respect to a fixed rectangular Cartesian coordinate system moves to a position $x_i(\tau)$ at some later time τ.

By consideration of invariance requirements under the deformation, Green and Rivlin (1959) have shown that for this material

$$\sigma = RSR^T \qquad\qquad A.IV.1$$

where σ = the stress matrix $\left[\sigma_{ij}\right]$

$S = S(E)$ is a matrix functional of the strain matrix E.

$$E = \left[E_{ij}\right]$$

where

$$2E_{ij} = \frac{\partial x_k}{\partial X_i} \frac{\partial x_k}{\partial X_j} - \delta_{ij}$$

$$\delta_{ij} = \begin{bmatrix} 1 \text{ if } i = j \\ 0 \text{ if } i \neq j \end{bmatrix}$$

The matrix R is obtained by separating the deformation into a rigid rotation and a pure homogeneous strain.

Thus if $F = \left[F_{ij}\right]$

where

$$F_{ij} = \frac{\partial x_i(\tau)}{\partial X_j(\tau)}$$

defines the deformation in terms of the displacement gradients at particle x_i at time τ, then $F = RM$ where R is an orthogonal matrix and represents a rigid rotation and M is a symmetric matrix representing a pure homogeneous strain.

Only the component R appears explicitly in equation A.IV.1, R^T denoting the transpose of R.

Equation A.IV.1 gives the stress matrix σ in terms of the strain. To obtain the inverse relation A.IV.1 can be written in the form:

$$R^T \sigma R = S(E) \qquad\qquad \text{A.IV.2}$$

then, if the inverse of functional S exists:

$$E = S^{-1}(R^T \sigma R) \qquad\qquad \text{A.IV.3}$$

This is not an explicit relation as the matrix R which is related to the strain appears in combination with the stress matrix σ.

The equations A.IV.2 and A.IV.3 may be considered simultaneously by writing:

$$Q = D(P) \qquad\qquad \text{A.IV.4}$$

where, either

$$Q = R^T \sigma R \qquad P = E$$

or $\qquad Q = E \qquad P = R^T \sigma R$

and D is a matrix functional.

Green and Rivlin (1959) have shown that for the

material being considered, this functional can be written in the form:

$$Q(t) = \theta_0 I + \int_0^t \theta_1(t - \tau_1) \, \dot{p}(\tau_1) d\tau_1$$

$$+ \int_0^t \int_0^t \theta_2(t - \tau_1; \; t - \tau_2) \, \dot{p}(\tau_1)\dot{p}(\tau_2)d\tau_1 d\tau_2$$

$$+ \int_0^t \int_0^t \int_0^t \theta_3(t - \tau_1; \; t - \tau_2; \; t - \tau_3)\dot{p}(\tau_1)\dot{p}(\tau_2)\dot{p}(\tau_3)d\tau_1 d\tau_2 d\tau_3$$

$$+ \; \ldots\ldots\ldots\ldots \qquad\qquad A.IV.5$$

where I = the unit matrix. θ_α are functions of their indicated arguments and are polynomials of the invariants

$$\int_0^t \eta_\alpha(t - \tau) \; tr \; \dot{p}(t) \quad d\tau$$

$$\int_0^t \int_0^t \eta_\beta(t - \tau_1; \; t - \tau_2) \; tr \; \dot{p}(\tau_1) \; \dot{p}(\tau_2) \quad d\tau_1 d\tau_2$$

etc.

Finally, equation A.IV.5 can be written in the form:

$$Q)t) = \int_0^t \Big[I\psi_1 T_1 + \psi_2 M_1 \Big] d\tau_1$$

$$+ \int_0^t \int_0^t \Big[I\psi_3 T_1 T_2 + I\psi_4 T_{12} + \psi_5 T_1 M_2 + \psi_6 M_1 M_2 \Big] d\tau_1 d\tau_2$$

$$+ \; \ldots\ldots\ldots \qquad\qquad A.IV.6$$

where

$$T_\alpha = tr \; \dot{p}(\tau_\alpha)$$

$$T_{\alpha\beta} = tr \; \dot{p}(\tau_\alpha) \; \dot{p}(\tau_\beta) \quad , \; etc.$$

$$M_\alpha = \dot{p}(\tau_\alpha)$$

ψ_1; ψ_2 are functions of $t - \tau_1$, $\psi_3 \ldots \psi_6$ are functions of $t - \tau_1$ and $t - \tau_2$, etc.

Appendix A.V

Analysis of Uniaxial Experiments on Non-linear Viscoelastic Material

The constitutive relation is:

$$E(t) = \int_0^t J(t - \tau_1) \, \dot{\sigma}(\tau_1) \, d\tau_1$$

$$+ \int_0^t \int_0^t K(t - \tau_1; \, t - \tau_2) \, \dot{\sigma}(\tau_1) \, \dot{\sigma}(\tau_2) \, d\tau_1 d\tau_2$$

$$+ \int_0^t \int_0^t \int_0^t L(t - \tau_1; \, t - \tau_2; \, t - \tau_3) \dot{\sigma}(\tau_1) \dot{\sigma}(\tau_2) \dot{\sigma}(\tau_3) d\tau_1 d\tau_2 d\tau_3$$

$$+ \,\ldots\ldots\ldots \qquad\qquad\qquad A.V.1$$

Only the first three terms will be considered.

Consider a single step loading programme of the form:

$$\sigma(t) = c_i H(t) \qquad (i = 1, 2, 3)$$

where $H(t)$ is the Heaviside function and is defined by:

$$H(t) = \begin{cases} 0, & t < 0 \\ 1, & t \geq 1 \end{cases}$$

Substituting in A.V.1 and integrating gives

$$E(t; \, i) = c_i \, J(t) + c_i^2 \, K(t,t) + c_1^3 L(t,t,t) \qquad A.V.2.$$

Thus, if three such tests are carried out with different values of c_i then at a given value of t, it is possible to write down three simultaneous equations in $J(t)$, $K(t,t)$, $L(t,t,t,)$ and thus obtain values of these functions at

the chosen value of t.   By considering other values of t, it is thus possible to define the functions for the range of t covered by the tests.   The function J(t) is thus fully determined, but the other two functions are only determined for the case of equal arguments.

Consider a two step loading programme:

$$\sigma(t) = a_i \, h(t) + b_j \, H(t - k)$$

Substituting in A.V.1 it is found that since the functions K, L are symmetrical with respect to their arguments (i.e. K(t, t - k) = K(t - k, t), etc.

$$E(t; i, j, k) = 2 \, a_i b_j K(t, t - k)$$

$$+ \, 3 \, a_i^2 b_j \, L(t, t, t - k) + 3 a_i b_j^2 \, L(t, t - k, t - k)$$

$$+ \quad a_i \, J(t) + b_j \, J(t - k)$$

$$+ \, a_i^2 \, K(t, t) + b_j^2 \, K(t - k, t - k)$$

$$+ \, a_i^3 \, L(t, t, t) + b_j^3 \, L(t - k, t - k, t - k)$$

. . . .   A.V.3

Note that the terms in the square brackets can be determined from the results of the single step tests. Therefore, by performing three tests with different values of i and j, it is again possible to write down simultaneous equations and solve for K(t, t - k), L(t, t, t - k) and L(t, t - k, t - k).   If these tests are repeated for a sufficient number of values of k, the function

K(t, t - k) will be completely determined and the function
L will be determined for the case when two of its
arguments are equal.   To determine L completely it is
necessary to consider the three step test:

$$\sigma(t) = aH(t) + bH(t - k) + cH(t - \ell)$$

Substituting in A.V.1 gives:

$$E(t; k, \ell) = 6abc\ L(t, t - k, t - \ell)$$

$$+ \quad \ldots\ldots\ldots\ldots\ldots\ldots \qquad\qquad A.V.4$$

when the terms in the square bracket can all be
determined from the single step and double step tests.
Thus, a single test will yield a value for $L(t, t - k, t - \ell)$ for a given k and ℓ.

Further tests with a number of different values
of k and ℓ in the range $(0 < k < \ell)$ will allow the complete
determination of the functions $L(t, t - k, t - \ell)$.

Appendix A.VI
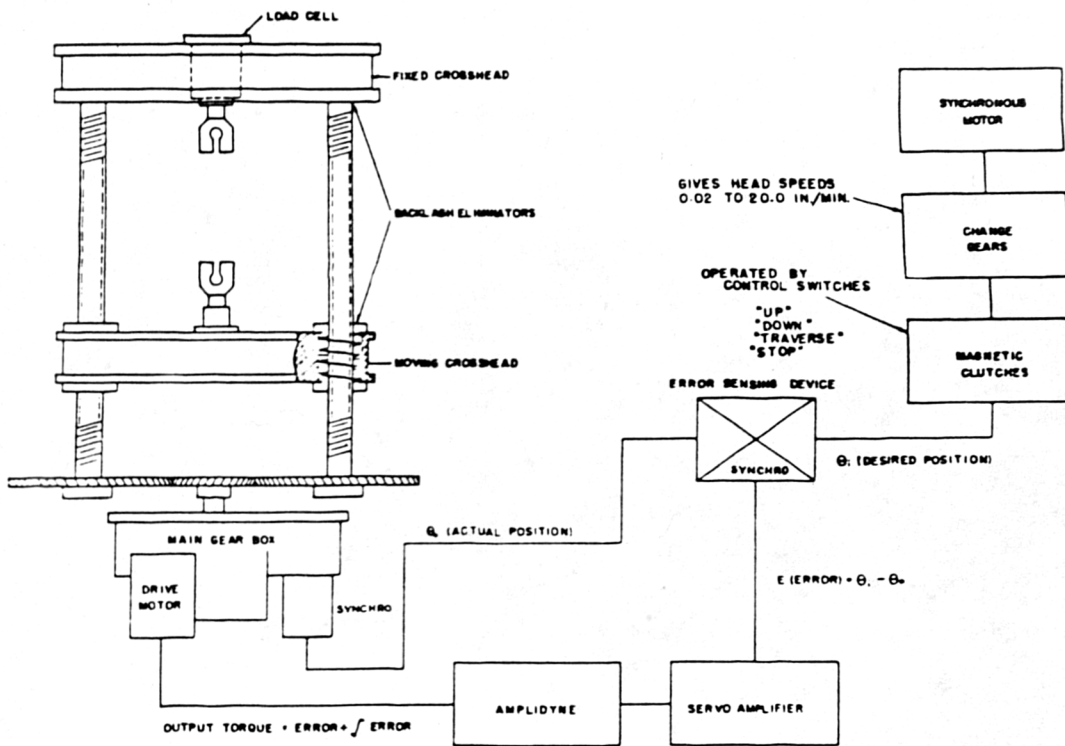
FIG. A. VI. 1.   INSTRON   CROSSHEAD
DRIVE   SYSTEM

The Instron Tensile Testing Machine

The Instron Tensile Testing Machine is a precision instrument incorporating many features that have been found essential in the testing of biological materials. Some of these are discussed in the brief description of the operation of this machine given below.

The function of this machine may be split into two distinct sections:-

(i) the crosshead drive mechanism
(ii) the load weighing and recording system

A block diagram of the crosshead drive system is shown in Fig A.VI.1. A constant speed synchronous motor drives a synchro transmitter unit *via* lightweight change gears. The gear ratio selected here determines the crosshead speed. The output from the servo transmitter is compared with the output of a reference synchro unit driven by the crosshead lead screw gear box. Any error signal between the two synchros is suitably amplified and used to operate the main crosshead drive motor in such a direction as to reduce the error. This is a positional servo system so that the only error produced in operation is in the form of a slight phase lag between the synchros. There is no error in the crosshead speed, this being an exact function of the speed of the synchronous motor. This system gives very precise control over the crosshead movement.

The load weighing system is outlined in Fig A.VI.2. This system is very precise and stable and, because it has no mechanical inertia, it does not influence
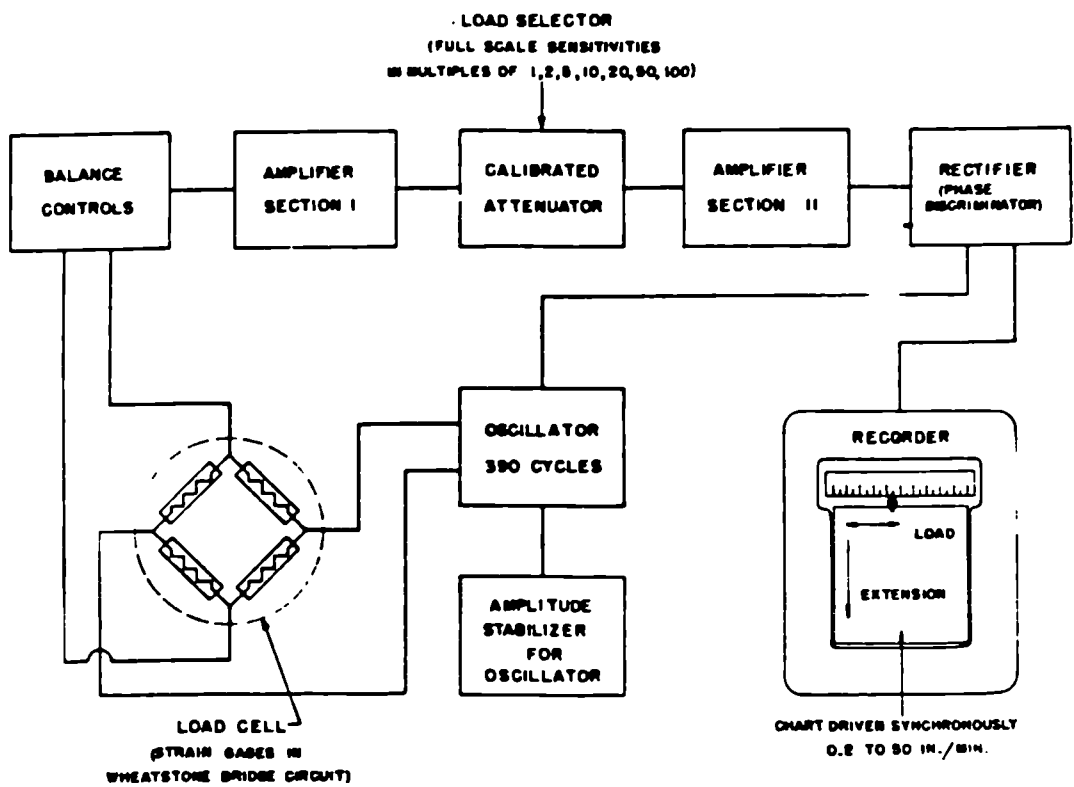
FIG. A. VI: 2   INSTRON LOAD MEASURING

AND RECORDING SYSTEM

the measurement of mechanical properties of the material
being tested.   The system is readily calibrated by dead
weight loading and has been found to maintain this
calibration over a period of several days to within 1%.
The weight of grips, etc. can be readily balanced out over
a wide range.   It is also possible to obtain a X5 gain in
sensititivy with any load cell at the price of a loss of
long term stability.

The extension of the specimen is recorded on
the chart of the pen recorder in two different ways.

(i)   The chart is driven by a synchronous
motor so that its movement is proportional
to the crosshead movement, the magnification
factor being determined by the crosshead
and chart drive gear box ratios in use.
This system records the extension of the
whole specimen between the grips.

(ii) If it is desired to measure the
extension of a gauge length on the
specimen, the X-Y Chart Drive system
allows the chart to be driven by an
amount proportional to the extension of
such a gauge length.   This extension
may be measured by a variety of
mechanical extensometers, directly by
strain gauges or by the Instron Optical
Extensometer described in the main text
and in Appendix A.VII.

Appendix A.VII

Strain Measuring Techniques

Three different optical strain measuring techniques were used during the investigations described in this thesis:-

(i)   a photographic system used with the Bioengineering Unit machine

(ii)   a photographic system used with the Instron machine

(iii)   the Instron Optical Extensometer

A.VII.1   Photographic Method No 1 - Bioengineering Unit Machine

The camera used in this system was a Zenza Bronica single lens reflex type. This produced 12 negatives of 6 x 6 cm. format from 120 roll film.

The film used was Ilford F.P.3 fine grain panchromatic, this being developed in Ilford "Monophen", a combined developer-fixer solution. This solution greatly decreases the processing time at the expense of an increase in emulsion grain size, although this was still perfectly acceptable. The accuracy of this system was checked by replacing the skin specimen with a precision grid and measuring the resulting negative. The maximum error found was of the order of 0.3%, this being at the extreme corners of the negative. There was no detectable error at the centre of the negative where the image of the skin specimen would normally be placed.

By using an electronic flash unit to illuminate the specimen, an effective exposure time of 1 millisecond was obtained. This was found to be necessary because the camera and its supporting slide were mounted at the extreme end of a cantilevered support. This system was

found to perform vertical oscillations of appreciable amplitude at a frequency of 10 cycles/sec. There was, therefore, a possibility of the image being distorted and blurred if this vibration was to occur while a shot was being taken as the transit time of the focal plane shutter was approximately 1/10 sec. This effect did not occur when using electronic flash as the shutter was fully opened, the whole area of the negative exposed only for the duration of the flash, and the shutter was then closed.

Although the photographic results obtained with this equipment were excellent, several problems were encountered in use:-

(i)   Only 12 shots were obtainable without reloading the camera although this could be done quickly using the spare film back. This was not always convenient.

(ii) Because of the amount of cranking required to wind on the film and cock the shutter mechanism, the minimum interval between shots was about 5 seconds.

(iii) The flash synchronisation mechanism in the camera was somewhat unreliable. This resulted in several hold-ups in the test programme while this was being rectified.

Because of these difficulties, a different system was developed for use with the Instron.

A.VII.2   <u>Photographic Method No 2 - Instron</u>

This method was similar in principle to that described above but the numerous refinements incorporated made for much more satisfactory operation.

A Nikon F single lens reflex camera was used. This produced up to 36 exposures of 24 x 36 mm. format on

35 mm. roll film, the film used being Ilford PAN F extra fine grain film.   Again, an acceptable grain size was obtained with Ilford "Monophen" combined developer-fixer solution. By using a 105 mm. lens mounted on a bellows attachment, the image size obtained on the negative was the same as that produced by the Bronica so that no further errors were introduced into the measurement of the negatives. Test photographs taken of a precision grid showed that the errors in the optical system were less than 0.1% of the ·negative size.

The camera was fitted with an electrical motor driven unit which enabled shots to be taken at rates up to 4 per second.   This drive was triggered externally by the Camera Timer Unit so that shots could ·be· taken automatically at intervals of up to 1 hour.

To maintain the optical axis of the camera in line with the specimen centre during the test, the camera was mounted on a pantograph arrangement so that it moved downwards at half crosshead speed.   This mounting arrangement was quite rigid and no vibration troubles were encountered.   However, the electronic flash equipment was used again as it was much more convenient than the photoflood lamps which would otherwise be necessary.

This apparatus was completely automatic in operation and was found to be much more convenient and reliable than the previous method.   The only drawback to this system is the time-consuming analysis of the negatives.

A.VII.3   ·The Instron Optical Extensometer

A direct record of load v. extension of a specimen was produced by this instrument at the expense of only having a uniaxial strain measurement, i.e. no

GAUGE LENGTH
MARKER.

IMAGE OF
SPECIMEN.
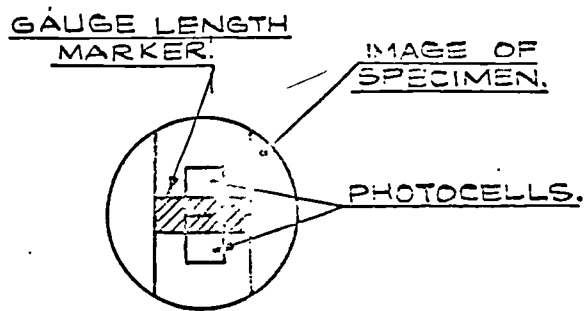
PHOTOCELLS.

(i) IMAGE OF SPECIMEN WITH GAUGE LENGTH MARK
IS FOCUSSED ON PHOTO CELLS.

EQUAL
AREAS
ILLUMINATED.
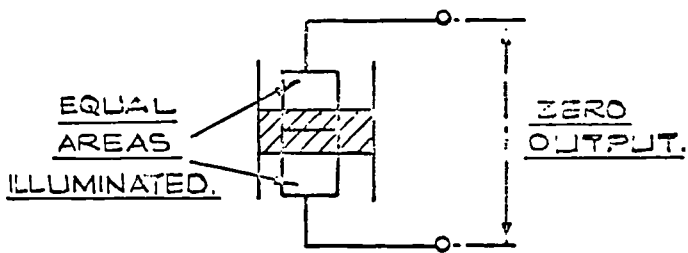
ZERO
OUTPUT.

(ii) WHEN GAUGE LENGTH MARK IS CENTRAL THE
RESULTANT ELECTRICAL OUTPUT IS ZERO.
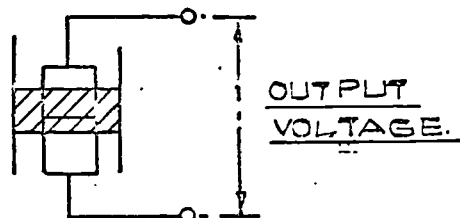
OUTPUT
VOLTAGE.

(iii) WHEN MARK IS OFF CENTRE THE RESULTANT
OUTPUT VOLTAGE IS AMPLIFIED AND USED TO DRIVE
THE OPTICAL / HEAD UNTIL THE MARK IS CENTRAL.

FIG. A VII. 1.- OPERATION OF OPTICAL HEADS.

data is produced regarding the contraction in specimen width which accompanies extension.

The principle of operation of the optical heads of this instrument is shown in Fig A.VI.1. The outputs of the two photo cells are connected in opposite phase so that with the image of the gauge length mark centrally placed, the cells are equally illuminated and there is no output. Any deviation of the mark produces an output voltage. This in turn operates a servo system to bring the head back into alignment with the mark. In this way the two heads "lock on" to the gauge length markers and follow their movements.

By means of a further servo system, the chart of the Instron pen recorder is caused to move by a distance which is proportional to the _relative_ movement of the optical heads. In this way, a load v. gauge length extension curve is obtained automatically. This was found to be a very considerable advance over the time-consuming analysis of negatives involved in the photo-graphic method. Using this equipment, the only limit to the number of tests which were performed was the supply of skin specimens. The only significant problem encountered was that the light transmission losses caused by the glass wall of the immersion tank and the Ringer's solution itself were so great as to render the operation of the heads very sluggish. The self-contained illumination system on the heads had, therefore, to be supplemented by fluorescent tubes attached to the tank. Excellent head following was obtained by this means.

Appendix A.VIII

Grid Printing Technique

For the purposes of the photographic strain
measuring technique described in Appendix A.VII, it was
necessary to print a fine accurate grid on the epidermal
surface of the skin.   This was done by the offset
lithographic printing process.   This had the advantage
that the process depends only on surface effects so that
the image on the plate used was on the same level as the
surface of the plate.   There was therefore no distortion
of the skin surface during printing.

The image on the plate consisted of a fine
grid of 0.064 in. squares.   The surface properties of
the plate were such that a film of water would adhere
readily to the plate surface except on the lines of the
grid which were strongly water-repellent.

The first step of the printing process was to
dampen the plate surface lightly with water.   An inked
roller was then run over the plate surface several times.
As the ink used was also water-repellent, it adhered only
to the grid lines which did not have a surface film of
water.   The skin was placed, epidermis up, onto a piece
of thin card to which it adhered.   The surface of the
epidermis was carefully dried and the whole assembly was
placed, epidermis down, on the inked plate and pressed
gently into contact.   On removal from the plate, a very
well defined grid was transferred to the surface of the
epidermis.

Appendix A.IX

Analysis of Stress Relaxation Data

(a)   Empirical analysis of stress-relaxation curves

Using the graphical method described by the
British Rheologists Club (1944), it is possible to analyse
the result of a stress relaxation test into the form:

$$\sigma(t) = A_o + \sum_{r=1}^{n} A_r \exp(-t/\tau_r)$$

· A.IX.1

This method can be used only when the time
constants τ_r have widely spaced values, as it is not
accurate enough to resolve values which are not so spaced.

The first step in this method is to write out
the results in tabular form thus:

t	....
$\sigma(t)$	....

From equation A.IX.1

as $t \to \infty$ $\sigma(t) \to A_o$

i.e. the stress $\sigma(t)$ tends to a stable value.   This was
found to occur in skin at times greater than about 5000
seconds.   The value of A_o found in this way is
subtracted from the data so that:

$$\sigma(t) - A_o = A_1 \exp(-t/\tau_1) + ...$$

A.IX.2

The vertical axis is labelled $\text{LOG} [\sigma(t) - A_0]$ and the horizontal axis is labelled $time \ \ t$.

$\text{LOG} \ A_1$

SLOPE OF STRAIGHT LINE
PORTION OF CURVE
$$= -\frac{1}{\tau_1}$$

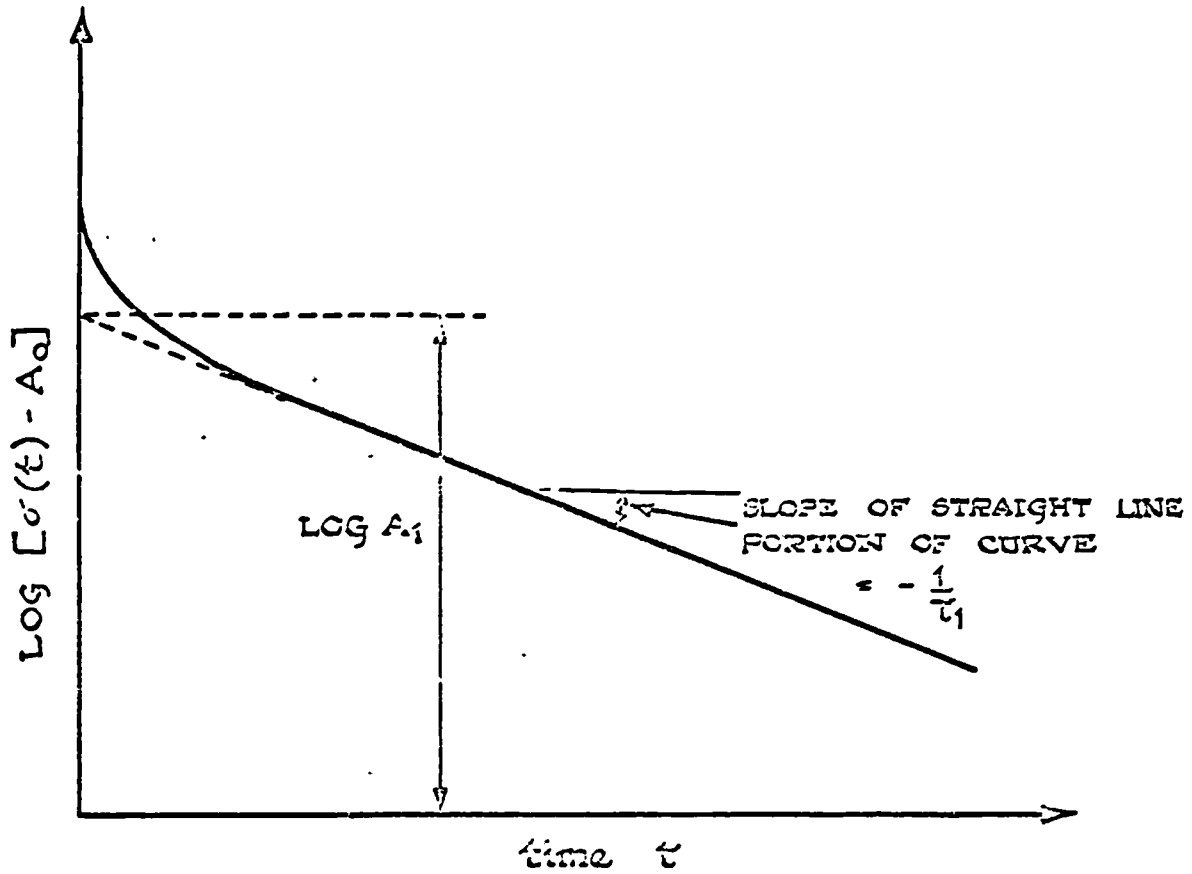FIG. A.IX 1. GRAPHICAL METHOD OF OBTAINING COEFFICIENTS AND TIME CONSTANTS OF EXPONENTIAL SERIES.

if $\tau_1 \gg \tau_2$ etc. and $t = \tau_1$:

then $\log \sigma(t) - A_o = -\dfrac{t}{\tau_1} \log A_1$ A.IX.3

     if $\log \sigma(t) - A_o$ is plotted against t

a straight line graph is obtained for $t = \tau_1$.
This is shown in Fig A.IX.1. The slope of this line can
be measured and is equal to $-\dfrac{1}{\tau_1}$. The intercept of this
line on the $\log \sigma(t) - A_o$ axis is equal to $\log A_1$. Thus
both τ_1 and A_1 are determined.

       Values of $A_1 \exp(-t/\tau_1)$ can now be calculated
for the values of τ used to tabulate the original data.
These values are then subtracted from the values of
$\sigma(t) - A_o$ so that:

$$\sigma(t) - A_o - A_1 \exp(-t/\tau_1) = A_2 \exp(-t/\tau_2) + \ldots\ldots \quad \text{A.IX.4}$$

The above process is then repeated for $t = \tau_2$ so that τ_2
and A_2 can be evaluated. Further terms of the series
can be determined as necessary.

(b)   <u>Sample calculations of stress relaxation</u>
         <u>behaviour of network model</u>
         The model is defined by:

$\alpha = 53^{\circ}$ $\beta(0) = 130 \text{ lb/in}^2$ $\gamma = 0.4 \text{ lb/in}^6$

t sec.	1	2	5	10	20	50	100
$\beta(t)$ lb/in^2	117	107	96	87.5	79.5	67.5	62.5

Case (i)

The model is given a strain $\epsilon_1 = 0.22$ at $t = 0$, and then held at this strain. Under these conditions at $t = 0$:

$$\theta = 42.8^\circ \qquad \sigma(0) = 0.21 \text{ lb/in}^2$$

the side link stress $= \dfrac{\sigma(0)}{2 \cos\theta} = 0.143 \text{ lb/in}^2$

the cross link stress $= \dfrac{\sigma(0)}{\tan\theta} = 0.216 \text{ lb/in}^2$

The deformations in the network under this action consist of two distinct effects:-

(i) an immediate response to the applied stress at $t = 0$. This may be considered as the elastic part of the overall viscoelastic behaviour.

(ii) a time-dependent response. This is the viscous part of the overall viscoelastic behaviour. It is these time-dependent deformations which are considered below. The effect of these deformations is added to the initial elastic deformation. When the viscous deformation is described as negligible, it is to be understood that it is very much smaller than the initial elastic deformation.

In analysing the stresses in the network, it is found convenient to consider the stress in the cross member. As this has no time-dependent properties, a change in the stress in the cross member must be

accompanied by a change in the length of this member.
Under stress relaxation conditions the ends of the model
are held at a fixed separation so that any stress
relaxation effect must imply:-

(i)   a reduction in cross member stress
hence
(ii)   an increase in cross member length
hence   .
(iii) an increase in side member length.

The relative importance of these effects depends
considerably on network configuration angle θ and thus
on the initial stress and can best be assessed by
considering the relative significance of the time-
dependent deformations of the viscoelastic side members.
The side link is assumed to have linear viscoelastic
properties defined by a stress relaxation test carried out
at a high stress level.
Considering the side link independently of the
network, the maximum possible time-dependent deformation
which can occur in this link in a time t is the creep
deformation which would result if the stress σ in this
member remained constant during t.   As in the network
being considered, σ   cannot increase with time, any
other deformation of the side link must have a smaller
value. · To determine whether the time-dependent
deformation of the side link will produce a significant .
change in the network geometry, the effect of this maximum
deformation is first considered.   To calculate the creep
deformation of the side links it is necessary to obtain
the creep compliance $\Gamma(t)$ of the side links, this function
being defined by the equation:

$$\varepsilon_f(t) = \sigma_i \ \Gamma(t)$$

when σ_i is the suddenly applied stress in a creep test.

By assuming that the side links have linear viscoelastic properties $\Gamma(t)$ can be calculated from $\beta(t)$ by the approximate method described by Ferry (1961). The appropriate equation is:

$$\Gamma(t) = (\sin m\pi)/m\pi \ \beta(t) \qquad\qquad \text{A.IX.5}$$

when m is the slope of the graph of log $\beta(t)$ against log t at a given time t. The function $\Gamma(t)$ calculated in this way is:

t - sec.	1	2	5	10	20	50	100
$\Gamma(t)$ in²/lb	.0083	.0090	.0101	.0111	.0122	.0144	.0155

at t = 0 the instantaneous deformation of side links is a purely elastic effect, therefore:

$$\Gamma(0) = \frac{1}{\beta(0)} = .0077 \ \text{in}^2/\text{lb}$$

In the example being considered, the maximum possible deformation of the side links in time t is given by the creep deformation:

$$\sigma \qquad \Gamma(t) - \Gamma(0)$$

thus, with $\sigma = 0.143$ lb/in²

$\qquad$ t = 100 secs.

this deformation is 0.0011 in./in.

If this deformation occurs with the side links in the
network the resulting change in θ is 0.06° and this in
turn implies a change in the cross link stress of less
than 0.4%. This may be considered negligible. Therefore,
in the time scale of the experiment being considered, the
maximum possible change in the network stress is negligibly
small. There are thus no apparent stress-relaxation
effects. This also implies that the stress in the side
link is constant during t and, therefore, that the maximum
possible side link deformation is the actual deformation
under these conditions.

Case (ii)

$$\varepsilon_1 = 0.66 \qquad \theta = 11^{\circ} \qquad \sigma(0) = 3.7 \text{ lb/in}^2$$

Repeating the calculation described above, the
percentage decrease in the cross link stress which would
result from the maximum possible side link deformation
after 100 seconds is found to be 33%. This is obviously
significant and implies that the effect of the time-
dependent deformation on the network geometry can no longer
be neglected over a period of 100 seconds. Because of the
number of variables involved, it is not possible to obtain
a simple estimate of the point at which this effect becomes
significant. This is best done by trial calculations.
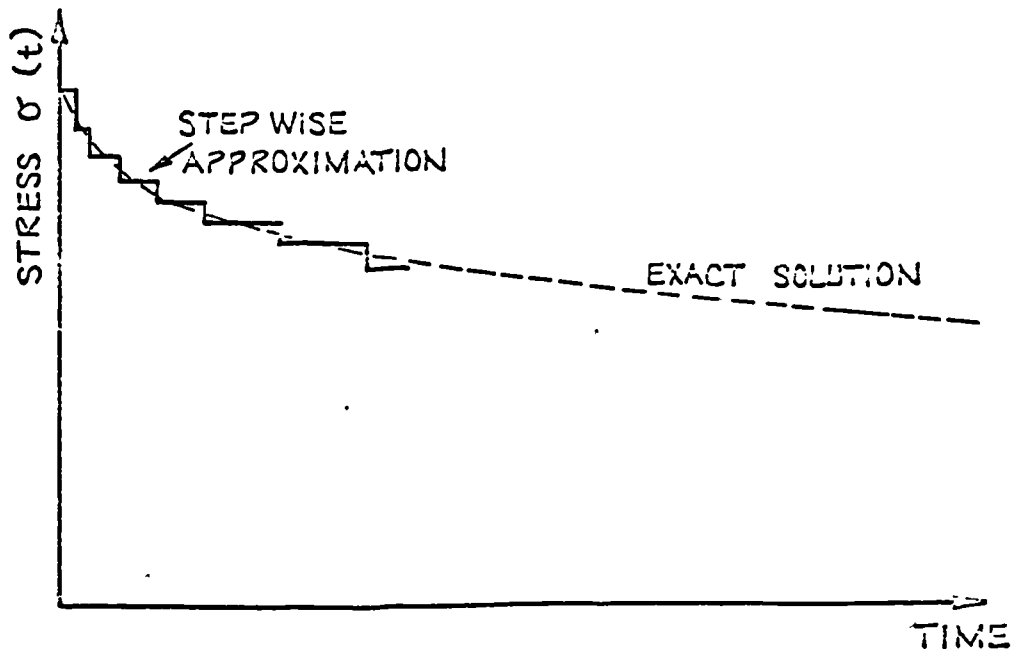This point is, of course, chosen arbitrarily, in this case

FIG. A IX.2. NETWORK THEORY — APPROXIMATE CALCULATION
OF STRESS RELAXATION CURVE.

a percentage decrease of cross link stress of greater than 10% was considered significant, this corresponding to an initial strain ε_1 = 0.6.

It should be appreciated that it is not the overall change in stress that is significant but the difference between the actual and maximum possible deformations of the side link.

In the case now being considered, this effect is significant over a period of 100 seconds so that it is not possible to consider that the stress in the side links is constant over this period in calculating the time-dependent deformations. However, during a short time interval δt, it is still possible to make this assumption. The deformation is therefore considered to occur in a number of discrete short steps with the stress being reduced at each step. As the side links are assumed to have linear viscoelastic properties, the deformation corresponding to each step can be directly added to give the total deformation. This property of linear viscoelastic materials is known as the Boltzmann superposition principle.

Considering the deformation of the network in a short time interval from t = 0 to t = δt_1 it is assumed that, during this time, the stress in the side links is constant. The creep strain in the side links in the time δt_1 is then calculated as in the first example. The resulting deformation of the network and hence the small change $\delta \sigma_1$ in applied stress is then found. It is then assumed that this change in σ occurs suddenly at t = δt_1. The resulting creep strain in the side links during a second short time interval δt_2 is then calculated, making use of the Boltzmann superposition principle, i.e.:

at $t = \delta t_1$ $\varepsilon_1 = \sigma_0 \; \Gamma(\delta t_1)$

at $t = \delta t_1 + \delta t_2$ $\varepsilon_2 = \sigma_0 \; \Gamma(\delta t_1 + \delta t_2) - \delta \sigma_1 \; \Gamma(\delta \tau_2)$

The resulting change $\delta \sigma_2$ in σ is then calculated and the process repeated until $t = 100$ seconds.

Thus, at the nth increment $\tau = \sum_{r=1}^{n} \delta t_r$

$\varepsilon_n = \sigma_0 \; \Gamma(t) - \delta \sigma_1 \; \Gamma(t - \delta t_1) - \ldots\ldots$

$- \delta \sigma_{n-1} \; \Gamma(\delta t_n)$

Fig A.IX.2 shows how this type of incremental analysis approximates to the exact solution.

Case (iii)

With further increase in the initial strain it was found possible to dispense with the above calculations. As the angle σ becomes small ($<5^\circ$) it is possible for large changes to occur in the cross member.stress and hence the side member stress without appreciable deformation occurring in the side links. This is because this deformation is a function of $\cos\theta$ which is very insensitive to variations in θ when θ is small. Under these conditions, it may be assumed that the length of the side member is constant and that stress relaxation conditions prevail. Thus the network behaviour is a direct function of $\beta(t)$ and no further calculation is necessary.

Appendix A.X

Development Problems with Constant Strain Rate Testing
in Vivo

In the course of the constant strain rate tests
in vivo, described in Chapter VI, several problems were
encountered. In view of the fundamental nature of some
of these, no further tests were attempted.

The major difficulty was found in the use of
the Instron Optical Extensometer as a strain measuring
device. Because of the small extension of the gauge
length which obtained (< 0.15 in.) it was necessary to
use this instrument at its highest magnification setting.
In this condition, the chart movement is ten times the
gauge length extension. This meant that the strain
record was only about 1.5 in. long. Much more serious
than this was an effect known as "stepping" of the
chart drive servo system. This was caused by the
considerable frictional forces arising in the chart
mechanism. To overcome these forces, it was necessary
for the chart servo motor to develop a considerable torque
while remaining stationary. When friction was overcome,
the drive mechanism would then advance in a sudden step
until the servo system reached its correct null position.
Thus the chart advanced in a series of steps of about
0.15 in. instead of in a smooth manner. As lower
magnifications were obtained by altering the gear ratio
between the servo motor and the chart this effect was
much less troublesome at these settings.

The result of the stepping effect was that any
given strain value could have had an error of ±10%.
Also, it was found that consecutive time marker pips
used to correlated the load and strain readings would
occur without movement of the chart. It was thus
difficult to correlate the load and strain readings.

Instron Limited have suggested that this
stepping problem can be overcome by increasing the gain

of the system at the optical head gear box. A larger
output at this point would allow the use of a lower
magnification at the chart drive end of the system, and,
as explained above, this would reduce the stepping effect.
Also, arrangements are being made to record the load
output on the Instron pen recorder so that the load-
strain record will appear on one chart.

The method of support for the subject's arm
was not entirely satisfactory as any large movements of
the subject resulted in erroneous strain readings. One
solution of this problem would be to discourage facetious
remarks among those concerned!

Problems such as the support of the arm will
obviously arise at any site which is used for this type
of experiment and their solution has to be related to
the particular difficulties involved in a given case.

When the above difficulties have been resolved,
it is anticipated that this technique will prove to be
convenient and valuable.